

Crossover Chemistry on ROMP-Polymers

Dissertation

For the attainment of the academic degree
doctor rerum naturalium (Dr. rer. nat.)

submitted to the
Faculty of Natural Sciences II
Martin-Luther-University Halle-Wittenberg

by

Steffen Kurzhals

Born on the 6th of April 1984

under the supervision of

Prof. Dr. Wolfgang H. Binder
Professor of the Macromolecular Chemistry
Martin-Luther-University Halle-Wittenberg

Reviewers:

1. Prof. Dr. Wolfgang H. Binder (Martin-Luther-University Halle-Wittenberg)
2. Prof. Dr. Franz Stelzer (Graz University of Technology)

Day of dissertation defense: July, 19, 2013

Halle (Saale), July 22, 2013

Überkreuzungsreaktionen an ROMP-Polymeren

Dissertation

zur Erlangung des

Doktorgrades der Naturwissenschaften (Dr. rer. nat.)

der

Naturwissenschaftlichen Fakultät II

der Martin-Luther-Universität

Halle-Wittenberg,

vorgelegt

von Herr Steffen Kurzhals

geb. am 6. April 1984 in Halle (Saale)

ausgeführt unter der Leitung von

Prof. Dr. Wolfgang H. Binder

Professor der Makromolekularen Chemie

Martin-Luther-Universität Halle-Wittenberg

Gutachter:

1. Prof. Dr. Wolfgang H. Binder (Martin-Luther-Universität Halle-Wittenberg)
2. Prof. Dr. Franz Stelzer (Technische Universität Graz)

Tag der Verteidigung: 19.07.2013

Halle (Saale), den 22.07.2013

Danksagungen

Ich möchte die Gelegenheit nutzen um Danke zu sagen

- meinem Betreuer Prof. Dr. Wolfgang H. Binder, der mich seit meiner Diplomarbeit betreut hat für die kleinen und großen Diskussionen rund ums Thema, die stets positive Sichtweise, die aufmunternden Worte und den speziellen Humor.
- an alle Mitglieder der Arbeitsgruppe, die mich die letzten fünf und ein halbes Jahr begleitet haben für die freundliche Atmosphäre und die hilfreichen Diskussionen.
- bei Anke Hassi für ihre Hilfe bei Problemen aller Art, sei es Organisatorisches oder das Zurechtfinden im Formulardschungel.
- bei Susanne und Norman, die das Arbeiten im Labor erst möglich gemacht haben.
- an alle aktuellen und vergangenen Mitgliedern des Büros 4.06 für das gemeinsame Lachen allen voran "meinen Mädels" Elena, Marlen, Claudia und den beiden Marias.
- den beiden anderen Mitgliedern des "ROMP-Trios" Bhanu und Onur für die nützlichen Diskussionen rund um das Thema Olefin-Metathese.
- an alle Mitorganisatoren des Praktikums, allen voran Claudia, Anja, Philipp und Diana.
- den Kollegen Onur und Haitham für die schöne Zeit als WG.
- dem NMR-Team von Dr. Schröder für die Anfertigung unzähliger Spektren, im Besonderen Frau Yvonne Schiller für das Messen der NMR-Kinetiken und ihre schier unendliche Geduld beim Auswerten dergleichen.
- an die Umicore GmbH für die Bereitstellung der Katalysatoren.
- an meine Familie und Freunde, die mich in all den Jahren unterstützt haben.

Abstract

Ring-opening metathesis polymerization (ROMP) has been established as a powerful tool for the preparation of homo- and block copolymers, as well as end functionalized polymers. However, it is still challenging to prepare end functionalized polymers with the desired functional group or block copolymers in any composition or order of monomers. In both cases the underlying cross over reaction is crucial for the success of the process. This thesis describes the investigation of the cross over step in block copolymerization reactions as well as termination reactions. As a model system for both processes, poly(5-norbornene-2,3-dicarboxylic acid dimethylester) (poly(**1**)) was chosen, as it can be polymerized with several ruthenium catalysts in a living manner. For the investigation of the cross over step in block copolymerization reactions, living poly(**1**) chains were reacted with three structurally different cycloolefins (1-4 equiv. with respect to the living chain). After quenching, the resulting block copolymers were studied by GPC and MALDI-TOF MS. Monitoring this process with mass spectrometry allowed the detection and semi quantification of the intermediate species. The results obtained show that the efficiency of the process depends strongly on the monomer/catalyst couple used as well as GPC methods alone are insufficient to determine the point of crossover. To obtain information about the propagating species in this process, co-oligomerization reactions were conducted and subsequently investigated via ESI-TOF MS.

The results confirm the general accepted dissociative olefin metathesis mechanism and show the strong dependency of the process on the catalytic system used. For the investigation of the cross over reaction in termination reactions, the model system was reacted with symmetric olefins. The resulting polymers were investigated via GPC, NMR and MALDI-TOF MS. The efficiency of the quenching process clearly depends on the structure of the terminating agent, the applied catalyst as well as the reaction time and the initial ratio of terminating agent/living chain. This quenching process was then applied on poly(norbornene). The comparison of these two systems showed the higher tendency of poly(norbornene) to undergo secondary metathesis in the quenching process. Additionally, the prepared poly(norbornene)s and their hydrogenated counterparts were studied by DSC-methods.

Inhaltsangabe

Die Ringöffnungsmetathese-Polymerisation (ROMP) hat sich seit der Entwicklung von Single-Site-Katalysatoren durch Robert Grubbs und Richard Schrock als Methode zur Herstellung von Homo- und Blockcopolymeren, sowie von endfunktionalisierten Polymeren etabliert. Dennoch ist es nicht immer möglich endfunktionalisierte Polymere mit beliebiger Endgruppe oder Blockcopolymeren mit frei wählbarer Zusammensetzung oder Reihenfolge der Monomeren darzustellen. In beiden Fällen ist der Überkreuzungsschritt entscheidend für den Erfolg der jeweiligen Reaktion. Daher war es das Ziel dieser Arbeit die Überkreuzungsreaktion in Blockcopolymerisationen und Terminierungsreaktionen von ROMP-Polymeren zu untersuchen. Als Modellsystem dieser beiden Prozesse wurde Poly(5-Norbornen-2,3-dicarbonsäuredimethylester) (Poly(**1**)) gewählt, welches mit verschiedenen Ruthenium-Katalysatoren lebend polymerisiert werden kann. Zur Untersuchung der Überkreuzung in Blockcopolymerisationen wurden lebende Polymerketten, hergestellt durch Polymerisation von Monomer **1**, mit drei strukturell unterschiedlichen Cycloolefinen (1-4 Equiv. in Bezug auf die lebende Kette) zur Reaktion gebracht. Nach Terminierung der Polymerisation wurden die resultierenden Polymere mittels GPC und MALDI-TOF MS charakterisiert. Die Verfolgung des Reaktionsprozesses durch Massenspektrometrie erlaubt die Detektion und Semiquantifizierung der im Überkreuzungsschritt auftretenden Zwischenprodukte. Die Ergebnisse zeigen, dass die Effizienz des Überkreuzungsprozesses stark vom gewählten System aus Katalysator und Monomer abhängt und die GPC-Messungen nicht hinreichend exakt genug sind um den Überkreuzungspunkt zu bestimmen. Derselbe Prozess wurde auch an lebenden Oligomeren mittels ESI-TOF MS untersucht.

Die so gewonnenen Ergebnisse bestätigen einen dissoziativen Olefin Metathese Mechanismus und zeigen erneut eine Abhängigkeit der Überkreuzungseffizienz von dem verwendeten Katalysator. Zur Untersuchung der Überkreuzungsreaktion in Terminierungsreaktionen wurde das gewählte Modellsystem mit symmetrischen Olefinen umgesetzt. Dabei konnte gezeigt werden, dass die Effizienz der Endgruppeneinführung von der Struktur des symmetrischen Olefins, dem verwendeten Katalysator, der Reaktionszeit und dem Molverhältnis zwischen Terminierungsagens und lebender Kette abhängt. Die Endgruppeneinführung mittels symmetrischer Olefine wurde dann analog am unsubstituierten Poly(norbornen)-System durchgeführt. Ein Vergleich der zwei Polymere zeigt dass das unsubstituierte Poly(norbornen) im

Gegensatz zum substituierten Poly(norbornen) (Poly(**1**)) sekundäre Metathesereaktionen eingeht. Desweiteren wurden sowohl die synthetisierten Poly(norbornene) als auch die hydrierten Poly(norbornene) durch DSC-Messungen charakterisiert.

Index of contents

1. INTRODUCTION AND MOTIVATION	1
1.1. Ring-opening metathesis polymerization (ROMP)	1
1.2 ROMP: influence of catalyst, monomer and additives	2
1.2.1 Role of monomer/catalyst couple	2
1.2.2. Role of additives and temperature	5
1.3 MALDI- / ESI-MS of olefin metathesis and metathesis catalysts	7
1.3.1. General	7
1.3.2. MALDI-TOF MS of olefin metathesis and metathesis catalysts	8
1.3.3. ESI-TOF MS of olefin metathesis and metathesis catalysts	9
1.4 Cross metathesis	11
1.4.1. General	11
1.4.2. Product control in cross metathesis	12
1.5. End functionalization of ROMP-polymers	16
1.5.1. Functionalized catalysts	17
1.5.2. Quenching with enol ethers	18
1.5.3. Quenching with molecular oxygen	20
1.5.4. Sacrificial synthesis	21
1.5.5. Quenching with vinylene carbonate/ 3H-furanone	22
1.5.6. Quenching with acrylates/acrylamides	23
1.5.7. Quenching with symmetric olefins	23
1.5.8. Telechelic polymers via chain transfer agents	25
1.5.9. Telechelic polymers via bimetallic catalysts	27
1.6 Aims	30
2. RESULTS AND DISCUSSION	31
2.1. Concept	31
POLYMERIZATION	33
2.2. Polymerization of monomer 1	33
2.2.1. NMR-kinetics	33
2.2.2. GPC-kinetics	36
2.2.3. Stereochemistry of poly(1)	38
2.3. Polymerization of monomers 11 and 12	40
2.3.1. Poly(<i>p</i> -phenylene vinylene)s via ROMP	40
2.3.2. Monomer synthesis	41
2.3.3. Polymerization results	45

2.4. Polymerization of norbornene (13)	50
2.4.1. Polymerization results	50
2.4.2. Stereochemistry of poly(13)	52
CROSSOVER REACTIONS	53
2.5. Investigation of the crossover step in block copolymerization reactions via MALDI-TOF MS	53
2.5.1. GPC-kinetics of the block copolymerization reactions	54
2.5.2. NMR-kinetics of the block copolymerization reactions	56
2.5.3. Monitoring the crossover efficiency via MALDI-TOF MS	58
2.5.4. MALDI-TOF quantification	62
2.6. Investigation of the crossover step in co-oligomerization reactions via ESI-TOF MS	66
2.6.1. Overview of detected ions	67
2.6.2. Reaction of catalysts G1, U1 with monomer 1	69
2.6.3. Reaction of catalysts G3, U3 with monomer 1	72
2.6.4. Reaction of catalysts G1, U1 with monomer 1 and subsequent addition of monomers 2-4	74
2.6.5. Reaction of catalysts G3, U3 with monomer 1 and subsequent addition of monomers 2-4	76
2.6.6. ESI-TOF MS semi-quantification	77
2.6.7. Connecting ESI-TOF MS semi-quantification with NMR-kinetics	80
2.7. End functionalization of poly(1) with symmetric olefins	82
2.7.1. Quencher synthesis	83
2.7.2. Termination of living chains with α -olefin 20 and symmetric olefin 24	85
2.7.3. Termination of living chains with compound 21	87
2.7.4. Termination of living chains with compound 23	90
2.7.5. MALDI-TOF analysis	92
2.8. End functionalization of poly(13) with symmetric olefins	94
2.8.1. Quenching efficiency for poly(13)	95
2.8.2. HPLC-analysis of poly(13)	98
2.8.3. Hydrogenation of poly(13)	103
2.8.4. DSC-studies on poly(13) and poly(14)	106
Summary	109
3. EXPERIMENTAL	115
4. REFERENCES	126
5. APPENDIX	132
Chapter 2.2.	132
Chapter 2.3.	136
Chapter 2.4.	146
Chapter 2.5.	147
Chapter 2.6.	154
Chapter 2.7.	177
Chapter 2.8.	183

Experimental Procedures	188
Curriculum Vitae	206
List of Publications	208

Results of this dissertation have been published

Parts of the chapters 2.2, 2.5 have been published in Binder, W. H.; Pulamagatta, B.; Onur, K.; Kurzhals, S.; Barqawi, H.; Tanner, S., Monitoring Block-Copolymer Crossover-Chemistry in ROMP: Catalyst Evaluation via Mass-Spectrometry (MALDI). *Macromolecules* **2009**, *42*, 9457–9466. Text, Schemes 2.14-2.15, Figures 2.1.-2.2., 2.10-2.16, 5.25-5.37 and Tables 2.1-2.2, 2.6-2.10 **adapted** with permission from *Macromolecules* **2009**, *42*, 9457–9466. Copyright **2009** American Chemical Society. Tables 2.1-2.2 adapted from *Macromolecules*, Article ASAP, DOI: 10.1021/ma302555q. Copyright **2013** American Chemical Society.

Parts of the chapters 1.2, 1.3, 2.2, 2.6 have been published in Kurzhals, S.; Enders, C., Binder, W. H., Monitoring ROMP Crossover Chemistry via ESI-TOF MS, *Macromolecules*, Article ASAP, DOI: 10.1021/ma302555q. Text, Schemes 2.16-2.19, Figures 2.17-2.22, 5.1, 5.38-5.48 and Tables 2.10, 5.1-5.18 **adapted** with permission from *Macromolecules*, Article ASAP DOI: 10.1021/ma302555q, Copyright **2013** American Chemical Society.

Parts of chapters 1.5, 2.7 have been published in Kurzhals, S.; Binder, W. H., Telechelic polynorbornenes with hydrogen bonding moieties by direct end capping of living chains. *J. Polym. Sci., Part A: Polym. Chem.* **2010**, *48*, (23), 5522-553, Text, Figures 2.23-2.29, 5.49-5.59, Tables 2.11-2.13 and Scheme 2.21 **adapted** with permission from *J. Polym. Sci., Part A: Polym. Chem.* **2010**, *48*, (23), 5522-5532, Copyright **2010** John Wiley and Sons.

List of abbreviations

Ac	acetyl
ACN	acetonitrile
ADMET	acyclic diene metathesis
ATRP	atom transfer radical polymerization
B.p.	boiling point
CID	collision induced dissociation
CM	cross metathesis
COSY	correlated spectroscopy
CTA	chain transfer agent
d	Doublet
Da	Dalton
DCM	Dichloromethane
DMSO	Dimethylsulfoxide
DSC	differential scanning calorimetry
equiv.	Equivalents
ESI-MS	electrospray ionization mass spectrometry
GPC	gel permeation chromatography
Hex	hexane
HMDS	hexamethyldisilazane
Hz	Hertz
<i>i</i> -Pr-OH	Isopropanol
k_{Br}	brutto rate constant
KBr	potassium bromide
k_p/k_i	ratio of propagation rate constant to initiation rate constant
MALDI-MS	matrix assisted laser desorption ionization mass spectrometry
M_e	molecular weight of entanglement
MeOH	Methanol
min	Minute
M_n	number average molecular weight
M_e	molecular weight of entanglement

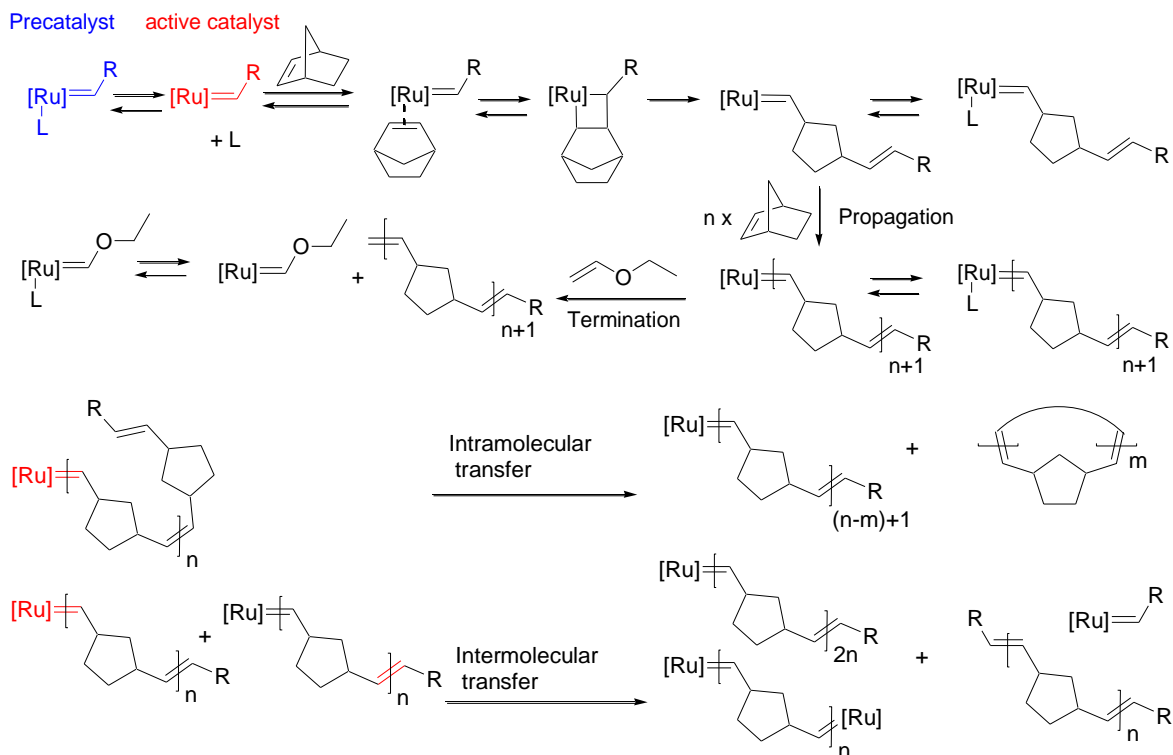
M_w	weight average molecular weight
M/C	monomer to catalyst ratio
Mes	Mesityl
m/z	mass to charge ratio
NHC	<i>N</i> -heterocyclic carbene
NMP	<i>N</i> -methylpyrrolidone
NMR	nuclear magnetic resonance
OLED	organic light emitting device
PCy ₃	tricyclohexylphosphine
PDI	polydispersity index
PPh ₃	Triphenylphosphine
ppm	parts per million
PPV	poly(<i>p</i> -phenylene vinylene)
s	Singlet
t	Triplet
TA	termination agent
T_g	glass transition temperature
THF	Tetrahydrofuran
T_m	melting temperature
TOF	time of flight
RCM	ring closing metathesis
ROM	ring opening metathesis
ROMP	ring opening metathesis polymerization
TEMPO	(2,2,6,6-tetramethylpiperidin-1-yl)oxyl
TMSCI	

1. Introduction and Motivation

Polymeric materials have nowadays found access into all parts of life, covering e.g. medical science, clothing, transport, information technology or energy harvesting. Living polymerization techniques have thereby been a boost in the development of these materials with complex molecular architecture or functionality. In the past two decades, the ring-opening metathesis polymerization (ROMP) has emerged in the field of living polymerization reactions, as a powerful tool for the preparation of homo- and block copolymers¹⁻⁹ together with the synthesis of telechelic and semi telechelic functionalized polymers.¹⁰⁻¹² A pivotal point in this history of success was the development of single site metathesis catalysts,^{13,14} which have led to a huge increase in interest for olefin metathesis, ranging from organic to polymer chemistry. The development of these catalysts by Robert Grubbs and Richard Schrock together with the elucidation of olefin metathesis mechanism by Yves Chauvin was awarded with Nobel Prize in 2005. With commercial catalysts in hand a wide array of cycloolefins could then be polymerized in a living fashion. Especially the catalysts based on ruthenium have shown unexampled tolerance to functional groups, air and moisture, allowing the preparation of functional materials by direct polymerization of monomers carrying carbohydrates, hydrogen bonding moieties, nucleosides, drugs, dyes etc. With potential use ranging from electronically/optically active materials, self-healing and responsive polymers or drug carrier-purposes, ROMP has become a valuable tool for material science.

1.1. Ring-opening metathesis polymerization (ROMP)

The ring opening metathesis polymerization (ROMP) is a metal catalyzed insertion polymerization. As for other ring opening polymerizations (ROP), the thermodynamic driving force is the release of ring strain. ROMP, like all other olefin metathesis reactions (ROM, RCM, CM, ADMET), proceeds via the mechanism, first proposed by Chauvin et al.,¹⁵ which includes the coordination of the monomer, the [2+2] cycloaddition to form the metallacyclobutane intermediate and the final cycloreversion (Scheme 1.1). Side reactions include the intramolecular chain transfer (backbiting), generating macrocycles, and the intermolecular chain transfer, leading to a scrambling of end groups.



Scheme 1.1. Mechanism of ROMP on the example of the reaction of norbornene with a ruthenium catalyst, e.g. Grubbs catalyst 1st-generation, $L = PCy_3$, termination with ethyl vinyl ether.

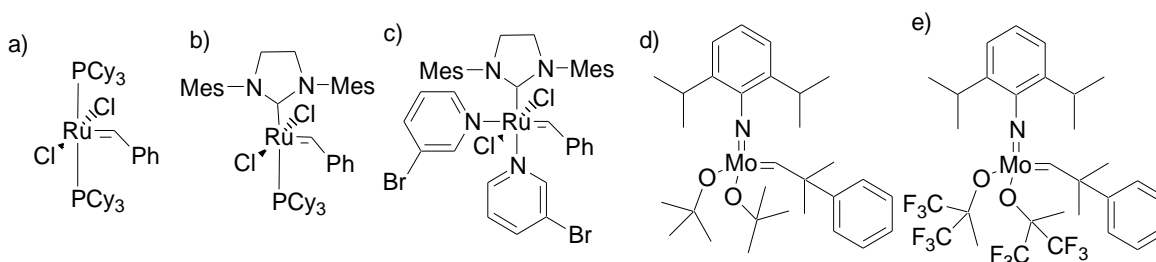
The unsaturation of the monomer is retained in the polymer in contrast to vinyl polymerizations. This feature of the ROMP is advantageous for the preparation of conductive polymers or the post functionalization of the obtained structures (cross linking, hydrogenation, thiol-ene reaction etc.).

1.2 ROMP: influence of catalyst, monomer and additives

1.2.1 Role of monomer/catalyst couple

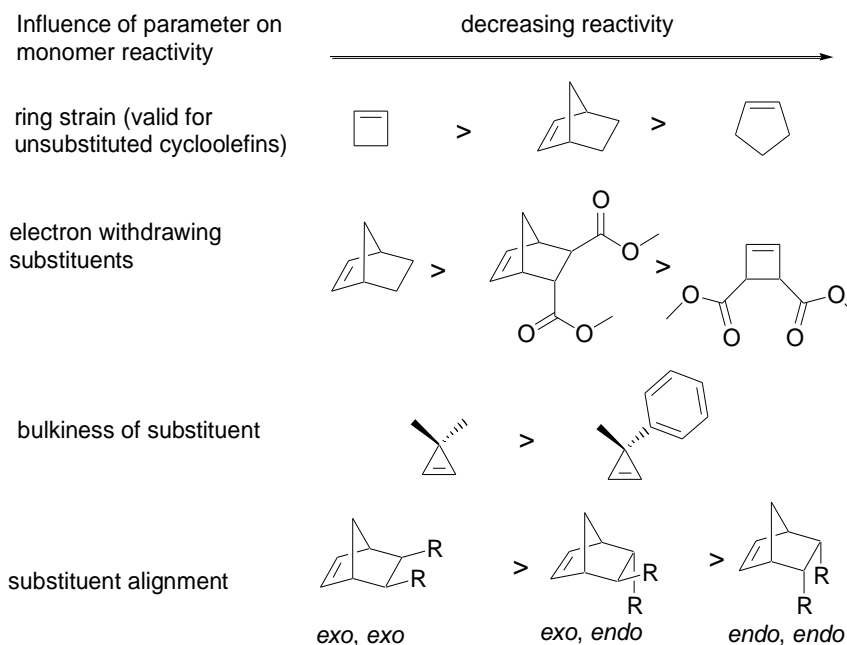
For the successful synthesis of block copolymers and functionalized polymers with defined molecular weights and narrow PDI a living polymerization process^{7,16,17} is crucial. Only in this case, the active species is maintained throughout the polymerization reaction and secondary metathesis such as backbiting¹⁸ or chain transfer-reactions⁸ are suppressed. Several parameters

have to be taken into consideration to obtain a living polymerization. The right selection of a monomer/catalyst combination is one central parameter for a successful polymerization. An important point is that the used catalyst must be able to tolerate all functional groups on the monomer. Ruthenium catalysts like Grubbs catalyst 1st, 2nd- and 3rd-generation display a greater tolerance^{19,20} of functional groups compared to molybdenum catalysts (see Scheme 1.2 for catalyst structures). For molybdenum catalysts, the reactivity with functional groups increases in the following order: ester/amides < ketones < olefins < aldehydes < water/alcohols < acids.²⁰ This order of reactivities explains the sensitivity of molybdenum catalysts against moisture and the use of aldehydes as termination agents.



Scheme 1.2. Chemical structure of metathesis catalysts, a) Grubbs catalyst 1st-generation, b) Grubbs catalyst 2nd-generation, c) Grubbs catalyst 3rd-generation, d-e Schrock molybdenum catalysts.

For ruthenium catalysts the order of reactivity is as follows: ester/amides < ketones < aldehydes < water/alcohols < acids < olefins.²⁰ Thus, ruthenium catalysts will react preferentially with olefinic bonds in comparison to all other functional groups. This feature of the ruthenium catalysts allows the direct polymerization of functional monomers carrying carbohydrates, hydrogen bonding motifs, fluorinated chains or bioactive molecules such as drugs or dyes. To ensure a living polymerization, the monomer should not carry a functional group that is more reactive towards the catalyst than the actual olefinic bond. A further point, influencing the reactivity, is the monomer structure itself. In general, the monomers for ROMP should possess sufficient ring strain for the polymerization process to be irreversible and thereby avoid polymerization/depolymerization equilibria. The reactivity of the monomer is linked to its ring strain and its substitution (Scheme 1.3).



Scheme 1.3. Influence of ring strain and substituents on the monomer reactivity.

Cazalis et al. have shown that an increase in ring strain leads to an increase in the reactivity by comparing the ROMP of norbornene and the more strained bicyclo[3.2.0]hept-6-ene, which includes a cyclobutene ring.²¹ The influence of the substituents (electronic and steric factors) on the monomer reactivity was investigated e.g. on substituted cyclobutenes,²² norbornenes²³ or cyclopropenes.²⁴ A decrease in the reactivity was thereby observed when electron withdrawing groups were attached at the monomer structure. This effect can be explained by the preference of the electron-poor catalyst to coordinate electron rich olefins. The monomer reactivity is also decreased by increasing the bulkiness of the substituents.²²⁻²⁴ Investigations on the ROMP of cyclopropenes in our work group have shown that the reactivity significantly decreases when going from 3,3-dimethylcyclopropene to 3-methyl-3-phenylcyclopropene.²⁴ The decrease in reactivity can be explained by the stronger sterical shielding of the double bond, by the more bulky phenyl group in allylic position.

Studies on 2,3-disubstituted norbornenes and oxo-norbornenes have shown that the reactivity of the monomer depends on the alignment of the substituents as well.²⁵⁻²⁹ The reactivity of the monomer with the substituents in a given configuration decreases in the following order *exo, exo* > *exo, endo* > *endo, endo*, as a result of the increasing sterical shielding of the double bond.^{26,27} Furthermore, the choice of the substituents can have significant influence on the

polymerization kinetics. Norbornenes with oxygen containing substituents tend to coordinate to the ruthenium center after incorporation in the polymer chain. The tendency of the substituents for coordination thereby increases in the following order: ester \approx ether < ketone.²⁷ The ability of the incorporated monomer to coordinate and thereby to form favorable six membered resting states with the ruthenium center increases the control over the polymerization process but decreases the overall reaction rate.²⁷

A successful polymerization however is linked to several parameters, and not only limited to the functional tolerance of the catalyst and the monomer structure. This can be seen by the fact that polymerization results of structurally similar monomers with the same type of catalyst can still differ significantly, regarding the livingness of the process. Thus, block copolymers prepared from these monomers would suffer from an uncontrolled molecular weight and broad polydispersity as a result of a poor crossover reaction and the different kinetics of each block. For the synthesis of narrowly dispersed polymers as well as molecular weights comparable to the calculated values, the initiation of the polymerization should be sufficiently fast for a selected catalyst/monomer couple. In case of $k_p/k_i \gg 1$, very often the formation of high molecular weight polymer is observed along with a broad polydispersity (PDI > 1.5). This initiation behavior is often observed with Grubbs catalyst 2nd-generation. Grubbs 1st-generation and especially Grubbs 3rd-generation have a more favorable k_p/k_i -ratio which often allows the preparation of polymers with narrow molecular weight distributions (PDI < 1.2).

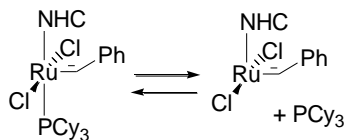
1.2.2. Role of additives and temperature

The reactivity of metathesis catalysts and their k_p/k_i ratio can be adjusted by using additives, such as ligands (phosphines, pyridines), solvents or acids. A common strategy to increase the activity of ruthenium carbenes is to add additives like acids,^{30,31} copper chloride or copper iodide³² that act as scavenger for the phosphine or pyridine-ligands (Scheme 1.4). Thus, the inactive 16 electron-precatalyst is converted into a 14-electron active catalyst species.^{33,34} Since the cleaved off phosphine ligand is irreversibly bound as phosphonium salt or copper complex, the catalytic cycle is not interrupted by back binding of free phosphine. Therefore, the active species is already present at the start of the reaction which leads to an improvement, both in initiation and propagation.

decrease in the activity by addition of

phosphines

addition of solvents acting as ligands
acetonitrile, pyridine, DMSO



increase in the activity by addition of

acids (HCl, H₃PO₄)
copper salts (CuCl, CuI)
perfluorinated solvents
donor solvents (*i*-PrOH, acetone)

Scheme 1.4. Influence of additives on the catalytic activity.

In contrast to the mentioned accelerators (acids, copper salts), the addition of phosphines slows down the polymerization since the equilibrium between precatalyst and active catalyst species is shifted towards the inactive site. In some examples, the addition of phosphine was used to control the polymerization of norbornene or cyclopentene with ruthenium-³⁵ and molybdenum catalysts.³⁶ The addition of trimethylphosphine to a polymerization of norbornene with Schrock catalyst prevents the formation of high molecular weight polymer by binding more strongly to the propagating species.³⁶ Thus, the reactivity of the propagating species is reduced, resulting in a change of the k_p/k_t ratio. The addition of solvents or the change of the reaction solvent has shown as well influence on the activity of metathesis catalysts.^{26,37,38} Grubbs et al. have shown that the initiation rate constant (k_i) for ruthenium catalysts is roughly proportional to the dielectric constant of the reaction solvent.³⁷ On the example of Grubbs catalyst 2nd-generation, the change of the solvent from toluene ($\epsilon = 2.38$) to tetrahydrofuran ($\epsilon = 7.32$) results in an increase of the initiation rate constant by a factor of 2.³⁷

Slugovc et al. reported that the addition of donor solvents like acetone or isopropanol can increase the metathesis activity of ruthenium catalysts by stabilizing the active species.²⁶ Solvents like acetonitrile, dimethylsulfoxide or pyridine on the other hand decrease the activity, as they can act as ligands, competing with the monomer insertion.²⁶ Perfluorinated solvents as additive have proven to increase the activity of Grubbs catalyst 2nd-generation in cross metathesis due to π/π interactions with the mesityl-groups of the *N*-heterocyclic carbene attached to the catalyst.³⁹ In case of Schrock molybdenum catalysts, polymerizations in tetrahydrofuran are slower than for example in toluene since tetrahydrofuran is acting as ligand and therefore competing with the monomer insertion.⁴⁰

Another point that has to be considered is that the used polymer system does not undergo secondary metathesis which would lead to molecular weight degradation and broader polydispersities. An increase in the reactivity of the catalysts often comes along with an increased tendency for secondary metathesis reactions (backbiting or intermolecular transfer).

These side reactions are often observed in the ROMP of unsubstituted cycloolefins (cyclopentene, cyclooctadiene) with Grubbs catalyst 2nd generation. The internal double bonds in the formed polymer chains are not protected from intra- or intermolecular chain transfer due to missing sterical hindrance. As an increase in the reaction temperature results in an increase in the activity along with secondary metathesis, it can be advantageous to conduct polymerization reactions at lower temperatures to suppress unwanted side reactions. While the polymerization of norbornene with Grubbs catalyst 3rd-generation for example is uncontrolled at room temperature; the polymerization is living at -20°C.⁴¹ Hence, with catalysts, solvents, additives and temperature, polymer chemists have a “ROMP toolbox”²⁶ for achieving optimal results.

1.3 MALDI- / ESI-MS of olefin metathesis and metathesis catalysts

1.3.1. General

With the advent of ESI MS and MALDI MS in the late 1980s,⁴² biochemists and polymer chemists was given a tool for the structural elucidation of biomacromolecules (proteins, carbohydrates) and synthetic polymers respectively. Electrospray ionization (ESI) and matrix assisted laser desorption ionization (MALDI) allow the transfer of ionized but unfragmented macromolecules to the gas phase. The formed ions can then be separated like in conventional mass spectrometry by using analyzers e.g. time of flight tubes (TOF), quadrupole or hexapole. The obtained information can then be used for the structural elucidation e.g. composition of copolymers,^{43,44} polymer end groups⁴⁵⁻⁵⁶ or peptide sequencing.

MALDI MS covers the broader range of molecular weights to be investigated (1-100 kg/mol). However, the mass range that can be detected depends strongly on the used polymer, with an often observed suppression of higher molecular weights. Thus, the upper detection limit for synthetic polymers is often in the range of ~15000-20000 m/z. Still MALDI MS is superior in the detection limit compared to ESI-TOF MS, not exceeding ~ 6000 m/z.^{57,58} In contrast to this limitation in the detection range, ESI-TOF MS covers better the small molecular weight range < 2000 g/mol, as there is no overlap with matrix clusters like in MALDI-MS and displays a better mass accuracy and resolution of the spectra. Ionization in both techniques can be tuned by the sample preparation. While in MALDI, the selected matrix/salt combination is of importance, the ESI-process can be tuned by addition of solvents and salts. Molecules and polymers carrying

already charged moieties greatly facilitate both processes, as no charge has to be attached at the analyte.

MALDI- and ESI-MS have been applied in olefin metathesis to study polymers, oligomers, catalysts and reaction mechanisms. For polymers/oligomers, the resulting mass spectra comprise information on the end group, molecular weight, the polydispersity and the purity of the investigated sample. Conclusions on the molecular weight and the purity have to be taken with care as ionization strongly depends on the chemical structure and the molecular weight. Thus, often the molecular weight is smaller and the obtained polydispersity is narrower compared to other techniques, e.g. GPC. For the investigation of reaction mechanisms, the resulting mass spectra obtain information e.g. on reactive intermediates, side products, and fragmentation pathways. ESI-TOF MS is hereby better suited than MALDI-TOF MS as samples can be taken directly from solution. For analysis of polymers as well as monitoring reactions, the isotopic pattern (visible below 4000 m/z) states on the number of charges attached to the molecule and can be used for identification of species by comparison with simulated structures. Like most analytical techniques, ESI- and MALDI-MS display some drawbacks which include suppression of high molecular weight species or preferential ionization of certain species.

1.3.2. MALDI-TOF MS of olefin metathesis and metathesis catalysts

From the two mentioned methods, MALDI covers a broader range of molecular weights to be detected. Thus, it is better suited for the analysis of polymers. Investigated ROMP polymers are most often norbornene based polymers with polar moieties like poly(norbornene dicarboxyimide)s^{49,51,52} or poly(norbornene dicarboxylic acid diester)s^{44,59,60} or derived from cyclophanedienes.^{61,62} A polymer backbone with polar substituents is often chosen as in general nonpolar polymers like poly(ethylene) or poly(propylene) are hardly ionized in the MALDI-process, excluding these materials from the analysis. Most measurements on end functionalized polymers were done for samples with M_n smaller than 10000 g/mol, to obtain spectra with peaks, displaying isotopic patterns. The presence or the absence of certain species in the mass spectrum can then be used to conclude on the quenching efficiency,^{45,49,51,52,60} the copolymer composition^{44,59} or secondary metathesis.⁶²

Besides the analysis of polymers, living oligomers and metathesis catalysts were studied via MALDI-TOF MS. The investigation of living chains via MALDI-TOF MS was conducted by Gibson et al.⁶³ In this study, Grubbs catalyst 1st-generation was used for the polymerization of norbornene dicarboxylic acid anhydride. The living species, generated by the ROMP process, were investigated prior to the termination via MALDI-TOF MS by mixing the reaction solution with indoleacetic acid as matrix, followed by deposition on a MALDI target. The mass spectrum showed as main series aldehyde capped oligomers (1000-5000 m/z) as a result of the non-anaerobic sample preparation. As side series, polymer chains still attached to the ruthenium catalyst were detected as $[M+H]^+$, $[M+Na]^+$, $[M+K]$ -adducts.

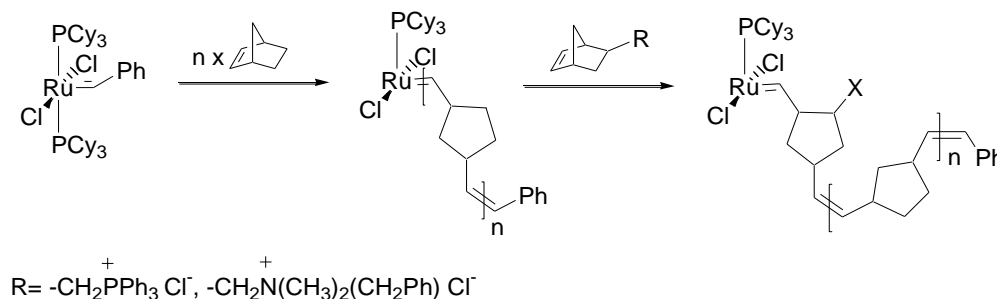
Fogg et al. were successful in the investigation of late transition metal complexes by MALDI-TOF MS including Piers metathesis catalyst or Grubbs catalyst 1st-generation, which were detected as cation or radical cation respectively.⁶⁴ The sample preparation (matrices: pyrene, anthracene) and transfer to the MALDI mass spectrometer was thereby conducted under an inert atmosphere.⁶⁴ This was achieved by combining a glovebox with a MALDI mass spectrometer in such a way that the entry of the loading chamber of the mass spectrometer is located inside the glovebox.⁶⁴ An investigation of Grubbs catalyst 1st- and 2nd-generation via MALDI MS using elemental sulfur, anthracene or pyrene as matrix was reported by Zhu et al.⁶⁵ The best results were obtained with elemental sulfur as matrix, allowing to observe the ruthenium complexes as radical cations.⁶⁵

1.3.3. ESI-TOF MS of olefin metathesis and metathesis catalysts

ESI-TOF MS can be seen as a complementary technique to MALDI-TOF MS in the investigation of olefin metathesis and metathesis catalysts. While MALDI-TOF MS was utilized for the analysis of polymers, ESI-TOF MS was applied for monitoring olefin metathesis reactions such as RCM, ADMET or ROMP. The great advantage over MALDI-TOF is that the samples can be directly taken from solution and thus also reactive intermediates can be accessed by this technique. Using this advantage, ESI-MS has proven to be a powerful tool for the investigation of reactions in solution and elucidation of their mechanisms,⁶⁶ especially in metal catalyzed reactions like formylation,⁶⁷ Suzuki-⁶⁸, Heck-,⁶⁹ Stille-coupling⁷⁰ and, as mentioned, olefin metathesis.^{66,71-81}

Previous works on the investigation of olefin metathesis with Grubbs catalyst 1st-generation by Chen^{71-73,77} and Metzger⁷⁸ have shown the necessity of charged comonomers, charged catalysts

or ligand exchange with charge-labeled ligands for the ionization of the ruthenium carbenes and oligomers or reaction products attached to the catalyst. The investigations included ROMP of norbornene (5 equiv.) and a charge carrying norbornene derivate (0.1 equiv.), (ammonium, or phosphonium-moiety) with Grubbs catalyst 1st-generation, with the incorporated charged monomer acting as “fishhook” for the oligomers attached to the neutral catalyst (Scheme 1.5).⁷¹



Scheme 1.5. Polymerization of norbornene with Grubbs catalyst 1st-generation and charged comonomers [⁷¹].

By using monocationic 1st-generation complexes (charge located at the phosphine-ligand) which are generated from dicationic precursors, Chen and coworkers monitored gas phase reactions with 1-butene, styrene and norbornene in order to determine the influence of the alkylidene moiety on the reaction rate.⁷² Monocationic ruthenium complexes, carrying the charge at the carbene moiety were used as well for comparing the reactivity of active species from 1st and 2nd-generation catalysts in the ROMP of norbornene.⁷⁴ Metzger et al. investigated the reaction of Grubbs catalyst 1st-generation with ethylene and diallyl-compounds in cross metathesis and ring closing metathesis reactions.⁷⁸ Ionization of the metal complexes was achieved by ligand exchange of tricyclohexylphosphine with charge labeled phosphine generating mono, di and tricationic complexes.⁷⁸ Thus, species were detected bearing up to 3 phosphine units. An ESI-TOF MS study on the decomposition of Grubbs catalyst 1st-generation in a mixture of dichloromethane/acetonitrile (v/v = 82/18) was performed by Zhao et al.⁸⁰ The investigation showed that acetonitrile acts as ligand and can promote decomposition.⁸⁰ The ruthenium species ionized by loss of chloride were detected with up to three acetonitrile ligands attached.⁸⁰

Metzger et al. were then able to overcome the necessity of charged ligands, monomers or catalysts by using alkali salts MeCl (Me: Li⁺, Na⁺, K⁺, Cs⁺) as additives to ionize neutral catalysts

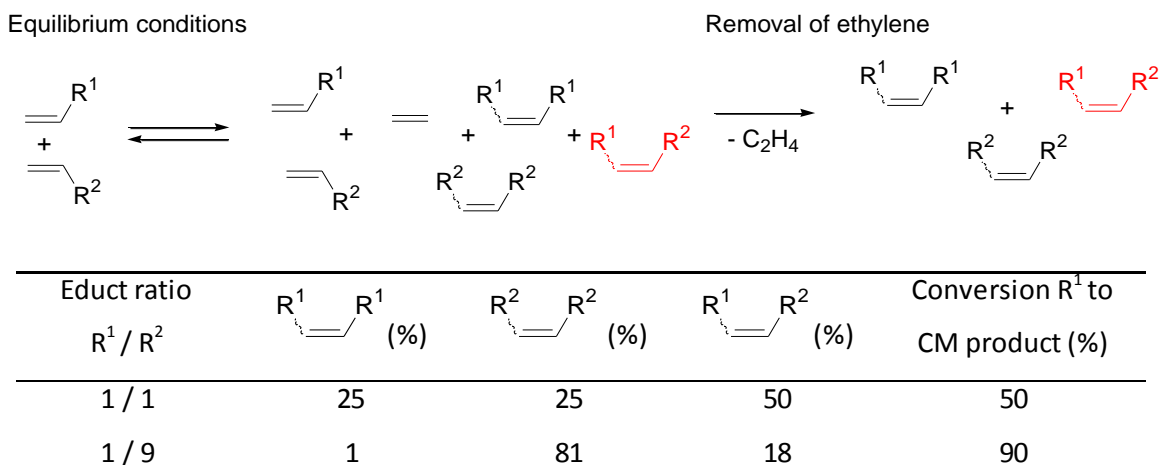
and neutral oligomers or reaction products attached to the catalyst. The alkali salts are added in a four times excess to the ruthenium carbenes which are detected as alkali metal adducts $[M+Me]^+$. Using this approach, Grubbs 1st-⁷⁹ and 2nd-generation catalysts⁸¹ and their reaction with 1-butene, ethylene (cross metathesis)⁷⁹, α,ω -dienes (ring closing metathesis, ADMET)⁷⁹ and cyclooctene (ROMP)⁷⁹ were investigated. The intermediates of these reactions could be identified; some selected peaks (bisphosphine and monophosphine complex-alkali metal adducts) were defragmented using collision induced dissociation (CID) with argon.⁷⁹

The fragmentation pattern of the investigated catalysts shows that both chlorines and the benzylidene ligand can be cleaved off during the ESI-process. The loss of the chlorines thereby takes place as chloride-anion and neutral hydrogen chloride, while the benzylidene moiety is cleaved off as C_7H_8 (toluene). Thus, in previous works it was shown that ESI-MS is not only suited to detect pure catalyst species but also reaction products from olefin metathesis reactions which are still attached to the catalyst.

1.4 Cross metathesis

1.4.1. General

The preparation of 1,2-disubstituted olefins can be achieved by different pathways, including e.g. palladium catalyzed coupling reactions (Heck-, Stille- or Suzuki-coupling), Wittig type olefination or by metathesis. In the mentioned coupling reactions e.g. Stille coupling, orthogonal functional groups are reacted with each other, generating one set of products. This orthogonality of the functional groups is not given in the cross metathesis, where both educts are olefins. Thus, favored by entropy, a statistical distribution of products can be expected in the cross metathesis of two olefins. The enthalpic contribution to the reaction energy is negligible ($\Delta_R H \sim 0$), because no ring strain is released or bond transformation is taking place. The cross metathesis of two terminal olefins is depicted in Scheme 1.6.



Scheme 1.6. Statistical product distribution for the cross metathesis of two terminal olefins, product distribution dependent on the educt ratio (under the assumption of efficient removal of ethylene, similar reactivity of the educts and full conversion of the educts), red: cross metathesis product, conversion R^1 to CM product (%): efficiency of the transformation from educt with substituent R^1 to the cross metathesis product.

Products formed in the reaction consist of the starting olefins, two homo- and one heterodimer in *cis* and *trans* configuration as well as ethylene. By removing ethylene from the mixture, the reaction equilibrium is shifted to the product side. The desired cross metathesis product is the one present with two homo metathesis products. The product distribution is dependent on the educt ratio. A mixture of the starting olefins (R^1 and R^2) in a ratio of 1:1 would give only 50% conversion to the desired cross metathesis product, under the assumption of similar reactivity of the educts (Scheme 1.6). By increasing the amount of one reaction partner, e.g. $R^1 / R^2 = 1 / 9$, it is possible to improve the conversion of one educt (R^1) to the cross metathesis product. For a mixture of two olefins ($R^1 / R^2 = 1 / 9$), the conversion of the educt R^1 to the cross metathesis product would be 90%, but its fraction in the product mixture would only be 18% (Scheme 1.6).

1.4.2. Product control in cross metathesis

Similar reactivity of the starting olefins is often not given in real systems. Thus, the product formation does not only depend on the ratio of the starting olefins but also on the reactivity of the olefins towards the catalyst and their tendency for homo metathesis.

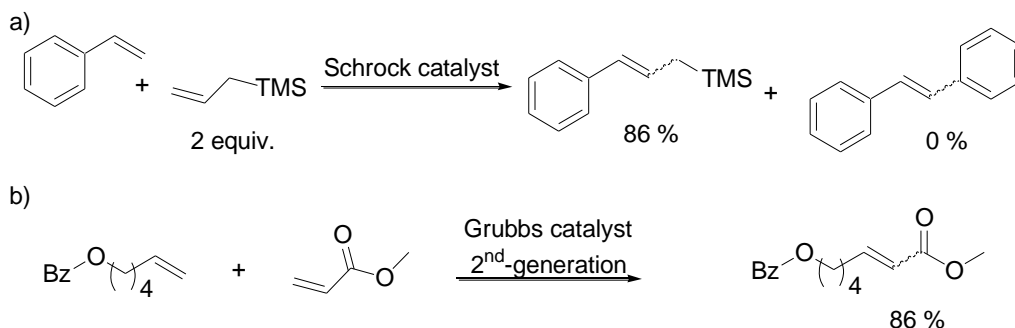
By controlling the product formation, one can avoid using a large excess of one reaction partner and by this reduce the catalyst loadings. Chatterjee and Grubbs⁸² have presented a model for the selectivity in cross metathesis, dividing substrates into four groups regarding their ability to homo-dimerize and to participate in the cross metathesis. Grubbs et al.⁸² classified olefins as follows: type I (fast homo-dimerization), type II (slow homo-dimerization), type III (no homo-dimerization) and type IV (not reactive in cross metathesis), (Table 1.1).

Table 1.1. Model for selectivity in cross metathesis by Chatterjee and Grubbs with a selection of substrates. For full table please refer to [⁸²], Table adapted from [⁸²].

Olefin type	Grubbs catalyst 1 st -generation	Grubbs catalyst 2 nd -generation	Schrock catalyst OR = OC(CF ₃) ₂ CH ₃
Type I (fast homodimerization)	terminal olefins, allyl silanes, allyl halides	terminal olefins, allyl silanes, styrene, allyl halides	terminal olefins, allyl silanes
Type II (slow homodimerization)	styrene	acrylates, acrylamides, perfluorinated alkane olefins, vinyl ketones	styrene, allyl stannanes
Type III (no homodimerization)	vinyl siloxanes	1,1-disubstituted olefins, phenyl vinyl sulfone	acrylonitrile
Type IV (not reactive)	1,1-disubstituted olefins, perfluorinated alkane olefins	vinyl nitro olefins	1,1-disubstituted olefins

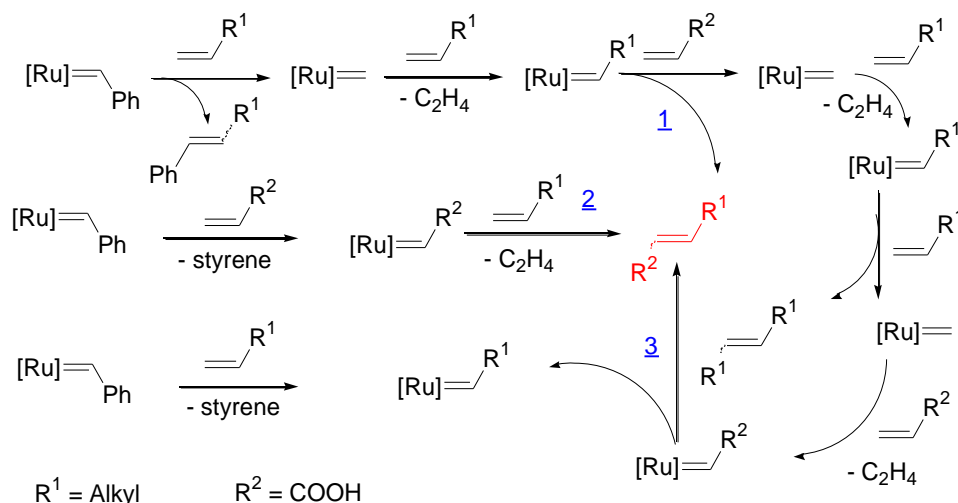
As catalytic systems, Grubbs catalyst 1st and 2nd-generation as well as a Schrock molybdenum catalyst were investigated. Despite the fact that the Schrock molybdenum catalyst displays the lowest tolerance of functional groups, it allows the cross metathesis with acrylonitrile and allyl stannanes in contrast to the tested ruthenium catalysts. When comparing the two ruthenium catalysts, Grubbs catalyst 2nd-generation exhibits a higher reactivity and functional group tolerance than their 1st-generation analogue. With increased activity of Grubbs catalyst 2nd-generation, it is possible to use strong electron deficient olefins and sterically demanding 1,1-disubstituted olefins for cross metathesis reactions. Terminal olefins (type I olefin) for example display a fast homo dimerization with Grubbs catalyst 2nd-generation, whereas 1,1-disubstituted

olefins do not homo dimerize at all with this catalyst. For Grubbs catalyst 2nd-generation, olefins of the type II and III include e.g. 1,1-disubstituted olefins, styrenes with a large *ortho* substituent or olefins with alkyl substituent on the allylic carbon.⁸² Therefore, an approach to avoid homo-dimerization and thus to control the product distribution is to increase the steric hindrance at the carbon-carbon double bond or in the allylic position. A second way to suppress or at least to reduce the homo-dimerization of an olefin is to reduce the electron density at the double bond. Type II olefins for Grubbs catalyst 2nd-generation which match this requirement are e.g. perfluorinated olefins, vinyl ketones, acrylates or acrylamide.⁸² Thus, sterically hindered olefins like styrene (Scheme 1.7a) or electron deficient olefins like methylacrylate (Scheme 1.7b) will preferentially react with a second olefin in the catalytic cycle and favor the formation of the cross metathesis product.



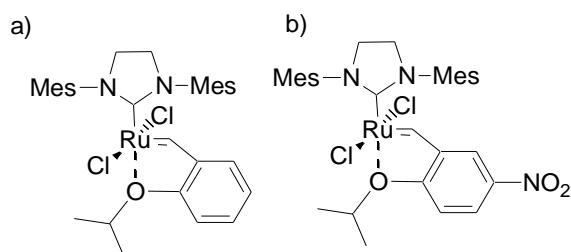
Scheme 1.7. Cross metathesis of a) styrene with allyltrimethylsilane,⁸³ b) Benzyl hexenyl ether with methylacrylate.⁸⁴

The catalytic cycle of a cross metathesis is depicted in Scheme 1.8. Nonproductive reaction steps are omitted because in this case product and educt side are identical. As it can be seen in Scheme 1.8, three alkylidene structures participate in the catalytic cycle ($[\text{Ru}]=\text{CHR}^1$, $[\text{Ru}]=\text{CHR}^2$ and $[\text{Ru}]=\text{CH}_2$). In contrast to the electron deficient olefin $\text{CH}_2=\text{CHR}^2$ ($\text{R}^2 = \text{COOH}$), the terminal olefin $\text{CH}_2=\text{CHR}^1$ ($\text{R}^1 = \text{alkyl}$) dimerizes fast. The formed dimer however is reactive in cross metathesis. The desired cross metathesis product is then formed over three pathways by the reaction of: 1) $[\text{Ru}]=\text{CHR}^1$ with $\text{CH}_2=\text{CHR}^2$, 2) $[\text{Ru}]=\text{CHR}^2$ with $\text{CH}_2=\text{CHR}^1$ and 3) $[\text{Ru}]=\text{CHR}^2$ with $\text{R}^1\text{CH}=\text{CHR}^1$.



Scheme 1.8. Catalytic cycle for the cross metathesis of a terminal olefin e.g. 1-butene with an electron deficient olefin (acrylic acid), non-productive reaction steps are omitted, blue underlined numbers: pathways to desired cross metathesis product.

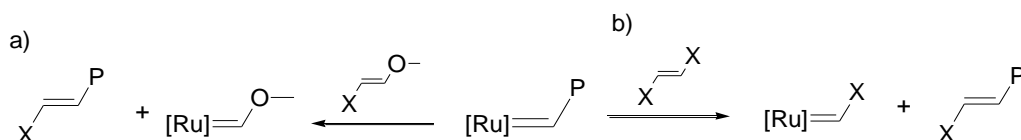
A further increase in the activity and selectivity of ruthenium catalysts in cross metathesis or ring closing metathesis was achieved by the development of Grubbs catalysts with chelating *o*-alkoxy-benzylidene ligands by Hoveyda⁸⁵⁻⁸⁷ and Blechert⁸⁸⁻⁹¹ (Scheme 1.9a).



Scheme 1.9. Chemical structure for a) Grubbs-Hoveyda catalyst (simultaneously developed by Hoveyda⁸⁷ and Blechert⁹² work group), b) Nitro-Grela catalyst.⁹³

The chelating *o*-alkoxy-benzylidene ligand stabilizes the catalyst and allows more reaction cycles. This type of catalysts showed improved activity towards electron deficient olefins and was able to catalyze cross metathesis reactions with acrylonitrile or olefins with perfluorinated substituents in high yields. Grela et al. reported on the modification of the *o*-isopropoxy benzylidene ligand e.g. by the introduction of a nitro-group, thereby improving the catalyst's performance (Scheme 1.9b).⁹³ Grubbs catalysts of the third generation have shown similar

activities to the *o*-alkoxy-benzylidene catalysts and allowed in contrast to Grubbs catalyst 2nd-generation the cross metathesis of acrylonitrile.⁹⁴ The fast initiation behavior of these 3rd-generation catalysts and the high activity makes them not only suitable for cross metathesis and thereby end functionalization but also for ring opening metathesis polymerization. For the end functionalization of polymers, the living chain end and the quencher react in a cross metathesis step. Therefore, the reaction should generate just one set of products. This can be achieved e.g. by reacting the living chain end with enol ethers,⁹⁵⁻¹⁰¹ trapping the ruthenium carbene irreversible (Scheme 1.10a) or by reacting with symmetric quenching agents¹² (Scheme 1.10b). In case of symmetric olefins, the cleaved catalyst as well as the polymer carries the same functional group. The following chapter describes the different methodologies and strategies for the end functionalization of ROMP polymers.

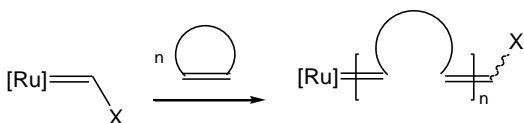


Scheme 1.10. Reaction of the living chain end with a) enol ethers, b) symmetric olefins.

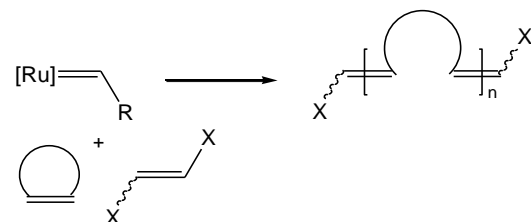
1.5. End functionalization of ROMP-polymers

Living polymerization reactions open the way for the preparation of defined molecular architectures. The introduction of an end group via ROMP can be performed in different ways including the reaction of the living chain end with terminating agents,^{98,102-104} the usage of functionalized catalysts, sacrificial synthesis or chain transfer agents.¹⁰⁵ Scheme 1.11 comprises the different methodologies used for the end functionalization of ROMP-polymers using ruthenium catalysts. For Schrock molybdenum catalysts, the end functionalization of polymers is usually done by using functionalized aldehydes, which react with the molybdenum carbene in a Wittig-type reaction.¹⁰⁶

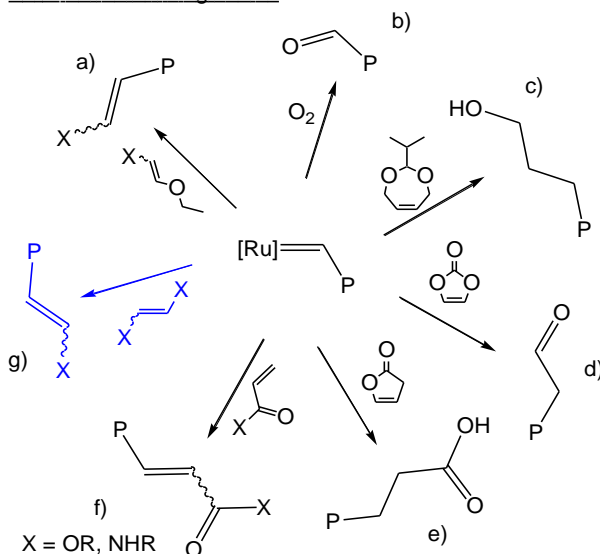
Functionalized catalysts



Telechelic polymers by chain transfer agents



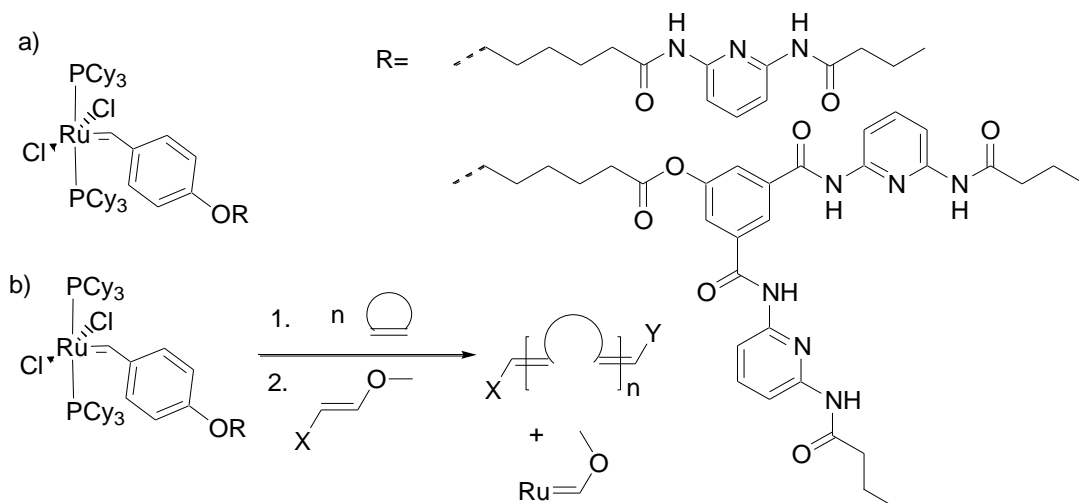
Termination of living chains



Scheme 1.11. End functionalization of ROMP-polymers by using functionalized catalysts, chain transfer agents or termination of the living chains with a) enol ethers, b) molecular oxygen, c) “Sacrificial synthesis”, d) vinylene carbonate, e) 3H-furanone, f) acrylates, acrylamides, g) symmetric olefins.

1.5.1. Functionalized catalysts

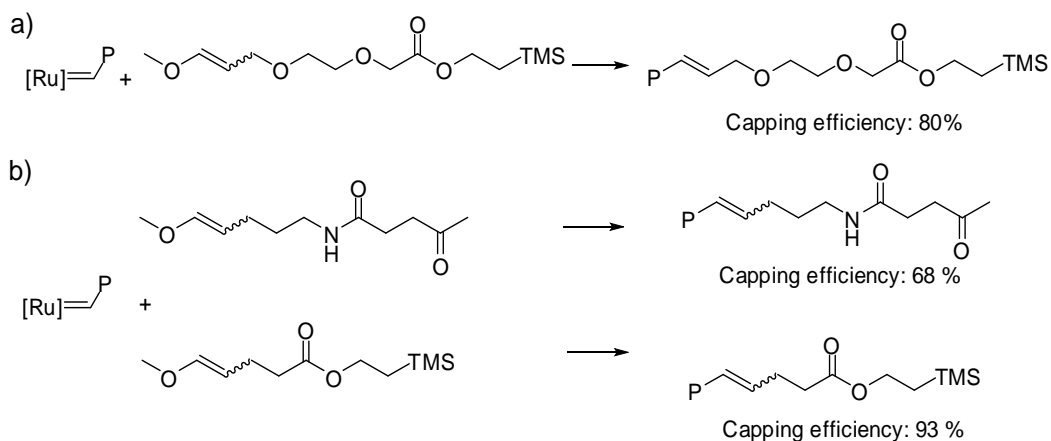
End functionalized polymers can be prepared by using modified metathesis catalysts, since the alkylidene moiety is transferred in the initiation step to the polymer chain. By modifying the alkylidene moiety it is possible to introduce a functional group in the polymer chain. Weck et al.¹⁰¹ prepared 1st-generation Grubbs catalysts bearing 2,6-diamidopyridine or the Hamilton receptor by reacting Grubbs catalyst 1st-generation with the corresponding functionalized styrene (Scheme 1.12). By quenching with functional enol ethers, (see chapter 1.5.2.) hetero telechelic poly(norbornene)s were prepared (M_n : 7000-9000 g/mol, PDI 1.4-1.7), which bear in contrast to homo telechelic polymers two different end groups. Although, functionalized catalysts represent an elegant way to introduce functional moieties, it requires much synthetic effort to prepare these catalysts. Often, purification of the air and moisture sensitive compounds via column chromatography is required, which is not without complication.



Scheme 1.12. Functionalized Grubbs catalysts 1st-generation, a) diimidopyridine, Hamilton receptor, b) synthesis of hetero telechelic polymers.

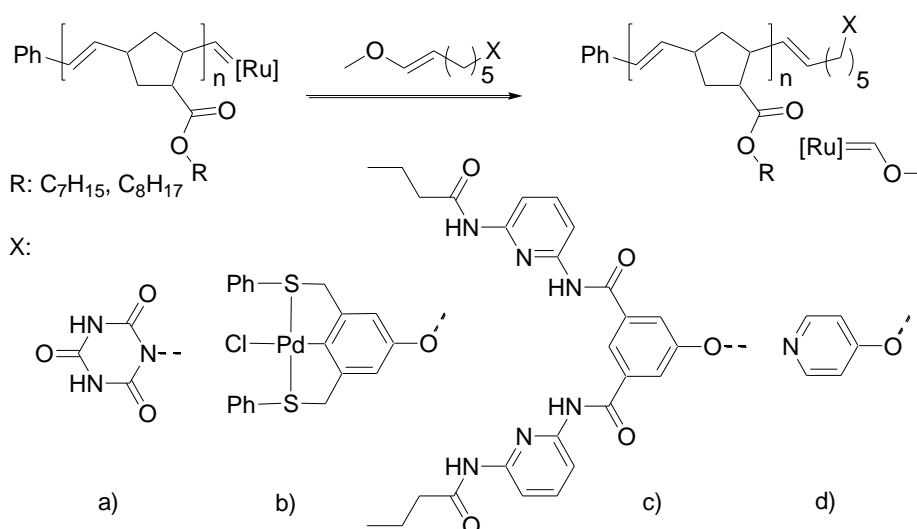
1.5.2. Quenching with enol ethers

The well-known reaction of the ruthenium carbene with ethyl vinyl ether yields the ruthenium trapped irreversibly in a Fischer-carbene complex and the methylene terminated carbene moiety. If the methylenide-moiety of the enol ether is replaced by functional moieties, it is possible to introduce end groups on the polymer chain^{10,11,95-97,99-101,107} (Scheme 1.13).



Scheme 1.13. Functionalized poly(norbornene)s by quenching with enol ethers: a) reaction conditions 15 equiv. terminating agent, 6-18 h, $[M]/[C] = 15$, Grubbs catalyst 1st-generation, results by Gordon et al.⁹⁶, b) 15 equiv., 3 h, $[M]/[C] = 50$, Grubbs catalyst 1st-generation, results by Owen et al.⁹⁹

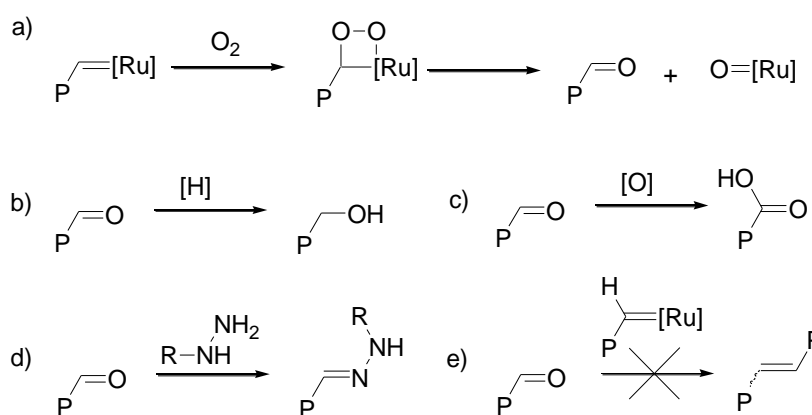
Gordon et al. described the quenching of poly(norbornene carboxylic acid methylester) with a TMS protected enol ether (15 equiv.) in an efficiency of 80 % (Scheme 1.13a).⁹⁶ Owen et al. reported on the quenching of the same polymer with enol ethers carrying e.g. amide, ester or urethane groups.⁹⁹ Efficiencies of 64 to 95 % were reported, with the lower efficiencies for the amide containing quenchers (Scheme 1.13b). Weck et al.^{10,11,100,101} used functionalized enol ethers (20 equiv.) to introduce pyridine, cyanurate and “palladated sulfur-carbon-sulfur pincer complex” end groups into norbornene-polymers (M_n : 7000-9000 g/mol, PDI 1.4-1.7), (Scheme 1.14). The bulky Hamilton receptor could also be successfully attached to poly(norbornene)s by using the same strategy.¹⁰ Near quantitative incorporation of the functional groups was reported, according to the disappearance of the propagating carbene in the ^1H NMR. In summary one can say that functional groups can be introduced by this method in efficiencies of 64 to 95 %, dependent on the functional moiety attached. A huge excess of the terminating agent is applied in the quenching process, although the reaction of the enol ether with the living polymer chain is favored by the formation of a Fischer carbene complex. The preparation of the enol ethers requires multistep synthetic procedures with often moderate yields and the formed terminating agents can dispose e.g. by acidic hydrolysis.



Scheme 1.14. End functionalized polymers by quenching with functionalized enol ethers, functional moieties a) cyanurate, b) “palladated sulfur-carbon-sulfur pincer complex”, c) Hamilton receptor, d) pyridine.

1.5.3. Quenching with molecular oxygen

In general, oxygen is to be avoided during ROMP to ensure a controlled polymerization; however, it can be used as terminating agent. The conversion of living poly(norbornene) chains into aldehyde-capped polymers (M_n : 13000-35000 g/mol, PDI 1.1-1.5), via bubbling oxygen through the reaction solution for 24 h, was described by Gibson et al.⁵⁴ The aldehyde end group can be further transformed into a primary alcohol or a carboxylic acid by reduction or oxidation respectively (Scheme 1.15a-c). Buchmeiser et al. reported on the functionalization of linear and cross-linked poly(norbornene)s with molecular oxygen using different metathesis catalysts (Grubbs catalyst 1st-, 2nd- and 3rd-generation).¹⁰⁸ Grubbs catalyst 1st-generation displayed the lowest stability against oxygen and therefore was best suited for the preparation of aldehyde capped polymers. The fraction of aldehyde end groups is 80%, 47% and 29% for polymers prepared with Grubbs catalyst 1st-, 2nd- and 3rd-generation respectively.

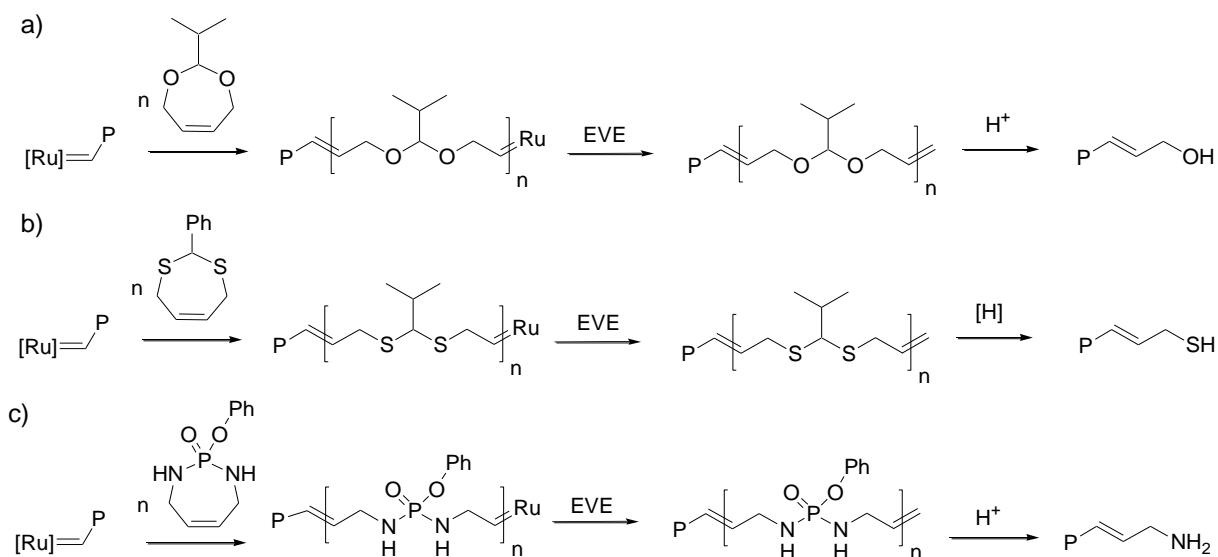


Scheme 1.15. a) Reaction of living chains (P: polymer) with molecular oxygen yielding aldehyde-end groups, b) reduction, c) oxidation, d) reaction with hydrazines, e) bimolecular coupling.

The aldehyde capped polymers were subsequently reacted with 2,4-dinitrophenylhydrazine or tetraethylenepentamine. Unlike their molybdenum analogues, the ruthenium carbene complexes show a low tendency to react with aldehydes. Thus, no significant bimolecular coupling is expected (Scheme 1.15e). A drawback of this method is the limitation to Grubbs catalysts of the 1st-generation.

1.5.4. Sacrificial synthesis

Kilbinger et al.¹⁰⁹ used the degradation of a block copolymer to introduce hydroxy, thiol and amine end groups onto poly(norbornene dicarboxyimide)s. For the introduction of hydroxy groups, the living polymer-chains, prepared with Grubbs catalyst 1st-generation, are reacted for 15 h with 20 to 25 equiv. of a dioxepine-monomer with respect to the ruthenium catalyst (Scheme 1.16). The living copolymer-species is then quenched with ethyl vinyl ether to generate the vinyl terminated polymer. The block consisting of dioxepine units is then degraded via acidic ether cleavage to form hydroxy-terminated poly(norbornene dicarboxyimide) (M_n 2000-5000 g/mol, PDI 1.1) which can be used for the esterification e.g. with propiolic acid. Hydroxy-telechelic poly(norbornene dicarboxyimide)s can be obtained by preparing ABA (A: dioxepine; B: norbornene dicarboxyimide) block copolymers (M_n : 2000-20000 g/mol, PDI 1.2-1.3). Thiol-end groups were introduced over the same pathway by reacting 40 equiv. of a thioacetal instead of dioxepine as 2nd monomer⁴⁹ with the poly(norbornene dicarboxyimide)s for 4 h (Scheme 1.16). Thiol-terminated polymers were prepared with Grubbs catalyst 3rd-generation in the molecular weight range from 7000 to 33000 g/mol with a PDI of 1.1-1.3.



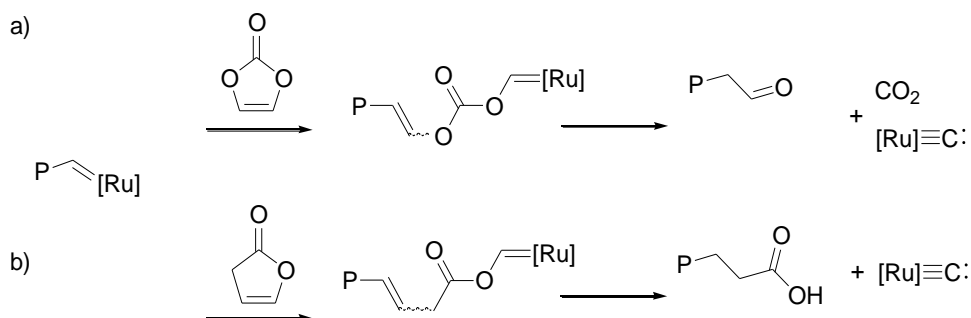
[H]: Raney Nickel / H₂ EVE: ethyl vinyl ether

Scheme 1.16. Sacrificial synthesis for the introduction of a) hydroxy, b) thiol and c) amine end groups, P: poly(norbornene dicarboxyimide).

The introduction of an amine end groups at the chain end was achieved by using a diazophosphepinoxide as second monomer.⁵² After termination with ethyl vinyl ether, the amine terminated polymer (M_n : 4000 g/mol, PDI: 1.2-1.3) is obtained by degradation of the second block using hydrochloric acid/acetone (Scheme 1.16). Grubbs catalyst 1st and 3rd-generation were applied as catalysts.

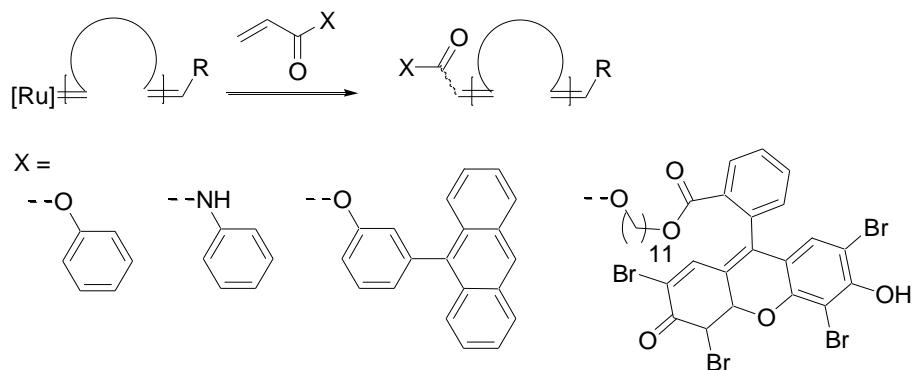
1.5.5. Quenching with vinylene carbonate/ 3H-furanone

Hilf and Kilbinger published another route to end group functionalized polymers by quenching poly(norbornene dicarboxyimide) chains with vinyl lactones⁴⁶, giving aldehyde or carboxylic acid terminated polymers (Scheme 1.17). Vinylene carbonate (50 equiv. with respect to the ruthenium catalyst) gives aldehyde-terminated polymers, 3H-furanone (20 equiv. with respect to the ruthenium catalyst) carboxylic acid-terminated polymers. The ruthenium catalyst is reduced in the process to a deactivated carbide-structure. A significant color-change of the solution to yellow indicates the completeness of the reaction. Polymers in the molecular weight range from 5000 to 15000 g/mol were prepared with PDI 1.1-1.3. In conclusion, "Sacrificial synthesis" and lactone quenching can be used to introduce simple functional moieties in a single reaction step. Subsequent reactions are then necessary to build up more complex molecular architectures.



Scheme 1.17. Aldehyde- and carboxyl-terminated poly(norbornene dicarboxylic imide)s via quenching with a) vinylene carbonate, b) 3H-furanone.

1.5.6. Quenching with acrylates/acrylamides



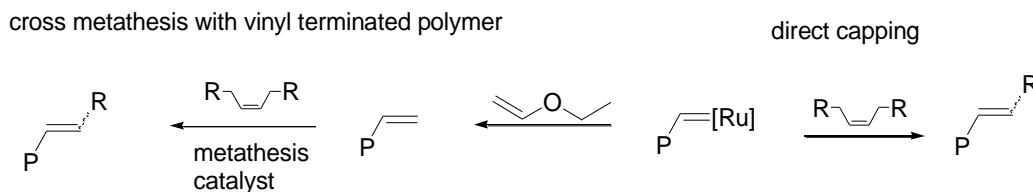
Scheme 1.18. Acrylates and acrylamides acting as termination agents.

Slugovc et al. used acrylates and acrylamides, carrying phenyl, anthracene and eosine moieties, for the termination of living poly(norbornene dicarboxylic diester)s.¹¹⁰ The living chains (M_n 2000-3500 g/mol, PDI 1.1), prepared with Grubbs catalyst 3rd-generation, were terminated with 2 equiv. of acrylate or acrylamide based quencher (Scheme 1.18). After final quenching with ethyl vinyl ether, a mixture of methylene terminated and functionalized polymer was obtained. End group efficiencies of 50 to 80 %, as judged from the intensities of the different species in the MALDI mass spectra, were reported.¹¹⁰ The occurrence of two species is caused by the asymmetry of the quencher which will either transfer the ester (amide) moiety or the methylene moiety onto the polymer. Secondary metathesis was observed when the amount of used acrylate or acrylamide was increased from 2 to 6 equiv., leading to fractions of telechelic polymers.¹¹⁰

1.5.7. Quenching with symmetric olefins

Symmetric olefins represent another class of terminating agents, which can be used to prepare end functionalized polymers (Scheme 1.19). This method is based on the cross metathesis of the living chain end with the symmetric olefin. Grubbs et al. reported on the direct end capping of poly(oxo-norbornene dicarboxyimide)s and poly(norbornene dicarboxyimide)s with symmetric *cis*-olefins.^{12,111} For the direct end capping, 5 equiv. of the symmetric olefin and reaction times of

approx. 6 h were applied to quench the polymer chains, giving in the most cases efficiencies for the end group introduction of 90 % and more (Table 1.2).



Scheme 1.19. Direct capping of living chains and cross metathesis of a methylene terminated polymer with *cis*-olefins, P: polymer.

Table 1.2. Results of the direct capping of living polymer chains with *cis*-olefins, initiated with Grubbs catalyst 3rd-generation or the cross metathesis of vinyl-terminated polymers with *cis*-olefins catalyzed with Grubbs-Hoveyda catalyst 2nd-generation, direct capping with 5 equiv. of symmetric olefin, cross metathesis (50 mol% catalyst), 5 equiv. of symmetric olefin, efficiency calculated from ¹H-NMR-spectroscopy, Table adapted from citation [12].

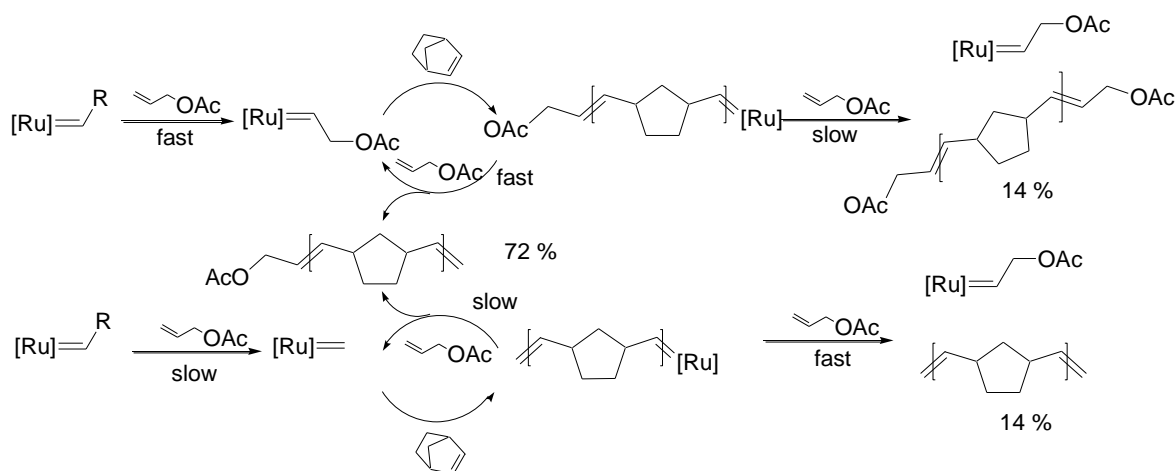
R =	% efficiency by direct capping	% efficiency by cross metathesis
OAc	97	89
OC(O)C(CH ₃) ₂ Br	> 98	> 90
CH ₂ C(O)H	59	36
CH ₂ C(O)NHS	80	44
CH ₂ CH ₂ OH	97	60
CH ₂ CH ₂ Br	> 98	> 90
CH ₂ CH ₂ SAc	91	70
Boc	> 98	> 90
Biotin	93	69
FITC	> 98	40

Additionally, Grubbs et al. investigated the cross metathesis of a methylene-terminated polymer with *cis*-olefins.¹² This reaction showed efficiencies of 40 to 90% (Table 1.2) for the end group introduction depending on the moieties pendant to the *cis*-olefin. The results for the reactions with Grubbs catalyst 3rd-generation (pyridine-ligands) are shown in Table 1.2. In all cases the direct end capping approach gives better results than the cross metathesis of the vinyl

terminated polymer. A deactivation of the catalyst was observed in both methods when a *cis*-olefin carrying azide moieties was used as terminating agent. Madkour et al. reported on the quenching of poly(oxo-norbornene)s ($M_n = 4000$ g/mol, PDI = 1.1) with symmetric olefins carrying pentafluorophenol groups.⁵⁵ The quenchers are based on *cis*-1,4-bis-hydroxy-2-butene. By using 10 equiv. of the symmetric olefin a complete end functionalization was achieved, according to MALDI MS. Grubbs catalyst 3rd-generation was applied for the polymerization. Direct capping of living polymer chains with symmetric olefins represents a simple approach which can introduce complex functional moieties in a single reaction step. The direct capping is to be preferred against the post functionalization approach (cross metathesis of a vinyl terminated with symmetric olefins) due to the better efficiencies.

1.5.8. Telechelic polymers via chain transfer agents

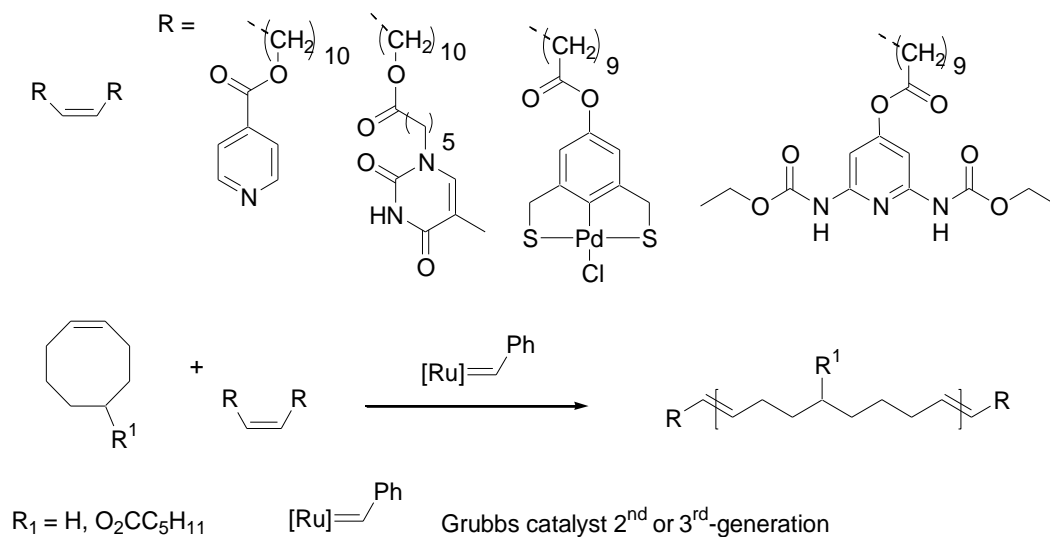
Instead of being applied at the end of the polymerization reaction, termination agents (enol ethers, asymmetric and symmetric olefins) can be used as chain transfer agents (CTA).^{105,112-114} Bielawski and Grubbs¹⁰⁵ reported on the synthesis of mono and bis-hydroxy telechelic poly(norbornene)s (M_n : 1500-8600 g/mol, PDI 1.7-2.1). If allylacetate was applied as CTA, three products are formed (Scheme 1.20).



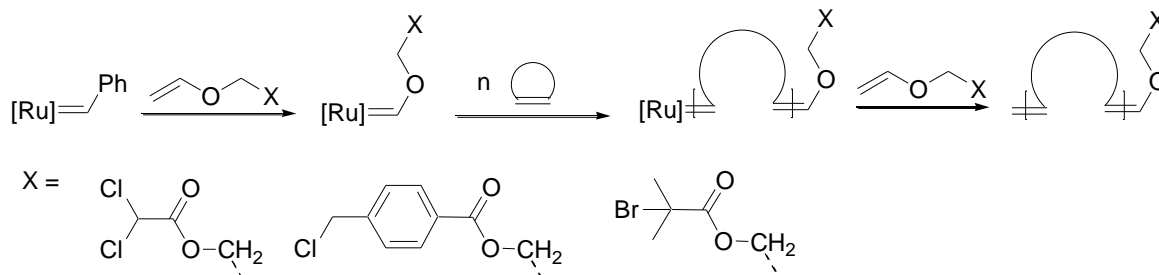
Scheme 1.20. Allylacetate as CTA in the synthesis of acetoxy-functionalized poly(norbornene), Scheme adapted from [104].

The major product is the mono-acetoxy-terminated poly(norbornene); minor products are the vinyl-telechelic- and the acetoxy-telechelic poly(norbornene) (Scheme 1.20). The reaction of the catalyst with the asymmetric quenching agent allylacetate generates two ruthenium alkylidenes,

the acetoxyethylidene complex ($\text{Ru}=\text{CHCH}_2\text{OAc}$) and the methylidene ($[\text{Ru}]=\text{CH}_2$) substituted complex. Based on the final product distribution, it is proposed that the acetoxyethylidene complex is generated faster than the methylidene complex. The growing chain is then terminated by allylacetate, generating methylene and acetoxy end groups at the polymer. Subsequently, new polymer chains are started by the cleaved off metal alkylidenes. Pure acetoxy telechelic poly(norbornene) can be prepared by using a symmetric chain transfer agent (*cis*-1,4-bisacetoxy-2-butene).¹⁰⁵ Weck et al.¹¹² prepared telechelic polymers from cyclooctene with CTAs bearing thymine and palladated sulfur carbon sulfur-ligands (M_n : 1000-12000 g/mol, PDI: 1.1-2.8) (Scheme 1.21).



Scheme 1.21. Symmetric chain transfer agents and the synthesis of telechelic poly(cyclooctene)s [¹¹²].

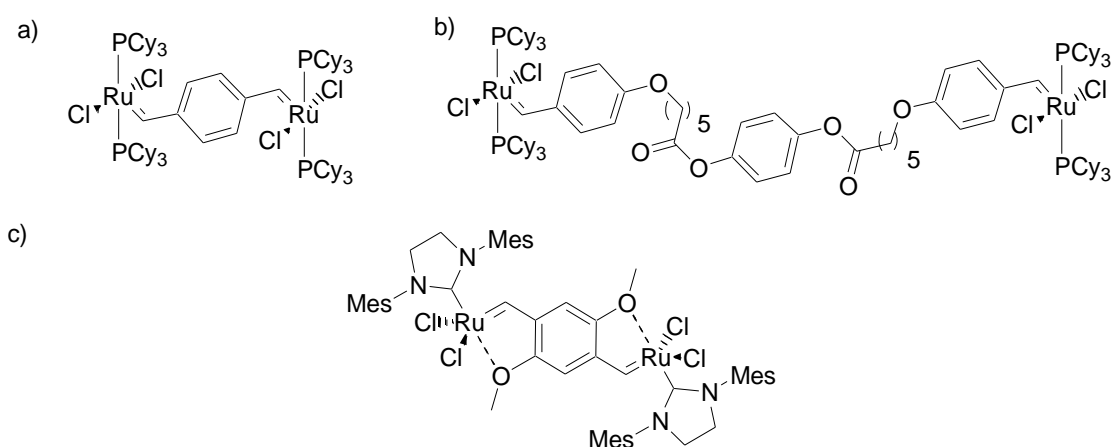


Scheme 1.22. Enol ethers acting as CTAs.

Katayama et al.⁹⁸ polymerized norbornene in the presence of functionalized enol ethers, acting as chain transfer agents to yield semi-telechelic polymers (M_n : 3000-10000 g/mol, PDI: 2.0-3.2) (Scheme 1.22). The formed polymers were used as macroinitiators for the ATRP of styrene. The use of chain transfer agents has the main disadvantage that the generated polymers display relatively high polydispersities (PDI \sim 2.0). The reactivity of the monomer and the chain transfer agent towards the catalyst has to be in a certain range to achieve a controlled molecular weight. Thus, the range of monomers is often limited to norbornene, cyclooctene or cyclooctadiene.

1.5.9. Telechelic polymers via bimetallic catalysts

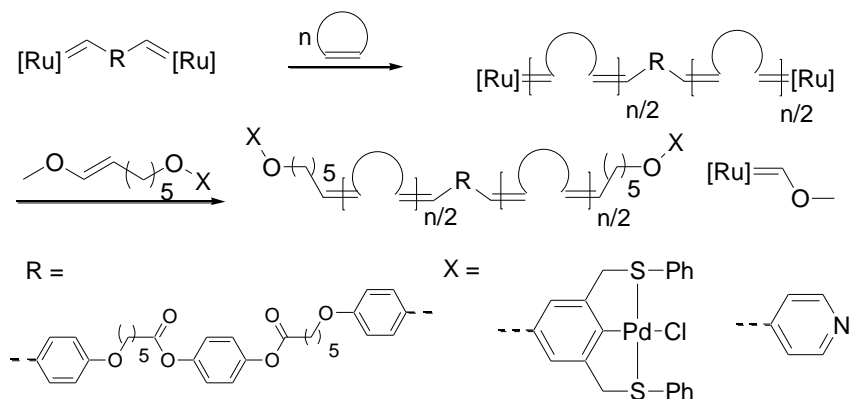
Another route to telechelic polymers can be bimetallic metathesis catalysts. This class of catalysts exhibits two reactive sites.^{8,100,115} Thus, each metal atom builds up a metal alkylidene bond, which enables the propagation and thus the termination on two reactive sites. Therefore, these catalysts are suitable for the preparation of triblock copolymers or telechelic polymers.



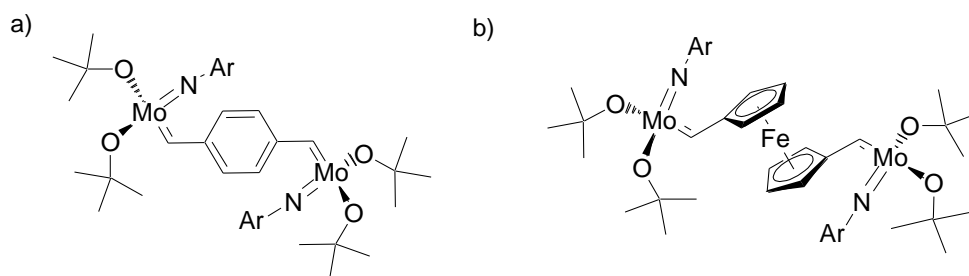
Scheme 1.23. Bivalent metathesis catalysts based on ruthenium [^{8,100,115}].

The termination of the growing chains can be conducted by one of the previously discussed methods (e.g. quenching with enol ethers, symmetric olefins or lactones). Two bimetallic ruthenium catalysts were reported by Weck et al. (Scheme 1.23a-b).^{8,100} These bivalent catalysts were applied for the synthesis of triblock copolymers of norbornenes and oxo-norbornenes⁸ as well as the synthesis of homo-telechelic poly(norbornene)s (M_n : 13000-96000 g/mol, PDI 1.2-

1.6) bearing hydrogen bonding donor and acceptor moieties (Scheme 1.24).¹⁰⁰ Grudzien et al. reported on a bivalent Grubbs-Hoveyda catalyst 2nd-generation and its application in ring closing metathesis (Scheme 1.23c).¹¹⁵

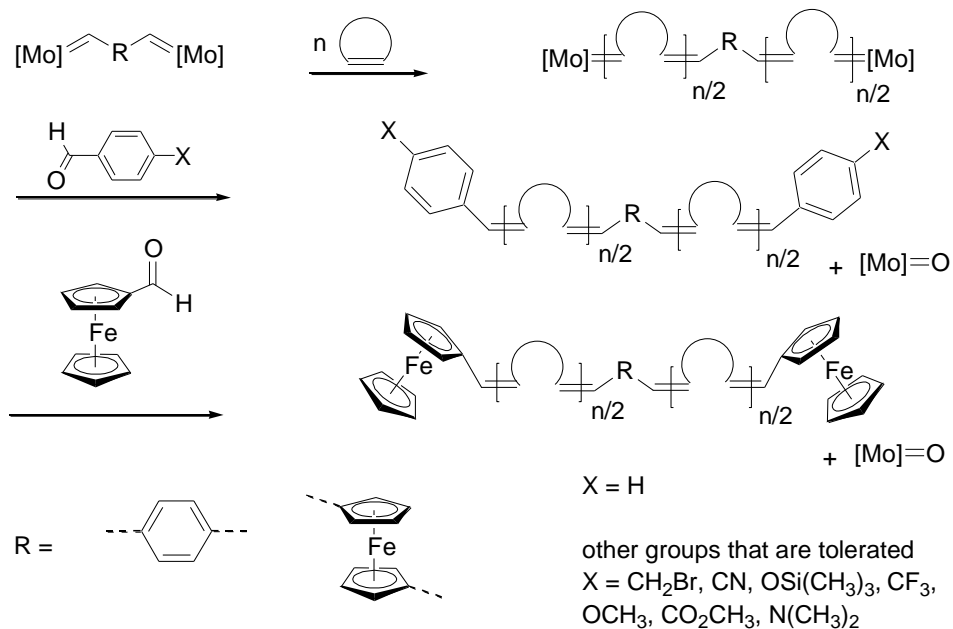


Scheme 1.24. Telechelic polymers by a bivalent ruthenium catalyst.¹⁰⁰



Scheme 1.25. Bivalent metathesis catalysts based on molybdenum.^{43,116}

Besides the mentioned ruthenium carbenes, bivalent catalysts based on molybdenum were reported in literature. Schrock et al. synthesized bivalent molybdenum catalysts⁴³ (Scheme 1.25a-b) via cross metathesis by reacting Schrock molybdenum catalysts with 1,4-divinylbenzene or 1,4-divinylferrocene. The catalyst prepared with 1,4-divinylferrocene was applied for the synthesis of triblock copolymers of norbornenes with liquid crystalline properties.¹¹⁶ Quenching was done with benzaldehyde or ferrocenecarboxaldehyde (Scheme 1.26).

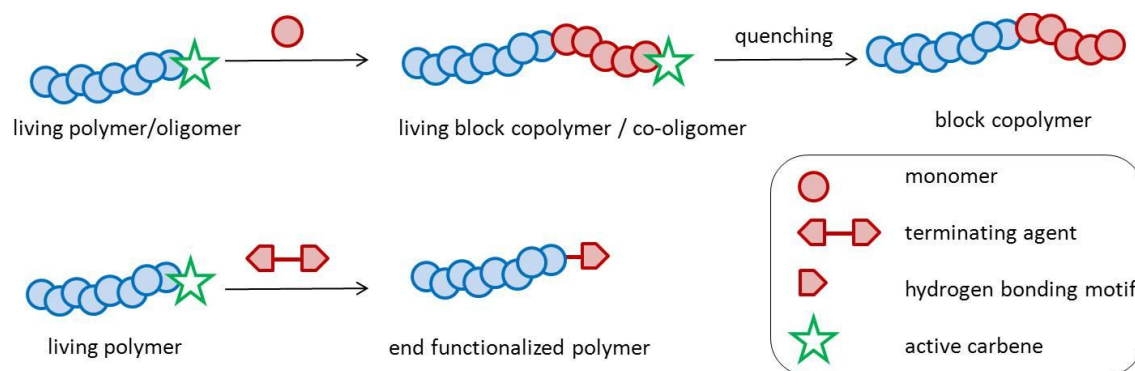


Scheme 1.26. Telechelic polymers by a bivalent molybdenum catalyst.

From literature it is also known that functionalized benzaldehydes, carrying e.g. bromomethyl, cyano, trimethylsiloxy or trifluoromethyl groups, are tolerated by the molybdenum carbenes.¹⁰⁶ Similar to the functionalized catalysts mentioned before, the synthesis of bimetallic catalysts is not without efforts and requires manipulation and purification of highly sensitive metal complexes, leading often to moderate yields.

1.6 Aims

This thesis aims to investigate and understand the crossover reaction in ROMP block copolymerization reactions and termination reactions of ROMP-polymers, as in both processes the underlying crossover reaction is crucial for the success of the reaction (Scheme 1.27). Furthermore, the monitoring of ROMP-processes via soft ionization mass spectrometry should be explored, further demonstrated via the synthesis of ROMP-polymers with hydrogen bonding motives at the chain end.



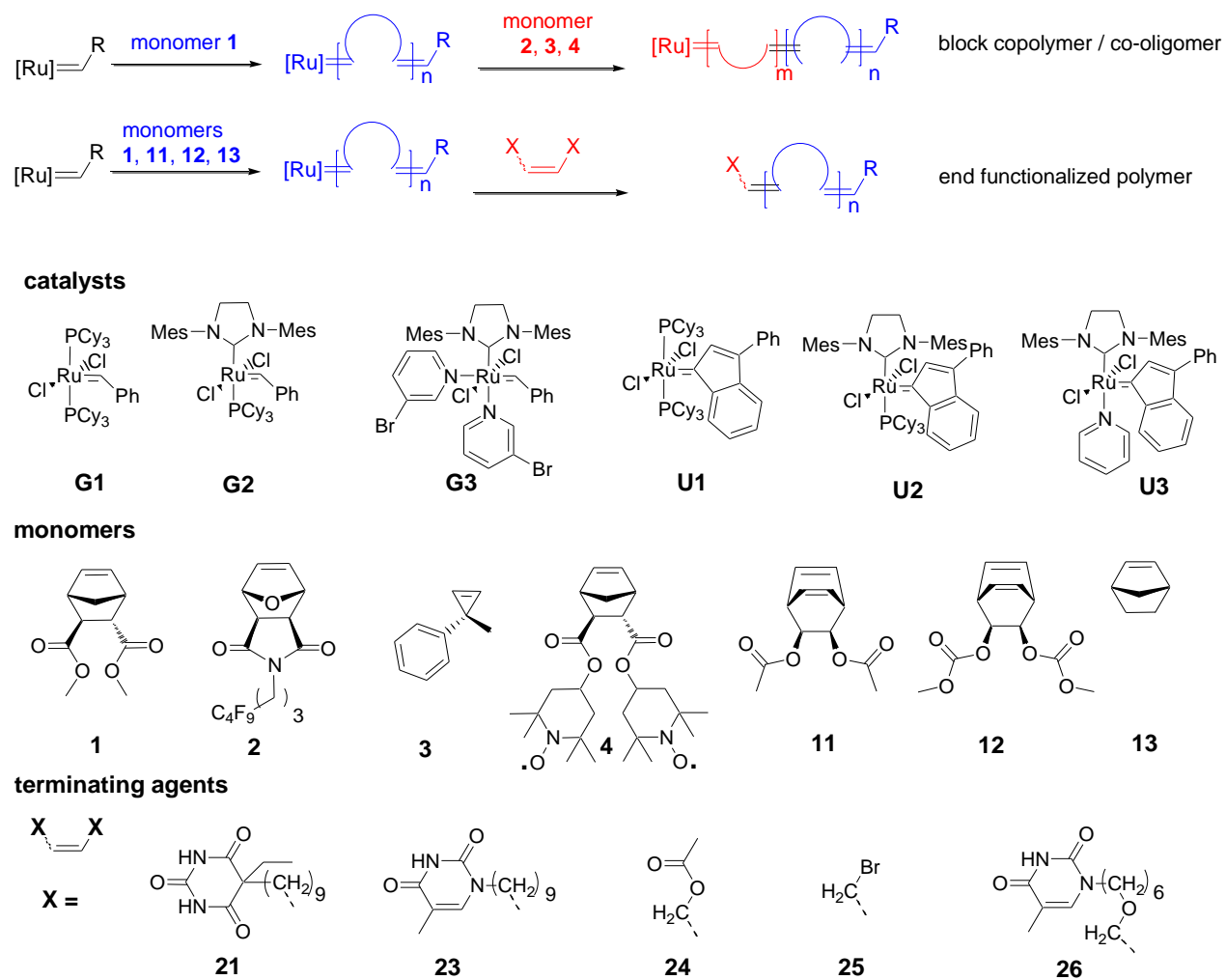
Scheme 1.27. Crossover reactions in ROMP block copolymerization and termination reactions.

In order to accomplish this task, living polymer chains should be either reacted with a second monomer in a stepwise approach or with a terminating agent. In consequence, the living polymer chains are converted into a block copolymer or an end functionalized polymer. A deeper insight into the cross over reaction should then be achieved by varying the reaction parameters involved (monomers, catalysts and termination agents) in the process. To gain further information, the kinetics of the polymerization and the crossover step has to be investigated. For the analysis of crossover reactions and the block copolymers, NMR, GPC and MALDI-TOF MS should be applied thus enabling a comparison of monomer and catalyst reactivities. In order to detect reactive species in the process, living oligomer and co-oligomer species should be synthesized and directly analyzed by ESI-TOF MS. The termination reactions are to be investigated with respect to their efficiency and the reaction conditions used.

2. Results and Discussion

2.1. Concept

The aim of this thesis concerns the investigation of the crossover step in ROMP block copolymerization reactions and termination reactions. An insight into this reaction step was thereby achieved by varying the catalysts, monomers and terminating agents (Scheme 2.1).



Scheme 2.1. Synthetic concept of the work.

As the cross over step is to be performed on living chains, the polymerization of the monomers **1-4** and **11-13** was studied with respect to its livingness via NMR and GPC-methods.

For the investigation of the crossover step in the block copolymerization reactions, living poly(**1**) chains were reacted with the cyclic olefins **2**, **3** or **4**. The block copolymerization kinetics were monitored by GPC and NMR-spectroscopy. As NMR-spectroscopy cannot distinguish regarding to the chain length of the copolymer species, MALDI- and ESI-TOF MS were applied to identify the individual species, which are generated in the process. MALDI-TOF MS was applied to identify the block copolymer species after quenching, while ESI-TOF MS was used to monitor living oligomer and co-oligomer species.

To study the crossover step in termination reactions, the termination with symmetric olefins was chosen as it allows the introduction of functional end groups in a single reaction step. Besides commercial available olefins, three symmetric olefins (**21**, **23** and **26**) were prepared by cross metathesis of the respective α -olefins. The functional symmetric olefins were then applied to study the influence of the pendant functional groups on the termination process by GPC, NMR and MALDI-TOF MS. The efficiency of the quenching was studied with respect to the reaction time, equivalents of terminating agent and catalyst used.

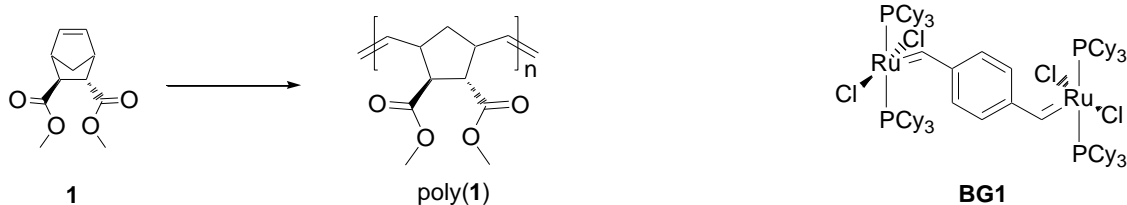
In this sense, the second part of this thesis "Results and Discussion" is divided into two sections. Section "Polymerization" (chapters 2.2. – 2.4.) focuses mainly on the actual polymerization of the different monomers and the livingness of the process. Section "Crossover reactions" (chapters 2.5. – 2.8.) comprises the investigation of the actual crossover reaction by NMR, GPC and mass spectrometric methods. A summary of the results is given in the end of the chapter "Results and Discussion". In chapters 3 and 4 the experimental procedures and the references are given respectively. The appendix with additional spectra and information follows in chapter 5.

Polymerization



2.2. Polymerization of monomer **1**

For the preparation of block copolymers as well as end group functionalized polymers a living polymerization is crucial. As test system for the investigation of the crossover step in block copolymerization- and functionalization reactions, polymers derived from monomer **1** were chosen. The polymerization of monomer **1** with the catalysts **G1**, **G3** and **U1**, **U3** was investigated with respect to its livingness (Scheme 2.2). Therefore, NMR and GPC-kinetics, M_n vs. time- and M_n vs. M/C -graphs were measured. Additionally, a bimetallic catalyst **BG1** (for synthesis see Appendix, chapter 2.2, Figures 5.4, 5.5) was applied for the polymerization of monomer **1**.



Scheme 2.2. Polymerization of monomer **1** and chemical structure of bimetallic catalyst **BG1**.

2.2.1. NMR-kinetics

NMR-kinetics on the polymerization of 5 equiv. of monomer **1** with the catalysts **G1**, **G3**, **U1** and **U3** and 50 equiv. of monomer **1** with **BG1** were conducted to obtain the brutto rate constant as well as the k_p/k_t -ratio. ^1H NMR-spectra show the disappearance of the olefinic resonances of monomer **1** at 6.26 and 6.09 ppm. Instead, new resonances which can be assigned to the olefinic protons of the polymer were observed at 5.42 and 5.20 ppm. The monomer conversion exceeded 90% for all the applied catalysts. A summary of the kinetic values is given in Table 2.1. The $\ln(M_0/M_t)$ vs. time graphs (Appendix, Figure 5.1) show linear slopes for the monomer conversion, irrespective of the catalyst used.

Table 2.1. Results of the NMR-Kinetics of monomer **1** with the catalysts **G1**, **G3**, **U1**, **U3** and **BG1**.

entry	experiment	catalyst	$[C]_0$ 10^{-2} (mol/L)	$k_p/k_i^{(1)}$	k_{br} (L/mol·s) ⁽²⁾
1	(1) ₅	G1	1.6	4.40	0.06
2	(1) ₂₀	G1	2.0	-	0.05
3	(1) ₅	G3	1.6	- ⁽⁴⁾	2.70
4	(1) ₂₀	G3	1.8	-	2.60
5	(1) ₅	U1	1.6	11.53	0.03
6	(1) ₅	U3	1.6	3.82	4.20
7	(1) ₅₀	BG1	0.2	-	0.015

(1): Ratio of propagation rate constant to initiation rate constant calculated according to Robson,¹¹⁷ (2): brutto-rate constant, (3) too fast to measure.

The brutto rate constants for the first generation catalysts **G1** and **U1** are in the same order of magnitude (Table 2.1, entries 1, 5). This is also observed for the third generation catalysts **G3** and **U3** (Table 2.1, entries 3, 6).¹¹⁸ Thereby, the third generation catalysts **G3** ($k_{br} = 2.7$ L/mol·s) and **U3** ($k_{br} = 4.2$ L/mol·s) clearly display an enhanced reactivity in comparison to their first generation analogues **G1** ($k_{br} = 0.06$ L/mol·s) and **U1** ($k_{br} = 0.03$ L/mol·s). The bivalent catalyst **BG1** displayed the lowest reactivity towards monomer **1** with a brutto rate constant of 0.015 L/mol·s. For catalysts **G1** (0.06 L/mol·s) and **G3** (2.7 L/mol·s) the k_{br} value was additionally determined from the polymerization reactions with different monomer (M) to catalyst (C) ratio (M/C = 5 and 20). The values obtained from the graphs are in good agreement, showing values of 0.06 L/mol·s (M/C = 5) and 0.05 L/mol·s (M/C = 20) for catalyst **G1**. Brutto rate constants obtained for catalyst **G3** match well with values of 2.7 L/mol·s (M/C = 5) and 2.6 L/mol·s (M/C = 20).

The initiating and propagating carbene for the different catalysts could be observed via ¹H NMR-spectroscopy (CDCl₃). Thereby it is worth to mention that the time between injection of the monomer and the first measurement was at least 35-40 s due to the instrumental setup. For **G1**, the initiating carbene appears at 20.01 ppm, while the resonance of the propagating carbene can be seen at 18.66 and 18.47 ppm. After complete monomer conversion, another carbene resonance can be seen at 19.35 and 19.16 ppm. This behavior, described by Slugovc et al.^{26,27} and Khosravi et al.,^{119,120} is observed in the ROMP of oxygen containing norbornenes. Two resting states for the propagating carbene exist in

solution; one as bisphosphine species and the other one complexed with the carbonyl group to form a six membered ring (Figure 2.1a).

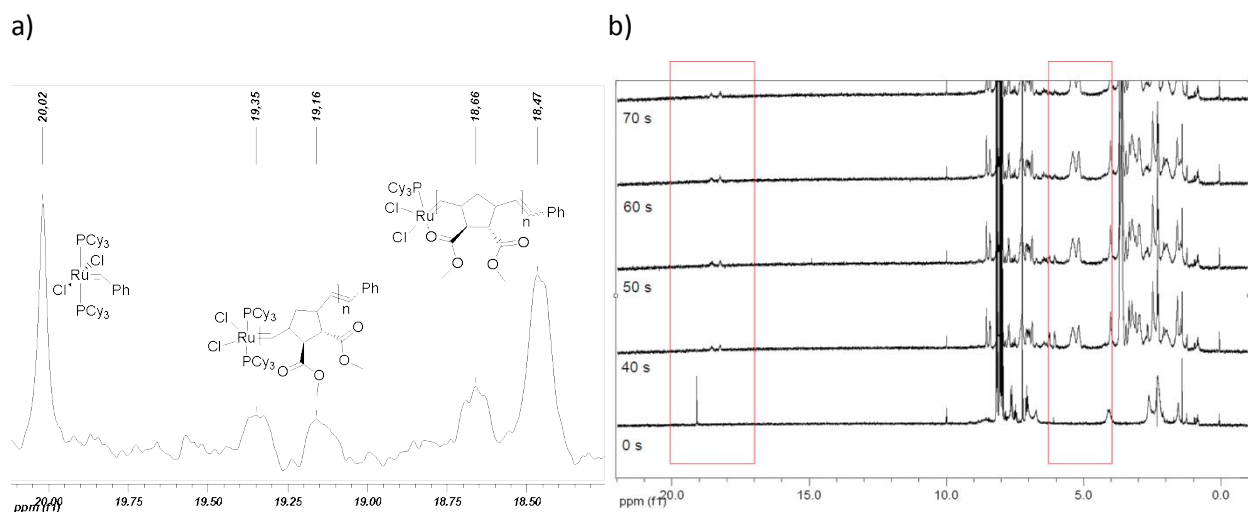
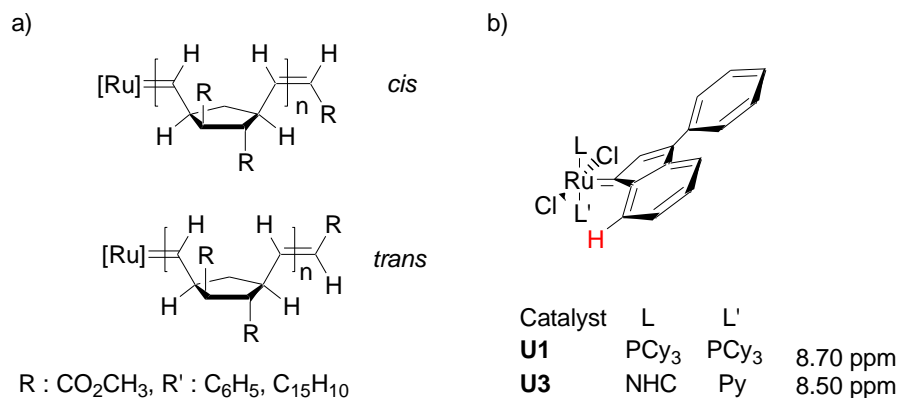


Figure 2.1. Polymerization of **1** (5 equiv.) a) with **G1**, alkydine region after complete monomer conversion, b) NMR Kinetics (5 equiv. of **1** with **G3**), highlighted: alkydine region on the left, olefinic region on the right.



Scheme 2.3. a) Ruthenium alkylidene with different configuration of the proximal backbone double bond, b) Proton used as signal for the initiating carbene for **U1** and **U3**, NHC: *N*-heterocyclic carbene, PCy₃: tricyclohexylphosphine, Py: pyridine.

For **G3**, the initiating carbene signal at 19.12 ppm is completely vanished at the first measuring point after 40 s (Figure 2.1b). Instead, the propagating carbene is observed at 18.59 and 18.27 ppm. In contrast to **G1**, a second type of propagating carbene is not observed. For catalysts **U1** and **U3** no alkydine proton for the initiating carbene can be observed due to the nature of the indenylidene

ligand, missing a proton in α -position. For tracing the initiation behavior, the doublet at 8.70 ppm (**U1**, 1H, $^3J_{\text{HH}} = 7$ Hz) and 8.50 ppm (**U3**, 1H, $^3J_{\text{HH}} = 7$ Hz) was monitored. This resonance is assigned to one of the aromatic protons of the indenylidene ligand (Scheme 2.3b). The propagating carbene for **U1** can be observed at 18.67 and 18.48 ppm. For catalyst **U3**, the resonance of the propagating carbene appears at 18.67 and 18.31 ppm. The splitting of the resonance of the propagating carbene for all the catalysts is likely to be explained by the configuration of the first backbone double bond, which can be either *cis* or *trans*. Thus, the proximal backbone creates a different chemical environment for the alkylidene proton (Scheme 2.3a). From the ratio of the initiating carbene at $t = 0$ and at the time of complete monomer conversion, the k_p/k_i ratio for the polymerization of monomer **1** with the catalysts **G1**, **G3** and **U1**, **U3** is calculated (Table 2.1). For all the applied catalysts, except **G3**, the k_p/k_i ratio is greater than 1, indicative for a slow initiation compared to the propagation. No k_p/k_i ratio could be determined for catalyst **G3**, since no initiating carbene was left at the first measuring point after 40 s. Thus, a k_p/k_i ratio < 1 is estimated for catalyst **G3**. From literature it is known that the k_i for **G3** is 6 magnitudes higher than for Grubbs catalyst 2nd-generation (**G2**).¹⁴ Also, the k_p/k_i ratio of the indenylidene-catalysts **U1** ($k_p/k_i = 11.53$) and **U3** ($k_p/k_i = 3.82$) is greater than for the benzylidene-catalysts **G1** ($k_p/k_i = 4.40$) and **G3** ($k_p/k_i = < 1$) as a result of the higher sterical hindrance created by the bulky indenylidene-ligand.

2.2.2. GPC-kinetics

Besides NMR-kinetics, the polymerization of monomer **1** was also monitored via GPC-analysis. In Figure 2.2 the development of the molecular weight with the time is depicted for the polymerization of monomer **1** ($M/C = 100$) with **G1** and ($M/C = 50$) with **G3**. For catalyst **G1**, the slope of the curve (Figure 2.2a) flattens with ongoing time, showing a dependence of the reaction rate on the monomer concentration. The same curve obtained for catalyst **G3** shows a linear slope, indicative that the reaction rate is more or less independent of the monomer concentration (Figure 2.2b). For both polymerizations, the PDI stays in the range of 1.1. No broadening of the polydispersity during the monitored time is observed, indicative for an absence of secondary metathesis such as backbiting, chain transfer.

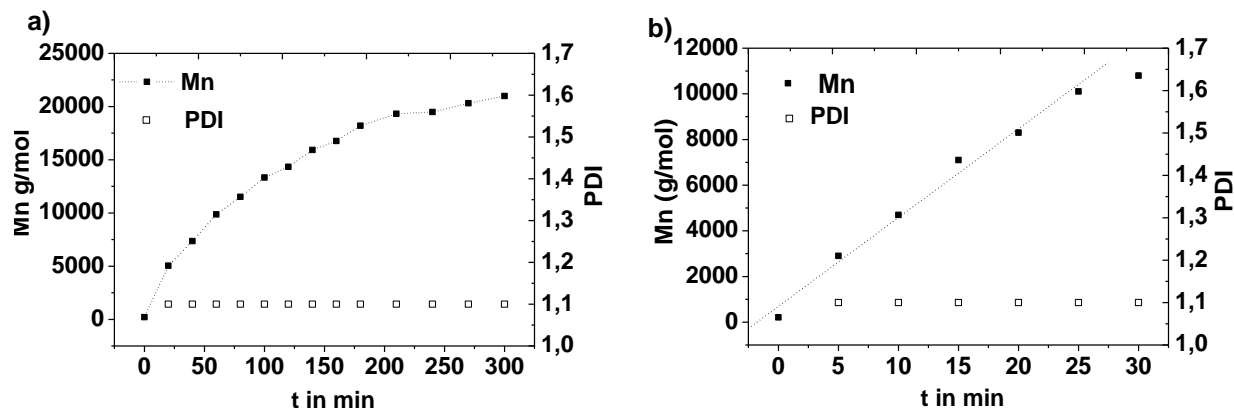


Figure 2.2. Number average molecular weight as a function of time for the polymerization of monomer **1** with a) **G1**, M/C = 100, b) **G3**, M/C = 50.

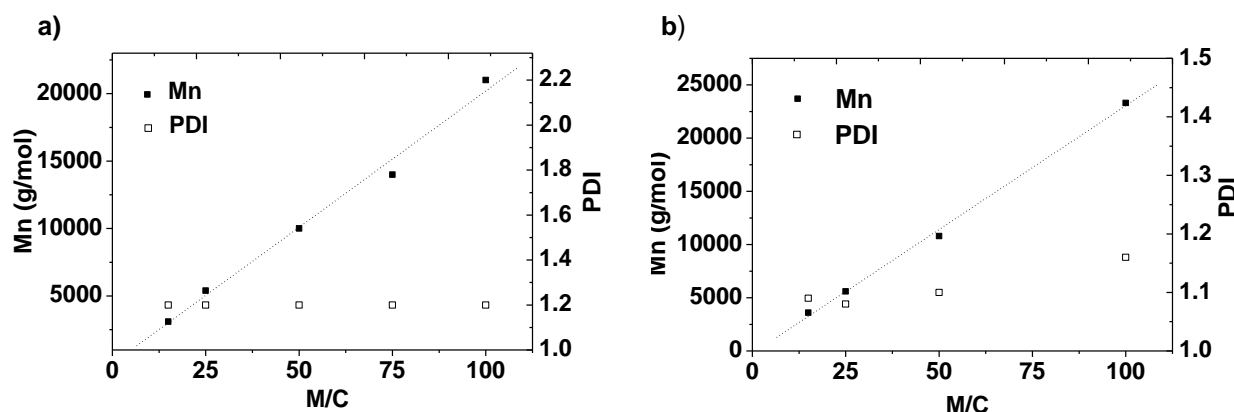


Figure 2.3. Number average molecular weight as a function of M/C ratio for the polymerization of monomer **1** a) with **G1**, b) with **G3**.

Additionally, the number average molecular weight as a function of the monomer to catalyst ratio was measured for the catalysts **G1** and **G3** (Figure 2.3). The molecular weight increases linearly with the M/C-ratio and the PDI stays in the range of 1.2 to 1.3 for catalyst **G1**. The same observation can be done for the M_n vs. M/C plot for **G3**, revealing a linear slope with PDIs for the prepared polymers in the range of 1.1. Table 2.2 summarizes the results of the polymerization reactions of monomer **1**. The molecular weights in the range of 2000 to 20000 g/mol are in a good agreement with the calculated values for the catalysts **G1**, **G3** and **U1**, **U3** with the best match for the catalysts **G1** and **G3**. For catalyst **BG1**, the molecular weights are higher than expected. Polymers with a polydispersity of 1.1-1.4 were obtained in yields of 80 to 90% (except Table 2.2, entries 12-13, yield 50 %).

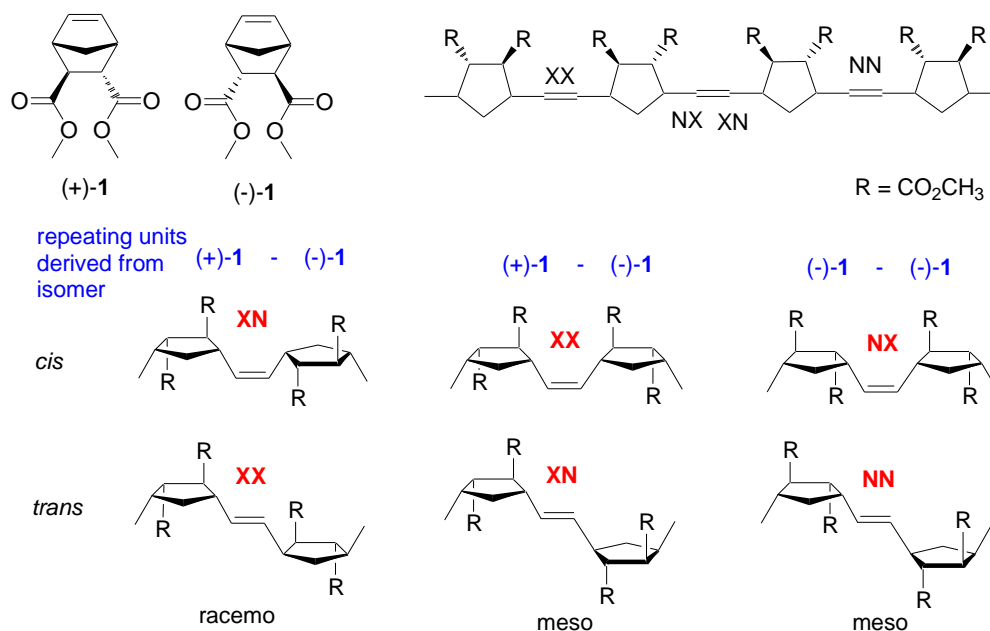
Table 2.2. Polymerization results of monomer **1** with catalysts **G1**, **G3**, **U1**, **U3** and **BG1**, entries 10-12 taken from Binder et al.¹²¹ Molecular weights determined by GPC in THF, against poly(styrene) standards.

entry	catalyst	M/C	M _n (calc)	M _n (exp)	PDI
1	G1	15	3254	3100	1.2
2	G1	25	5354	5400	1.2
3	G1	50	10604	10000	1.2
4	G1	75	15854	14000	1.2
5	G1	100	21104	21000	1.2
6	G3	15	3254	3600	1.1
7	G3	25	5354	5600	1.1
8	G3	50	10615	10800	1.1
9	G3	100	21126	23300	1.2
10	U1	50	10704	8500	1.2
11	U3	15	3354	2700	1.2
12	U3	25	5454	4400	1.2
13	BG1	25	5380	6400	1.4
14	BG1	25	5380	8300	1.3

2.2.3. Stereochemistry of poly(**1**)

After having studied the kinetics of the polymerization process, the microstructure of poly(**1**) was investigated. ROMP polymers in general and especially polymers such as poly(**1**) display a rich microstructure, having *cis* and *trans* double bonds as well as meso and racemo dyads. The *cis* / *trans* ratio of the double bonds is 60/40 for poly(**1**), prepared with **G1** and 80/20 for poly(**1**) prepared with **G3**. The assignment was done from the ¹H NMR spectrum (Appendix, Figure 5.2) in accordance to Keitz and Grubbs.¹²² In the ¹³C NMR for poly(**1**), prepared with **G3**, four resonances for the double bond carbons can be seen (133.1, 132.6, 130.4 and 129.9 ppm (Appendix, Figure 5.3). This splitting can be attributed to the presence of *cis* meso, *cis* racemo, *trans* meso and *trans* racemo dyads (Scheme 2.4). Hence, poly(**1**) is atactic, which is expected, since all the applied catalysts do not allow a stereo selective polymerization. As monomer **1** exhibits *endo* and *exo*-substituents and is used as a racemate for the polymerization, different alignments of the *endo* and *exo*-methylester groups of neighboring repeating units in the polymer chain are possible. Thus, two methylester groups can either point in the same

direction or in opposite directions, giving all in all four alignments (**XX** *exo, exo*, **NN** *endo, endo*, **XN** *exo, endo* and **NX** *endo, exo*).¹²³ A great variety of structures is possible with a racemic mixture of a monomer, since two neighboring repeating units can be derived from the following combinations (+)-**1** - (+)-**1**, (-)-**1** - (-)-**1**, (+)-**1** - (-)-**1** and (-)-**1** - (+)-**1**. A selection of possible dyads is given in Scheme 2.4.



Scheme 2.4. Stereochemistry of poly(**1**) and different alignments of the methylester groups, **XX** *exo, exo*, **NX** *endo, exo*, **XN** *exo, endo*, **NN** *endo, endo*, selection of dyads generated by polymerization of a racemic mixture of monomer **1**. Scheme adapted from Hamilton et al.¹²³

Summary of chapter 2.2.

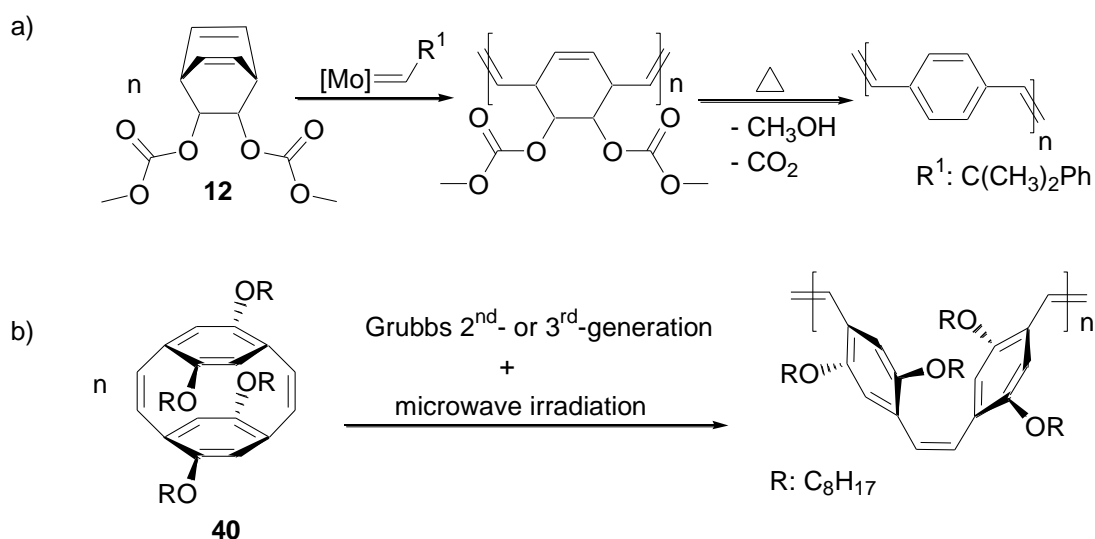
According to the linear plot of the $\ln(M_0/M_t)$ vs. time and M_n vs. M/C plots as well as the matching molecular weights and the low polydispersities, the polymerization of monomer **1** with catalysts **G1**, **G3**, **U1** and **U3** proceeds in a living manner. Best results were obtained with **G1**, **G3** and **U3**. With the bivalent catalyst **BG1**, monomer **1** can be polymerized in a controlled manner, but the polymerization reactions suffer from moderate yields and PDIs of 1.4. The catalysts **G2** and **U2** are not suited for the polymerization due to a $k_p/k_t \gg 1$, leading to high molecular weight polymer with a broad PDI ≥ 1.6 .

2.3. Polymerization of monomers 11 and 12

This chapter comprises a short overview on the preparation of poly(*p*-phenylene vinylene)s via ROMP, the synthesis of two barrelene-monomers and their polymerization.

2.3.1. Poly(*p*-phenylene vinylene)s via ROMP

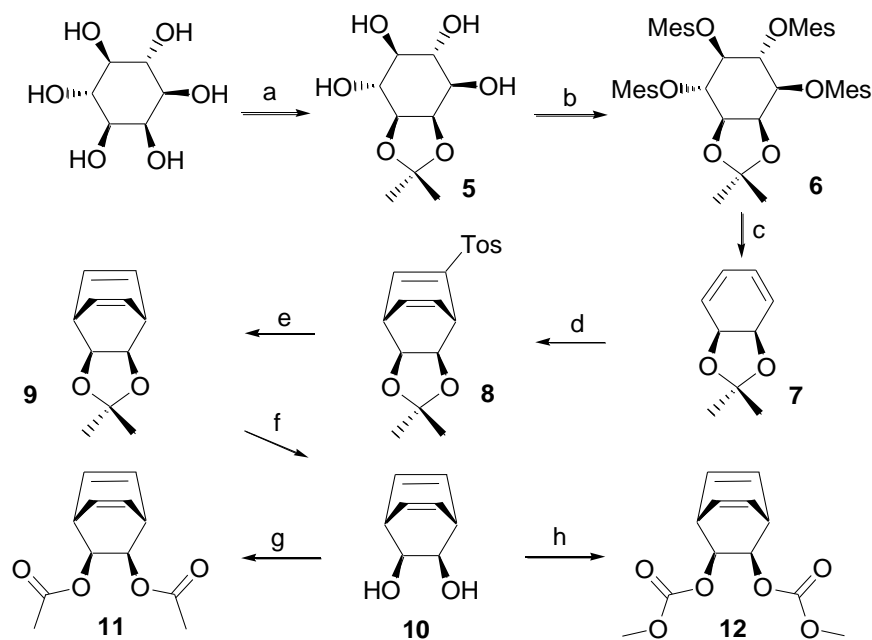
Poly(*p*-phenylene vinylene)s (PPVs) are an important class of semi-conductive polymers which find application in OLEDs or solar cells. These polymers can be prepared via multiple pathways including metal-catalyzed coupling reactions (Stille- and Heck-coupling), acyclic diene metathesis polymerization (ADMET) or ring-opening metathesis polymerization (ROMP). The approach via ROMP, assuming a living process, offers the advantage that the produced polymers have low polydispersities and defined molecular weights. PPV-polymers via ROMP can be either prepared by using paracyclophane dienes or substituted barrelene monomers. The polymerization of paracyclophane dienes, in contrast to substituted barrelenes, offers a direct access to PPV-polymers, since the conjugated system is already present in the monomer. Bazan et al. described the block copolymer synthesis from cyclophane ene and fluorinated norbornenes.¹²⁴



Scheme 2.5. Poly(*p*-phenylene vinylene)s via ROMP: a) polymerization of a methoxy carbonyloxy substituted barrelene, b) polymerization paracyclophane dienes

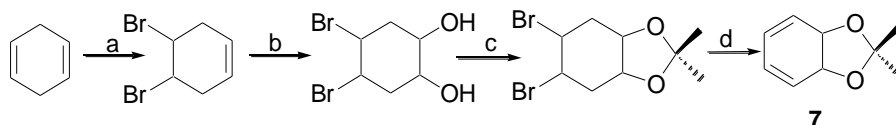
Yu and Turner^{61,62,125-127} described the polymerization and copolymerization of paracyclophane dienes with Grubbs catalyst 2nd- and 3rd-generation and microwave irradiation (Scheme 2.5b) yielding soluble PPVs (*cis/trans*-vinylene units = 1:1). The preparation of poly(*p*-phenylene vinylene) by polymerization of an acetoxy- (**11**) or methoxy carbonyloxy substituted barrelene (**12**) with a Schrock molybdenum catalyst was published by Conticello et al.¹²⁸ (Scheme 2.5a). In case of the acetoxy-substituted barrelene (**11**), the polymerization stopped after few turnovers due to carbonyl olefination of the acetoxy group with the molybdenum alkylidene. Only monomer **12** could be converted into polymer. Molecular weights (M_n) for poly(**12**) of 46000 g/mol (polymerization in THF, PDI = 1.2) and 63000 g/mol (polymerization in DCM, PDI = 1.3) were reported ($M/C = 100$, expected $M_n = 25400$ g/mol). The soluble precursor polymers (*cis/trans*-vinylene units = 1:1) were then converted into the insoluble conjugated poly(*p*-phenylene vinylene) via heating under cleavage of methyl carbonic acid, which decomposes into methanol and carbon dioxide.

2.3.2. Monomer synthesis



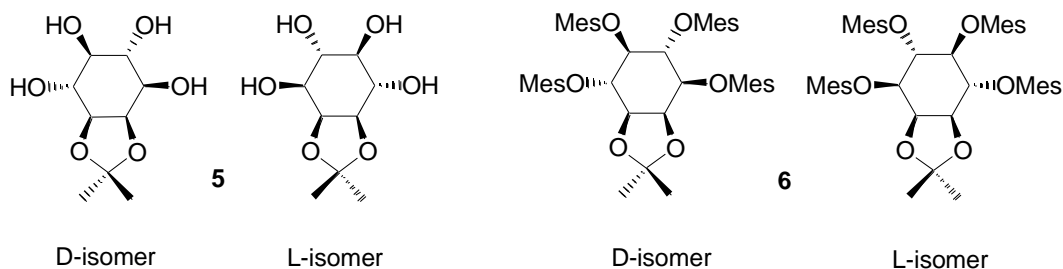
Scheme 2.6. Synthetic pathway to barrelene monomers **11** and **12**, a) 2,2-dimethoxypropane, (51 %), b) mesyl chloride, 0 °C, (93 %), c) Zn/Cu, NMP, 120 °C, (30 %), d) tosyl acetylene, benzene, (83 %), e) Sml₂, HMPA, (74 %), f) AcOH, H₂O, (63 %), g) Ac₂O, pyridine, (75 %), h) methyl chloroformate, pyridine, (80 %).

For the synthesis of soluble PPV-precursor polymers, two monomers based on barrelene were chosen. The preparation of the monomers bicyclo[2.2.2]oct-5,7-diene-2,3-diol di(acetate) (**11**) and bicyclo[2.2.2]oct-5,7-diene-2,3-diol di(methylcarbonate) (**12**) was performed in a seven step process¹²⁸⁻¹³⁰ starting from commercial available *myo*-inositol. The synthetic pathway is depicted in Scheme 2.6. An alternative route for the synthesis of compound **7**^{131,132} starting from cyclohexa-1,4-diene is depicted in Scheme 2.7, but was not pursued due to the extensive use of sulfur dioxide in the second step.



Scheme 2.7. Alternative route to compound **7** a) Br₂, CHCl₃, b) KMnO₄, c) 2,2-dimethoxypropane, d) 1,8-diazabicyclo[5,4,0]undec-7-ene.

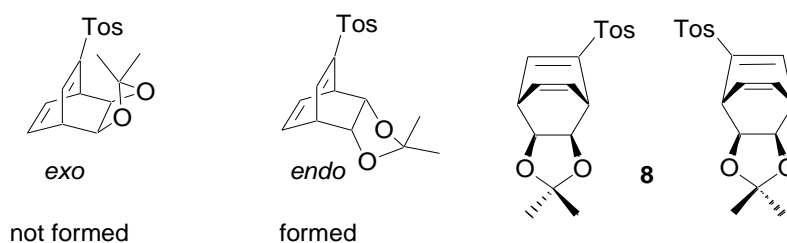
The chosen synthetic pathway starts with the reaction between *myo*-inositol and 2,2-dimethoxypropane to form the ketal **5** in a yield of 51%. The ¹H NMR spectrum (see appendix, Figure 5.6) shows the significant resonances for the hydroxyl protons and the methyl protons at 4.82-4.66 ppm and 1.39-1.25 ppm respectively. An analysis of the coupling constants, the ¹H/¹H COSY and the ¹³C NMR of compound **5** are given in the appendix (Figures 5.7, 5.8, 5.9). In the second step, the remaining hydroxyl-groups are esterified with mesyl chloride to give compound **6** in a yield of 93%. Compounds **5** and **6** consist of a mixture of two enantiomers (Scheme 2.8). The ¹H NMR for compound **6** (see appendix, Figure 5.10) shows no remaining resonances for hydroxyl protons but instead new resonances for the mesyl groups in the range of 3.37-3.33 ppm. As for compound **5** the ¹H/¹H COSY and the ¹³C NMR can be seen in the appendix (Figures 5.11, 5.12).



Scheme 2.8. Enantiomers of compounds **5** and **6**.

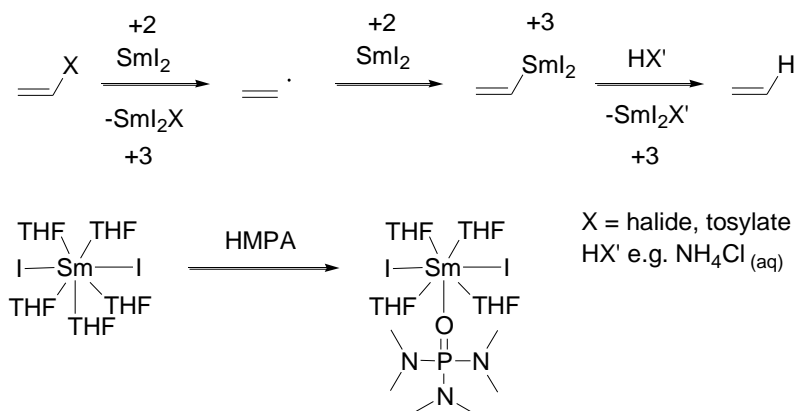
In the third step, the mesyl-groups of compound **6** are removed in an elimination reaction with a zinc/copper couple in *N*-methylpyrrolidone to form the crucial 3,5-cyclohexadiene-derivate **7** in a yield of 30%. The moderate yields can be a result of a partially deactivated zinc/copper couple. Compound **7** is unstable in neat and should be kept for storage as a solution in ethyl acetate or *N*-methylpyrrolidone. In the appendix (Figure 5.13), the ^1H NMR spectrum of **7** in a crude mixture with *N*-methylpyrrolidone is given, showing resonances for the olefinic protons at 5.93 and 5.82 ppm.

The fourth step in the synthesis of the barrelene monomers **11** and **12** is the Diels-Alder reaction of tosyl acetylene, acting as dienophile, with **7** to furnish compound **8** in a yield of 83%. As a product of a Diels-Alder reaction, compound **8** can be formed as an *exo*- and an *endo*-isomer (Scheme 2.9). According to the ^1H -NMR (see appendix, Figure 5.14) just one isomer is formed, which was assigned to the *endo*-isomer.¹³³ This isomer appears like **5** and **6** as a mixture of two enantiomers (Scheme 2.9). The reason for the exclusive formation of the *endo*-isomer can be explained by steric interactions, leading exclusively to an attack of tosyl acetylene on the less hindered site of the diene **7**.



Scheme 2.9. Isomers of compound **8**.

The tosyl group of compound **8** is removed in a subsequent reaction via reduction with samarium(II) iodide and HMPA to yield the barrelene derivative **9** in a yield of 74%. This reaction proceeds via a single electron transfer mechanism, depicted in Scheme 2.10. Samarium(II) iodide in THF appears as $\text{SmI}_2(\text{THF})_5$, a pentagonal bipyramidal complex,¹³⁴ with the iodine atoms in axial position. The reducing activity of this complex can be increased by the addition of hexamethylphosphortriamide (HMPA), replacing one THF-ligand. In the ^1H NMR spectrum of compound **9** (see appendix, Figure 5.15) two resonances for the olefinic protons are visible, showing that the protons at the two double bonds are not chemically equivalent. This is caused by the conformation of the molecule, where the ketal group is pointing towards one of the olefinic bonds.



Scheme 2.10. Reduction of alkyl- or alkenyl halides with samarium(II) iodide.

In the sixth step, the ketal group is removed by acidic hydrolysis using a mixture of acetic acid and water to give compound **10** in a yield of 63%. The ¹H NMR spectrum (see appendix, Figure 5.16) shows a broad resonance for the hydroxyl protons at 2.15 ppm. Subsequently, the esterification of compound **10** with acetic anhydride or methyl chloro formate gives the monomer **11** in a yield of 75% and the monomer **12** in a yield of 80% respectively. The ¹H NMR spectra of the monomers **11** and **12** are given in the Figures 2.4 and 2.5. Carbon NMR-spectra of these two compounds can be seen in the appendix, Figures 5.17 and 5.18.

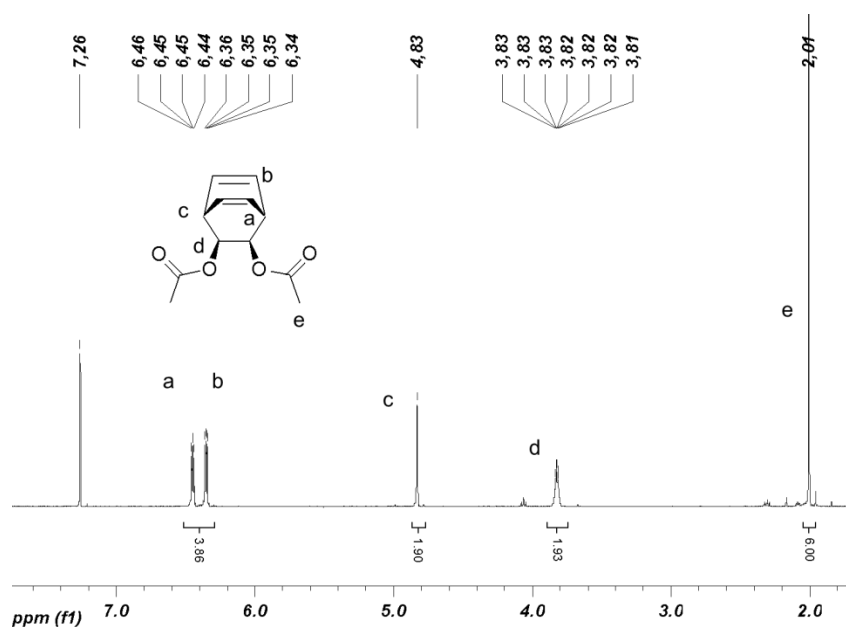


Figure 2.4. ¹H-NMR of **11** in CDCl₃.

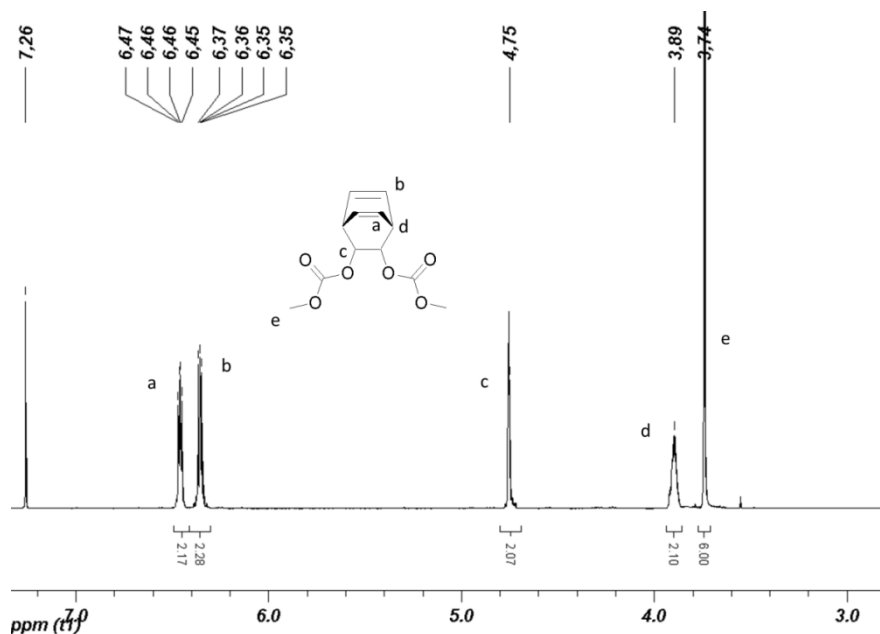
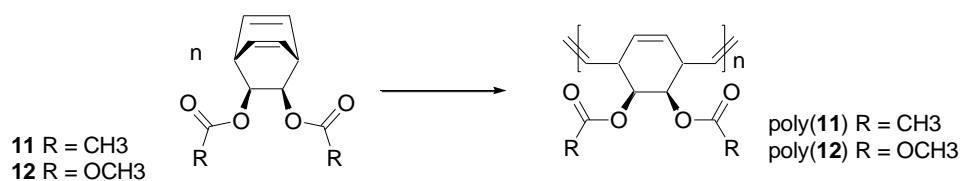


Figure 2.5. ^1H NMR of **12** in CDCl_3 .

2.3.3. Polymerization results

After their successful synthesis, the monomers **11** and **12** were polymerized with the catalysts **G1 - G3** and **U1 - U3** (Scheme 2.11).



Scheme 2.11. Polymerization of monomer **11** and **12**.

GPC Results

The polymerization results of monomers **11** and **12** are summarized in Table 2.3. It can be seen that monomer **11** displays reactivity towards all tested catalysts. Polymers were obtained with PDI values ranging from 1.6 to 2.7. The high PDI-values are attributed to a slow initiation and secondary metathesis reactions. The best results for the polymerization of **11** were obtained with Grubbs catalyst 2nd-generation (**G2**), showing molecular weights comparable to the calculated value (see Table 2.3, entry 2,

3). Best results for the polymerization of monomer **12** were obtained with catalysts **G2** and **G3** (60 °C, 2 equiv. HCl) with polymers with PDIs of 1.3 and comparable molecular weights to the calculated values (Table 2.3, entries 8, 14). In the other polymerization reactions, the molecular weight either exceeds or stays below the calculated value (Table 2.3, entry 10, 11, 12). Polymers with a PDI in the range of 1.3 to 2.4 were obtained. However, these values were lower than the PDIs measured for poly(**11**).

Table 2.3. GPC results for the polymerization of monomers **11** and **12** with different catalysts, conditions for polymerization of **11**: solvent DCM, room temperature, $[M]_0 = 0.08$ M, $[C]_0 = 3 \cdot 10^{-3}$ M, conditions for polymerization of **12**: solvent DCM, room temperature unless otherwise noted. * 2 equiv. HCl, 40 °C, # 2 equiv. HCl, solvent: CHCl_3 , 60 °C, $[M]_0 = 0.12$ M, $[C]_0 = 5.6 \cdot 10^{-3}$ M.

entry	M/C	monomer	catalyst	t (h)	M_n (calc)	M_n (exp)	PDI
1	21	11	G1	20	4771	7300	2.8
2	25	11	U1	2	5754	6600	2.2
3	21	11	G2	20	4771	4600	1.6
4	30	11	G2	20	6764	8500	1.8
5	25	11	U2	4	5754	7500	2.5
6	20	11	G3	20	4544	6100	2.7
7	18	11	U3	4	4200	1300	1.7
8	25	12	G2	6	6454	5500	1.3
9	12	12	G2	3	3152	11900	1.5
10	25	12	U2	6	6554	3200	1.4
11	21	12	G3	20	5438	1300	1.8
12	21	12	U3	20	5538	1400	1.7
13	15	12	G3*	20	3914	6000	1.3
14	18	12	G3#	20	4676	6900	1.3

NMR-kinetics

The NMR-kinetics of **11** (M/C = 20) with catalyst **G2** is given in Figure 2.6, showing complete monomer conversion after 17 hours. The NMR-spectra showed the disappearance of the olefinic resonances of the monomer at 6.44 and 6.33 ppm. Polymer formation was confirmed by the appearance of two new resonances at 5.53 and 5.28 ppm which can be assigned to the vinyl protons and the protons at the

double bond in the 1,4-cyclohexenylene groups (see Figure 2.6). The *cis/trans* ratio of the double bonds is approximately 1:1.

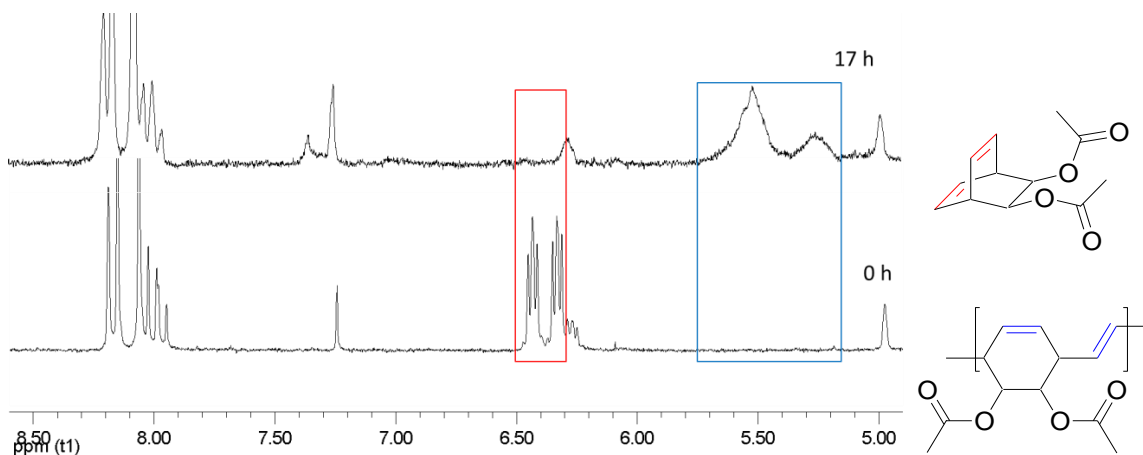


Figure 2.6. Stacked ^1H -NMR spectra (8.50 ppm - 5.00 ppm) from the polymerization of monomer **11** with **G2** (M/C = 20), highlighted in red: olefinic resonances of the monomer, highlighted in blue: olefinic resonances of the polymer.

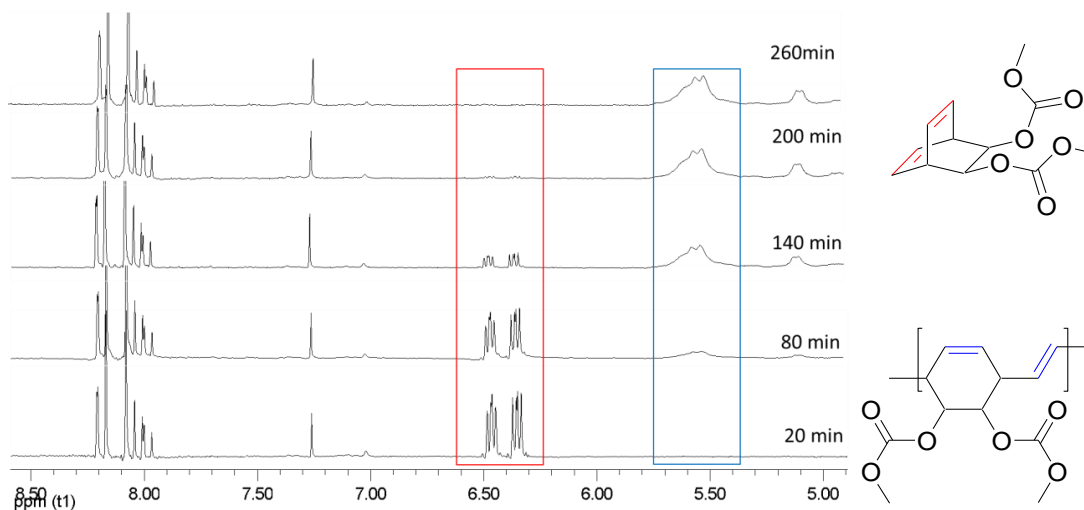


Figure 2.7. Stacked ^1H -NMR spectra (8.6-5.0 ppm) from the polymerization of monomer **12** with **G2** (M/C = 20), highlighted in red: olefinic resonances of the monomer, highlighted in blue: olefinic resonances of the polymer.

The spectrum from the NMR kinetics of monomer **12** with catalyst **G2** shows the disappearance of the olefinic resonances of the monomer at 6.46 and 6.36 ppm (Figure 2.7). Polymer formation was confirmed by the appearance of a new resonance at 5.53 which can be assigned to olefinic protons of the polymer. The *cis/trans* ratio for the double bonds is approximately 1:1 (for ^1H NMR, see appendix,

Figure 5.19). When comparing the two monomers, compound **12** displays faster polymerization kinetics with catalyst **G2** than monomer **11**, achieving complete monomer conversion ($M/C = 20$) already after ~ 4 hours (Figure 2.7). The result is surprising as the methoxy carbonyloxy groups in monomer **12** execute a stronger electron withdrawing effect (CH_3COOH , $\text{p}K_a$ 2.92),¹³⁵ compared to the acetoxy groups (CH_3COOH , $\text{p}K_a = 4.76$)¹³⁵ attached to monomer **11**. In general, the reactivity of the monomer, applied for ROMP, decreases with an increasing electron withdrawing effect. An explanation for this behavior cannot be given definitely but it is possible that the polymerization of monomer **12** is favored compared to monomer **11** due to less coordination of the methoxy carbonyloxy groups to the ruthenium center, compared to the acetoxy groups. Thus, coordination of the substituents would be less competing with the monomer coordination.

In the polymerization of **12** with **G2**, unreacted catalyst can be still observed in the ^1H NMR at 19.16 ppm after complete monomer conversion. The derived kinetic plot (Figure 2.8) is characteristic for a polymerization with a slow initiation. This was confirmed by the calculation of the k_p/k_i ratio, giving a value of 114 for the polymerization of monomer **12** with catalyst **G2**. Thus, the initiating and propagating carbene display a significant difference in the reactivity towards monomer **12**. For monomer **11**, statements about the initiation behavior cannot be done, due to the low resolution of the spectra. A similar behavior is expected judging from the broad PDI.

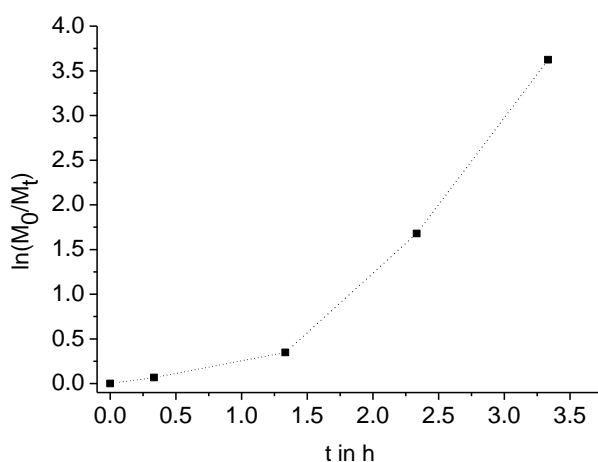


Figure 2.8. Kinetic plot $\ln(M_0/M_t)$ vs. time for the polymerization of monomer **12** with **G2**, $M/C = 20$, $[M]_0 = 0.13$ M, $[C]_0 = 0.65 \cdot 10^{-2}$ M, $k_p/k_i = 114$, $k_p \sim 0.25$ L/mol·s (calculated from the last 3 points).

MALDI-TOF MS

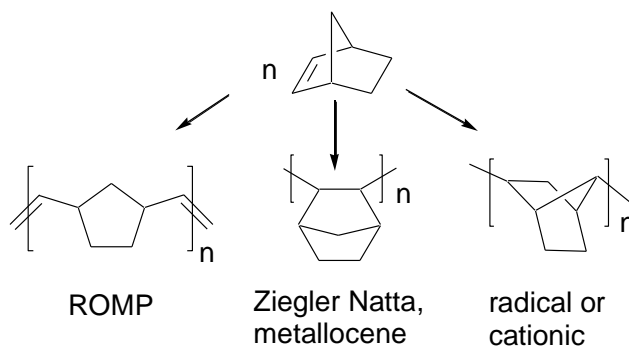
MALDI-TOF MS measurements of poly(**11**) and poly(**12**) have not led to satisfying results (see appendix, Figures 5.21 and 5.22). The recorded spectra with dithranol as matrix display multiple series with low intensity and resolution. Different matrices (dithranol, all-*trans*-retinoic acid, pencil lead, α -cyano-4-hydroxycinnamic acid, *trans*-2-[3-(4-*tert*-Butylphenyl)-2-methyl-2-propenylidene]malononitrile (DCTP), *trans*-3-indoleacrylic acid (IAA), 2-(4-Hydroxyphenylazo)benzoic acid (HABA), 2,5-dihydroxyacetophenone) and salts (sodium- and silver trifluoroacetate) were tried out to obtain better resolved spectra, but no improvement could be achieved. The distance between some of the peaks did correspond to the mass of the repetition unit (222 m/z ($C_{12}H_{14}O_4$) for **11** and 254 m/z ($C_{12}H_{14}O_6$) for **12**, but an unambiguously identification of the species was not possible. Therefore, an analysis of poly(**11**) and poly(**12**) via MALDI-TOF MS was not further pursued. The poor ionization of poly(**11**) shows that polymers derived from structurally similar monomers (e.g. monomer **1** and **11**) do not display the same tendency to ionize.

Summary of chapter 2.3.

The polymerizations of the monomers **11** and **12** have been tested with the catalysts **G1 - G3** and **U1 - U3**. Although complete conversion of the two monomers with catalyst **G2** was observed, the polymerizations suffer on an unfavorable k_p/k_t -ratio. With **G2**, the molecular weights are comparable to the calculated values in a limited range of 4000 to 6000 g/mol, with PDIs from 1.3 to 1.8. For the polymerization reactions with the other catalysts, the molecular weights are not comparable with the calculated values, with PDIs in the range of 1.3 to 2.7. Cross over reactions on poly(**11**) and poly(**12**) were not investigated due to the uncontrolled polymerization and the poor ionization in MALDI-TOF MS. Despite not having achieved a living polymerization with monomers **11** and **12**, it could be demonstrated that these monomers can be polymerized with the tested catalysts. Thus, it is possible to generate soluble PPV-precursor polymers from functionalized barrelene monomers not only by using a Schrock molybdenum catalyst¹³³ but also with the ruthenium carbenes **G1-G3** and **U1-U3**.

2.4. Polymerization of norbornene (13)

Poly(norbornene) was chosen as the third system for the crossover studies. The monomer bicyclo[2.2.1]hept-2-ene (norbornene) is versatile and can be polymerized over radical, cationic, complex coordinative or metathesis pathway (Scheme 2.12).



Scheme 2.12. Polymers from norbornene.

The polymers obtained from these polymerization pathways differ significantly from each other. Only in the case of ROMP the unsaturation of the monomer is retained in the polymer. Poly(norbornene) via ROMP is an attractive precursor polymer, since it can be transformed from an amorphous into a semi crystalline polymer via hydrogenation. The polymerization of norbornene via ROMP has been intensively studied with molybdenum^{36,136-139} and ruthenium catalysts.^{14,104} Norbornene is often used as a model monomer for measuring reaction kinetics^{21,40,140} as well as testing catalysts concerning their stereo control.¹⁴¹

2.4.1. Polymerization results

Polymerization with **G3** at room temperature is uncontrolled, since chain transfer and backbiting reactions are favored at this temperature. However, the polymerization can be changed into a living process by reducing the temperature to -20 °C as shown by Grubbs et al.¹⁴ In Table 2.5, the polymerization results of norbornene are summarized. Polymerization reactions were quenched with ethyl vinyl ether to furnish methylene terminated polymers. The measured molecular weights obtained by GPC were corrected by a factor of 0.5. This correction is necessary due to the different hydrodynamic radii of poly(norbornene) and poly(styrene). Polymerization of norbornene with Grubbs catalyst 1st-generation was uncontrolled. Thus, in order to gain more control over the polymerization process, triphenylphosphine as well as tricyclohexylphosphine (5 equiv.) were added. The obtained PDIs were

reduced to 1.4 to 1.5, but the measured molecular weights were still lower than the expected values (Table 2.5, entry 1-2). The formation of high molecular weight polymers is observed in the polymerization of norbornene with catalyst **G2** as a result of the unfavorable k_p/k_t ratio $\gg 1$. However, it was shown that control over the molecular weight could be achieved when catalyst **G2** was used together with chain transfer agents.¹⁰⁴ The best results were obtained with catalyst **G3**. In the range of 5000 to 100000 g/mol, the measured molecular weights match the calculated values. The polydispersity index for all prepared samples is in the range of 1.2-1.3 (Table 2.5, entries 3-7).

Table 2.5. GPC-results for poly(norbornene) (poly(**13**))

entry	M/C	catalyst	M_n (calc)	M_n (exp)	M_n (corr)*	PDI
1	100	G1 + 5 equiv. PPh ₃	9504	9000	4500	1.5
2	100	G1 + 5 equiv. PCy ₃	9504	16800	8400	1.4
3	50	G3	4804	9100	4550	1.3
4	100	G3	9504	20700	10350	1.2
5	200	G3	18904	43900	21950	1.2
6	500	G3	47104	96900	48450	1.3
7	1000	G3	94104	195000	97500	1.2

* Corrected by a factor of 0.5, isolated yield: entries 1, 2 (60%), entries 3-7 (75-85 %).

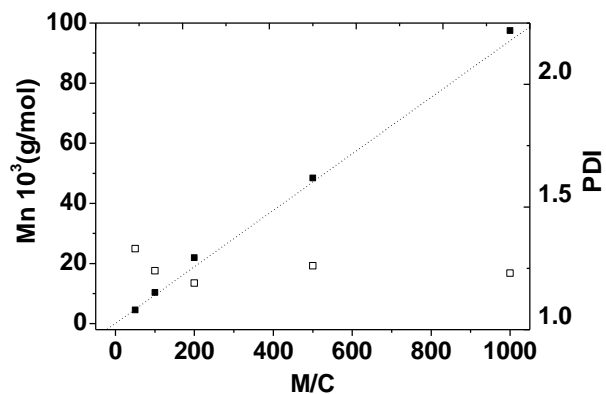
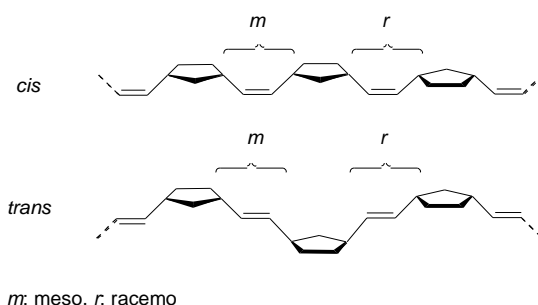


Figure 2.9. Number average molecular weight as a function of the M/C ratio for **G3**.

In Figure 2.9, the number average molecular weight as a function of the M/C-ratio is depicted, showing a linear slope of the curve. Thus, the polymerization of norbornene with **G3** can be considered as living process.

2.4.2. Stereochemistry of poly(13)

A stereo control was not achieved with the applied catalysts **G1** and **G3**. This is not unexpected for Grubbs catalysts, since the rotation of the carbene (ruthenium-carbon bond) is not hindered and therefore no site of the catalyst is favored for the monomer insertion.



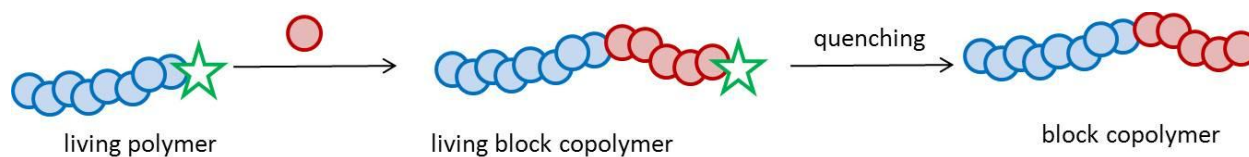
Scheme 2.13. Possible dyads formed in the polymerization of norbornene, *cis* meso, *cis* racemo, *trans* meso, *trans* racemo. Figure adapted from [123].

However, it is worth to mention that new ruthenium-¹²² and molybdenum-carbenes^{141,142} have been developed that display a high *cis*-selectivity. The ratio of *cis* to *trans* double bonds, calculated from the olefinic resonances at 5.35 and 5.21 ppm, is 60/40 with catalyst **G3** (see appendix, Figure 5.23 for the ¹H NMR-spectrum). The *cis/trans* ratio is dependent on the catalyst, showing e.g. a ratio of *cis* to *trans* double bonds of 34/64 for Schrock molybdenum catalyst.¹³⁷ In the ¹³C NMR-spectrum of a poly(norbornene) prepared with catalyst **G3**, (see appendix, Figure 5.24) each carbon resonance is split due to the presence of different dyads (*cis* meso, *cis* racemo, *trans* meso, *trans* racemo) in the polymer chain (Scheme 2.12). Hence, the prepared poly(norbornene)s display an atactic polymer structure.

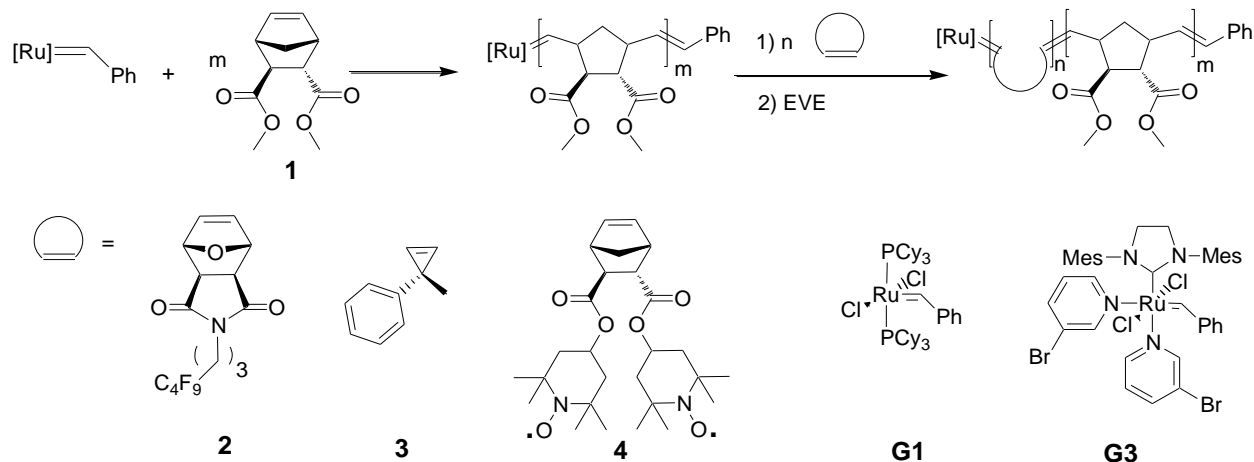
Crossover Reactions

In the previous chapters "2.2. - 2.4." it was shown that the polymerization of monomers **1** and **13** (norbornene) with selected catalysts is a living process. This was concluded on the basis of the data obtained from GPC and NMR-kinetics. Therefore, crossover reactions will be performed on these two systems. The chapter "Crossover Reactions" is divided in four parts. In the first two parts the reaction of living polymer chains and living oligomer-chains from monomer **1** with a second monomer is investigated and therefore the underlying crossover step in block copolymerization/ co-oligomerization reactions by means of NMR-spectroscopy, GPC, MALDI- and ESI-TOF MS. The third part will describe the termination of living poly(**1**) chains with symmetric olefins. In the last part, the end functionalization of poly(norbornene)s by the same method and the thermal investigation of the prepared poly(norbornene)s and hydrogenated poly(norbornene)s is described.

2.5. Investigation of the crossover step in block copolymerization reactions via MALDI-TOF MS



This chapter will describe the monitoring and evaluation of the crossover-reaction in ROMP via kinetic analysis and MALDI-mass-spectrometry. For this purpose, the prepared living poly(**1**) chains were reacted with three structurally different cycloolefins (**2** - **4**).^{24,143,144} Monomer **2** is an oxo-norbornene based monomer with a dicarboxyimide moiety, while monomer **4** is a norbornene based monomer with two TEMPO-moieties. Monomer **3** is a highly strained cyclopropene. The monomers chosen (monomer **1** - **4**) (see Scheme 2.14) display their best ROMP-processes with different catalysts such as monomer **1** and **2** with catalysts **G1** and **G3**;¹⁴³ monomer **3** with **G2** and **G3**²⁴ and monomer **4** with **G2**.¹⁴⁴ The classical investigation of block copolymers via GPC and NMR is limited to statements about M_n and PDI (GPC) as well as the block ratio (NMR). As a complementary technique, MALDI MS can reveal the intermediate species in the crossover step and by this allow a better understanding of poor or insufficient polymerization results in certain block copolymer systems.



Scheme 2.14. Crossover studies in block copolymerization reactions, monomer **1** - **4**, catalysts **G1** and **G3**, EVE, ethyl vinyl ether.

The samples for the investigation of the crossover-reactions were synthesized as follows: Monomer **1** was polymerized with the catalysts **G1** or **G3** and subsequently the second monomer **2**, **3**, or **4** was added in defined amounts. Poly(**1**)_n was chosen as first block since it is well desorbed and detected by MALDI-TOF MS.

2.5.1. GPC-kinetics of the block copolymerization reactions

The block copolymerization reactions were first investigated by GPC and NMR-methods. From Table 2.6, it can be seen that block copolymers from all three systems (poly((**1**)-*b*-(**2**)), poly((**1**)-*b*-(**3**)), poly((**1**)-*b*-(**4**))) could be prepared with molecular weights that are similar to the calculated values and PDIs in the range of 1.2 to 1.3.

Table 2.6. GPC data for block copolymerization of monomer **1** with monomers **2**, **3** and **4**.

entry	Sample	catalyst	M _n (calc)	M _n (exp)	PDI
1	(1) ₁₀₀ - <i>b</i> -(2) ₁₀₀	G1	63500	53800	1.2
2	(1) ₁₀₀ - <i>b</i> -(2) ₁₀₀	G3	63500	57000	1.2
3	(1) ₂₀ - <i>b</i> -(3) ₂₀	G1	6800	4900	1.3
4	(1) ₅₀ - <i>b</i> -(3) ₂₀	G3	13100	13500	1.1
5	(1) ₅₀ - <i>b</i> -(4) ₂₀	G3	20300	18200	1.2

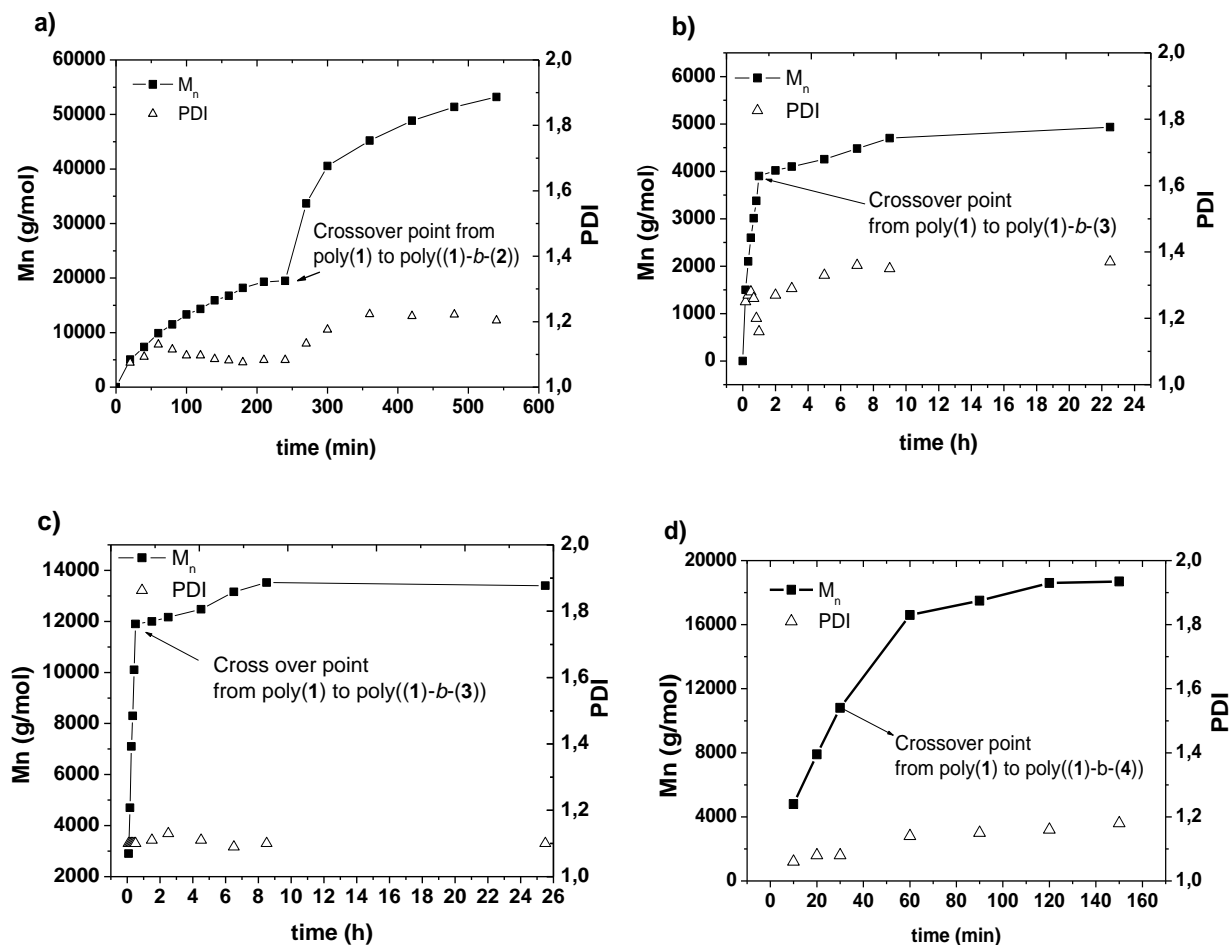


Figure 2.10. Increase in number average molecular weight with time a) $(1)_{100}\text{-}b\text{-}(2)_{100}$ using catalyst **G1**, b) $(1)_{20}\text{-}b\text{-}(3)_{20}$ using catalyst **G1**, c) $(1)_{50}\text{-}b\text{-}(3)_{20}$ using catalyst **G3**, d) $\text{poly}(1)_{50}\text{-}b\text{-}(4)_{20}$ using catalyst **G3**.

The M_n (GPC) vs. time-graphs for the block copolymer systems ($\text{poly}((1)\text{-}b\text{-}(2))$, $\text{poly}((1)\text{-}b\text{-}(3))$, and $\text{poly}((1)\text{-}b\text{-}(4))$) are depicted in Figure 2.10. For the system $\text{poly}(1)\text{-}b\text{-}(2)$, the slope of the curve increases after the point of crossover (Figure 2.10a), while it remains nearly constant in the system $\text{poly}(1)\text{-}b\text{-}(4)$ (Figure 2.10d). In contrast to this, a significant change in the kinetics for the crossover-reaction from monomer **1** to monomer **3** using catalysts **G1** and **G3** can be seen (Figure 2.10b-c). After the point of cross over, the slope of the curve is decreasing significantly, indicative for slower polymerization kinetics of monomer **3** compared to monomer **1**. The different slopes of the curves before and after the crossover reaction indicate already different kinetics for the polymerization of the individual monomers.

2.5.2. NMR-kinetics of the block copolymerization reactions

For further insight, the kinetics for the homo and block copolymerization reactions were monitored by $^1\text{H-NMR}$ -spectroscopy (see appendix for the $\ln(M_0/M_t)$ vs. time graphs, Figures 5.26 and 5.27).

Table 2.7. Polymerization kinetics data obtained from $^1\text{H-NMR}$ spectroscopy.

entry	experiment	catalyst	$[\text{C}]_0$ (mol/L)	k_{br} (L/mol·s)	
1	(2) ₂₀	G1	0.0065	homo- 2	2.20
2	(1) ₁₀ - <i>b</i> -(2) ₁₀	G1	0.015	block- 2	1.30
3	(2) ₂₀	G3	0.0066	homo- 2	5.70
4	(1) ₂₀ - <i>b</i> -(2) ₂₀	G3	0.0049	block- 2	11.90
5	(3) ₂₀	G1	0.02	homo- 3	0.0045
6	(1) ₂₀ - <i>b</i> -(3) ₂₀	G1	0.02	homo- 1	0.05
7	(1) ₂₀ - <i>b</i> -(3) ₂₀	G1	0.015	block- 3	0.0042
8	(3) ₂₀	G3	0.012	homo- 3	0.0016
9	(1) ₂₀ - <i>b</i> -(3) ₂₀	G3	0.018	homo- 1	2.60
10	(1) ₂₀ - <i>b</i> -(3) ₂₀	G3	0.014	block- 3	0.0079

The polymerization of monomer **4** could not be analyzed by $^1\text{H-NMR}$ -spectroscopy due to the attached free radical at the monomer. Assuming first-order kinetics, the brutto rate constants (k_{br}) can be derived from the $\ln(M_0/M_t)$ vs. time graphs, which are summarized in Table 2.7. From the values obtained one can say that the reactivity of the monomers towards the catalysts **G1** and **G3** increases in the following order (**3** < **1** < **2**). On the example of the kinetics with catalyst **G1**, monomer **1** ($k_{br} = 0.05$ L/(mol·s)) is consumed 10 times faster than **3** ($k_{br} = 0.0045$ L/(mol·s)), but approximately 50 times slower than **2** ($k_{br} = 2.2$ L/(mol·s)) (Table 2.7, entries 1, 5 and 6). As shown in chapter 2.2., a significant increase in the kinetics is observed when monomer **1** is polymerized with **G3** compared to **G1** ($k_{br} = 2.6$ L/(mol·s) with **G3** and 0.05 L/(mol·s) with **G1**). For the monomers **2** and **3**, a change from catalyst **G1** to **G3** does not lead to a significant acceleration in the polymerization kinetics. The change from the neat catalyst to the macro-initiator (living poly(**1**)₂₀) does only result in small changes in the k_{br} -values of the individual monomers (see Table 2.7, entries 5 and 7). Thus, the carbene ligand plays a minor role in the kinetics for the selected block copolymer systems.

The observation of the alkylidene region in the $^1\text{H NMR}$ gives statements about the initiation behavior of the living poly(**1**) chains. In case of the polymerization with catalyst **G3**, the initiating carbene at 18.56 and 18.26 ppm (living poly(**1**)-chains) is not observed at the first measuring point after the crossover. Instead, new alkylidene resonances appear at 18.72 and 18.59 for the system poly((**1**)-*b*-(**2**)) and 16.74 ppm for the system poly((**1**)-*b*-(**3**)) respectively. These resonances can be assigned to the propagating carbene of the 2nd block. For the experiments run with catalyst **G1**, a mixture of initiating carbene and newly formed carbene is observed directly after the point of cross over for the system poly((**1**)-*b*-(**3**)). The resonance of the initiating carbene is decreasing over time until it is completely converted to the propagating carbene of the 2nd block. Thus the signal at 18.66 and 18.47 disappears and new resonances can be observed at 17.80 and 17.45 for the system poly((**1**)-*b*-(**3**)). From these observations it can be concluded that poly(**1**) chains initiate faster when prepared with **G3** compared to **G1**.

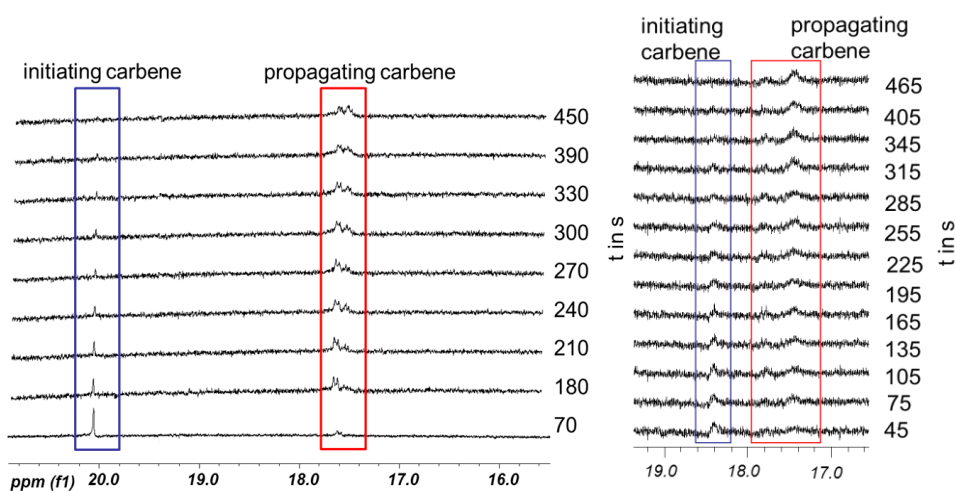
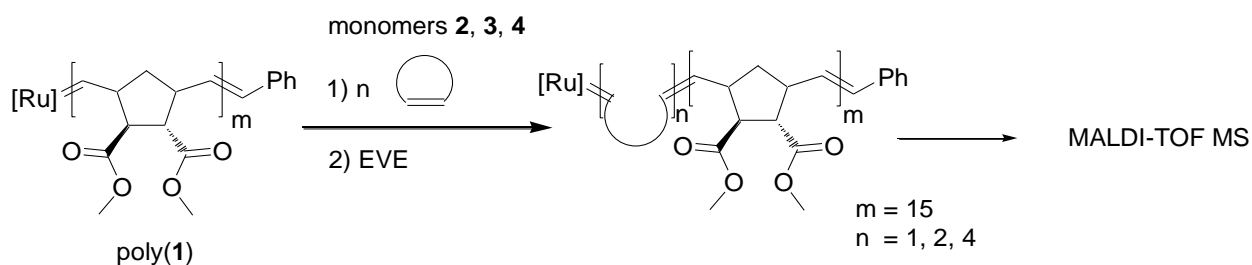


Figure 2.11. Crossover reaction of monomer **3**, a) with catalyst **G1**, b) living poly(**1**)₂₀ prepared with catalyst **G1**, blue: initiating carbene, red: propagating carbene.

No statement can be done about the system poly((**1**)-*b*-(**2**)) with **G1**, since the propagating carbene appears at the same position (18.67 and 18.45 ppm) as the carbene generated from monomer **1**. A comparison of monomer **3** initiated with **G1** and with poly(**1**) chains prepared with catalyst **G1** reveals no significant difference in the reactivity. In both cases the initiating carbene is consumed in approximately 8 minutes (Figure 2.11).

2.5.3. Monitoring the crossover efficiency via MALDI-TOF MS

To achieve a further insight into the crossover step in the selected block copolymerization reactions, living poly(**1**) chains with a degree of polymerization ($n = 15$) were reacted with 1, 2 or 4 equiv. of the monomer **2**, **3** and **4** similar to step-crossover-experiments in living anionic polymerization processes.¹⁴⁵ The chain length was limited to $n = 15$ to differentiate the individual species, especially for poly(**1**-*b*-**2**) due to similar masses of homo- and block copolymer species. Additionally, this chain length is well desorbed in the MALDI-process. After reaction completion, the chains were terminated with ethyl vinyl ether. The obtained polymers were then investigated via GPC and MALDI-TOF MS (Scheme 2.14).¹⁴⁶



Scheme 2.15. Investigation of block copolymerization reactions via MALDI-TOF MS.

The complete consumption of monomer **1** before the crossover-reaction was checked by thin layer chromatography. GPC measurements show the expected shift in the molecular weight with increasing amounts of the second monomer, e.g. Table 2.8, entry 1-3, 13-15). An overlay of the GPC-curves can be seen in the appendix, Figures 5.27-5.29. The polydispersity for the homo and block copolymers remains in the range of 1.1-1.2.

The mass spectra for the system poly(**1**-*b*-**2**) (Table 2.8, entries 1-6), (see appendix, Figures 5.36 and 5.37) show the picture of an incomplete crossover reaction, irrespective if catalyst **G1** or **G3** was used. After addition of 1 equiv. of monomer **2**, significant amounts of homopolymer (**1**)_{*n*} are still detected, along with peaks which can be assigned to (**1**)_{*n*}-*b*-**2**)₁ and (**1**)_{*n*}-*b*-**2**)₂ species. Even after addition of 4 equiv. of monomer **2**, homopolymer peaks can be detected together with block copolymer species up to (**1**)_{*n*}-*b*-**2**)₆. The measured mass spectra indicate a slow crossover-reaction for the system poly(**1**-*b*-**2**). It is surprising that both catalysts (**G1** and **G3**) give nearly the same picture, since the more reactive catalyst **G3** gives faster crossover and kinetics with the monomers **1** and **2**, as indicated by ¹H NMR spectroscopy.

Table 2.8. Results for block copolymers obtained by crossover-reaction from poly(**1**) to monomer **2–4**.

entry	sample	catalyst	M_n (calc.) ¹	M_n (GPC)	PDI (GPC)	M_{peak} (MALDI) ²	M_n (MALDI) ³	PDI (MALDI) ⁴
1	(1) ₁₅	G1	3255.4	2800	1.15	3280.3	2646.5	1.20
2	(1) ₁₅ (2) ₁	G1	3680.5	3300	1.16	3494.8	3350.1	1.13
3	(1) ₁₅ (2) ₄	G1	4955.7	3900	1.16	4556.0	4934.8	1.07
4	(1) ₁₅	G3	3255.4	2500	1.13	2018.5	2250.9	1.07
5	(1) ₁₅ (2) ₁	G3	3680.5	2900	1.18	3068.8	3888.3	1.09
6	(1) ₁₅ (2) ₄	G3	4955.7	3900	1.14	4979.0	5878.5	1.06
7	(1) ₁₅	G1	3255.4	4100	1.14	4733.4	4751.2	1.04
8	(1) ₁₅ (3) ₁	G1	3385.5	4200	1.14	4863.3	4805.1	1.03
9	(1) ₁₅ (3) ₄	G1	3775.7	4400	1.15	4913.4	4841.5	1.02
10	(1) ₁₅	G3	3255.4	3600	1.09	4734.2	5565.1	1.05
11	(1) ₁₅ (3) ₁	G3	3385.5	3800	1.10	5705.1	5847.7	1.03
12	(1) ₁₅ (3) ₄	G3	3775.7	3900	1.07	5705.3	5865.4	1.03
13	(1) ₁₅	G1	3278.4	3100	1.21	3911.2	3742.3	1.03
14	(1) ₁₅ (4) ₁	G1	3756.7	3300	1.14	4538.4	4330.6	1.01
15	(1) ₁₅ (4) ₂	G1	4233.0	3800	1.21	4537.6	4477.0	1.01
16	(1) ₁₅	G3	3278.4	3700	1.09	4751.1	5256.1	1.04
17	(1) ₁₅ (4) ₁	G3	3756.7	4700	1.10	5802.1	5842.5	1.02
18	(1) ₁₅ (4) ₂	G3	4233.0	4900	1.08	6432.9	6580.5	1.02

¹) Calculated monoisotopic peak value including starting group (Ph), end group (vinyl) and excluding ions,

²) Peak maximum of main series from MALDI spectra, ³) Calculated average M_n using Polytools® software,

⁴) M_w/M_n calculated using Polytools® software.

Figures 2.12 and 2.13 show the MALDI-spectra for the crossover-reaction of poly(**1**)_n (n = 15) with monomer **4** using **G1** and **G3**, respectively (Table 2.8, entries 13-18). The mass spectra for these samples resemble the picture seen for the system poly((**1**)-*b*-(**2**)). After the addition of two equivalents of monomer **4**, the main series can still be assigned to unreacted poly(**1**) chains (see Figures 2.12 e, f and 2.13 e, f). As side series, block copolymer species with the composition (**1**)_n-*b*-(**4**)₁ and (**1**)_n-*b*-(**4**)₂ are detected, which are more prominent for the copolymers synthesized with catalyst **G3**. Again, the measured mass spectra signify a slow crossover-reaction for the system poly((**1**)-*b*-(**4**)). However, the

higher intensities for the block copolymer species in the experiments with catalyst **G3** are an indication for a more efficient cross over reaction, compared to the block copolymer poly(**1**)-*b*-(**4**), prepared with catalyst **G1**.

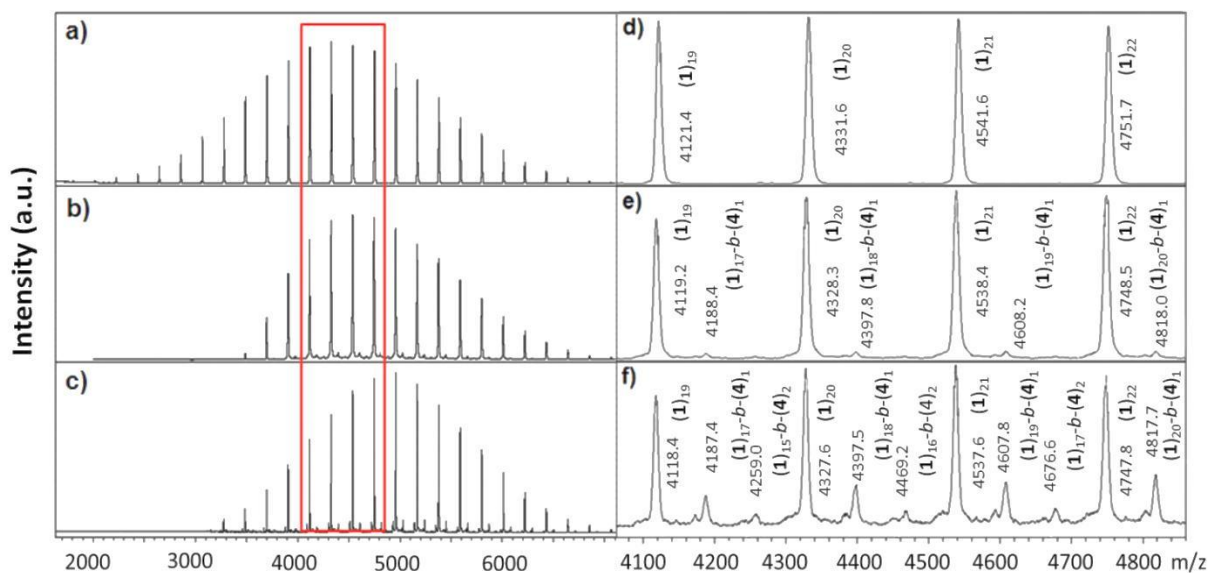


Figure 2.12. MALDI-TOF mass spectra of poly(**1**)₁₅ (a: complete spectra, d: enlargement), poly(**1**)₁₅-*b*-(**4**)₁ (b: complete spectra, e: enlargement) and poly(**1**)₁₅-*b*-(**4**)₂ (c: complete spectra, f: enlargement) prepared with catalyst **G1**, (all the chains of main series are desorbed as $[M+Na]^+$ ions).

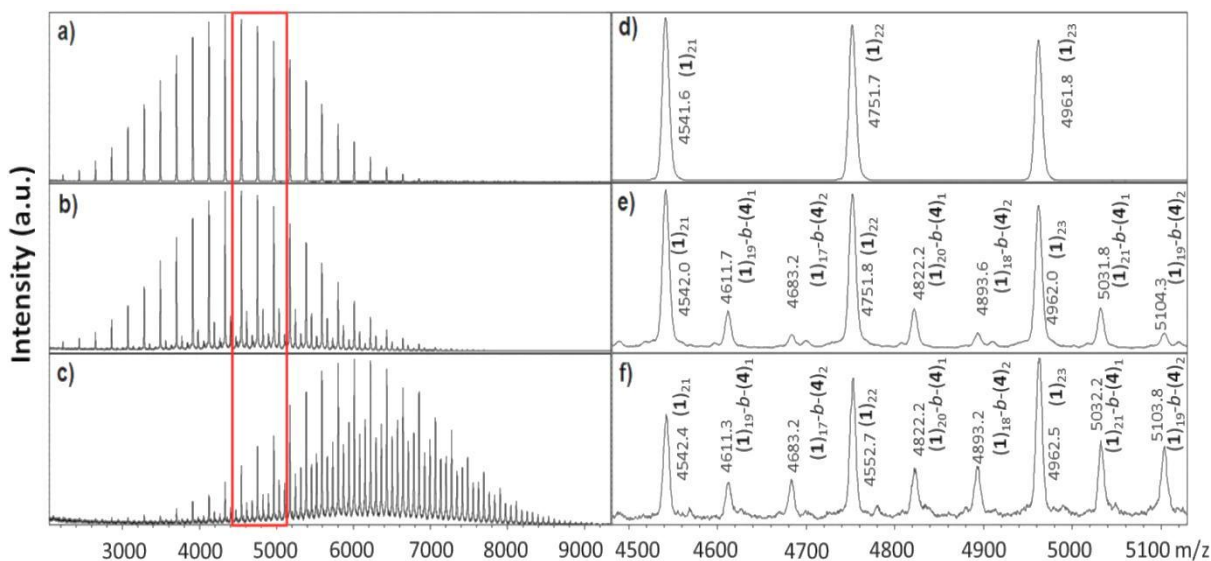


Figure 2.13. MALDI-TOF mass spectra of poly(**1**)₁₅ (a: complete spectra, d: enlargement), poly(**1**)₁₅-*b*-(**4**)₁ (b: complete spectra, e: enlargement) and poly(**1**)₁₅-*b*-(**4**)₂ (c: complete spectra, f: enlargement) prepared with catalyst **G1**, (all the chains of main series are desorbed as $[M+Na]^+$ ions).

For the third system, poly(**1**-*b*-**3**), a significant difference in the mass spectra is seen for the applied catalysts **G1** and **G3**. As for the other two systems, a shift in the molecular weight can be observed by GPC after addition of 1 and 4 equiv. of monomer **3** (Table 2.8, entries 7-12). However, the mass spectra show a different picture (Figures 2.14, 2.15). The addition of 1 equiv. of monomer **3** results in the case of poly(**1**), initiated with **G1**, to a mixture of $(\mathbf{1})_n$ and $(\mathbf{1})_n\text{-}b\text{-}(\mathbf{3})_1$ with comparable intensities (Figure 2.14e). The same experiment conducted with catalyst **G3**, shows already a strong reduction of the homopolymer species (Figure 2.15e). As main series, $(\mathbf{1})_n\text{-}b\text{-}(\mathbf{3})_1$ is detected along with copolymer species up to $(\mathbf{1})_n\text{-}b\text{-}(\mathbf{3})_3$. Addition of 4 equiv. of monomer **3** leads in the case of catalyst **G1** to a strong reduction of the homopolymer species $(\mathbf{1})_n$. The species $(\mathbf{1})_n\text{-}b\text{-}(\mathbf{3})_1$ is now detected as main series along with side series with up to $(\mathbf{1})_n\text{-}b\text{-}(\mathbf{3})_3$ (Figure 2.14f). In case of catalyst **G3**, the homopolymer species are nearly disappeared after addition of 4 equiv. of monomer **3** (Figure 2.15f). Block copolymer species with a composition up to $(\mathbf{1})_n\text{-}b\text{-}(\mathbf{3})_4$ are detected. However, the main series is still assigned to $(\mathbf{1})_n\text{-}b\text{-}(\mathbf{3})_1$. These observations can be explained by the faster initiation behavior of catalyst **G3** compared to **G1**, leading to a better crossover reaction after the addition of 1 equiv. of monomer **3**.

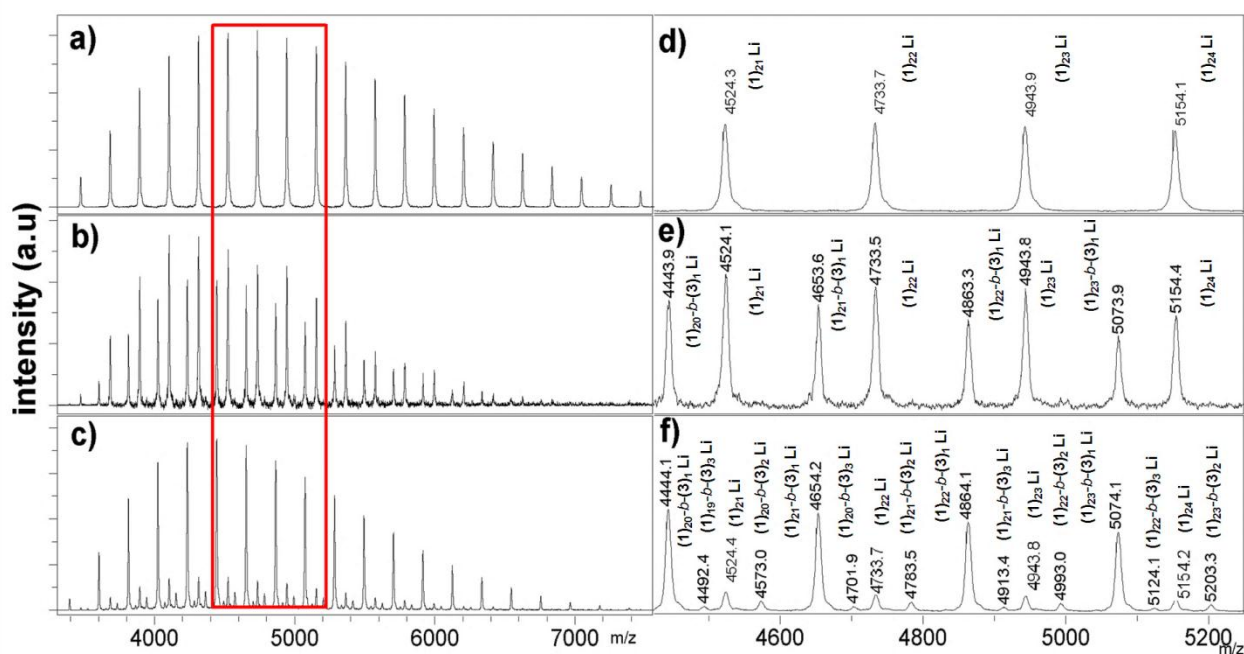


Figure 2.14. MALDI-TOF mass spectra of poly(**1**)₁₅ (a: complete spectra, d: enlargement), poly(**1**)₁₅-*b*-**3**₁ (b: complete spectra, e: enlargement) and poly(**1**)₁₅-*b*-**3**₄ (c: complete spectra, f: enlargement) prepared with catalyst **G1**, (all the chains of main series are desorbed as $[\text{M}+\text{Li}]^+$ ions).

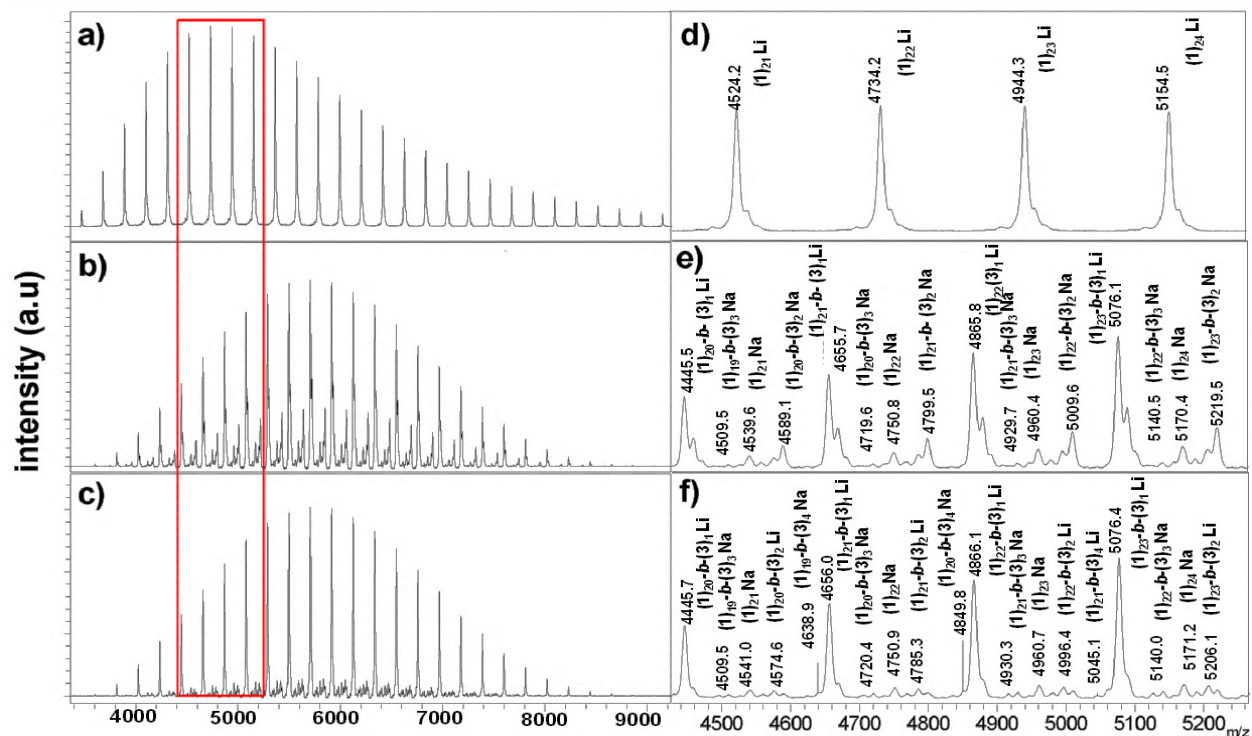


Figure 2.15. MALDI-TOF mass spectra of poly(**1**)₁₅ (a: complete spectra, d: enlargement), poly(**1**)₁₅-*b*-(**3**)₁ (b: complete spectra, e: enlargement) and poly(**1**)₁₅-*b*-(**3**)₄ (c: complete spectra, f: enlargement) prepared with catalyst **G3**, (most chains of main series are desorbed as [M-Li]⁺ ions and few as [M-Na]⁺ ions).

2.5.4. MALDI-TOF quantification

However, it is worth to note that MALDI mass spectra do not allow quantitative statements, since desorption of a species is dependent on the structure and the molecular weight.¹⁴⁷⁻¹⁵¹ Still it is possible to gain quantitative information by measuring sensitivity-plots for the individual species.^{147-149,152}

The sensitivity plots are obtained by measuring a concentration series of the sample with an added standard. The calculated intensity ratios between the standard and the individual species are then plotted as a function of the weight ratio between the standard and the sample. As standard for the block copolymer system, pure poly(**1**) was added. Derived from these plots is the desorption ratio, which gives the probability of a species to be ionized in relation to the standard. The sensitivity plots for the individual block copolymer species are shown in Figure 2.16. For the system poly(**1**)-*b*-(**2**), peaks with the chain length (**1**)_n, n = 15 were compared with each other. Peaks with the chain length of (**1**)_n, n = 20 were used for the other two systems. The desorption factors for the species (**1**)₁₅-*b*-(**2**)_n in relation to the

species $(\mathbf{1})_{15}$ are as follows: $(\mathbf{1})_{15}-b-(\mathbf{2})_1$ (2.14), $(\mathbf{1})_{15}-b-(\mathbf{2})_2$ (2.38), $(\mathbf{1})_{15}-b-(\mathbf{2})_3$ (2.02), $(\mathbf{1})_{15}-b-(\mathbf{2})_4$ (1.52) (all as sodium ions). Thus, a species $(\mathbf{1})_{15}$, compared to a species $(\mathbf{1})_{15}-b-(\mathbf{2})_1$ is desorbed better by a factor of 2.14. The factors for the individual species remain within the same range, showing that the chain length of the second block is not having a significant influence on the desorption.

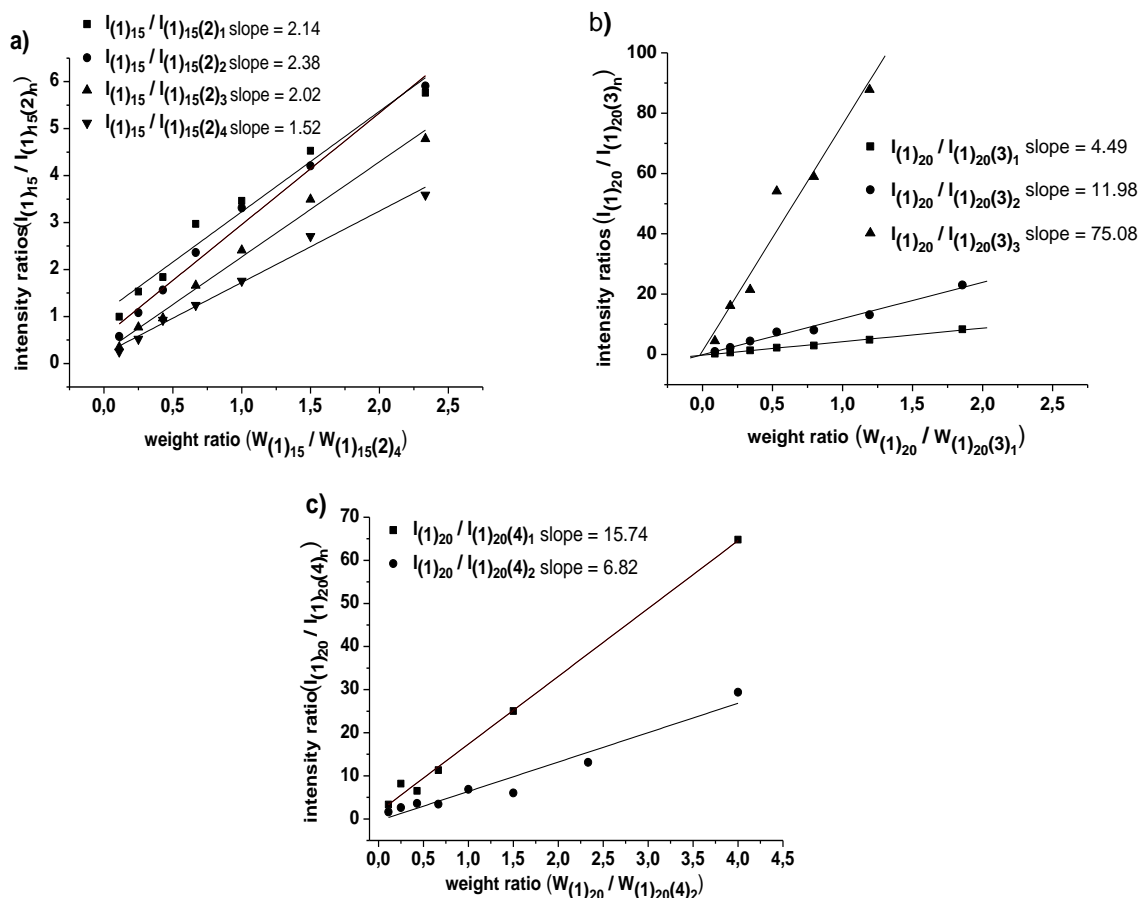


Figure 2.16. Plot of signal intensity ratios vs. weight ratios (MALDI-TOF mass spectra) of a) $(\mathbf{1})_{15}$ and $(\mathbf{1})_{15}-b-(\mathbf{2})_4$ mixtures, b) $(\mathbf{1})_{20}$ and $(\mathbf{1})_{20}-b-(\mathbf{3})_1$ mixtures and c) $(\mathbf{1})_{20}$ and $(\mathbf{1})_{20}-b-(\mathbf{4})_2$ mixtures. The intensities of the individual ions of $(\mathbf{1})_{15}-b-(\mathbf{X})_{1,2,3,4}[\text{Na}^+]$ ions for poly $(\mathbf{1})-b-(\mathbf{2})$ and $(\mathbf{1})_{20}-b-(\mathbf{X})_{1,2,3,4}[\text{Na}^+]$ ions for poly $(\mathbf{1})-b-(\mathbf{4})$ are plotted against the corresponding weight ratios, yielding the individual sensitivity-values for the corresponding desorbed ions, for Figure 2.16c) poly $(\mathbf{1})_{20}-b-(\mathbf{3})_n[\text{Li}^+]$ ions were compared with poly $(\mathbf{1})_{20}[\text{Li}^+]$ ions.

In contrast to this, the chain length of the second block plays an important role for the block copolymers poly $(\mathbf{1})-b-(\mathbf{3})$ and poly $(\mathbf{1})-b-(\mathbf{4})$. For these systems the desorption factors (measured in relation to the species $(\mathbf{1})_{20}$) are: $(\mathbf{1})_{20}-b-(\mathbf{3})_1$ (4.49), $(\mathbf{1})_{20}-b-(\mathbf{3})_2$ (11.98), $(\mathbf{1})_{20}-b-(\mathbf{3})_3$ (75.08) (all as lithium ions) and $(\mathbf{1})_{20}-b-(\mathbf{4})_1$ (15.74), $(\mathbf{1})_{20}-b-(\mathbf{4})_2$ (6.82) (all as sodium ions) respectively. On the example of poly $(\mathbf{1})-b-(\mathbf{3})$ it can

be seen that the probability of desorption is decreasing with increasing number of monomer **3** incorporated in the chain. This is in agreement with MALDI MS of poly(**3**) and poly(**4**) giving poor resolved spectra. Based on the derived desorption factors, the intensities of the homo- and copolymer species were corrected. Thereby, a semi quantification of the species generated by the cross over reaction can be achieved (see Table 2.9).

Table 2.9. MALDI signal intensity ratios of the crossover-reactions and corrected intensities in brackets*.

entry	sample	X	catalyst	N	(1) _n	(1) _n X ₁	(1) _n X ₂	(1) _n X ₃	(1) _n X ₄
1	(1) ₁₅ (2) ₁	2	G1	15	1.00	1.10 (2.35)	0.51 (1.22)	-	-
2	(1) ₁₅ (2) ₄	2	G1	15	1.00	1.55 (3.32)	2.03 (4.83)	2.10 (4.24)	1.92 (2.92)
3	(1) ₁₅ (2) ₁	2	G3	15	1.00	0.72 (1.54)	0.51 (1.22)	-	-
4	(1) ₁₅ (2) ₄	2	G3	15	1.00	0.53 (1.13)	1.64 (3.90)	1.73 (3.49)	1.65 (2.51)
5	(1) ₁₅ (3) ₁	3	G1	20	1.00	0.69 (3.10)	-	-	-
6	(1) ₁₅ (3) ₄	3	G1	20	1.00	5.00 (22.45)	0.40 (4.79)	0.15 (11.26)	-
7	(1) ₁₅ (3) ₁	3	G3	20	1.00	16.66 (74.80)	4.50 (53.91)	0.66 (49.55)	-
8	(1) ₁₅ (3) ₄	3	G3	20	1.00	20.00 (89.80)	3.60 (43.12)	2.00 (150.16)	2.80
9	(1) ₁₅ (4) ₁	4	G1	20	1.00	0.05 (0.79)	-	-	-
10	(1) ₁₅ (4) ₂	4	G1	20	1.00	0.06 (0.94)	0.01 (0.07)	-	-
11	(1) ₁₅ (4) ₁	4	G3	20	1.00	0.24 (3.78)	0.30 (2.05)	-	-
12	(1) ₁₅ (4) ₂	4	G3	20	1.00	0.24 (3.78)	0.31 (2.11)	-	-

(*) corrected intensities of the quantification number of (**1**)_nX_m species calculated by multiplying the MALDI peak intensity values with the respective slopes obtained from sensitivity plots of the individual ions (see Figure 2.21), intensity of the pure poly(**1**) species is set to 1.0.

The values in brackets give the corrected intensities which are obtained by multiplying the measured intensity ratio (derived from the pure sample) with the desorption ratios. Thus, a comparison between the qualitative description of the mass spectra and the obtained semi quantitative results can be done. For the experiments of poly(**1**) with monomer **2** (Table 2.9, entries 1-4), initial homopolymer ((**1**)₁₅-species) remains even after addition of 4 equiv. of monomer **2**, showing an incomplete cross over reaction with both the catalysts (**G1** and **G3**).

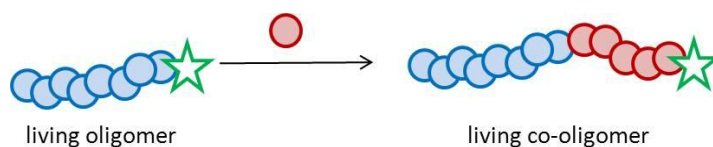
For the system poly(**1**)-*b*-(**4**), the amount of homopolymer remains significant after addition of 2 equiv. of monomer **4**, indicating a poor cross over reaction (Table 2.9, entries 9-12). The trend observed for the system poly(**1**)-*b*-(**3**) could be confirmed with the corrected intensities (Table 2.9, entries 5-8). For poly(**1**), initiated with **G1**, the addition of 4 equiv. of monomer **3** results in low amounts of homopolymer and high amounts of the block copolymer species (**1**)_n-*b*-(**3**)₁₋₃. With the more reactive catalyst **G3**, a strong reduction of the homopolymer is already achieved after addition of 1 equiv. of monomer **3** with a ratio of the species poly(**1**)₂₀ / poly(**1**)₂₀-*b*-(**3**)₁ / poly(**1**)₂₀-*b*-(**3**)₂ / poly(**1**)₂₀-*b*-(**3**)₃ = 1.00 / 74.80 / 53.91 / 49.55. With the addition of 4 equiv. of monomer **3**, the amount of homopolymer is further decreased and the crossover reaction is near to completion.

According to the amount of initial homopolymer, the crossover reaction in the systems poly(**1**)-*b*-(**3**) and poly(**1**)-*b*-(**4**) is more efficient with catalyst **G3**. For poly(**1**)-*b*-(**3**), the crossover step is fast and thereby preferred compared to the propagation of the 2nd block poly(**3**), as proven by the k_{br} -values (0.0042 L·mol⁻¹·s⁻¹ for **G1** and 0.0079 L·mol⁻¹·s⁻¹ for **G3**). The slow kinetics for **3** can be attributed to steric hindrance created by the phenyl-moiety at the cyclopropene monomer. Only small changes are observed in the system poly(**1**)-*b*-(**2**) when catalyst **G1** is replaced by **G3**.

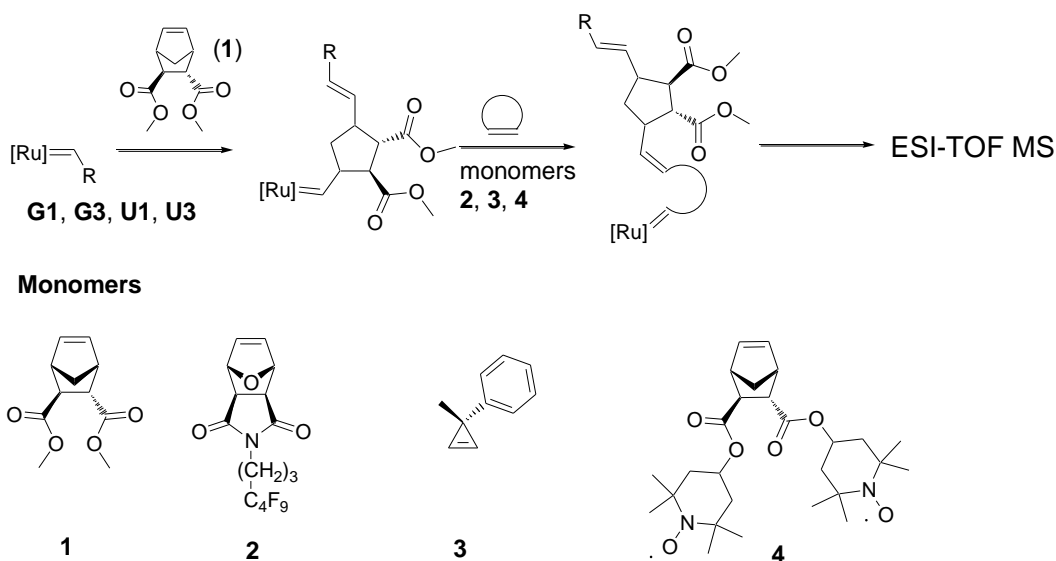
Summary of chapter 2.5.

In summary, one can say that mass spectrometry of the samples revealed the presence of homopolymer in the mixture, although the expected shift in GPC can be seen and the molecular weights of the prepared block copolymers match with the calculated values. This indicates that the point of cross over in block copolymerization reactions is different from what kinetic data (GPC) is showing. These results demonstrate the importance of mass spectrometry as a complimentary tool for the investigation of such processes.

2.6. Investigation of the crossover step in co-oligomerization reactions via ESI-TOF MS



The investigation of the polymer-species formed in the ROMP process after quenching was performed with MALDI-TOF mass spectrometry in the previous chapter. To detect and evaluate the catalyst species involved in this process, an analytical method was required that allowed the investigation directly from solution. The monitoring of the catalytic species via NMR spectroscopy is limited to the detection of the initiating and propagating carbene and the determination of the k_p/k_i ratio, with no detailed information on the number of monomer units incorporated. Thus, the catalytic species present in solution were investigated via ESI-TOF MS, which allowed the transfer of the living species from solution to the gas phase by a gentle ionization. For the investigations the selection of catalysts **G1** and **G3** was extended to the catalysts Umicore M1 (**U1**) and Umicore M3 (**U3**) which differ by their indenylidene-ligand from the Grubbs type catalysts. The set of monomers (**1-4**) remains unchanged (Scheme 2.16).



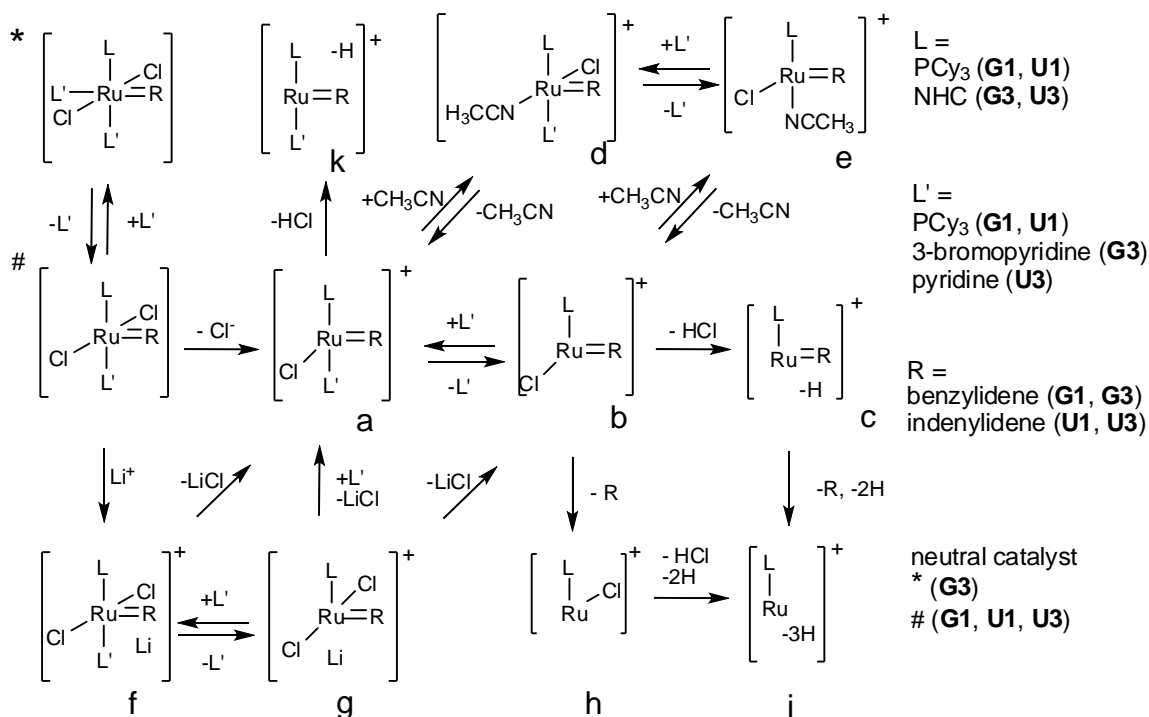
Scheme 2.16. Co-oligomerization reactions monitored via ESI-TOF MS, using the monomers (**1-4**) and catalysts (**G1**, **G3**, **U1** and **U3**), Mes: mesitylene, Ph: phenyl, sum formulas: **1** ($C_{11}H_{14}O_4$), **2** ($C_{15}H_{12}F_9N_1O_3$), **3** ($C_{10}H_{10}$), **4** ($C_{27}H_{42}N_2O_6$), **G1** ($C_{43}H_{72}Cl_2P_2Ru_1$), **G3** ($C_{38}H_{40}Br_2Cl_2N_4Ru_1$), **U1** ($C_{51}H_{76}Cl_2P_2Ru_1$), **U3** ($C_{41}H_{41}Cl_2N_3Ru_1$).

The chain length of the polymeric species during crossover reaction was significantly reduced in comparison to the samples measured by MALDI MS from 15 units of monomer **1** to one unit since ESI-TOF is limited in its detection of the mass range to about 6000 Da. Furthermore, the reduction in chain length allows to study the very first step of the initiation and propagation, thus visualizing the reacted and unreacted catalysts species as a result of the k_p/k_t -ratio.

The preparation of the samples for the measurement was done by diluting the reaction solution (DCM) by a factor of 100. The dilute solution is then mixed with a solution of LiCl (0.1 mg in 10 mL) in MeOH/acetonitrile (v/v = 100/1). Subsequently, the ESI MS measurements in ion positive mode were done by direct injection of the premixed analyte solution into the ESI mass spectrometer. To get an insight into the crossover reaction before and after the point of crossover, two sets of experiments were performed: as first experiments, the addition of 1 equiv. of monomer **1** to the catalysts **G1**, **G3** and **U1**, **U3** was conducted. Secondly the addition of 1 equiv. of monomer **1** and the subsequent addition of one equivalent of the monomers **2**, **3** or **4** to the selected catalysts (Scheme 2.16) was performed to study the crossover-reactions.

2.6.1. Overview of detected ions

Before starting the discussion of the mass spectra, a nomenclature for the different types of ions, detected via ESI-TOF MS, is introduced. An overview of this is given in Scheme 2.17, describing only the ions a letter, omitting neutral species, as they are not detected by ESI-TOF MS. As an example, the molecule ion by loss of chloride $[M - Cl]^+$ for Grubbs catalyst 1st-generation (**G1**) will be denominated as **G1a**. For oligomer species with inserted monomer the same nomenclature will be applied, thus designating an ion of Grubbs catalyst 1st-generation, generated by loss of one chlorine and one phosphine with two inserted units of **1** $[M + \text{two units of } \mathbf{1} - Cl - PCy_3]^+$ as **G1b-(1)₂**. The co-oligomer species will be named analogously, e.g. catalyst **G1** after insertion of one unit of monomer **1** followed by insertion of one unit of monomer **3** and ionized by loss of chloride and phosphine $[M + \text{one unit of } \mathbf{1} + \text{one unit of } \mathbf{3} - Cl - PCy_3]^+$ will be designated as **G1b-(3)₁(1)₁**. The order **G1-(3)_x(1)_y** is a consequence of the olefin metathesis mechanism where the monomer is always inserted into the metal carbene double bond, thus the second monomer is attached to the catalyst. The structures labeled with * and # in Scheme 2.17 depict the neutral catalysts and therefore the starting structures for catalyst **G3** and the catalysts **G1**, **U1**, **U3** respectively.



Scheme 2.17. Overview on types of detected ions and proposed fragmentation pathway, NHC: *N*-heterocyclic carbene ($\text{C}_{21}\text{H}_{26}\text{N}_2$), benzylidene (C_7H_6), indenylidene ($\text{C}_{15}\text{H}_{10}$).

In solution, the neutral catalysts cleave off and rebind the neutral ligands L' , thus e.g. an equilibrium exist between mono and bisphosphine species for catalyst **G1**. The types of detected ions in the mass spectrum show that there are multiple ways for the ruthenium complexes **G1**, **G3**, **U1** and **U3**, with or without oligomer attached, to be ionized. Structures **a** and **b**, ionized by loss of chloride, appear together with their acetonitrile adducts **d** and **e**. The loss of the second chlorine as hydrogen chloride leads to structure **c**. Further fragment ions (catalyst species **h** and **i**), generated by loss of the carbene ligand are detected in the range of 400-500 m/z . Structures **f** and **g** are formed by the addition of alkali metal ions like lithium to the neutral catalyst species, as described by Wang and Metzger.⁷⁹ Cleavage and rebinding of neutral ligands like L' or acetonitrile are likely to happen during the ESI-process.⁸⁰ Other fragmentation steps like loss of hydrogen chloride or the carbene ligand are assumed to be irreversible.

2.6.2. Reaction of catalysts **G1**, **U1** with monomer **1**

For the first experiments, 1 equiv. of monomer **1** was reacted with the catalysts **G1**, **G3**, **U1** and **U3**. For the reaction catalyst **G1** with 1 equiv. of monomer **1** the most prominent peaks could be assigned to unreacted catalyst species **G1a** (787.4 m/z), **G1b** (507.2 m/z), **G1c** (471.2 m/z) and **G1d** (828.4 m/z). Species with inserted monomer **1** (up to 5 units) could be detected with much lower intensities e.g. at **G1e-(1)₁** at 758.3 m/z and **G1e-(1)₂** at 968.4 m/z. compared to the unreacted catalyst species (Figure 2.17, appendix, Table 5.1). A similar picture is seen for the reaction of 1 equiv. of monomer **1** with catalyst **U1** (Appendix, Table 5.3). The main peaks can be assigned to the unreacted catalysts species **U1a** (887.4 m/z), **U1b** (607.2 m/z), **U1d** (928.4 m/z) and **U1e** (648.2 m/z). Species with inserted monomer **1** were detected with significant lower intensities e.g. **U1b-(1)₁** (817.3 m/z), **U1c-(1)₁** (781.3 m/z) and **U1e-(1)₁** (858.3 m/z).

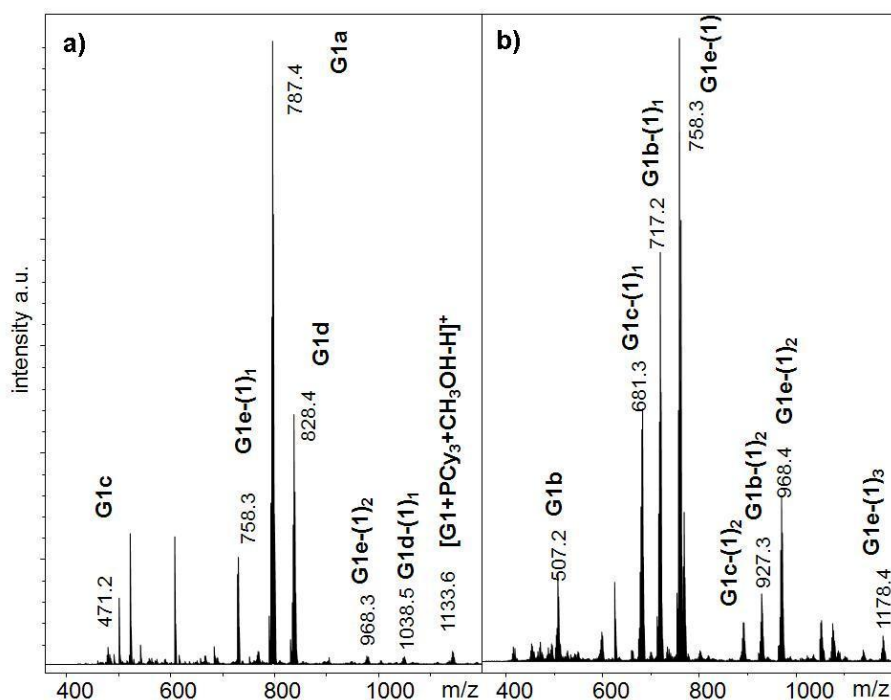
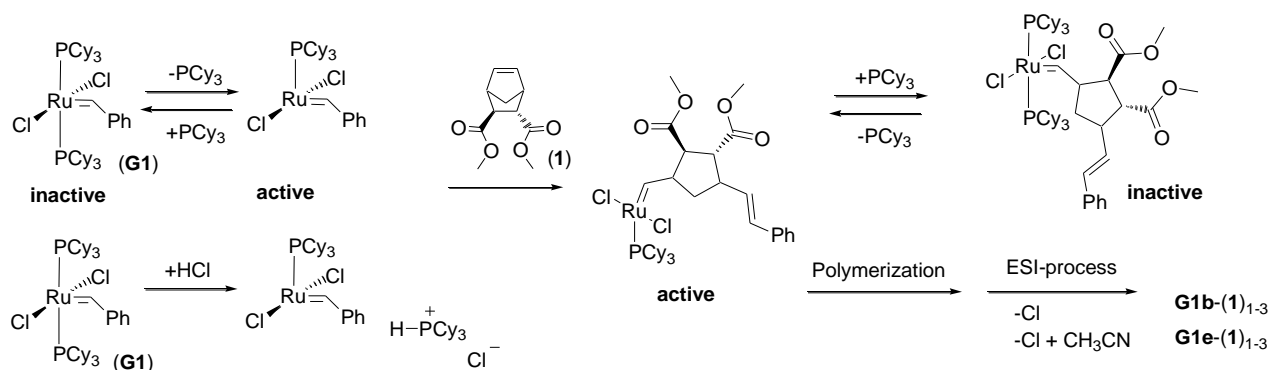


Figure 2.17. ESI-TOF MS spectra in the range of 400 to 1100 m/z, a) reaction of catalyst **G1** with 1 equiv. of monomer **1**, b) reaction of catalyst **G1** with 1 equiv. of monomer **1** with 5 equiv. of hydrochloric acid (solution in diethyl ether).

Thus in both the cases, unreacted catalyst species dominate the mass spectrum. Under the chosen measurement conditions the ruthenium complexes are mainly ionized by loss of chlorine. Acetonitrile as neutral ligand can coordinate to the ruthenium complexes, e.g. **G1d** (828.4 m/z) or **U1e-(1)₁** (858.3 m/z). The species with incorporated monomer are mostly observed as monophosphine complexes, while the unreacted catalyst species are observed as bisphosphine complexes e.g. **G1a**, **G1d**.

To investigate the effect of an additive, the reaction of catalyst **G1** with 1 equiv. of **1** was repeated in the presence of 5 equiv. of hydrochloric acid, since the addition of acid is known to accelerate the ROMP-process by trapping cleaved off phosphine as phosphonium salt thus converting the inactive catalyst in its active form (Scheme 2.18).^{30,31}



Scheme 2.18. Effect of the HCl-addition on the reaction of catalyst **G1** with monomer **1**, and possible ions formed in the ESI-process.

The mass spectrum for this experiment differs considerably from the one obtained for the reaction without acid (Figure 2.17, Appendix, Table 5.2). No bisphosphine species (e.g. **G1a** (787.4 m/z) or **G1d** (828.4 m/z)) are observed in the mass spectrum (see Figure 2.17b). The most prominent peaks can be assigned to monophosphine species with monomer **1** inserted e.g. **G1b-(1)₁** (717.2 m/z), **G1e-(1)₁** (758.3 m/z), **G1e-(1)₂** (968.4 m/z). Peaks for unreacted catalyst can be observed with a lower intensity e.g. **G1b** (507.2 m/z) and **G1c** (471.2 m/z). Thus, addition of acid clearly accelerates the ROMP-process. The absence of bisphosphine species after addition of acid confirms that acid acts as a phosphine scavenger (Figure 2.17b) and indicates a dissociative mechanism in olefin metathesis. A selection of identified ions for catalysts **G1** and **U1** is given in Figures 2.18 and 2.19 respectively.

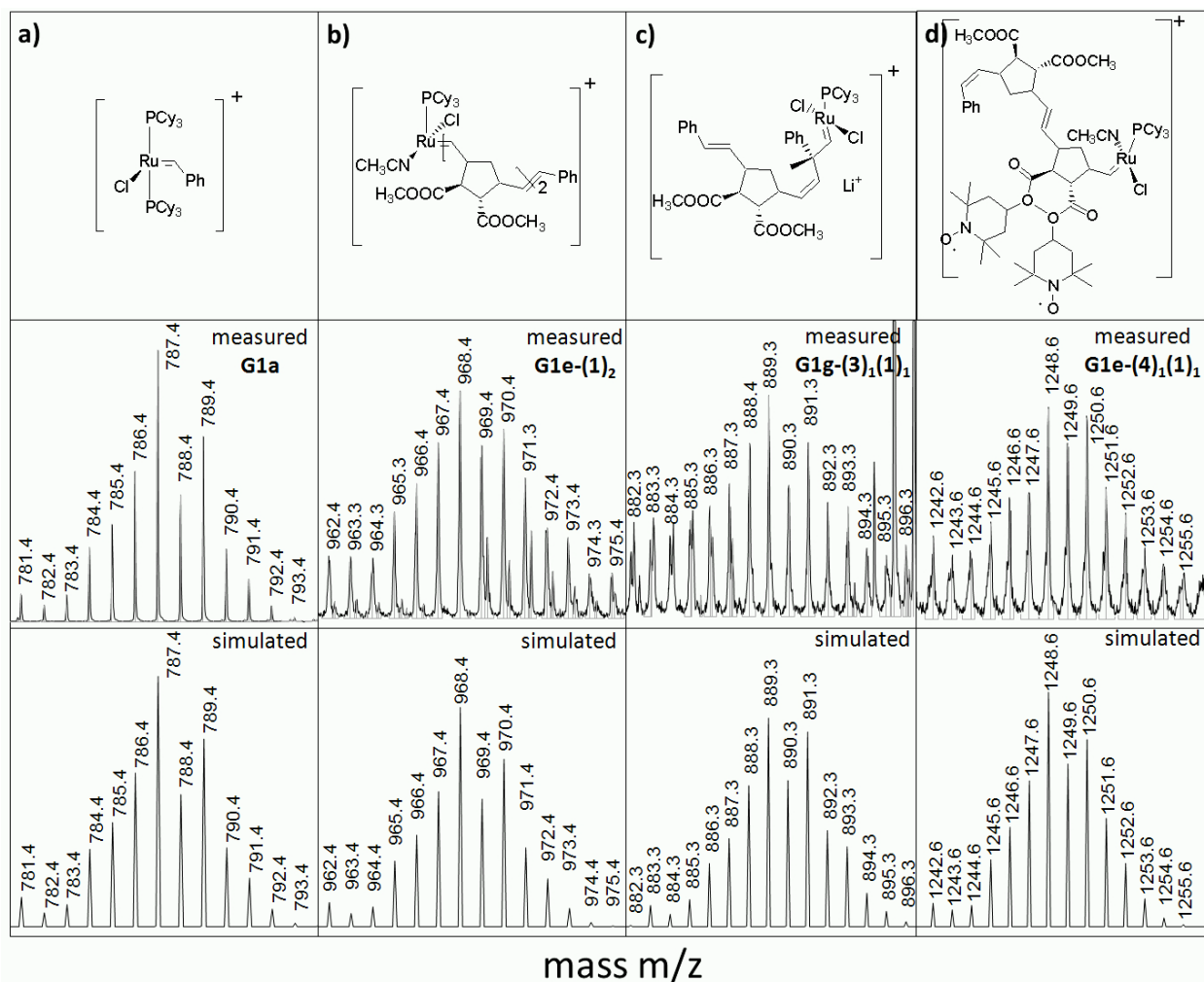


Figure 2.18. Selection of measured and simulated isotopic patterns, (a-b) for the reaction of catalyst **G1** with 1 equiv. of monomer **1**, (c) for the crossover experiment **1/3**, (d) for the crossover experiment **1/4**, a) **G1a**, b) **G1e-(1)₂**, c) **G1g-(1)₁(3)₁**, d) **G1e-(1)₁(4)₁**.

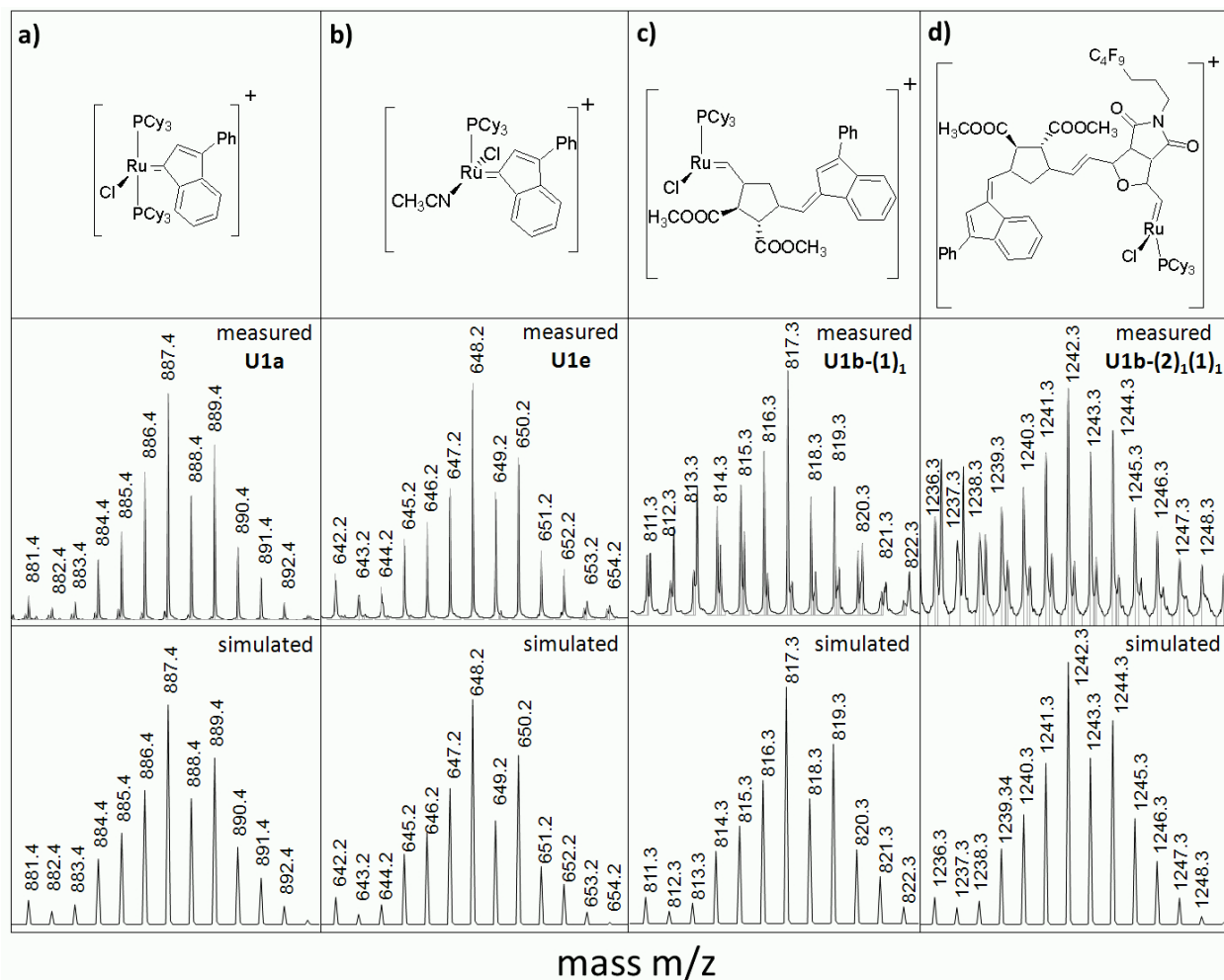


Figure 2.19. Selection of measured and simulated isotopic patterns, (a-c) for the reaction of catalyst **U1** with 1 equiv. of monomer **1**, (d) for the crossover experiment **1/2**, a) **U1a**, b) **U1e**, c) **U1b-(1)₁**, d) **U1b-(1)₁(2)₁**.

2.6.3. Reaction of catalysts **G3**, **U3** with monomer **1**

The experiments were then continued with the reaction of monomer **1** with the third generation catalysts **G3** and **U3**, which differ from their 1st-generation analogues by their *N*-heterocyclic carbene- and pyridine ligands. Since Grubbs catalyst 3rd-generation (**G3**) initiates faster than Grubbs catalyst 1st-generation (**G1**)^{37,41} one can expect a change in the resulting mass spectrum. This change can be seen by the strongly reduced signals of the starting catalyst species compared to the experiment performed with catalyst **G1**.

In the mass spectrum for the reaction of 1 equiv. of monomer **1** with catalyst **G3**, the main peaks can be assigned to oligomer species with up to 8 units of monomer **1** inserted (Appendix, Table 5.4). Ions with monomer **1** attached include **G3a-(1)₁₋₆**, **G3b-(1)₁₋₆**, **G3c-(1)₁₋₆** and **G3e-(1)₁₋₈**. Peaks assigned to unreacted catalyst include e.g. **G3b** (533.1 m/z), **G3c** (497.2 m/z) or **G3h** (443.1 m/z). The peaks with the highest intensity comprise ions without 3-bromopyridine ligand attached ($M - 2L'$), e.g. **G3c-(1)₁** (707.2 m/z), **G3e-(1)₂** (994.3 m/z). Ions with one 3-bromopyridine ligand ($M - L'$), e.g. **G3a-(1)₁** (902.2 m/z), **G3d** (733.1 m/z) are detected with lower intensities compared to ($M - 2L'$) species. This indicates that both ligands are cleaved off in the catalytic cycle to form a propagating 14-electron-species. In consequence, the propagating species formed from Grubbs catalyst 3rd-generation is identical to Grubbs catalyst 2nd-generation. For the same experiment, conducted with catalyst **U3**, the mass spectrum displays a mixture of unreacted catalyst and catalyst with inserted monomer units (Appendix, Table 5.5). The most prominent peaks from the unreacted catalyst appear at 712.2 m/z (**U3a**), 633.2 m/z (**U3b**) and 597.2 m/z (**U3c**). Complex species with incorporated monomer are observed with up to 8 units of monomer **1**, including **U3a-(1)₁₋₇**, **U3b-(1)₁₋₇**, **U3c-(1)₁₋₇** and **U3e-(1)₁₋₈**. The mass spectrum for this experiment is given in Figure 2.20, showing a descending intensity of the oligomer species with increasing chain length. As for catalyst **G3** the peaks with the highest intensities correspond to complex ions with no pyridine ligand attached, e.g. **U3b** (633.2 m/z), **U3c-(1)₁** (807.3 m/z) or **U3e-(1)₁** (884.3 m/z). A selection of identified ions for catalysts **G3** and **U3** is given in Figures 2.21 and 2.22 respectively.

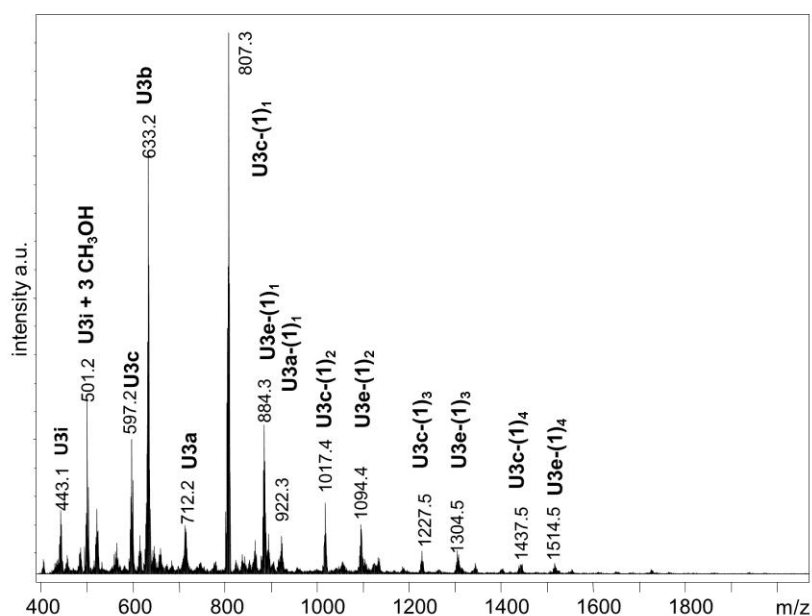


Figure 2.20. ESI-TOF mass spectrum for the reaction of catalyst **U3** with 1 equiv. of monomer **1**.

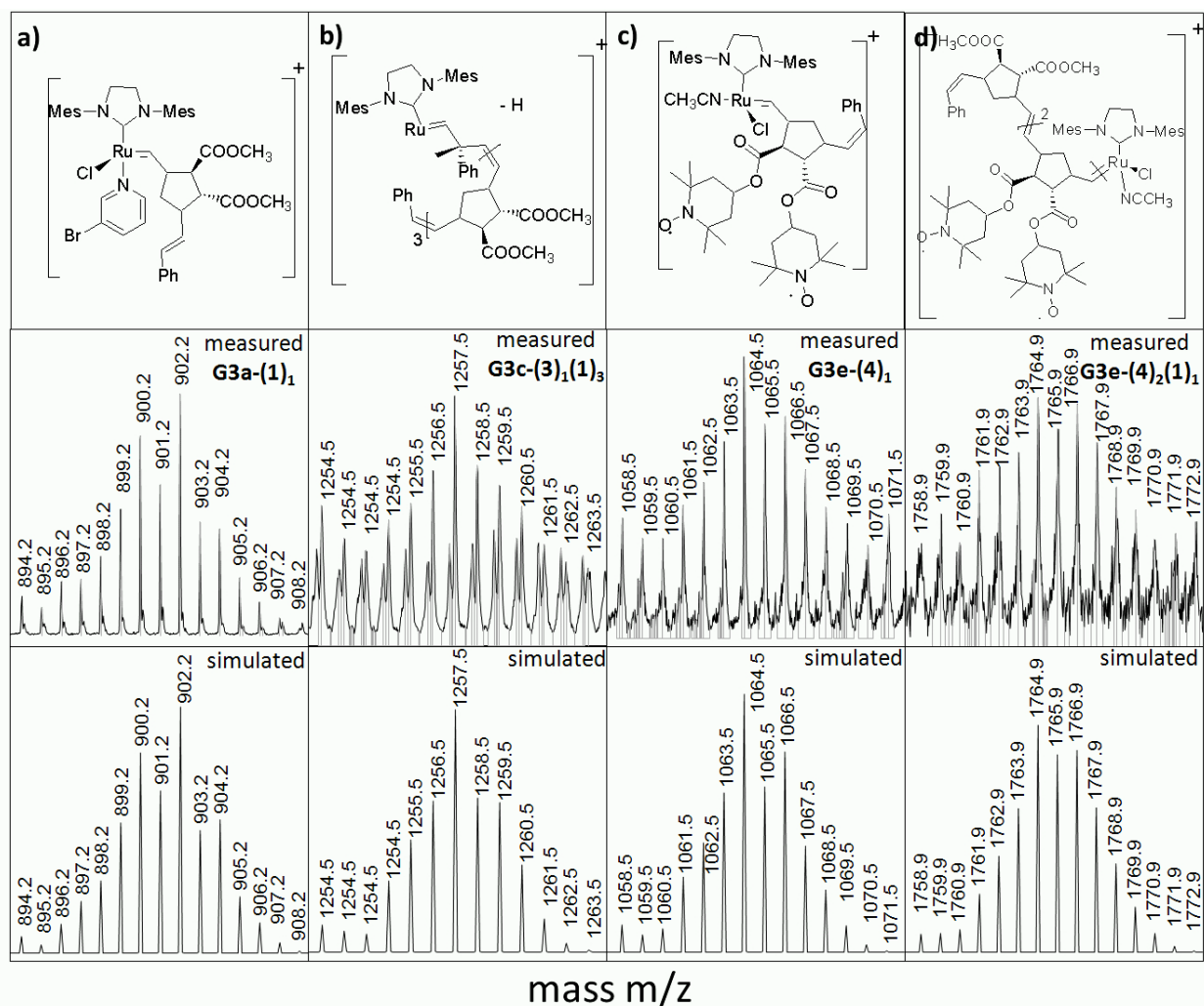


Figure 2.21. Selection of measured and simulated isotopic patterns, (a) for the reaction of catalyst **G3** with 1 equiv. of monomer **1**, (b) for the crossover experiment **1/3**, (c-d) for the crossover experiment **1/4**, a) **G3b-(1)₁**, b) **G3c-(1)₃(3)₁**, c) **G3e-(4)₁**, d) **G3e-(1)₁(4)₂**.

2.6.4. Reaction of catalysts **G1**, **U1** with monomer **1** and subsequent addition of monomers **2-4**

After completion of the reactions with monomer **1**, the set of experiments was extended by the reaction of the catalysts **G1**, **G3**, **U1** and **U3** with 1 equiv. of monomer **1** and subsequent addition of 1 equiv. of the monomers **2**, **3** or **4** (experiments **1/2**, **1/3** and **1/4**). The resulting mixtures were then analyzed analogously by ESI-TOF MS. The mass spectra obtained for the experiments **1/2**, **1/3** and **1/4**, performed with catalyst **G1** (Appendix, Tables 5.6-5.8), do not show a significant change in comparison to the

experiments conducted solely with monomer **1**. The main peaks can be still assigned to unreacted catalyst e.g. **G1a** (787.4 m/z), **G1b** (507.2 m/z), **G1c** (471.2 m/z) or **G1d** (828.4 m/z). Oligomer and co-oligomer species can be detected with significantly lower intensity compared to the peaks of the unreacted catalyst. The existence of oligomer species with only monomer **1** incorporated (up to $(\mathbf{1})_6$, e.g. **G1c-(1)₁** (681.3 m/z), **G1d-(1)₃** (1458.7 m/z) or **G1e-(1)₂** (1178.4 m/z)) shows that the crossover-reaction is not completed after addition of 1 equiv. of the second monomer. This is in agreement with the measurements done for the respective block copolymers via MALDI TOF MS.⁴⁴ Nonetheless, the formation of co-oligomer species up to $(\mathbf{2})_2(\mathbf{1})_x$, $(\mathbf{3})_1(\mathbf{1})_x$ and $(\mathbf{4})_2(\mathbf{1})_x$ could be confirmed for the respective experiments by the detection of the respective ions, e.g. **G1e-(2)₁(1)₁** (1183.3 m/z), **G1f-(3)₁(1)₁** (1169.5 m/z) or **G1e-(4)₂(1)₁** (1738.9 m/z). In case of experiment **1/3** and **1/4**, oligomer species containing solely the second monomer were observed as well e.g. **G1a-(3)₁** (917.5 m/z) or **G1e-(4)₁** (1038.5 m/z) and **G1e-(4)₂** (1528.8 m/z). For the experiments **1/2**, **1/3** and **1/4** with catalyst **U1** (Appendix, Tables 5.10-5.12), the main peaks in the mass spectra are assigned to residual unreacted catalyst e.g. **U1a** (887.4 m/z), **U1b** (607.2 m/z), **U1d** (928.4 m/z) and **U1e** (648.2 m/z). These catalyst species are present in a mixture with oligomer and co-oligomer species after the co-oligomerization reactions. Oligomer species up to $(\mathbf{1})_5$ units, e.g. **U1b-(1)₁** (817.3 m/z) and co-oligomer species up to $(\mathbf{2})_4(\mathbf{1})_x$, $(\mathbf{3})_1(\mathbf{1})_x$ and $(\mathbf{4})_2(\mathbf{1})_x$ can be observed, e.g. **U1e-(2)₃(1)₂** (2343.6 m/z), **U1e-(3)₁(1)₂** (1198.5 m/z), **U1e-(4)₂(1)₁** (1838.9 m/z). No higher co-oligomer species than $(\mathbf{3})_1(\mathbf{1})_x$ were observed in the experiment **1/3** with catalyst **G1** and **U1**. Similar to catalyst **G1**, oligomer-species of the second monomer are observed with monomer **4**, e.g. **U1e-(4)₁** (1138.5 m/z) and **U1e-(4)₂** (1628.8 m/z). The effect of HCl-addition on the crossover efficiency was probed on the experiment **1/3** with catalyst **G1** (Appendix, Table 5.9). The resulting spectrum displays a mixture of unreacted catalyst-species e.g. **G1b** (507.2 m/z), **G1h + Cl + CH₃CN** (493.1 m/z), oligomer species up to $(\mathbf{1})_4$ e.g. **G1b-(1)₃** (1137.4 m/z), **G1e-(1)₄** (1388.5 m/z) and co-oligomer species up to $(\mathbf{3})_2(\mathbf{1})_x$ e.g. **G1b-(3)₁(1)₃** (1267.5 m/z) and **G1g-(3)₂(1)₂** (1229.5 m/z) in similar intensities. In accordance to the experiment conducted solely with monomer **1** and addition of 5 equiv. of HCl no bisphosphine species are detected in the mass spectrum. The higher intensities for oligomer and co-oligomer species clearly show that hydrochloric acid accelerates the ROMP-process and leads to a more efficient crossover reaction. In Figures 2.18 and 2.19, a selection of oligomer and co-oligomer species for catalyst **G1** and **U1** is given respectively.

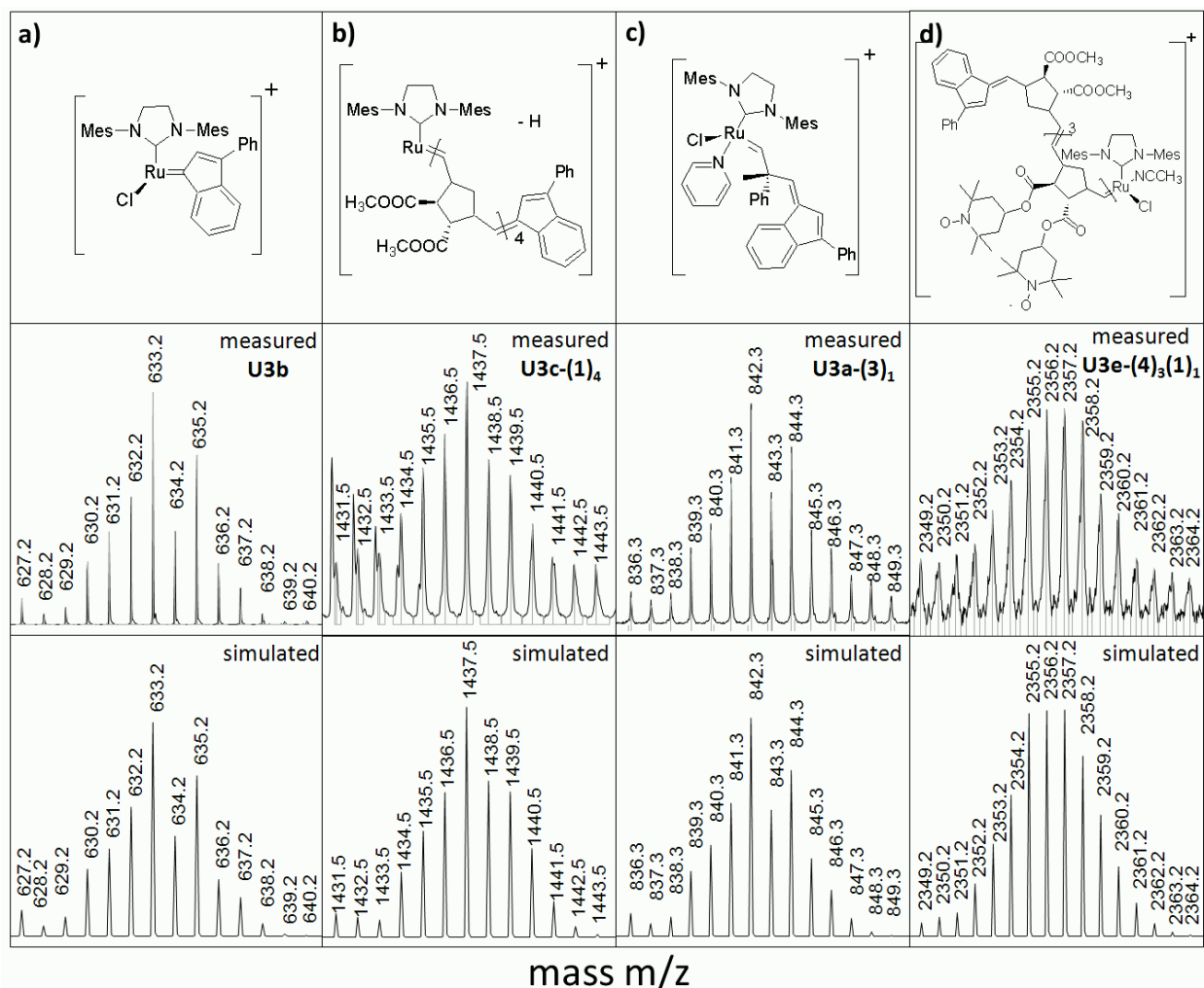


Figure 2.22. Selection of measured and simulated isotopic patterns, (a-b) for the reaction of catalyst **U3** with 1 equiv. of monomer **1**, (c) for the crossover experiment **1/3**, (d) for the crossover experiment **1/4**, a) **U3b**, b) **U3c-(1)₄**, c) **U3a-(3)₁**, d) **U3e-(1)₁(4)₃**.

2.6.5. Reaction of catalysts **G3**, **U3** with monomer **1** and subsequent addition of monomers **2-4**

For the co-oligomerization reactions **1/2**, **1/3** and **1/4** with catalyst **G3** (Appendix, Tables 5.13-5.15), a mixture of unreacted catalyst, e.g. **G3b** (533.1 m/z), oligomer species up to **(1)₆**, e.g. **G3e-(1)₆** (1834.7 m/z) and co-oligomer species up to **(2)₂(1)_x**, **(3)₁(1)_x** and **(4)₃(1)_x**, e.g. **G3j-(2)₂(1)₂** (1926.4 m/z), **G3c-(3)₁(1)₃** (1257.5 m/z), **G3e-(4)₂(1)₄** (2397.1 m/z) are obtained. Species containing only the 2nd monomer are detected in the monomer combinations **1/3** and **1/4**, e.g. **G3c-(3)₁** (627.2 m/z), **G3e-(4)₁** (1064.5 m/z).

It has to be mentioned that for the reaction **1/2**, oligomer and co-oligomer species for all catalysts appear in a similar mass range, which often leads to overlapping peaks which makes the detection of certain species difficult.

For the co-oligomerization reactions with catalyst **U3** (Appendix, Tables 5.16-5.18), a similar picture to catalyst **G3** is observed. After the crossover reaction with the second monomer, a mixture of unreacted catalyst, e.g. **U3a** (712.2 m/z), **U3b** (633.2 m/z), **U3c** (597.2 m/z) oligomer species up to $(\mathbf{1})_6$, e.g. **U3e- $(\mathbf{1})_6$** (1934.7 m/z) and co-oligomer species up to $(\mathbf{2})_4(\mathbf{1})_x$, $(\mathbf{3})_1(\mathbf{1})_x$ and $(\mathbf{4})_4(\mathbf{1})_x$, e.g. **U3e- $(\mathbf{4})_4(\mathbf{1})_1$** (2584.5 m/z), **U3g- $(\mathbf{3})_1(\mathbf{1})_1$** (1015.3 m/z), **U3e- $(\mathbf{4})_3(\mathbf{1})_2$** (2567.3 m/z), is obtained. These co-oligomer species confirm the successful crossover reaction. However, neither with catalyst **G3** nor with catalyst **U3**, the crossover is complete after the addition of the 2nd-monomer **2**, **3** or **4**, proven by the presence of residual oligomer species $(\mathbf{1})_x$ composed solely of monomer **1**. This complies with the results obtained for catalyst **G3** during the investigation of the block copolymers via MALDI-TOF MS (chapter 2.5).⁴⁴

Similar to the catalyst **G3**, oligomer species of the second monomer are observed with catalyst **U3** up to $(\mathbf{2})_2$, $(\mathbf{3})_1$ and $(\mathbf{4})_2$, e.g. **U3e- $(\mathbf{2})_2$** (1524.3 m/z), **U3c- $(\mathbf{3})_1$** (727.3 m/z), **U3e- $(\mathbf{4})_2$** (2145.1 m/z) as a consequence of the reaction of unreacted catalyst with the 2nd-monomer (**2**, **3** or **4**). In case of catalysts **G3** and **U3**, the propagation of the 2nd monomer is only observed in the combinations of **1/2** and **1/4**. In the reaction **1/3**, the propagation stops after insertion of one unit of **3**. This observation was made with all applied catalysts (**G1**, **G3**, **U1** and **U3**) except experiment **1/3** conducted with catalyst **G1** and addition of 5 equiv. of hydrochloric acid. This can be explained with the low reaction rate of monomer **3** with these catalysts caused by the steric hindrance of the phenyl group attached to the cyclopropene ring.⁴⁴ A selection of detected species for catalysts **G3** and **U3** is given in the Figures 2.26 and 2.27 respectively. More measured and simulated isotopic patterns are given in the appendix (Figures 5.38-5.48).

2.6.6. ESI-TOF MS semi-quantification

As it was seen in the previous chapter (2.5. Investigation of the crossover step in block copolymerization reactions via MALDI-TOF MS) quantitative statements from mass spectra are difficult to make, since species which differ in their chemical structure or molecular weight can possess different probabilities of ionization^{44,147,148,151} and the measuring conditions affect the obtained results. Nonetheless, a quantification of the detected species via ESI-TOF MS was done for a better comparison. The fraction of an individual ion was thereby derived from the sum of intensities of a single isotopic pattern in

comparison with the sum of the intensities of all identified peaks. Ions without monomer attached and with oligomer or co-oligomers attached were grouped for a better overview, comparing benzylidene complexes **G1** and **G3** as well as indenylidene catalysts **U1** and **U3** (Table 2.10).

Table 2.10. Quantification of the catalyst-species for the reaction of 1 equiv. monomer **1** and 1 equiv. of **1** + 1 equiv. of monomer **2-4** with the catalysts **G1**, **G3** and **U1**, **U3** measured via ESI-TOF.

Reaction			ESI-TOF MS quantification			
entry	experiment	catalyst	catalyst %	(1) %	(2, 3, 4) (%)	COS (%)
1	1	G1	90.2	9.8	-	-
2	1	G1 + 5 equiv. HCl [*]	7.3	92.7	-	-
3	1	G3	12.9	87.1	-	-
4	1	U1	95.4	4.6	-	-
5	1	U3	65.6	34.6	-	-
6	1/2	G1	96.9	2.4	-	0.7
7	1/2	G3	12.5	82.2	-	6.3
8	1/2	U1	91.0	6.3	-	2.7
9	1/2	U3	77.4	18.8	1.6	2.2
10	1/3	G1	88.2	10.3	-	1.5
11	1/3	G1 + 5 equiv. HCl [*]	33.9	39.8	-	26.3
12	1/3	G3	8.7	70.5	3.5	17.3
13	1/3	U1	91.9	5.9	-	2.2
14	1/3	U3	62.8	30	3.9	3.3
15	1/4	G1	93.9	4.6	0.9	0.9
16	1/4	G3	21.0	44.8	14.0	22.2
17	1/4	U1	94.2	4.3	0.9	0.6
18	1/4	U3	73.3	13.3	9.7	3.7

Catalyst (%): Fraction of catalyst-species with no monomer attached, (**1**) (%): Oligomer species containing only monomer **1**, (**2, 3, 4**) (%): Oligomer-species containing only monomer **2, 3** or **4**, COS: Co-oligomer-species containing monomer **1** and either monomer **2, 3** or **4**, * solution of hydrochloric acid in dry diethyl ether.

For more detailed information on the individual ions see also appendix, Tables 5.1-5.18. It is worth to mention that the values in Table 2.10 are derived under the assumption of equal probability of ionization, irrespective of molecular weight or chemical structure and assigning the ionic species displaying no carbene ligand to the unreacted catalyst fraction. Therefore, these values do not represent absolute values but estimation.

For the reaction of monomer **1** with catalyst **G1** or **G3**, the fractions of the species show significant differences (Table 2.10). In case of catalyst **G1**, pure catalyst species dominate the mass spectrum with a fraction of 90 % (Table 2.10, entry 1). The reverse picture is seen with catalyst **G3** where the main fraction is formed by oligomer species (**1**)_x with a fraction of 87 % (Table 2.10, entry 3). When the reaction of monomer **1** with catalyst **G1** was performed in the presence of 5 equiv. of hydrochloric acid, the fraction of pure catalyst species is clearly decreased from 90% to 7%, while the fraction of oligomer species is increased from 10 to 93 % (Table 2.10, entry 2). For the crossover experiments **1/2**, **1/3** and **1/4** with catalyst **G1** (Table 2.10, entries 6, 10, 15), the values for the different fractions resemble each other with only small fractions of co-oligomer species (1%).

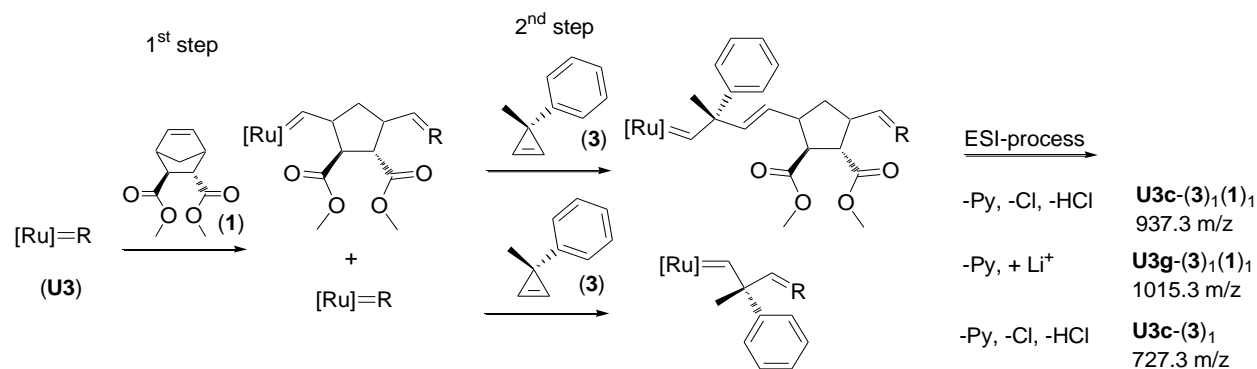
In contrast to catalyst **G1**, higher amounts of oligomer and co-oligomer species are observed with catalyst **G3** (Table 2.10, entries 7, 12 and 16). However, the main fraction is still composed of oligomer species containing solely monomer **1**. In case of catalyst **G3**, the highest amounts of co-oligomer species are visible for the experiments **1/3** and **1/4** with 17 % and 22 %, respectively. The crossover experiment **1/3** conducted with catalyst **G1** and addition of 5 equiv. HCl shows a significant change to the experiment conducted without acid (Table 2.10, entries 10, 11). The fraction of unreacted catalyst species is decreased from 87 to 33 while the fractions of oligomer species (**1**)_x and co-oligomer species are increased from 10 % to 40 % and 1 % to 26 % respectively. Additionally, it is the only experiment where species are observed with more than one unit of monomer **3** inserted, e.g. **G1g-(3)₂(1)₂** (1229.5 m/z). Thus, catalyst **G1** with HCl as additive gives similar results as catalyst **G3**, judging from the fractions of oligomer and co-oligomer species (Table 2.10, entries 11 and 12).

The same trend as for the catalysts **G1** and **G3** can be observed for the indenylidene catalysts **U1** and **U3**. In case of catalyst **U1**, similar to catalyst **G1**, pure catalyst species dominate the mass spectrum (Table 2.10, entry 4). In accordance with catalyst **G3**, a significant increase in oligomer species is observed with catalyst **U3** (Table 2.10, entry 5). In the crossover experiments **1/2**, **1/3** and **1/4**, catalyst **U1** gives similar results to catalyst **5** with only small fractions of co-oligomer species (0.6-2.7 %) in the mixture (Table 2.10, entries 8, 13 and 17). The highest fraction on co-oligomer species is observed for the experiment **1/2** with 2.7 %. In accordance to catalyst **G3**, higher amounts of oligomer and co-

oligomer species, can be detected in the crossover experiments with catalyst **U3** in comparison with catalyst **U1**, e.g. Table 2.10, entries 14 and 18. The highest amounts of co-oligomer species (22 %) with catalyst **U3** are observed in the experiment **1/4** along with a significant amount (10 %) of oligomer species (**4**)_x (Table 2.10, entry 18).

2.6.7. Connecting ESI-TOF MS semi-quantification with NMR-kinetics

According to the kinetic investigations performed on the polymerization of monomer **1** (chapter 2.2.), the low values for species containing monomer **1** or crossover species for catalyst **G1** and **U1** can be explained by the initiation behavior of these catalysts. Only a fraction of the catalyst is reacting with the monomer **1**, generating oligomer species and therefore leaving unreacted catalyst in the mixture after addition of 1 equiv. of monomer **1**. The reaction of the subsequently added monomers **2**, **3** or **4** with a mixture of propagating species and unreacted catalyst is subjected again to an initiation process generating co-oligomer-species and oligomer species (Scheme 2.19) containing exclusively the 2nd monomer (Table 2.10, entries 9, 12, 14, 16 and 18). These newly formed species would be present in a mixture with unreacted catalyst and oligomer species from monomer **1** attached to the catalyst (Table 2.10, entries 10, 12, 14-18). Only for catalyst **G3**, the rate of initiation exceeds the rate of propagation, leading to a small amount of residual catalyst. In contrast to catalyst **G3**, a significant amount of unreacted catalyst resides in the experiments with catalyst **U3**. This can again be explained by the k_p/k_i ratio which amounts 3.82 for catalyst **U3**. A residual amount of unreacted catalyst cannot be avoided for the third generation catalysts since the mixing of monomer and catalyst solution is slow compared to the polymerization rate.

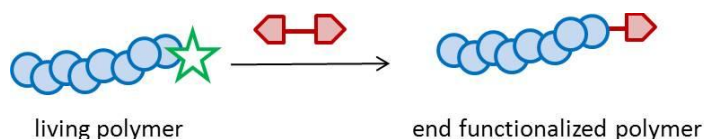


Scheme 2.19. Formation of oligomer species of the 2nd monomer on the example of experiment **1/3** with catalyst **U3**, Py: pyridine (C₅H₅N), R: indenylidene (C₁₅H₁₀).

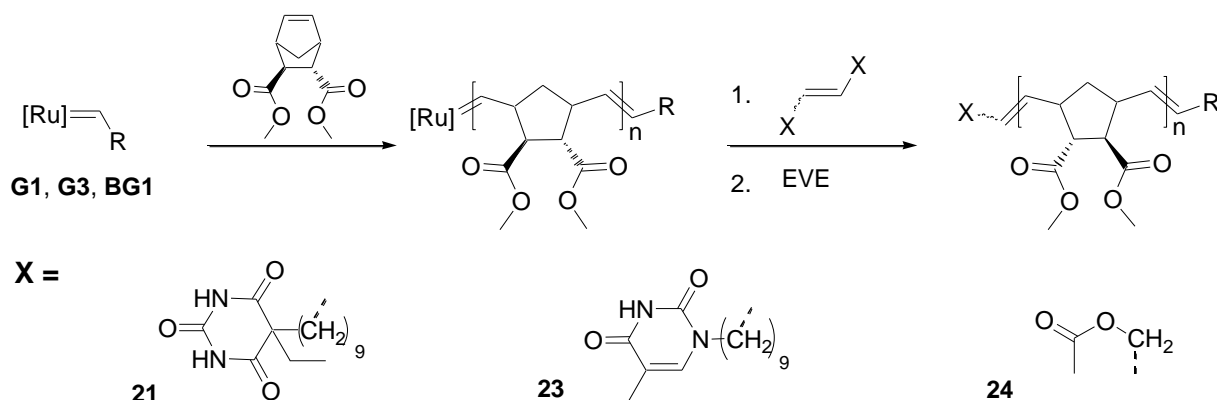
Summary of chapter 2.6.

ROMP of non-charged monomers in oligomerization and co-oligomerization reactions can be monitored by ESI-TOF MS using the method of Metzger et al.⁷⁸ Co-oligomer species could be detected in all three systems **1/2**, **1/3** and **1/4** confirming the occurring crossover reaction. Propagation of the second “block” is only observed in the combinations **1/2**, **1/4** indicative of the higher reactivity of the oxo-norbornene **2** and norbornene **4** compared to the cyclopropene **3**. Propagation of **3** required the addition of hydrochloric acid, which proved to be an efficient accelerator for ROMP-reactions. The results obtained are in agreement to the investigations via MALDI-TOF MS (chapter 2.5), showing an incomplete crossover reaction after addition of 1 equiv. of a monomer. The measured spectra display a significant difference between the reactions conducted with 1st (**G1**, **U1**) and 3rd-generation catalysts (**G3**, **U3**) as a result of the different k_p/k_i ratios and reactivities of the tested catalysts. The highest fractions of oligomer- and co-oligomer species were observed with catalyst **G3**.

2.7. End functionalization of poly(**1**) with symmetric olefins



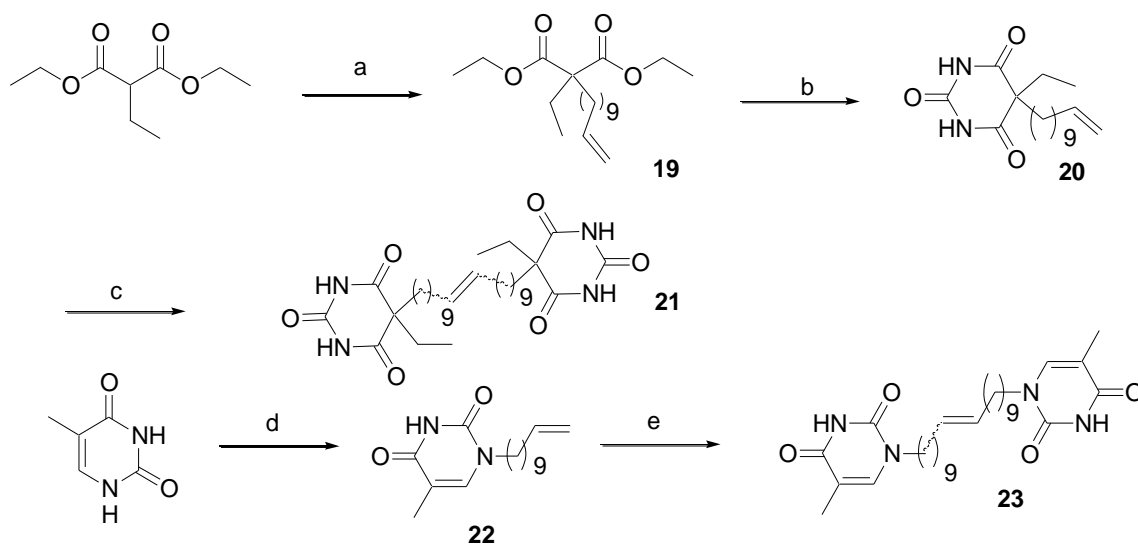
The cross over reaction plays not only a crucial role in block copolymerization reaction but also in the introduction of functional end groups by termination of the living polymer chain. In block copolymerization reactions, the living chain end performs a cross metathesis with a second monomer and propagates further. In contrast to this, in termination reactions, the living chain end is cleaved off in the process. The cross metathesis of the living polymer species with symmetric olefins was chosen as type of reaction since it allows to attach complex functional moieties in a single reaction step (Scheme 2.20). Thymine- as well as barbituric acid moieties at the symmetric olefins (**21**, **23**) were selected as end groups, as they are able to build up supramolecular interactions (H-bonding).^{112,153-167} In order to study the cross over step in termination reactions, living poly(**1**) chains, initiated with the catalysts **G1**, **G3** or **BG1**, were reacted with the symmetric olefins **21**, **23** and **24** (Scheme 2.20).



Scheme 2.20. End functionalization of poly(**1**) via symmetric terminating agents. Semi-telechelic polymers for catalysts **G1**, **G3** and telechelic polymers for catalyst **BG1** are generated, EVE: ethyl vinyl ether.

2.7.1. Quencher synthesis

Two olefins bearing thymine and barbiturate moieties were synthesized as quenchers. The third olefin used for quenching of poly(**1**) is the commercial available *cis*-1,4-bisacetoxy-2-butene (**24**). This compound was already successfully applied by Matson and Grubbs for the end functionalization of poly(norbornene dicarboxyimides).¹² The barbiturate containing olefin (**21**)^{156,168} was prepared in a three step process (Scheme 2.21). In the first step diethyl 2-ethylmalonate was converted to diethyl 2-ethyl-2-(undec-10-enyl)malonate (**19**) via nucleophilic substitution with bromoundecene in 63% yield. The ¹H NMR spectrum (see appendix, Figure 5.49) shows the significant resonances for the terminal double bond at 5.80 and 4.96 ppm.



Scheme 2.21. Synthesis of the terminating agents **21** and **23** (a) 11-bromoundecene, sodium hydride (63 %), (b) urea, sodium hydride (63 %), (c) catalyst **G2**, copper(I) iodide (74 %), (d) HDMS, TMSCl, 11-bromoundecene (61 %), (e) catalyst **G2**, copper(I) iodide (60 %).

In the second step urea was deprotonated with sodium hydride and reacted with compound **19** to generate **20** in 63% yield. The ¹H NMR (see appendix, Figure 5.50) shows the NH-protons of the newly formed ring at 8.88 ppm and the disappearance of the ester-groups from compound **19** at 4.17 ppm (CH₃-CH₂-OC(O)). The second α -olefin **22**, based on thymine, was prepared by reaction of thymine with HMDS and TMSCl and subsequent nucleophilic substitution with 11-bromoundecene¹⁶⁹ in a yield of 61%. The ¹H NMR (see appendix, Figure 5.55) shows the protons of the terminal olefinic group at 5.80 and

4.96 ppm. The respective α -olefins **20** and **22** were then converted to the symmetric bivalent olefins **21** and **23** in a homo metathesis step using Grubbs-catalyst 2nd-generation.

Two methods for the homo metathesis were investigated. The first one is the acceleration of the reaction via microwave irradiation (DCM, 100°C, 30 W). In a second approach, the addition of 3 mol% copper(I) iodide was performed.³² Better conversions were achieved by the addition of copper iodide, which acts as phosphine scavenger, thus leading to a higher concentration of the active catalyst species in the reaction cycle. Additionally, this method allowed the catalyst loading to be decreased from 5 mol% to 2 mol% in comparison to the reaction performed under microwave conditions. Compounds **21** and **23** were obtained in yields of 74 and 60% respectively. The formation of the internal olefins **21** and **23** can be observed in the ¹H NMR by the formation of the resonance at 5.36 ppm and 5.37 ppm respectively (Figure 2.23), together with a disappearance of the resonances of the vinyl-group from the α -olefins at 5.80 and 4.96 ppm. In Figure 2.28, the ¹H NMR spectra of the symmetric olefins are depicted. The products (**21**, **23**) obtained from the homo metathesis are a mixture of *cis*- and *trans*-olefin.

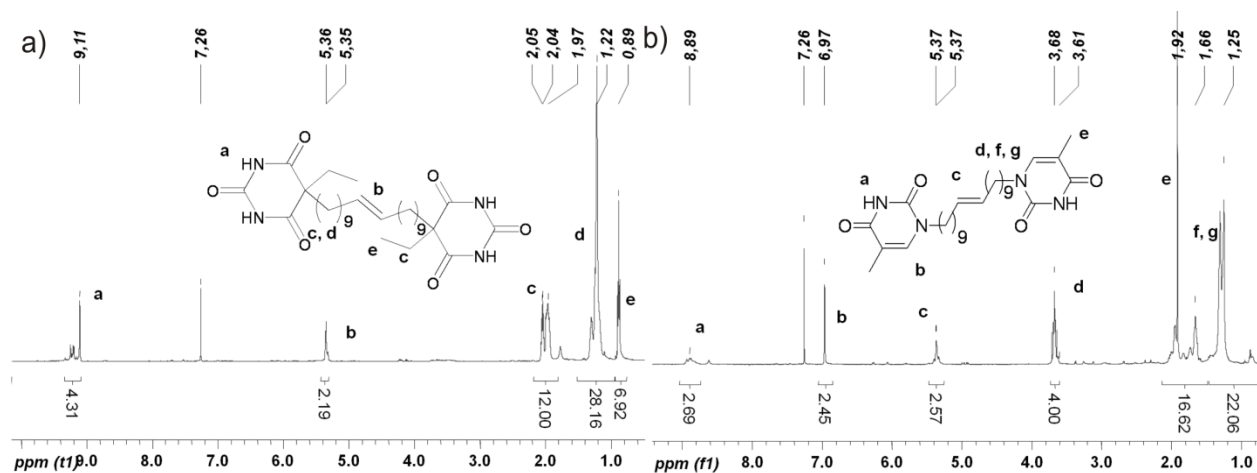


Figure 2.23. ¹H-NMR spectra of symmetric terminating agents, a) compound **21**, b) compound **23**.

Compound **21**, for example, displays two resonances in the ¹³C NMR (see appendix, Figure 5.54) at 130.35 ppm (*trans* olefinic carbon) and 129.86 ppm (*cis* olefinic carbon).¹⁷⁰ From the intensity in the ¹³C NMR, the ratio of *trans*- to *cis*- configured olefin can be estimated to be 3.3 / 1 for compound **21** and 2.1 / 1 for compound **23** (see appendix, Figure 5.57 for ¹³C NMR).

2.7.2. Termination of living chains with α -olefin **20** and symmetric olefin **24**

Symmetric olefins were chosen for the termination reactions because quenching of polymers with asymmetric olefins results in two products. This could be seen in the reaction of poly(**1**) with the α -olefin **20** (Table 2.11, entry 1). The MALDI-TOF spectrum for this reaction (see appendix, Figure 5.58) revealed two series which are assigned to methylene capped poly(**1**) $[M+Na]^+$ as main series and barbiturate capped poly(**1**) $[M+Na]^+$ as side series. The formation of methylene-terminated polymer is preferred in contrast to barbiturate capped polymer according to the intensity ratio of methylene capped polymer to barbiturate capped polymer. This is in agreement with quenching experiments using allylacetate by Grubbs et al., showing a preference for the formation of methylene capped polymer.¹⁰⁴ A possible explanation for the preference of methylene capped polymer is that the polar barbiturate moiety complexes with the ruthenium center and by this influences the product distribution. In contrast to this, the termination reaction with symmetric olefins generates just one set of products. Thus, they are better suited for the preparation of end functionalized polymers.

Table 2.11. GPC and MALDI-TOF MS results for poly(**1**) quenched with compounds **20** and **24** as terminating agents.

entry	cat.	TA	equiv. TA	time (h)	M_n (GPC) g/mol	PDI (GPC)	M_n^a MALDI m/z	PDI ^a MALDI	M_p^b MALDI m/z	$I(\text{meth})/I(\text{eg})^c$
1	G1	20	10	24	4200	1.18	3993	1.11	3911.1	49 ^d
2	G1	24	10	24	5000	1.21	4614	1.13	5228.4	0.21
3	G3	24	10	24	9700	1.19	13317	1.05	14917.5	^e
4	BG1	24	10	24	6400	1.39	8200	1.24	8920.6	^f

^a calculated with Polytools software, ^b mass of the peak with the highest intensity, ^c ratio of intensities of methylene terminated poly(**1**) and poly(**1**) bearing functionalized end group, ^d quenching efficiency determined by MALDI-quantification: 38%, ^e full conversion, no methylene capped species detected, ^f ratio semi telechelic to telechelic acetoxy capped polymer = 0.09, monomer to catalyst ratio (calculated molecular weight): 25 (5640 g/mol) for entry 1, 25 (5431 g/mol) for entry 2, 30 (6482) for entry 3, 25 (5530 g/mol) for entry 4.

In a model reaction, living poly(**1**) chains, initiated with catalyst **G1**, were terminated with symmetric olefin **24**. Final quenching was performed with ethyl vinyl ether. The MALDI spectrum for this product shows a mixture of semi telechelic acetoxy capped poly(**1**), e.g. $[(C_{11}H_{14}O_4)_{19}C_{11}H_{12}O_2Na]^+$ as main series and methylene capped poly(**1**), e.g. $[(C_{11}H_{14}O_4)_{20}C_8H_8Na]^+$ as side series (Figure 2.24a). When poly(**1**)

chains, initiated with catalyst **G3**, were terminated with compound **24**, only semi telechelic acetoxy capped poly(**1**) was observed in the MALDI-spectrum, e.g. $[(C_{11}H_{14}O_4)_{62}C_{11}H_{12}O_2Na]^+$ (Figure 2.24b). Thus, poly(**1**) chains initiated with **G3** are more reactive in the reaction with symmetric olefins. With the bivalent catalyst **BG1** it was possible to generate telechelic acetoxy capped poly(**1**). The MALDI spectrum displays two series which are assigned to telechelic acetoxy capped poly(**1**), e.g. $[(C_{11}H_{14}O_4)_{28}C_8H_{12}O_4Na]^+$ as main series and semi telechelic acetoxy capped poly(**1**), e.g. $[(C_{11}H_{14}O_4)_{29}C_{11}H_{12}O_2Na]^+$ as side series (Figure 2.24c-d). Thus, the symmetric olefin **24** proved to be a highly reactive quencher, generating acetoxy capped poly(**1**) in high efficiencies. These results are comparable with the work of Matson and Grubbs,¹² showing termination efficiencies for compound **24** of up to 97%, calculated by NMR-spectroscopy.

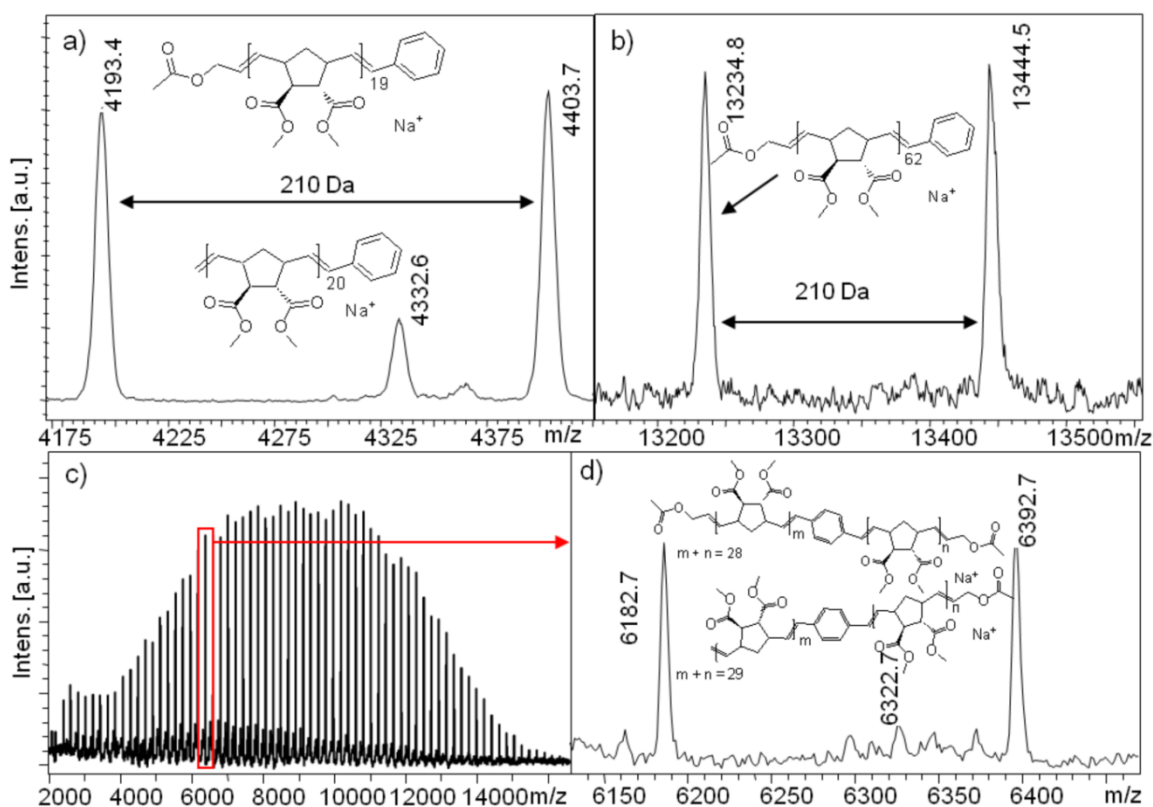


Figure 2.24. MALDI-TOF MS spectra of poly(**1**) quenched with *cis*-1,4-bisacetoxy-2-butene (**24**), a) with **G1**, 10 equiv. of **24**, 24h, enlargement from 4175 to 4425 m/z, b) initiated with **G3**, 10 equiv. of **24**, 24h, enlargement from 13150 to 13500 m/z, c) with **BG1**, 10 equiv. of **24**, 24h, full spectrum, d) enlargement from 6100 to 6500 m/z, final quenching with ethyl vinyl ether.

2.7.3. Termination of living chains with compound **21**

The terminating agents (TA) **21** and **23** were reacted analogously to compound **24** with the living poly(**1**)-chains, initiated with catalysts **G1** and **G3**. Ethyl vinyl ether was added at the end of the reaction to terminate all remaining chains. The excess of the symmetric olefins **21** and **23** was subsequently removed by column chromatography. The efficiency of the quenching reaction with the olefins **21** and **23** was investigated by varying the reaction time (1-100 h) as well as the amount of terminating agent with respect to the living end group (TA/C = 1/1 - 20/1), (Table 2.12, entries 1, 4, 8) and (Table 2.13, entry 1, 3). The incorporation of the end group could be proven by NMR-spectroscopy as shown in Figure 2.25 on the example of poly(**1**) reacted with 2 equiv. of compound **21** for 2 h.

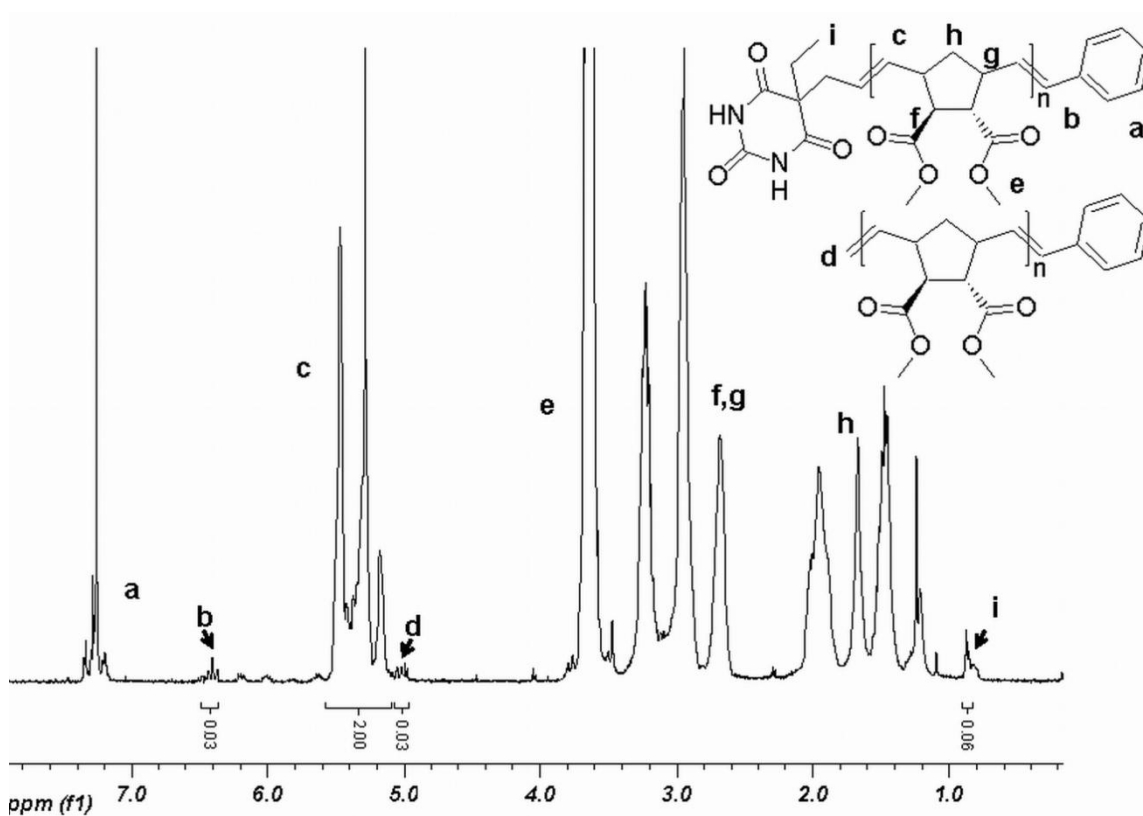


Figure 2.25. ^1H -NMR-spectrum for poly(**1**) initiated with **G1**, quenched with 2 equiv. of **21** for 2h.

A resonance of the benzyldiene end group can be seen at 6.40 ppm ($=\text{CH}-\text{Ph}$). The resonances appearing at 4.99 ppm and 0.87 ppm can be assigned to the methylene end group ($=\text{CH}_2$) and the methyl group of the barbiturate end group, respectively. An integration of these end group signal gives a ratio of 1.33/1

of barbiturate-end groups vs. the methylene-end groups and thereby an efficiency of the quenching reaction of 57 %. The polymers, obtained from the quenching reactions were investigated via MALDI-TOF MS.^{171,172} In most of the cases, the mass spectra of the end functionalized polymers (Figures 2.26, 2.27, 2.28) show two series, which could be assigned to the methylene capped polymer and functionalized polymer. Extracted from the mass spectrum, the ratio of methylene capped polymer to functionalized polymer (Table 2.12, 2.13) gives an indication of the quenching efficiency. This ratio is derived from the intensities of both species, which are calculated according to equation 1. Simplified, the total intensity of each species is obtained from the sum of single intensities multiplied with the degree of polymerization.

$$I_t = \sum I_p \times \frac{M_P - M_{E1} - M_{E2} - M_C}{M_R}$$

Equation 1. I_t : total intensity of a species, I_p : intensity of a single peak, M_{E1} , M_{E2} , mass of end groups, M_C : mass of cation, M_R : mass of repetition unit

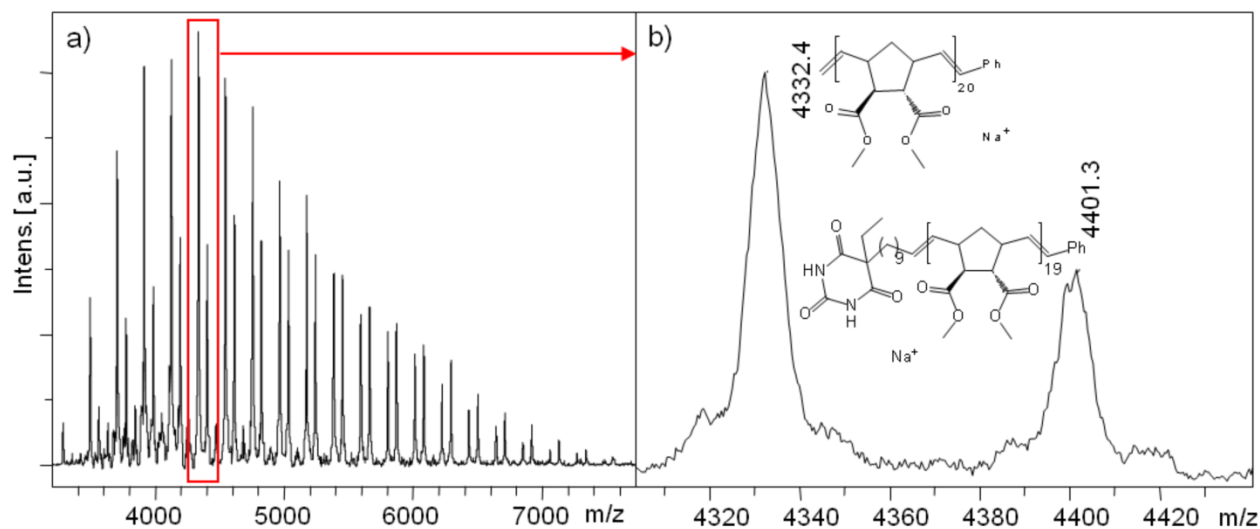


Figure 2.26. MALDI-TOF MS spectrum of poly(**1**) initiated with **G1** and quenched with 5 equiv. of TA **21** for 100 h, a) full spectrum b) enlargement from 4310 to 4430 m/z.

In Figure 2.26, the MALDI-TOF spectrum of poly(**1**) initiated with catalyst **G1** and quenched with 5 equiv. of **21** for 100 h is depicted. The mass distance between the peaks of the individual series is $m/z = 210$ Da which corresponds to the mass of monomer **1**. In the enlarged spectrum (Figure 2.31 b), two series are observed, which can be assigned to methylene-capped poly(**1**), e.g. $[(C_{11}H_{14}O_4)_{20}C_8H_8Na]^+$ as main series and barbiturate capped poly(**1**), e.g. $[(C_{11}H_{14}O_4)_{19}C_{23}H_{32}N_2O_3Na]^+$ as side series.

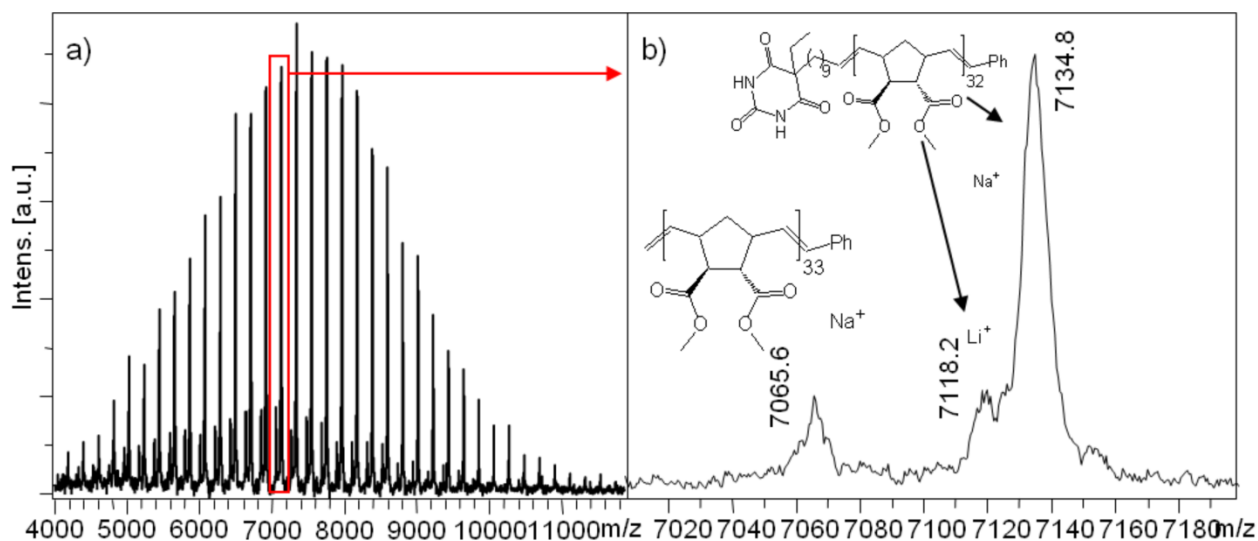


Figure 2.27. MALDI-TOF MS spectrum of poly(**1**) initiated with **G3** and quenched with 20 equiv. of TA **21** for 100 h, a) full spectra b) enlargement from 7000 to 7200 m/z, for comparison of measured spectrum and simulated isotopic patterns see appendix, Figure 5.59.

In Figure 2.26, the MALDI-TOF spectrum of poly(**1**) initiated with catalyst **G3** and quenching with 20 equiv. of **21** for 100 h is depicted. An enlargement of the spectrum (Figure 2.32 b) shows three series with barbiturate capped poly(**1**), e.g. $[(C_{11}H_{14}O_4)_{32}C_{23}H_{32}N_2O_3Na]^+$ as main series. The two side series are assigned to barbiturate capped poly(**1**) ionized with lithium e.g. $[(C_{11}H_{14}O_4)_{32}C_{23}H_{32}N_2O_3Li]^+$ and methylene-capped poly(**1**), e.g. $[(C_{11}H_{14}O_4)_{33}C_8H_8Na]^+$. According to the mass spectra, the change from catalyst **G1** to **G3** leads to a significant decrease of the methylene capped species (Figure 2.26b, 2.27b). The best results were achieved by reacting poly(**1**) chains, initiated with **G3**, with 20 equiv. of the terminating agent (**21**) for 100 h.

Table 2.12. GPC and MALDI-TOF MS results for poly(**1**) quenched with compound **21**.

entry	cat.	equiv. TA (21)	time (h)	M _n (GPC) g/mol	PDI (GPC)	M _n ^a MALDI m/z	PDI ^a MALDI	M _p ^b MALDI m/z	I(meth)/I(barb) ^c	corrected value ^d
1	G1	1	2	5500	1.15	5969	1.05	4750.6	50	1.6 (38.5 %)
2	G1	2	2	5400	1.31	5861	1.05	4960.8	14.3	0.47 (68 %)
3	G1	5	2	5400	1.23	5724	1.05	5380.9	3.2	0.11 (90 %)
4	G1	10	2	5200	1.22	5907	1.03	5590.4	2.4	0.077 (93 %)
5	G1	5	20	6500	1.24	6172	1.06	4751.3	1.6	0.050 (95.2 %)
6	G1	5	100	4400	1.32	4661	1.03	4332.8	1.4	0.046 (96 %)
7	G3	5	50	8000	1.18	10583	1.05	11547.0	2.0	0.0645 (94 %)
8	G3	20	50	7600	1.19	9867	1.07	11267.1	0.47	0.015 (98.5 %)
9	G3	20	100	6400	1.15	7429	1.03	7346.2	0.17	0.005 (99.5 %)

^a calculated with Polytools software, ^b mass of the peak with the highest intensity, ^c ratio of intensities of methylene terminated poly(**1**) and poly(**1**) bearing barbiturate end group, ^d corrected intensity ratio by applying the desorption, ratio from the quantification, monomer to catalyst ratio (calculated molecular weight): 25 (5640 g/mol) for entries 1-6, 30 (6691 g/mol) for entries 7-9, for the ratio of methylene capped polymer to end functionalized polymer, only the species ionized with sodium were taken into consideration.

2.7.4. Termination of living chains with compound **23**

Symmetric olefin **23** was reacted analogously with living poly(**1**) chains (Table 2.13). In Figure 2.28a, the enlarged MALDI-TOF spectrum of poly(**1**) initiated with **G1** and quenched with 5 equiv. of compound **23** for 100h is shown. The main series is assigned to methylene capped poly(**1**), e.g. [(C₁₁H₁₄O₄)₂₃C₈H₈Na]⁺. Thymine capped poly(**1**), e.g. [(C₁₁H₁₄O₄)₂₂C₂₂H₃₀N₂O₂Na]⁺ could be detected as side series. The enlarged MALDI-TOF spectrum of poly(**1**) initiated with catalyst **G3** and quenched with 5 equiv. of compound **23** for 100h is depicted in Figure 2.28b. Methylene capped poly(**1**) [(C₁₁H₁₄O₄)₄₂C₈H₈Na]⁺ is observed as main series whereas thymine capped poly(**1**) ionized with lithium or with sodium e.g.

$[(C_{11}H_{14}O_4)_{41}C_{22}H_{30}N_2O_2Li]^+$, $[(C_{11}H_{14}O_4)_{41}C_{22}H_{30}N_2O_2Na]^+$ are assigned as side series. A fourth series was observed which could not be definitely assigned but might overlap with methylene capped poly(**1**) ionized with potassium $[(C_{11}H_{14}O_4)_{42}C_8H_8K]^+$. For terminating agent **23**, the change from catalyst **G1** to **G3** did not lead to a significant change in the intensity ratio of methylene capped to thymine capped poly(**1**) (Table 2.13, entries 3, 4), (Figure 2.28a-b).

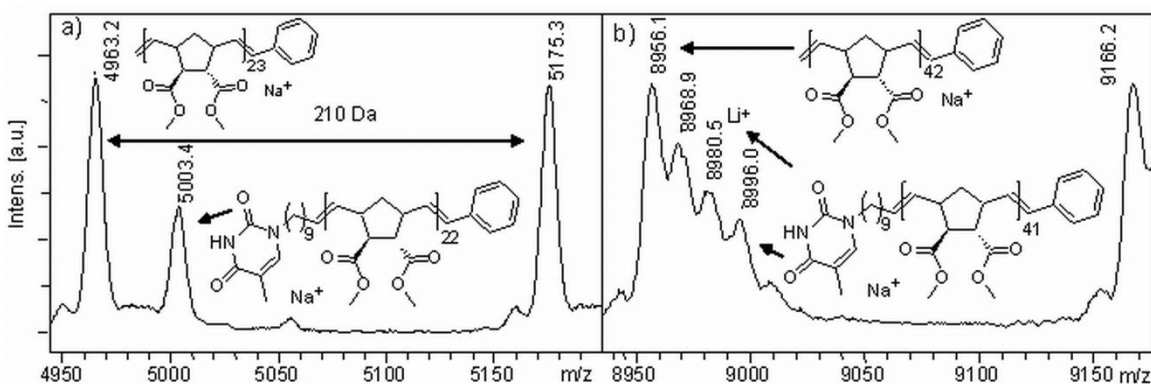


Figure 2.28. MALDI-TOF MS spectra of poly(**1**) quenched with terminating agent (**23**), a) initiated with **G1**, 5 equiv. (**23**), 100 h, enlargement from 4950-5200 m/z, b) initiated with **G3**, 5 equiv. (**23**), 100 h, enlargement from 8950 to 9170 m/z

Table 2.13. GPC and MALDI-TOF MS results for poly(**1**) quenched with compound **23**.

entry	cat.	equiv. TA (23)	time (h)	M_n (GPC) g/mol	PDI (GPC)	M_n^a MALDI m/z	PDI ^a MALDI	M_p^b MALDI m/z	$I(\text{meth})/I(\text{thym})^c$	corrected value ^d
1	G1	1	100	5600	1.22	4929	1.12	4961.7	2.03	0.11 (90 %)
2	G1	2	100	5900	1.19	5106	1.12	4962.1	2.00	0.11 (90 %)
3	G1	5 (35°C)	100	5800	1.22	5695	1.12	4961.7	1.49	0.08 (92 %)
4	G3	5	100	8700	1.15	8682	1.03	9166.4	2.42 ^e	0.13 (88 %)

^a calculated with Polytools software, ^b mass of the peak with the highest intensity, ^c ratio of intensities of methylene terminated poly(**1**) and poly(**1**) bearing thymine end group, ^d corrected intensity ratio by applying the desorption ratio from the quantification, ^e only the sodium series were considered for the quantification, monomer to catalyst ratio (calculated molecular weight): 25 (5610 g/mol) for entries 1-3, 30 (6661 g/mol) for entry 4.

2.7.5. MALDI-TOF analysis

As it can be seen from the ratio of methylene capped polymer to functionalized polymer, the fraction of functionalized polymer increases with time and added amount of terminating agent **21** and **23** (Table 2.12, entries 1, 3, 4, 6, Table 2.13, entries 1, 3). Running the termination reaction for more than 100 h did not increase the fraction of functionalized polymer. By changing from catalyst **G1** to the more reactive catalyst **G3** and using an excess (20 equiv.) of the terminating agent (**21**), the fraction of barbiturate capped polymer could be further increased (Table 2.12, entries 8, 9). In contrast to this, the fraction of thymine capped polymer did not increase by changing from catalyst **G1** to **G3** (Table 2.13, entry 3, 4). As the extracted ratios of methylene capped polymer to functionalized polymer does not give a quantitative statement, a quantification^{147,148} of the different polymer species was done by using the same method which was already applied for the quantification of block copolymers in the previous chapter (2.5.).¹⁴⁷⁻¹⁵¹

In order to perform the quantification, a sample of the end functionalized polymer was measured in different mixtures with methylene capped poly(**1**). In this way it is possible to get a correlation between the intensity and the fraction of the different desorbed species. In Figure 2.29, the graphs for barbiturate capped and thymine capped poly(**1**) are given. The slope of the curve (Figure 2.29) gives the desorption ratio between methylene capped poly(**1**) and poly(**1**) with the functional end group, with values of 18 for thymine and 30 for barbiturate capped polymer.

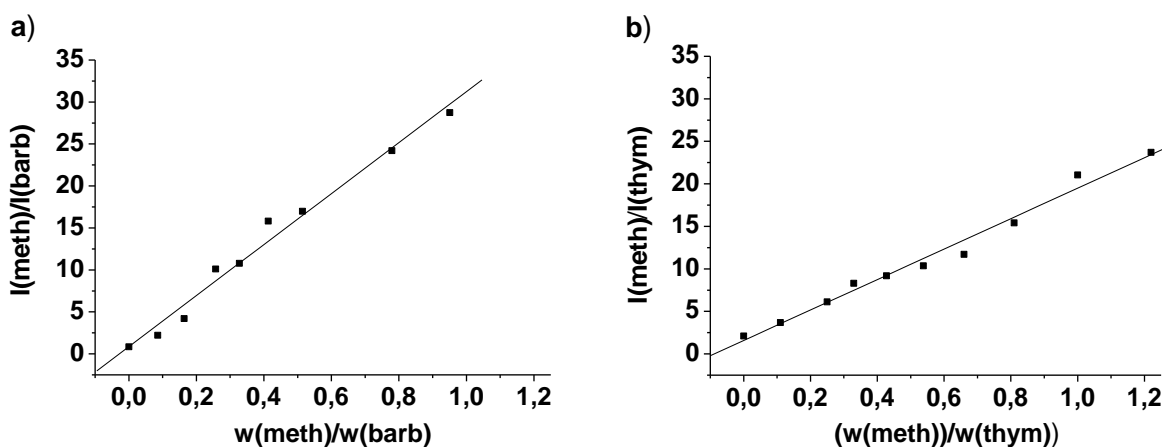


Figure 2.29. Quantification curves for poly(**1**) a) capped with barbiturate end group (**21**), b) capped with thymine-end group (**23**), $I(\text{meth})/I(\text{barb})$: intensity ratio of methylene capped poly(**1**) against barbiturate capped poly(**1**), $w(\text{meth})/w(\text{barb})$: mixing ratio of methylene capped poly(**1**) against barbiturate capped poly(**1**), $I(\text{meth})/I(\text{thym})$: intensity ratio of methylene capped poly(**1**) against thymine capped poly(**1**), $w(\text{meth})/w(\text{thym})$: mixing ratio of methylene capped poly(**1**) against thymine capped poly(**1**).

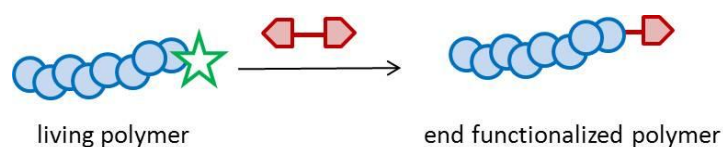
Thus, methylene capped polymer is preferentially desorbed in comparison to thymine or barbiturate capped polymer.

Without taking this desorption ratio into account, the fraction of the end functionalized polymer is underestimated. Therefore, the extracted intensity ratios of methylene capped poly(**1**) against end group functionalized poly(**1**) (Tables 2.12 and 2.13) are corrected by the desorption ratio for an estimation of the actual fraction of the functionalized polymer. In so doing, the fraction of barbiturate capped polymer in the mixture is calculated to be 38 to 99 %. Thus, barbiturate capped polymer of 99 % could be prepared by reacting poly(**1**), initiated with catalyst **G3**, with an excess of 20 equiv. of terminating agent **21** and a reaction time of 100 h (Table 2.12, entry 9). By applying the correction for poly(**1**) quenched with terminating agent **23**, the fraction of thymine-capped poly(**1**) is in between 88 and 92 %. A comparison of the terminating agents **21** and **23** under the same reaction conditions (**G1**, 5 equiv. of terminating agent, 100 h reaction time) gives fractions of functionalized polymer of 96 % and 92 % respectively (Table 2.12, entry 6), (Table 2.13, entry 3). Hence, no significant change in the reactivity of the symmetric olefins **21** and **23** is observed when the barbiturate group at the symmetric olefin is replaced by a thymine moiety.

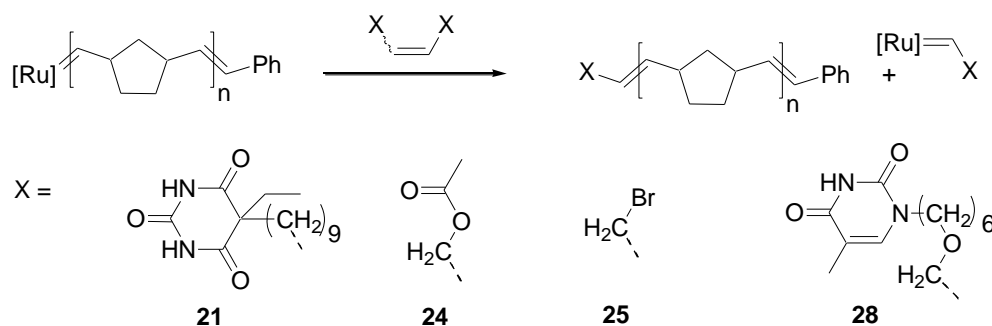
Summary of chapter 2.7.

Summarizing this chapter, it can be said that the reaction of living chains with symmetric olefins represents a simple approach for the end group introduction of ROMP polymers. Symmetric olefins **21** and **23**, carrying the hydrogen bonding motives thymine and barbiturate respectively, can be prepared by cross metathesis and subsequently utilized as terminating agents, as the ruthenium catalysts are tolerant of a wide array of functional groups. The efficiency of the quenching process depends on the reaction time as well as on the amount of added terminating agent. A quantification of the end group fractions can be achieved via MALDI-TOF MS. Efficiencies for the end group introduction of 92 % for thymine and 99% for barbiturate could be achieved. In agreement to the block copolymerization/oligomerization reactions (chapters 2.5-2.6), catalyst **G3** gives better crossover efficiencies.

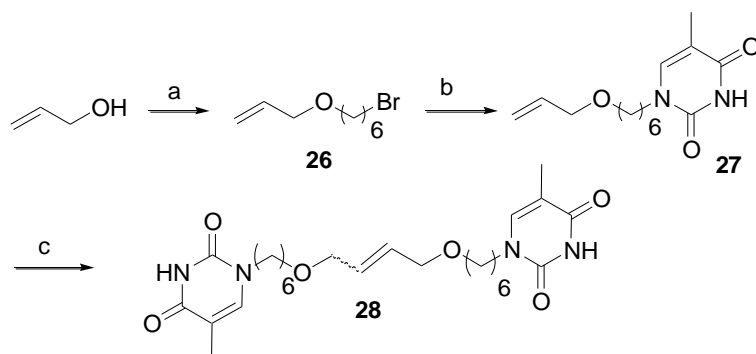
2.8. End functionalization of poly(**13**) with symmetric olefins



After proving that the direct capping with symmetric olefins is an efficient termination reaction, the strategy was transferred to poly(norbornene), (poly(**13**)). The living polymerization of norbornene (**13**) with **G3** was described in chapter 2.4. Different symmetric olefins were reacted with the living poly(norbornene) chains to obtain end functionalized polymers. Addition of the quenching agents were done at -20°C , with a slow warm up, followed by reaction for 24 to 100 h. The symmetric olefins for the termination are depicted in Scheme 2.22.



Scheme 2.22. End functionalization of poly(norbornene) with symmetric olefins.



Scheme 2.23. Synthesis of symmetric terminating agent **28**, a) 1,6-dibromohexane, KOH_{aq} , b) Thymine/HMDS/TMSCl, c) homometathesis, catalyst **G2**, copper(I) iodide.

Quencher **28** was used as to see if a heteroatom near to the olefinic bond ($=\text{CH}-\text{CH}_2-\text{O}-\text{CH}_2$) would change the reactivity of this quencher. Terminating agent **28** was synthesized in a three step process, depicted in Scheme 2.23. The first step is the reaction of allyl alcohol with 1,6-dibromohexane, furnishing the ether **26** in a yield of 79 %. Subsequent reaction of compound **26** with bis(O-trimethylsilyl)thymine furnished compound **27** in a yield of 40 %. The final product **28** was obtained by homo metathesis of compound **27**, using catalyst **G2** and copper iodide, in a yield of 59 %. The ^1H NMR spectra for the compounds **26-28** are given in the appendix, Figures 5.60-5.62.

2.8.1. Quenching efficiency for poly(**13**)

Analysis of the end functionalized poly(norbornene)s was performed by NMR spectroscopy. The efficiency was determined by the integral ratio of the proton from the initiator group ($\text{CH}-\text{Ph}$) at 6.40-6.27 ppm against the resonances from the newly introduced end group.

Table 2.14. End group efficiencies for the termination of poly(norbornene), (poly(**13**)) with symmetric olefins.

entry	M/C	cat.	TA	equiv. TA/C	time (h)	Mn (calc)	Mn* (GPC)	PDI	Y %	EG%
1	100	G3	EVE	exc.	1	9400	12200	1.1	80	100
2	50	G3	21	20	100	4700	4450	1.3	70	75
3	100	G3	24	10	24	9400	11000	1.2	89	89''
4	100	G3	24	10	24	9400	12600	1.1	80	89
5	2000	G2	25	50	24	4700	2600	2.0	60	+
6	50	G3	25	20	24	4700	6950	1.4	80	#
7	100	G3	28	10	100	9400	10500	1.3	70	50
8	100	G3	28	20	100	9400	11900	1.1	70	70

*corrected by factor of 0.5, '' quenching at room temperature, mixture of semi-telechelic and telechelic acetoxy terminated poly(**13**), + 20% semi-telechelic, 80% telechelic, # only bromomethyl end groups detected, no initiator group.

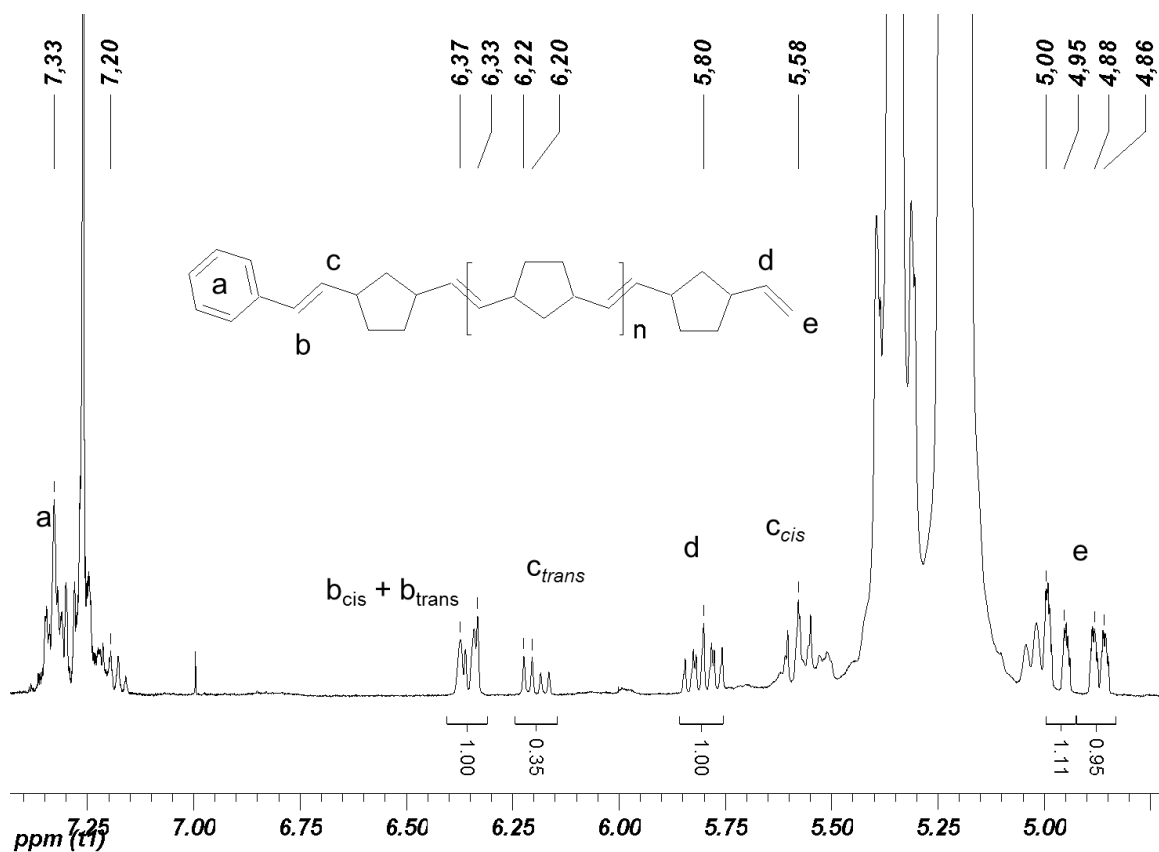
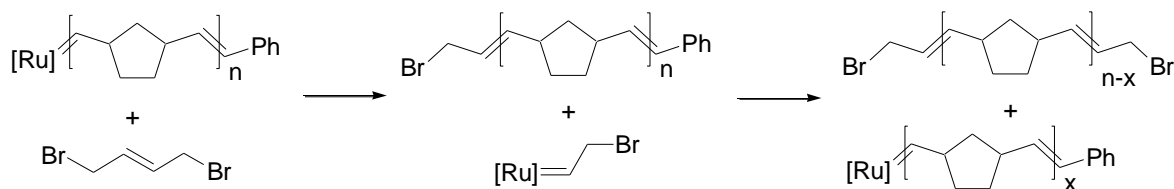


Figure 2.30. $^1\text{H-NMR}$ spectrum of poly(**13**) quenched with ethyl vinyl ether, magnification from 7.5 to 4.5 ppm.

Quenching with ethyl vinyl ether at -20°C leads to polymers with narrow polydispersity (Table 2.14, entry 1) with the methylene end group observed at 5.00–4.85 ppm (2H, dd, $^3J_{\text{HH}} = 10.1\text{ Hz}$, $^3J_{\text{HH}} = 17.3\text{ Hz}$, $=\text{CH}_2$), (Figure 2.30). Termination of living poly(norbornene) chains with compound **24** produced acetoxy-capped poly(norbornene). New resonances for the acetoxy group could be observed at 4.63 ppm and 4.50 ppm for the methylene group neighboring a *cis* or *trans* double bond respectively (2H, $=\text{CH-CH}_2\text{-O}$) and for the methyl group at 2.06 ppm (3H, s, $\text{CH}_3\text{C(O)O}$).

From the ratio of the end groups it was concluded that the polymer consists of a mixture of telechelic and semi-telechelic acetoxy capped poly(**13**). By maintaining the temperature for 4 h at -20°C after addition of compound **24**, the loss of the initiator group could be avoided and semi-telechelic acetoxy capped polymer was obtained (Table 2.14, entries 3, 4 and appendix, Figure 5.63 ($^1\text{H-NMR}$)) This is in agreement with the work of Matson and Grubbs¹² reporting on quenching efficiencies for this compound of up to 97%.

The use of *trans*-1,4-dibromo-2-butene (**25**) as quencher (Table 2.14, entry 6) led to telechelic bromomethyl capped poly(**13**). This was confirmed by the disappearance of the resonance of the initiator group at 6.37 (=CH-Ph). Thus, the cleaved off catalyst reacts with internal double bonds of the polymer backbone to generate telechelic polymer (Scheme 2.24).



Scheme 2.24. Chain transfer reactions on the example of termination with 1,4-dibromomethyl-2-butene (**25**).

These chain transfer reactions are often observed for polymers with sterically unhindered double bonds (ROMP polymers generated from cyclopentene, cyclooctene, norbornene). The presence of the bromomethyl end group can be confirmed by the appearance of two resonances at 4.01 and 3.94 ppm (2H, d, $^3J_{\text{HH}(\text{cis})} = 7.6 \text{ Hz}$, $^3J_{\text{HH}(\text{trans})} = 7.2 \text{ Hz}$, =CH-CH₂-Br), which can be assigned to the methylene groups neighboring a *cis* or a *trans* double bond respectively. The PDI broadens from 1.1 to 1.4, indicative of chain transfer reactions. Compound **25** was additionally tested as chain transfer with catalyst **G2**. Thus, compound **25** is already added at the beginning of the polymerization. The formation of high molecular weight polymer, precipitating from solution, was observed instantaneously. However, the polymer becomes soluble again over the course of the reaction. This behavior can be explained due to the molecular weight degradation by chain transfer reactions. The polydispersity with a value of 2.0 is within the expected value for this kind of reactions.¹⁰⁴ Investigation by NMR showed the presence of telechelic and semi-telechelic bromomethyl capped poly(norbornene) in a ratio ~ 80/20 (Figure 5.65).

The quenching of the living chains with the internal olefins **21** and **28** was done analogously to the model system poly(**1**) with a reaction time of 100 h. An increase in the end group fraction from 50 to 70% was observed by increasing the number of equivalents of the terminating agent from 10 to 20 equiv. (Table 2.14, entries 7 and 8). By using an excess of quenching agents **21** and **28** (20 equiv.) it was possible to prepare semi-telechelic barbiturate and thymine capped poly(norbornene) with an end group fraction of 75 % and 70% respectively. The residual end groups are capped with methylene as a result of the final quenching with ethyl vinyl ether (NMR, =CH₂, 5.00-4.85 ppm). In the NMR, the presence of the barbituric acid moiety can be seen on the resonance at 0.88 ppm which was assigned to

the methyl group ($\text{CH}_3\text{-CH}_2\text{-}$). For the poly(norbornene) quenched with compound **28**, the thymine moiety can be seen at 3.89 ppm ($=\text{CH-CH}_2\text{-O}$), 3.68 ($\text{CH}_2\text{-CH}_2\text{-N}$) and 3.39 ($\text{O-CH}_2\text{-CH}_2$), see appendix Figure 5.64 ($^1\text{H NMR}$).

The efficiency values obtained for the termination reaction with different olefins show that the compounds **24** and **25** are more reactive in the crossover process than the olefins **21** and **28**.

Higher end group efficiencies can be obtained with the olefins **24** and **25**, compared to **21** and **28** with smaller amount of terminating agent and in less time. The different reactivities of the olefins towards cross metathesis with the polymer can be explained by steric factors. As compounds **24** and **25** are small in size compared to the olefins **21** and **28**, their coordination to the ruthenium center of Grubbs catalyst 3rd-generation is less sterically hindered. It is noteworthy to mention that in literature most often *cis*-configured olefins are used out of steric reasons. Nonetheless, compound **25** which is configured *trans* and compounds **21** and **28** which are mixtures of *cis* and *trans* undergo reaction with the living poly(norbornene)-species. An important point is that the cleaved off catalyst formed by the reaction of the living polymer chain with olefins **24** or **25** tends to perform chain transfer reactions by attacking the internal double bonds of the poly(norbornene) backbone in contrast to the catalyst formed after reaction with olefins **21** and **28**. MALDI TOF MS of poly(**13**) did not deliver well resolved spectra but showed peaks separated by the mass of the repetition unit (94 Da, C_7H_{10}). A spectrum for the sample (Table 2.14, entry 3) is given in the appendix, Figure 5.67.

2.8.2. HPLC-analysis of poly(**13**)

In an attempt to quantify the fractions of different end groups attached to the poly(norbornene)s besides NMR-methods, HPLC measurements on poly(norbornene)s were performed. For quantitative statements a separation of the different functionalized polymer species is crucial. Liquid chromatography for macromolecules can be conducted in three different modes: size exclusion chromatography (SEC), liquid adsorption chromatography (LAC) and liquid chromatography under critical conditions (LCCC). Parameters which can be used to obtain a certain mode or to switch between the modes include the solvent composition, temperature and the used column. In SEC, the macromolecules are separated by their hydrodynamic volumes due to exclusion from column pores. The separation in this case is dominated by entropic forces leading to an elution of higher molecular weight samples at earlier retention times compared to lower molecular weight samples. LAC on the other hand

separates the polymers according to their polarity, thus separation is based on enthalpic interactions. As a consequence, higher molecular weight samples, having more units to interact with the stationary phase, elute later. The third mode, LCCC, is a special case where polymer samples of different molecular weights elute at the same time, caused by a compensation of entropic and enthalpic forces. Hence, the aim is to obtain LCCC-conditions for poly(norbornene)s to achieve a separation of methylene terminated and end functionalized poly(norbornene). Before conducting LC measurements, the solubility of the poly(norbornene)s (sample $M_n = 7000$ g/mol) was tested in a couple of solvent/nonsolvent pairs. The limit to insolubility, as judged by a beginning turbidity of the solution, was observed as follows: v/v %, THF/H₂O: 95/5, THF/MeOH: 83/17, THF/Hex: 80/20, DCM/MeOH 83/17. As samples, methylene terminated poly(norbornene) with molecular weights from M_n : 7000 g/mol – 100000 g/mol were used. For setting the conditions it is important that the polymers display the same end group distribution, as different end groups will significantly alter the retention times. The first measurements were conducted at normal phase columns (Nucleosil 100-5 and Nucleosil 300-5), see Table 2.15. The results show that higher molecular weight polymers are eluted faster than lower molecular weight samples. Neither a change in the solvent composition, nor a reduction in temperature could shift the system towards LAC or LCCC-conditions (Table 2.15, entries 1-5, 12-13). From this it was concluded that the poly(norbornene) does not interact with the normal phase columns. Therefore, the type of column was changed to reverse phase columns exhibiting C18 chains.

Measurements on a reverse phase system were first conducted on a Novapak C18 column. Surprisingly, a measurement in pure THF showed for all measured molecular weights approximately the same retention time. The same result was observed when the measurement was conducted e.g. in pure toluene (Table 2.16, entries 1, 4-5). To check if these conditions correspond to LCCC-conditions, poly(norbornene) with a thymine end group (70 % functionalized, $M_n = 11900$ g/mol) was measured under the same conditions (pure THF) and compared with an methylene terminated poly(norbornene) ($M_n = 12000$ g/mol), Table 2.16, entry 2. No difference was observed, judging the retention times of 3.59 min (poly(norbornene), $M_n = 12000$ g/mol) and 3.61 min for thymine functionalized (poly(norbornene), $M_n = 11900$ g/mol). Thus, it was concluded that no polymer has entered the pores of the column since species which differ significantly in their polarity and therefore should have different interactions with the stationary phase are eluted at the same time.

Table 2.15. Results of LC measurements of methylene terminated poly(norbornene)s poly(**13**) on normal phase columns: Entries 1-14: Nucleosil-OH 100-5 column (100 Å pore size, 5 µm particle size), Entry 15: Nucleosil-OH 300-5 column (300 Å pore size, 5 µm particle size), Column dimensions for Nucleosil-OH 100-5 and 300-5, ID x L = 4.6 x 250 mm, inner diameter (ID), length (L).

entry	sample	M _n (g/mol)	solvent v/v %	flow rate (mL/min)	T (°C)	t _{ret} (min)
1	poly(13)	7000	THF	0.3	35	6.50
		12000				5.86
2	poly(13)	7000	THF/MeOH 91/9	0.3	35	6.55
		12000				5.90
3	poly(13)	7000	DCM	0.3	35	6.70
		12000				5.98
4	poly(13)	7000	DCM/MeOH 95/5	0.3	35	6.54
		12000				5.84
5	poly(13)	7000	DCM/MeOH 90/10	0.3	35	6.89
		12000				6.26
6	poly(13)	7000	DCM/MeOH 94/6	0.3	35	6.47
		12000				5.86
7	poly(13)	7000	DCM/MeOH 92/8	0.3	35	6.56
		12000				5.96
8	poly(13)	7000	DCM/MeOH 92/8	0.3	22	6.69
		12000				6.09
9	poly(13)	7000	DCM/MeOH 91/9	0.3	22	6.87
		12000				6.24
10	poly(13)	7000	DCM/MeOH 90/10	0.3	22	6.91
		12000				6.31
11	poly(13)	7000	DCM/MeOH 85/15	0.3	35	6.80
		12000				6.22
12	poly(13)	7000	DCM/ACN 95/5	0.3	10	6.96
		12000				6.27
13	poly(13)	7000	DCM/ACN 95/5	0.3	35	7.14
		12000				6.47
14	poly(13)	7000	DCM/THF 95/5	0.5	35	3.88
		12000				3.48
15	poly(13)	7000	THF	0.3	35	10.94
		12000				10.24
		20000				9.58
		50000				8.75
		75000				8.33

Table 2.16. Results of LC measurements of methylene terminated poly(norbornene)s poly(**13**) and poly(norbornene) quenched with compound **28**, poly(**13**)-**28** (fraction of thymine end group 70 % by NMR) on reverse phase column Nova-Pak C18 (C18-chains, 60 Å pore size, 4 µm particle size), Column dimensions: ID x L = 3.9 x 150 mm, inner diameter (ID), length (L).

entry	sample	M _n (g/mol)	solvent v/v %	flow rate (mL/min)	T (°C)	t _{ret} (min)
1	poly(13)	7000	THF	0.3	35	2.97
		12000				2.94
		20000				2.93
		50000				2.92
		75000				2.91
		100000				2.97
2	poly(13)	12000	THF	0.3	35	3.59
	poly(13)- 28	11900				3.61
3	poly(13)	7000	THF/Hex 80/20	0.1	35	16.90
		12000				16.04
	poly(13)- 28	11900				15.77
4	poly(13)	7000	toluene	0.3	35	2.96
		12000				2.94
		20000				2.91
5	poly(13)	7000	toluene	0.3	9	3.05
		12000				3.05
		20000				2.99
6	poly(13)	7000	toluene/MeOH 9:1	0.3	35	2.98
		12000				2.92
		20000				2.88
7	Uracil	112	ACN/H ₂ O 1/1	0.3	35	3.30

In consequence, the polymer should elute at the void volume. The void volume, using uracil as marker, corresponds to a value of 0.99 mL. The polymer gives a similar retention volume with a value of 0.9 mL. Since both values are similar, taking different measuring conditions (solvent mixture, pump pressure) into account, it can be concluded that the total exclusion of poly(norbornene) chains starts for this column already at 7000 g/mol. To avoid the exclusion of the polymer chains from the column pores a different column (Atlantis T3) was chosen with an average pore size of 100 Å. The results for these measurements are summarized in Table 2.17. Measurements were again started in pure THF with the result that the poly(norbornene)s from M_n ≥ 20000 g/mol display the same retention time. Thus, total exclusion of the poly(norbornene) chains on the Atlantis T3 column starts approximately at 20000 g/mol. From these values it can be concluded that the void volume for this column (Atlantis T3) is

approximately 1.6-1.8 mL. SEC-conditions were also observed for the other experiments, Table 2.17, entries 2-4, 7-10. By using a mixture of THF/hexane the enthalpic interactions could be increased, leading to an approximation of the retention times compared to measurements in pure THF, see Table 2.17, entries 1, 5. A further increase in the hexane fraction (above 20 vol-%) was not possible since the poly(norbornene) will precipitate.

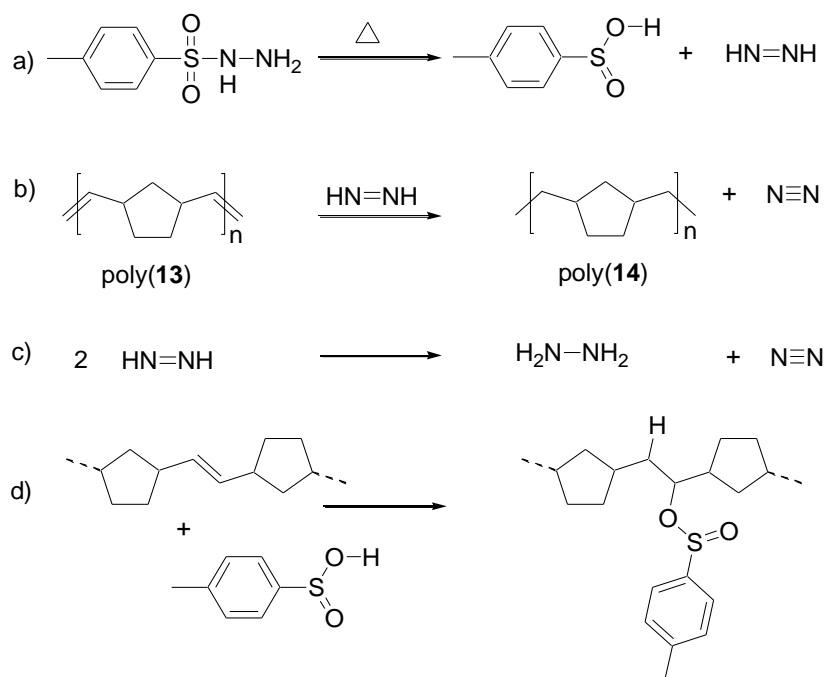
Table 2.17. Results of LC measurements of methylene terminated poly(norbornene)s poly(**13**) on reverse phase column Atlantis T3 column (C18-chains, 100 Å pore size, 5 µm particle size), Column dimensions: ID x L = 4.6 x 250 mm, inner diameter (ID), length (L).

entry	sample	Mn (g/mol)	solvent v/v %	flow rate (mL/min)	T (°C)	t _{ret} (min)
1	poly(13)	7000	THF	0.3	35	7.01
		12000				6.61
		20000				6.41
		50000				6.43
		75000				6.42
		100000				6.43
2	poly(13)	7000	THF	0.3	6	6.46
		12000				6.03
		20000				5.85
3	poly(13)	7000	THF/MeOH 90/10	0.3	35	6.50
		12000				6.00
		20000				5.78
4	poly(13)	7000	THF/ACN 90/10	0.3	35	6.80
		12000				6.18
		20000				5.91
5	poly(13)	7000	THF/Hex 80/20	0.3	35	5.92
		12000				5.70
		20000				5.60
		50000				5.65
6	poly(13)	7000	THF/Hex 80/20	0.3	6	5.97
		12000				5.64
		50000				5.50
7	poly(13)	7000	DCM	0.3	35	6.51
		12000				5.96
8	poly(13)	7000	DCM	0.3	7	6.97
		12000				6.24
9	poly(13)	7000	toluene	0.3	35	6.12
		12000				5.75
		20000				5.60
10	poly(13)	7000	toluene/MeOH 90/10	0.3	35	6.50
		12000				5.92
		20000				5.70

For a better understanding of the size exclusion, an estimation of the poly(norbornene) coil dimensions was conducted. By taking into account that the molecular weights for poly(norbornene) are corrected by a factor of 0.5 against polystyrene standards in GPC, one can assume that e.g. the hydrodynamic radius of a polystyrene in THF (100000 g/mol), which is given in literature as 100 Å,¹⁷³ corresponds to a poly(norbornene) with a molecular weight of 50000 g/mol. Hence, the polymer coil has a diameter of approximately 200 Å, which is too large to enter the pores. A further improvement and therefore an approximation to the LCCC-conditions would require columns with higher pore sizes¹⁷⁴ (≥ 300 Å) to reduce the entropic interactions and more apolar solvent mixtures, e.g. cyclohexane to augment the enthalpic interactions.

2.8.3. Hydrogenation of poly(13)

Hydrogenation of the amorphous poly(norbornene)s was accomplished with tosylhydrazide. The mechanism of this reaction is depicted in Scheme 2.25. Tosylhydrazide decomposes under heating in *p*-tolylsulfonic acid and the reducing agent diazene, which hydrogenates the double bonds of the polymer.



Scheme 2.25. Hydrogenation of polymers via diazene, a) formation of diazene, b) hydrogenation reaction, c) diazene disproportionation, d) addition of sulfonic acid.

Tosylhydrazide is used in excess (5 equiv.) due to disproportionation of the diazene into hydrazine and nitrogen (Scheme 2.25c). A side reaction in the hydrogenation process can be the addition of formed sulfonic acid onto a double bond (Scheme 2.25d). Hydrogenated poly(norbornene) is a semi crystalline polymer which is poorly soluble in organic solvents at room temperature. Although the range of solvents is limited, solvation can be achieved in toluene, xylene or cyclohexane at elevated temperatures. Investigation of the hydrogenated samples via ^1H NMR revealed a degree of hydrogenation of 99.8% (Figure 2.31) The ^{13}C NMR of a hydrogenated poly(norbornene) is depicted in Figure 2.32, showing four resonances in the aliphatic range. Thus, a saturated hydrocarbon polymer has been prepared by successful hydrogenation of the *cis* and *trans*-double bonds of poly(norbornene). The tacticity is not changed by the hydrogenation process and therefore remains atactic.

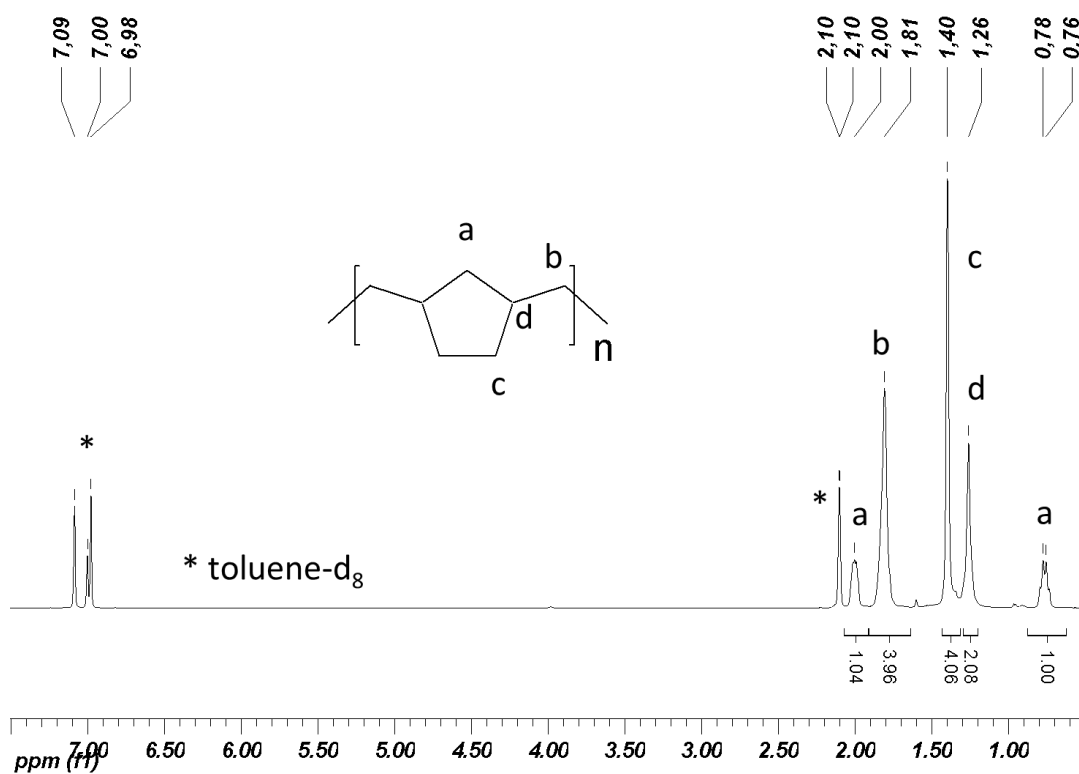


Figure 2.31. ^1H NMR of hydrogenated poly(norbornene) in toluene-d_8 , measured at 70°C .

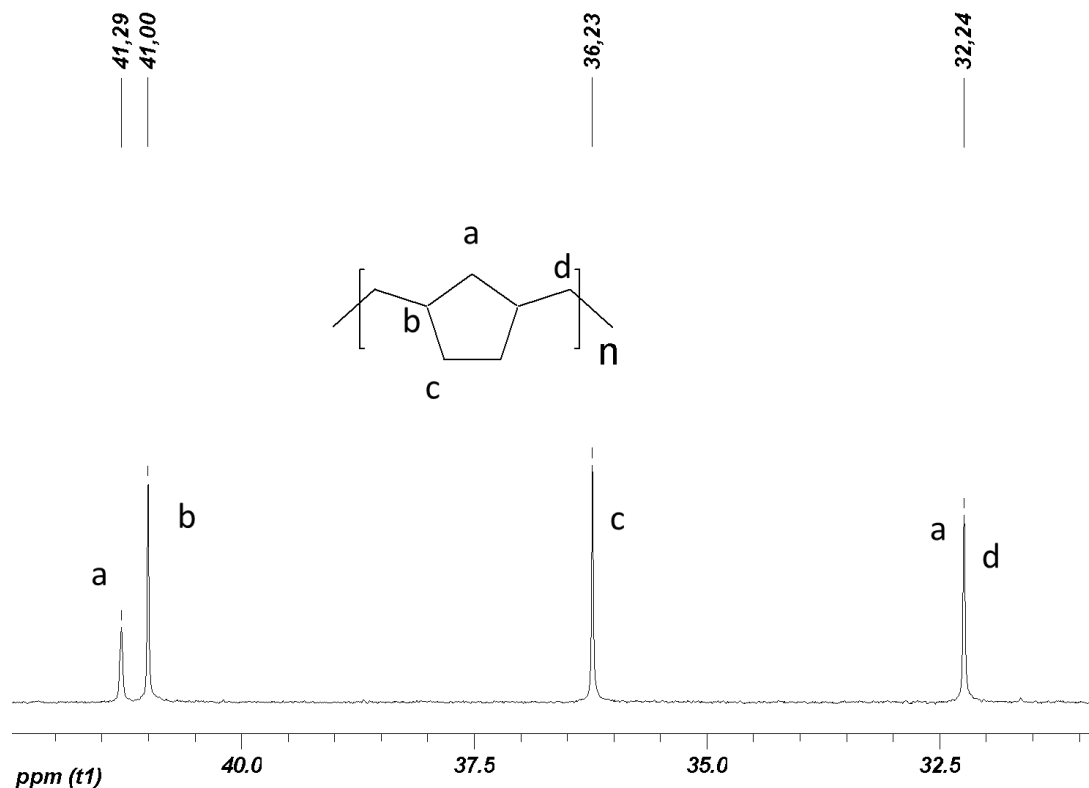
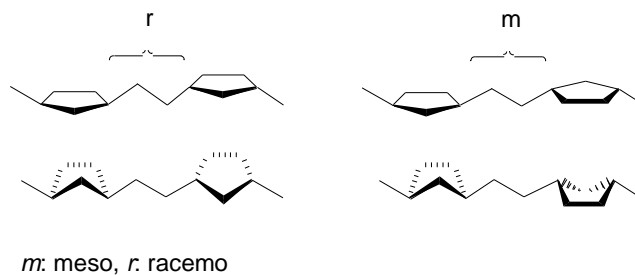


Figure 2.32. ^{13}C NMR of hydrogenated poly(norbornene) in toluene- d_8 , measured at 70 °C.



Scheme 2.26. Meso and racemo dyads in hydrogenated poly(norbornene), drawings in the second line represent the same structure with emphasis on the zigzag conformation.

In general, crystallinity in polymers requires a tactic structure of the polymer chain. Thus, the crystallinity in atactic hydrogenated poly(norbornene) is unexpected. In Scheme 2.26, the meso and racemo dyads of hydrogenated poly(norbornene) are presented. All cyclopentylene rings are *cis* configured which is predetermined by the monomer norbornene.³⁶ The cyclopentylene rings can alter their conformation which allows nearly a zigzag conformation, of the polymer chain, independent of the

participating dyads.³⁶ This zigzag or all *trans* conformation, which is also found in crystalline poly(ethylene), facilitates the crystallization of hydrogenated poly(norbornene).³⁶

2.8.4. DSC-studies on poly(13) and poly(14)

Table 2.18. Glass transition temperatures of poly(norbornene)s, entries 1, 3, 4 and 5, methylene terminated poly(13), entry 2, poly(13) quenched with compound 28, fraction of thymine end group: 70%.

entry	sample	M _n (g/mol) (GPC)	T _g (°C)
1	poly(13)	10350	43
2	poly(13)-28	11900	43
3	poly(13)	21950	48
4	poly(13)	48450	50
5	poly(13)	97500	51

Measuring conditions: poly(norbornene)s: 25 – 100 - (-50) - 100 (°C),

Table 2.19. Melting and crystallization temperatures of hydrogenated poly(norbornene)s, entries 1, 3, 4 and 5, poly(14) obtained by hydrogenation of methylene terminated poly(13), entry 2, thymine functionalized poly(14), obtained by hydrogenation of thymine terminated poly(13) (sample poly(13)-28), fraction of thymine end group: 70%.

entry	sample	M _n (g/mol) (GPC)	T _m (°C) 1 st / 2 nd heating run	ΔH _m 1 st / 2 nd heating run	T _c (°C)
1	poly(14)	10350	140.8 / 137.2	60.7 / 66.8	126.3
2	poly(14)-28	11900	139.2 / 138.2	47.5 / 54.6	125.2
3	poly(14)	21950	145.5 / 142.6	63.9 / 63.9	129.1
4	poly(14)	48450	147.5 / 143.3, 136.4	63.5 / 36.5	126.6, 112.5
5	poly(14)	97500	149.8 / 145.8	65.1 / 54.4	124.5

Measuring conditions: hydrogenated poly(norbornene)s: 25 - 170 - (-30) - 170 (°C), heating rate 10 K/min

The results of the DSC measurements for the poly(norbornene)s and hydrogenated poly(norbornene)s are summarized in the Tables 2.18 and 2.19. DSC measurements showed that the poly(norbornene)s are amorphous materials with a glass transition in the range of 43 to 51°C (Figure 2.33a). This temperature range can be explained by the molecular weight dependence of the glass transition.¹⁷⁵ Curves measured for poly(styrene)s and poly(butadiene)s displayed two characteristic points where the slope of the curve changed.¹⁷⁵ The first one is at M_e , the molecular weight of entanglement, the second one, called M_T , is the molecular weight from where the T_g is independent from the molecular weight ($M_T \sim 10 \pm 2 M_e$).¹⁷⁵ The measured glass transition temperatures for poly(norbornene) are higher than values reported for poly(norbornene) (35-45 °C).^{104,176,177} However, a comparison is difficult due to different *cis/trans* ratios of the double bonds and tacticity. For DSC curves see also appendix, Figures 5.68-5.70.

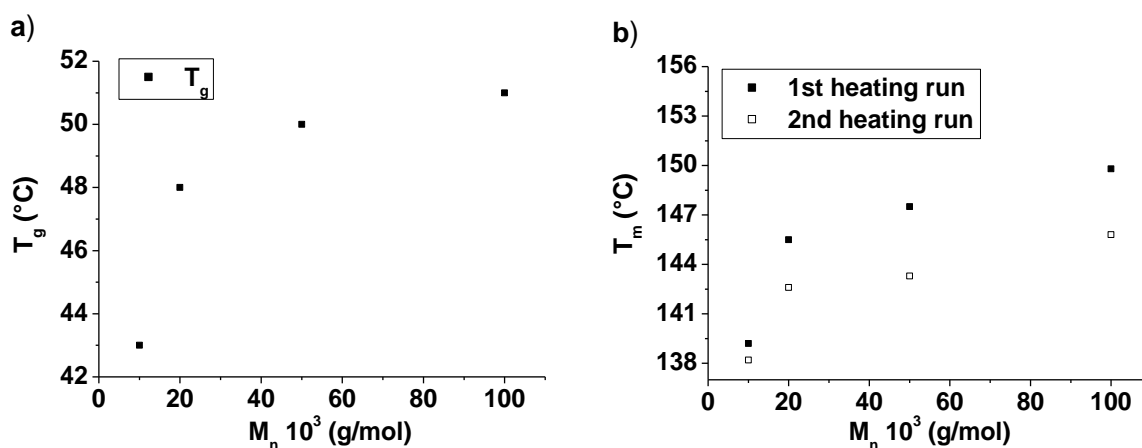


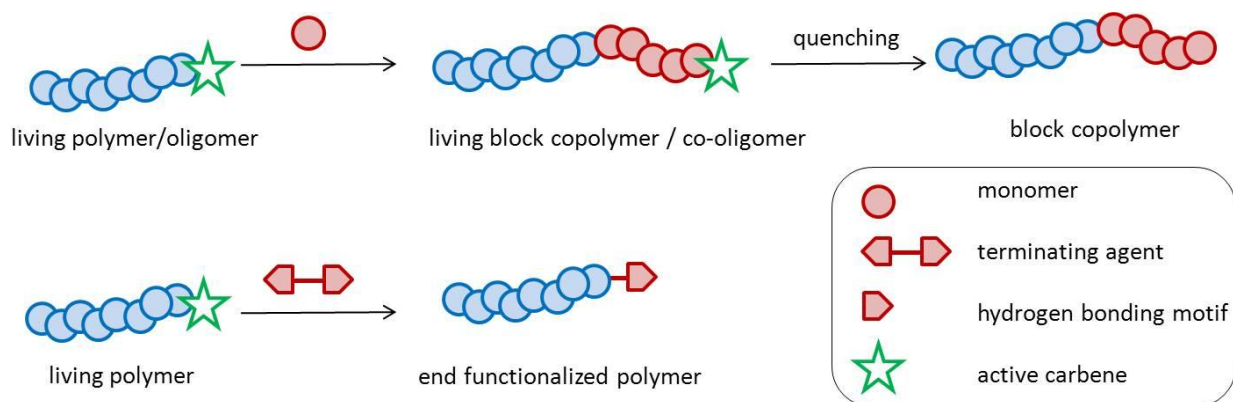
Figure 2.33. DSC results a) glass transition temperature of methylene terminated poly(norbornene)s in dependency of the molecular weight, b) melting temperature of the hydrogenated poly(norbornene)s (end groups: benzyl and methyl) in dependency of the molecular weight, samples prepared with Grubbs catalyst 3rd-generation, for the sample with $M_n = 50$ kDa the value from the main peak is used.

The hydrogenated poly(norbornene)s are semi crystalline polymers showing melting temperatures in the range of 139 to 149°C (equilibrium melting temperature = 156 °C).³⁶ Again, the observed temperature range of the melting temperature can be explained by a molecular weight dependence (2.33b). Longer polymer chains tend to build up larger and therefore thermally more stable crystals. For all samples a drop in the melting temperature was observed when comparing the first and second heating run. Thus, the crystals grown from the precipitation are larger than after cooling from the melt with 10 K/min. This behavior was reported for poly(ϵ -caprolactone) showing a difference in the melting temperature between 1st and 2nd heating of approx. 5 °C.¹⁷⁸ The crystallinity, judged from the melting enthalpy in the first heating run (Table 2.19) is similar for the unmodified samples (60-65 J/g). This

shows that the molecular weight has not a strong influence on the initial amount of crystals formed from solution. A glass transition temperature could not be determined for the hydrogenated poly(norbornene)s even after repeated cycles or by using higher cooling rates (40 K/min). To our best knowledge, no T_g value was reported in literature. The introduction of a thymine moiety (poly(**14**)-**28**, for ^1H NMR see appendix, Figure 5.66) led to small change of 1 °C in the measured crystallization temperature and a drop in the measured heating enthalpy. Thus, the crystallinity of the polymer is reduced by the introduction of a large functional moiety.

Summary

This thesis was aimed at the investigation of the crossover step in ROMP block copolymerization and termination reactions.

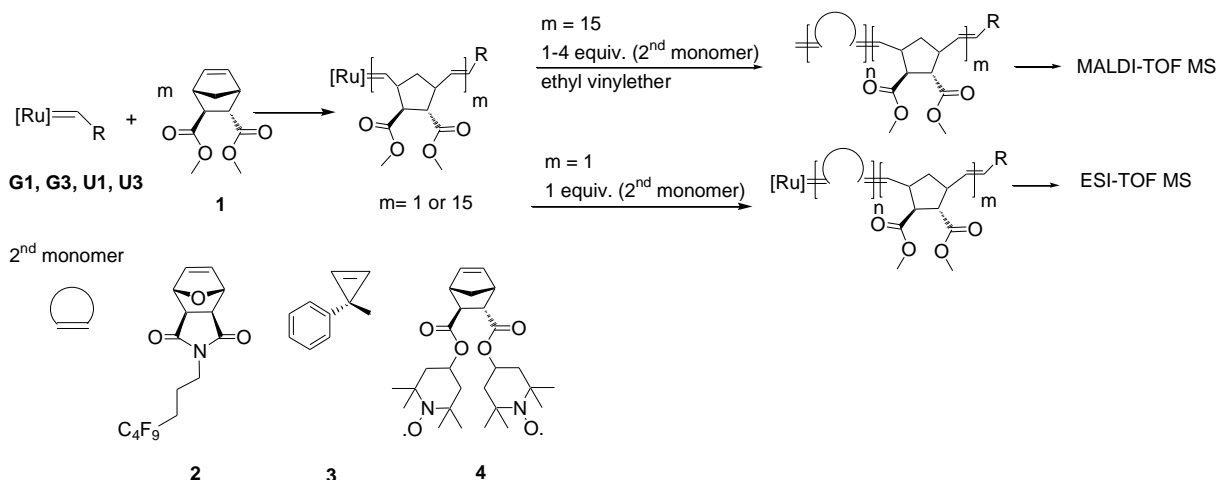


As for the crossover step, living polymer chains are required, the first part of this work focused on the polymerization of three different systems and the investigation of their polymerization kinetics by means of gel permeation chromatography (GPC) and NMR-methods.

Polymerization of monomer **1** with the catalysts **G1**, **U1**, **G3** and **U3** can be considered a living process. This can be concluded by the linear slope of the $\ln(M_0/M_t)$ vs. time curves, the linear increases in the molecular weight with time and applied $[M]/[C]$ ratio. The molecular weights are comparable with the expected values and the polydispersity displays values of 1.1-1.2. As judged from NMR-kinetics, the third generation catalysts **G3** and **U3** show a significant increase in the reactivity compared to their first generation analogues **G1** and **U1**. For all the applied catalysts except **G3**, the k_p/k_i is greater than 1 for the polymerization of monomer **1**. Still, narrow dispersed polymers can be prepared with the catalysts **G1**, **U1** and **U3**, displaying k_p/k_i ratios for the polymerization of monomer **1** up to ~ 10 .

For the second system, two barrelene based monomers exhibiting acetoxy- (**11**) or methoxycarbonyloxy-groups (**12**) could successfully be synthesized in a seven step process starting from *myo*-inositol. The monomers showed reactivity towards all the tested catalysts. Best results were obtained with Grubbs catalyst 2nd-generation (**G2**) producing polymers in a molecular weight range of 4000 to 6000 g/mol with a polydispersity of 1.4 to 1.6. In comparison, monomer **12** showed faster polymerization kinetics than monomer **11**. Although not considered as living process, it could be shown that soluble poly(*p*-phenylene vinylene) polymers can be prepared with ruthenium catalysts.

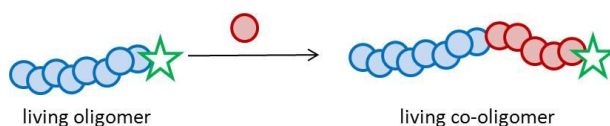
For the third system, based on norbornene, a living polymerization could be achieved by using catalyst **G3** at -20°C in agreement with works from Choi and Grubbs.¹⁴ Poly(norbornene)s (poly(**13**)) in the range from 5000 to 100000 g/mol could be prepared with polydispersities of 1.1 to 1.2. For all systems, poly(**1**), poly(**11**), poly(**12**) and poly(**13**), the polymers display an atactic structure and a mixture of *cis* and *trans* double bonds. As only monomer **1** and **13** could be polymerized in a living fashion, crossover experiments were then done with living chains of poly(**1**) and poly(**13**).



Crossover studies of a living polymer chain with a second monomer were performed with poly(**1**) and the monomers **2**, **3** and **4** (1, 2 and 4 equiv.). As catalytic systems, catalysts **G1** and **G3** were used. NMR kinetics on the homo and copolymerization showed strong differences in the reactivity of the individual monomers. The monomers arranged in increasing activity (**3** < **1** < **2**) show that the cyclopropene **3** is the least reactive, although it possess the highest ring strain. Thus, sufficient ring strain is a requirement for successful ROMP but it is not rate determining. As well, monomer **2** is more reactive than monomer **1**, which follows the rule that *exo,exo*-substituted norbornenes are more reactive than *exo,endo*-substituted monomers.

To obtain information on the individual species involved in the crossover process, the polymers were terminated and investigated via MALDI-TOF MS. Poly(**1**) proved as an excellent probe for the monitoring of crossover reactions since it is well desorbed in MALDI-TOF MS. For the systems (**1**)-*b*-(**2**) the crossover is not completed after addition of 1 and 4 equiv. of monomer **2** respectively, independent of the applied catalyst. For the system poly(**1**)-*b*-(**3**), a significant change can be seen when using **G3** compared to **G1**. In case of **G3**, the homopolymer is nearly vanished after addition of 1 equiv. of monomer **3** whereas with **G1** a mixture of homopolymer and copolymer species is observed. After the addition of 4 equiv. the crossover is completed with catalyst **G3**, but the main series remains (**1**)_x(**3**)₁, showing the poor

propagation in the polymerization of **3**. In the system poly(**1**)-*b*-(**4**), a similar picture is observed as in block copolymer system poly(**1**)-*b*-(**2**), with an incomplete crossover even after the addition of 2 equiv. of monomer **2**. In contrast, GPC measurements of these copolymerization reactions showed the expected shift in molecular weight. However, the presence of homopolymer in the mixture revealed by MALDI MS shows that one cannot rely solely on GPC measurements for judging the point of crossover.



ESI-TOF MS investigations were performed on the living oligomer- and co-oligomer species before termination to obtain information of the catalyst species involved in the process. To see the effect of the k_p/k_i ratio, the chain length of the polymer species was reduced from $(\mathbf{1})_{15}(\mathbf{2}, \mathbf{3}, \mathbf{4})_{1-4}$ to $(\mathbf{1})_1(\mathbf{2}, \mathbf{3}, \mathbf{4})_1$. The samples, dissolved in dichloromethane, were measured with a solution of lithium chloride in methanol/acetonitrile (100/1) similar to the method of Wang et al.⁷⁸ Thereby, it was possible to investigate the ROMP of non-charged monomers and to overcome the necessity of charged co-monomers.

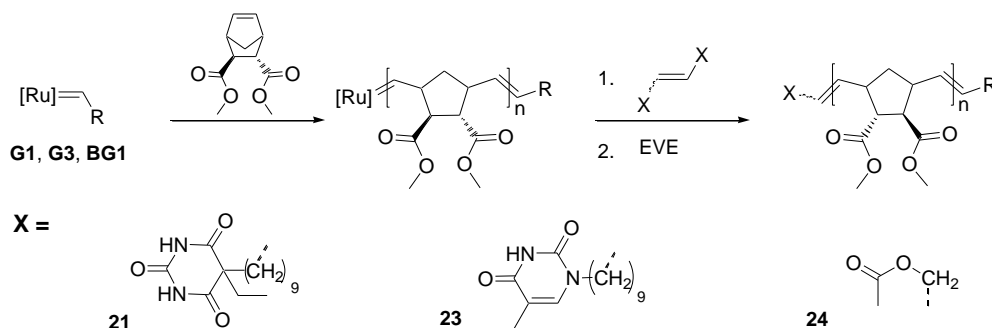
The measured spectra display a significant difference between the reactions conducted with 1st and 3rd-generation catalysts. For the first generation catalysts **G1** and **U1**, the main peaks can be assigned to unreacted catalyst species. Just a small fraction is composed out of oligomer- and co-oligomer species. The high fraction of unreacted catalyst in the reaction mixture is a result of the k_p/k_i ratio of catalysts **G1** and **U1**. The propagating species is observed as monophosphine complex, which is in agreement to a dissociative mechanism for olefin metathesis.³³

For the 3rd-generation catalysts **G3** and **U3**, a significant reduction of the relative amounts of catalyst species and an increase in the fractions of oligomer and co-oligomer species is observed. The smallest fraction of unreacted catalyst can be seen with **G3**, which has the most favorable k_p/k_i ratio of all the tested catalysts. The highest fraction of co-oligomers is observed for the system **1/2** and **1/4**. Identical to the reactions with the catalysts **G1** and **U1**, only in the case of the systems **1/2** and **1/4** propagation of the second monomer is observed. For the crossover reaction **1/3**, propagation stops after insertion of one unit of **3**. This behavior confirms the low reactivity of monomer **3** which is caused by the steric hindrance of the substituents on the ring opened cyclopropene, hindering further coordination and insertion. Experiments conducted with hydrochloric acid as additive displayed higher fractions of

oligomer and co-oligomer-species compared to experiments without acid. Thus, hydrochloric acid proved as an efficient additive to accelerate the ROMP-process.

The propagating species observed for **G3** contain no or only one pyridine ligand. Thus, both pyridines are labile and can be cleaved off during the catalytic cycle. In this process, a 14-electron active species is generated which is identical to the one formed from Grubbs catalyst 2nd-generation. The results obtained are in a good agreement to the investigation of the block copolymers via MALDI MS, showing incomplete crossover after addition of 1 equiv. of the second monomer and the strong influence of the applied catalyst on the product distribution by its k_p/k_t ratio and its reactivity.

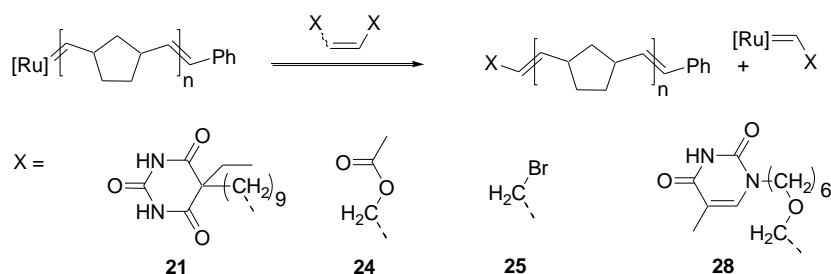
The second major reaction depending on the cross over reaction, besides the block copolymerization, is the end group introduction by termination of living chains.



For the end functionalization of poly(**1**) the quenching with symmetric olefins was chosen since it allows the introduction of functional end groups in a single reaction step. Two symmetric olefins (**21** and **23**) carrying barbiturate and thymine groups were prepared by homo metathesis of the corresponding α -olefins **20** and **22** respectively. The synthesis was performed with catalyst **G2** either by microwave heating or by the addition of copper(I) iodide. Ruthenium catalysts are favored for this kind of reaction due to their tolerance of the most functional groups. However, it is worth to note, that it is necessary to separate the functional group and the terminal olefin by a spacer unit to avoid complexation and deactivation of the metathesis catalyst. The addition of copper(I) iodide, acting as phosphine scavenger has led to better reaction efficiencies compared to microwave heating. The efficiency of the termination process depends on the reaction time and the amount of added terminating agent.

Quantification of the termination efficiency was achieved by MALDI-TOF MS. The highest efficiencies could be achieved by a reaction time of 100 h and by using an excess (20 equiv.) of the terminating agent with respect to the living chain. A comparison of the applied catalysts showed a higher reactivity

for catalyst **G3** than for **G1**. Thus, 3rd-generation catalysts do not only display enhanced reactivity during the polymerization and block copolymerization but also for the cross metathesis with terminating agents. With the applied conditions, poly(**1**) with an end group fraction of 99 % of barbiturate and 92 % of thymine end groups could be obtained. Hence, the reaction of living chains with symmetric olefins represents a simple approach for the introduction of complex functional moieties.



Crossover reactions were done on poly(norbornene) by quenching living chains with symmetric olefins (**21**, **24**, **25** and **28**). By using this approach end functionalized poly(norbornene)s could be prepared exhibiting bromomethyl-, acetoxy-, barbituric acid- and thymine-moieties with fractions of the desired end group of up to 89 %. For the quenching with 1,4-bis(acetoxy)-2-butene (**24**) and 1,4-dibromo-2-butene (**25**), telechelic and semi-telechelic polymers could be observed. The presence of telechelic polymer is a result of the cross metathesis of the cleaved catalyst with internal double bonds of the polymeric backbone. This side reaction could be reduced by maintaining the temperature at -20°C for a certain time after the addition of the quencher. The internal olefins **24** and **25** displayed enhanced reactivity in the cross metathesis compared to the olefins **21** and **28**. Higher fractions of end groups can be achieved by using less amount of quenching agent and less reaction time. The less sterical hindrance of the olefins **24** and **25** in comparison to the symmetric olefins **21** and **28** makes them more reactive in the cross metathesis with the living polymer chains, although they are more electron deficient. The presence of telechelic polymers shows that poly(norbornene) is more prone to secondary metathesis reactions than poly(**1**) as a result of the lower sterical hindrance of the internal double bonds at poly(norbornene) backbone.

Hydrogenation of the prepared poly(norbornene)s (methylene- and thymine-capped) was successfully accomplished by using tosylhydrazide, with hydrogenation efficiencies of up to 99.8 %. DSC-studies on the methylene terminated poly(norbornene)s revealed a molecular weight dependence of the glass transition for the poly(norbornene)s and of the melting point for the hydrogenated poly(norbornene)s.

The introduction of a thymine end-group (poly(**14**)-**28**) had no effect on the melting temperature but on the crystallinity, which was reduced in comparison to the unmodified sample.

3. Experimental

Solvents/reagents/materials

All chemicals were purchased from Sigma Aldrich and were used without further purification unless otherwise noted. Dichloromethane, chloroform, diethyl ether were predried over calcium chloride. Diethyl ether and THF were distilled over sodium, benzophenone and degassed with argon prior to use. Dimethylsulfoxide, xylene, chloroform and dichloromethane were distilled over calcium hydride and degassed with argon prior to use. Grubbs catalysts 1st- (**G1**), 2nd- (**G2**) and 3rd-generation (**G3**) were purchased from Sigma Aldrich. Umicore catalysts M1 (**U1**), M2 (**U2**) and M3 (**U3**) were kindly provided by Umicore AG & Co. KG.

Analytics

NMR was measured on Varian Gemini 2000 FT NMR spectrometer (200 and 400 MHz). Chloroform-d₁, THF-d₈, DMSO-d₆, toluene-d₈ were used as solvents. Kinetics of the polymerization reactions were measured on a 200 MHz FT-NMR spectrometer at 27 °C using CDCl₃ as solvent. Chemical shifts were recorded in parts per million (δ) and referenced to residual protonated solvent (CDCl₃: 7.26 ppm (¹H), 77.0 ppm (¹³C), THF-d₈: 1.75 and 3.60 ppm (¹H), DMSO-d₆: 2.50 ppm (¹H), 39.4 ppm (¹³C), toluene-d₈: 2.09 ppm (¹H), 20.4 ppm (¹³C)). For analysis of the FIDs Mestrec 4.9.9.9 was used. GPC measurements were done at Viscotek GPCmax VE 2001 with a Styragel linear column GMH_{HR}; THF was used as carrier-solvent at 1 mL/min at RT. The sample concentration was approximately 3 mg/mL. Polystyrene standards ($M_p = 1050 - 125000$ g/mol) were used for conventional external calibration, using a Waters RI 3580 refractive index detector. Chromatograms were analyzed using Malvern Viscotec OmniSEC software, version 4.6.2. MALDI-TOF MS measurements were done at Bruker autoflex III smartbeam, equipped with a nitrogen laser (337 nm), in linear and reflector positive mode. As matrix, dithranol (1,8-dihydroxy-9,10-dihydroanthracen-9-one) was used as solution of 20 mg/mL in THF. Polymer samples were dissolved in THF at a concentration of 5 mg/mL. As salts, sodium trifluoroacetate, lithium trifluoroacetate or silver trifluoroacetate were used as solutions of 20 mg/mL in THF. In a typical sample preparation a solution was mixed with a ratio of 100:40:5 with regard to matrix/polymer/salt and spotted on the target. For the investigation of the block copolymer species the MALDI-TOF MS samples were prepared by mixing solutions of matrix (20 mg/mL THF), polymer (20 mg/mL THF), and salt (20

mg/mL THF) in a ratio of 100/10/1. Mass spectra were analyzed with Bruker Daltonics flex analysis software, version 3.0.

Example for ESI-MS sample preparation:

Polymerizations were conducted in septum sealed vials. Catalyst **U3** (3.6 mg, 0.005 mmol) was weighed into a vial. The vial is flushed with argon and sealed prior to use. A solution of monomer **1** (1 mg, 0.005 mmol) in 0.5 ml dry Dichloromethane is added, shaken and reacted for 10 min. Then a solution of monomer **2** (2 mg, 0.005 mmol) in 0.5 ml dry dichloromethane is added and reacted for further 10 min. The mixture is diluted to 1/100 of the original concentration. A sample of 0.2 ml is withdrawn and mixed with 0.2 ml of a solution of lithium chloride in methanol (0.1 mg/ml). Concentration of ruthenium carbenes is approx. $2.5 \cdot 10^{-5}$ mol/L.

ESI-TOF MS

Mass spectrometric measurements were conducted at a Bruker Daltonics micrOTOF II. The samples were measured via direct injection, with a flow rate of 300 μ L/h. Measurements were done in positive mode with a capillary voltage of 4.5 kV. Temperature of dry gas (N_2) was adjusted to 50 °C. Calibration was done by measuring Tunemix in a mixture of Acetonitrile/Water 95/5. Data were recorded in the range from 50 to 3000 m/z with a hexapole RF-voltage of 700 V. Recorded spectra were analyzed with Bruker DataAnalysis 4.0 software, isotopic patterns are simulated with Bruker Compass IsotopePattern.

HPLC-measurements

HPLC measurements were conducted on an Elite-LaChrom-HPLC from *Hitachi VWR*, equipped with autosampler (Hitachi L-2200), column oven (Hitachi L-2300, temperature 0 - 70 °C), semi-micro pump (Hitachi L-2100, max. flow rate 2.5 mL/min) and diode array detector (Hitachi L-2455, deuterium and tungsten lamp), operating from 190 to 900 nm. Normal phase columns Nucleosil-OH 100-5 and Nucleosil-OH 300-5 from *Macherey Nagel* and C_{18} -reverse phase columns Nova-Pak C18 and Atlantis T3 from *Waters* were used. Samples were dissolved at a concentration of 3 mg/mL and injected into the column in a volume of 20 μ L. Chromatographic runs were recorded in the range of 190-400 nm with EZChrom Elite-Software.

Monomers: The synthesis of the monomers **1-4** is described in the appendix.

D- and L-1,2-O-isopropylidene-myo-inositol (5)

A mixture of *myo*-inositol (5 g, 27 mmol), 2,2-dimethoxypropane (9 mL, 73 mmol), toluene-*p*-sulfonic acid (50 mg, 0.29 mmol) and dimethyl sulfoxide (16 mL) was stirred at 90 °C until a clear solution was obtained. After cooling the solution to 20 °C, ethanol (20 mL) and diethyl ether (100 mL) were added. The solution was stirred for 2 h after which triethylamine (1 mL) was added. The mixture was stirred for further 4 h and then left at room temperature. The white solid was filtered off, washed with methanol/diethyl ether (1:5) (42 mL) and dried. The crude product was recrystallized with ethanol to furnish compound **5**. Yield: 3.1 g (51%). ¹H NMR (400 MHz, DMSO-*d*₆, 27 °C): δ (ppm) = 4.81 (1H, d, ³J_{HH} = 4.7 Hz), 4.78 (1H, d, ³J_{HH} = 5.3 Hz), 4.71 (1H, d, ³J_{HH} = 4.2 Hz), 4.67 (1H, d, ³J_{HH} = 4.4 Hz), 4.16 (1H, dd, ³J_{HH} = 4.1 Hz, ³J_{HH} = 5.1 Hz), 3.79 (1H, dd, ³J_{HH} = 5.3 Hz, ³J_{HH} = 7.4 Hz), 3.48 (1H, ddd, ³J_{HH} = 4.1 Hz, ³J_{HH} = 5.1 Hz, ³J_{HH} = 9.1 Hz), 3.33 (2H, m), 2.90 (1H, dt, ³J_{HH} = 4.4 Hz, ³J_{HH} = 9.4 Hz). ¹³C NMR (100 MHz, DMSO-*d*₆, 27 °C): δ (ppm) = 107.8, 79.0, 76.2, 74.4, 74.0, 72.2, 69.7, 28.1, 25.9.

1,2-O-isopropylidene-3,4,5,6-tetra(methanesulfonyl)-myo-inositol (6)

Mesyl chloride (5.5 mL, 72 mmol) was added to a solution of **5** (3g, 13.6 mmol) and 4-dimethylaminopyridine (0.1 g, 0.81 mmol) in dry pyridine (23 mL) under argon. The reaction temperature was maintained at 0 °C. After complete addition, the mixture was allowed to warm up to room temperature and to stay overnight. The next day the mixture was poured on ice (75 g) and the precipitated white solid was filtered, washed with cold water (3 × 10 mL), isopropanol (2 × 10 mL) and dried *in vacuo* at 50 °C. Yield: 6.8 g (93%). ¹H NMR (400 MHz, DMSO-*d*₆, 27 °C): δ (ppm) = 5.32 (1H, m), 5.15 (2H, m), 4.82 (1H, m), 4.64 (1H, m), 3.35 (3H, s), 3.33 (3H, s), 3.30 (3H, s), 3.28 (3H, s), 1.56 (3H, s), 1.35 (3H, s). ¹³C NMR (100 MHz, DMSO-*d*₆, 27 °C): δ (ppm) = 110.8, 80.7, 75.6, 74.8, 74.4, 73.7, 73.6, 39.2, 38.9, 38.7, 27.0, 25.6.

***cis*-O-isopropylidene-3,5-cyclohexadien-1,2-diol (7)**

A 500 mL round bottom flask was charged with potassium iodide (24 g, 132 mmol), compound **6** (10 g, 19.2 mmol) and N-methyl-2-pyrrolidone (200 mL). The mixture was heated at 120 °C until a clear solution was achieved. Approximately 36 mL of volatile material was distilled off at 120 °C, 10 Torr to remove residual water. Fresh prepared zinc/copper couple (15 g) was added and the mixture was heated at 120 °C for 24 h. All volatile materials were distilled off at 145 °C, 20 Torr (B.p. 88 - 100 °C). The distillate was poured in a mixture of brine/water (3/2, 500 mL) and the aqueous solution was extracted with ethyl acetate (3 × 50 mL). The organic phase was washed with water (5 × 50 mL), brine (3 × 50 mL)

and dried over sodium sulfate. The organic phase was concentrated *in vacuo* to yield compound **7**. Yield: 830 mg (30%). ^1H NMR (400 MHz, CDCl_3 , 27 °C): δ (ppm) = 5.92 (2H, m), 5.83 (2H, m), 4.59 (2H, m, $^3J_{\text{HH}} = 1.6$ Hz), 1.36 (3H, s), 1.34 (3H, s).

4,4-Dimethyl-8-(toluene-4-sulfonyl)-3,5-dioxo-tricyclo[5.2.2.0^{2,6}]undeca-8,10-diene (8)

A flask was charged with ethynyl-*p*-toluenesulfonate (240 mg, 1.3 mmol) and purged with argon. Dry benzene (1.5 mL) was added to dissolve the solid. Compound **7** (200 mg, 1.3 mmol) in dry benzene (1 mL) was added and the resulting mixture was heated at 80 °C for 14 h. After cooling to room temperature, the solvent was removed and the residue was recrystallized in acetone. The solution was cooled to -50 °C to yield white crystals which were filtered and washed with -78 °C cold acetone. Yield: 220 mg (50%). ^1H NMR (400 MHz, CDCl_3 , 27 °C): δ (ppm) = 7.70 (2H, d, $^3J_{\text{HH}} = 8.3$ Hz), 7.33 (2H, d, $^3J_{\text{HH}} = 8.1$ Hz), 7.14 (1H, dd, $^3J_{\text{HH}} = 1.9$ Hz, $^3J_{\text{HH}} = 6.5$ Hz), 6.27 (1H, t, $^3J_{\text{HH}} = 6.2$ Hz), 6.20 (1H, t, $^3J_{\text{HH}} = 6.6$ Hz), 4.25 (1H, dd, $^3J_{\text{HH}} = 3.3$ Hz, $^3J_{\text{HH}} = 6.9$ Hz), 4.13 (1H, dd, $^3J_{\text{HH}} = 3.5$ Hz, $^3J_{\text{HH}} = 6.8$ Hz), 4.08 (1H, m), 4.02 (1H, ddd, $^3J_{\text{HH}} = 1.6$ Hz, $^3J_{\text{HH}} = 3.4$ Hz, $^3J_{\text{HH}} = 7.2$ Hz), 2.44 (3H, s), 1.28 (3H, s), 1.21 (3H, s).

4,4-Dimethyl-3,5-dioxo-tricyclo[5.2.2.0^{2,6}]undeca-8,10-diene (9)

A flask was charged with compound **8** (977 mg, 2.72 mmol) and then evacuated and backfilled with argon three times. Samarium iodide in THF (0.1 M, 150 mL) was added and the mixture was cooled to -20 °C. Hexamethylphosphortriamide (8.2 mL), which was stirred over calcium hydride and distilled prior to use, was added in one shot. The reaction was kept at -20 °C and monitored via TLC. After completion, the reaction was terminated by the addition of saturated ammonium chloride solution. The solution was stirred for another hour while warming up to room temperature. THF was removed *in vacuo* and the solid residue was diluted with water and extracted with diethyl ether (3 times). The solvent was removed and the residue was dissolved in hexane/ethyl acetate 1:1 and filtered through a pad of silica. Compound **9** was purified via column chromatography (hexane/ethyl acetate 10:1). Yield: 330 mg (59%). ^1H NMR (400 MHz, CDCl_3 , 27 °C): δ (ppm) = 6.32 (2H, dd, $^3J_{\text{HH}} = 3.1$ Hz, $^3J_{\text{HH}} = 4.3$ Hz), 6.26 (2H, dd, $^3J_{\text{HH}} = 3.0$ Hz, $^3J_{\text{HH}} = 4.4$ Hz), 4.22 (2H, t, $^3J_{\text{HH}} = 1.6$ Hz), 3.83 (2H, m), 1.34 (3H, s), 1.27 (3H, s).

Bicyclo[2.2.2]octa-5,7-diene-2,3-diol (10)

Compound **9** (100 mg, 0.56 mmol) was dissolved in acetic acid (3.5 mL). Water was added until the solution turned turbid and the resulting mixture was heated at 100 °C for 3.5 h. The solution was concentrated at 10 Torr, 40 °C and the solid residue was purified via column chromatography

(hexane/ethyl acetate from 4/1 to 1/1) to obtain a white solid in a yield of 55 mg (71%). ^1H NMR (400 MHz, CDCl_3 , 27 °C): δ (ppm) = 6.41 (2H, dd, $^3J_{\text{HH}} = 3.1$ Hz, $^3J_{\text{HH}} = 4.3$ Hz), 6.24 (2H, dd, $^3J_{\text{HH}} = 3.2$ Hz, $^3J_{\text{HH}} = 4.4$ Hz), 3.82 (2H, m), 3.71 (2H, s), 2.15 (2H, s).

Bicyclo[2.2.2]octa-5,7-diene-2,3-diol di(acetate) (11)

To a solution of compound **10** (150 mg, 1.1 mmol) in acetic anhydride (1.5 mL) was added anhydrous pyridine (1 mL). After stirring for 3 days the reaction solution was poured onto an acidic water/ice mixture. The aqueous phase was extracted with chloroform. The organic phases were combined and dried over sodium sulfate. After removal of the solvent and drying *in vacuo*, compound **11** was obtained. Yield 205 mg (80%). ^1H NMR (400 MHz, CDCl_3 , 27 °C): δ (ppm) = 6.45 (2H, dd, $^3J_{\text{HH}} = 3.2$ Hz, $^3J_{\text{HH}} = 4.4$ Hz), 6.35 (2H, dd, $^3J_{\text{HH}} = 3.1$ Hz, $^3J_{\text{HH}} = 4.5$ Hz), 4.83 (2H, t, $^3J_{\text{HH}} = 1.6$ Hz) 3.82 (2H, dtdd, $^3J_{\text{HH}} = 1.5$ Hz, $^3J_{\text{HH}} = 3.2$ Hz, $^3J_{\text{HH}} = 4.5$ Hz, $^3J_{\text{HH}} = 6.1$ Hz), 2.00 (6H, s). ^{13}C NMR (100 MHz, CDCl_3 , 27 °C): δ (ppm) = 170.2, 133.6, 132.5, 69.2, 41.3, 20.8.

Bicyclo[2.2.2]octa-5,7-diene-2,3-diol di(methyl carbonate) (12)

Methyl chloroformate (0.45 ml, 5.84 mmol) was added to a solution of compound **10** (219 mg, 1.58 mmol) in anhydrous dichloromethane (4 mL) and dry pyridine (0.32 mL), cooled with an ice bath. After stirring for 3 days the reaction solution was poured onto an acidic water/ice mixture. The aqueous phase was extracted with chloroform. The organic phases were combined and dried over sodium sulfate. After removal of the solvent and drying *in vacuo*, compound **12** was obtained in a yield of 321 mg (80%). ^1H NMR (400 MHz, CDCl_3 , 27 °C): δ (ppm) = 6.46 (2H, dd, $^3J_{\text{HH}} = 3.1$ Hz, $^3J_{\text{HH}} = 4.3$ Hz), 6.36 (2H, dd, $^3J_{\text{HH}} = 3.2$ Hz, $^3J_{\text{HH}} = 4.5$ Hz), 4.76 (2H, m) 3.90 (2H, m), 3.74 (6H, s). ^{13}C NMR (100 MHz, CDCl_3 , 27 °C): δ (ppm) = 155.3, 133.5, 133.2, 72.0, 54.8, 41.1.

General polymerization procedure of monomers 11 and 12

A penicillin vial with magnetic stirrer was dried in the oven at 150 °C and allowed to cool down in a desiccator. The vial was charged with catalyst **G2** (4 mg, 0.005 mmol) and monomer **12** (30 mg, 0.118 mmol), flushed with argon and sealed with a cap. Dry dichloromethane (1 mL) was added via syringe and the resulting mixture was stirred for 6 h. The polymerization was quenched by adding 3 drops of ethyl vinyl ether. Stirring was continued for another hour. The reaction solution was passed through a pipette of silica gel. After removal of the solvent, the residue was repeatedly washed with methanol. Poly(**12**) was obtained after drying *in vacuo*. Yield: 20 mg (66%). Poly(**11**) ^1H NMR (400 MHz, CDCl_3 , 27 °C): δ

(ppm) = 5.53 (4H, m), 5.26 (2H, m), 3.25 (1H, m), 3.08 (1H, m), 2.05 (6H, s). **Poly(12)** ^1H NMR (400 MHz, CDCl_3 , 27 °C): δ (ppm) = 5.55 (4H, m), 5.10 (1H, m), 4.92 (1H, m), 3.77 (6H, s), 3.29 (2H, m).

Polymerization of norbornene (poly(13)₁₀₀)

Norbornene was dried by stirring 2 h over sodium at 50 °C and then vacuum transferred (oil bath 50 °C, 50 mbar) into a collection flask, cooled with ice. A penicillin vial with magnetic stirrer was dried in the oven at 150 °C, flushed with argon and sealed with a cap and equipped with a balloon of argon. A stock solution of Grubbs catalyst 3rd-generation in dry dichloromethane (9.4 mg/1 mL) was prepared. 1 mL of this solution is withdrawn via syringe and injected into the vial. The vial is cooled down to -25 °C. A stock solution of norbornene in dry dichloromethane was prepared (100 mg/1.5 mL). 1.5 mL of the monomer solution were withdrawn and injected into the precooled vial. The temperature was maintained below -20 °C. After 0.5 h, the polymerization was quenched by adding 3 drops of ethyl vinyl ether. Stirring was continued for another hour. The polymer was precipitated by dropping the dichloromethane solution into 100 mL of methanol. After centrifugation and drying the polymer was obtained as a white solid. Yield: 75 mg (75%). For preparation of poly(norbornene) M/C = 500, 1000 the solvent was changed to THF and the concentration of the monomer solution was decreased to 100 mg/3 mL.

Synthesis of hydrogenated poly(norbornene) (14)

A flask was charged with poly(norbornene) (50 mg, 0.53 mmol of double bonds), tosylhydrazide (400 mg, 2.14 mmol) and dry xylene (10 mL). After purging the solution with nitrogen, the flask was connected to a reflux condenser with attached bubbler. The reaction was heated for 5 h at 160 °C. The reaction was allowed to cool down to room temperature and the solution was precipitated into methanol (100 mL). The fine white precipitate was collected by centrifugation and dried *in vacuo*. Yield: 40 mg (80%)

Terephthalaldehyde dihydrazone (15)

Hydrazine hydrate (150 mL, 3.0 mol) in ethanol was dropped to a solution of terephthalaldehyde (2 g, 14.9 mmol) in ethanol. The solution was cooled during the addition with an ice bath. The solution was allowed to warm up to room temperature and stand for several days. After evaporating the solution to dryness, the residue was recrystallized with ethanol and the obtained yellow solid was filtered off and dried *in vacuo*. Yield: 1.4 g (57%). ^1H NMR (400 MHz, THF-d₈, 27 °C): δ (ppm) = 7.58 (2H, s), 7.41 (4H, s), 6.15 (4H, s).

1,4-Bis(diazomethyl)benzene (16)

To a solution of **15** (100mg, 0.61 mmol), sodium sulfate (617 mg, 4.3 mmol) and yellow mercury(II) oxide (666 mg, 3 mmol) in benzene (38 mL) was added a saturated solution of potassium hydroxide in ethanol (0.15 mL). The solution was stirred for 100 minutes in which a color change from orange to brown can be observed. The reaction was monitored via IR-spectroscopy. The solution was filtered and evaporated to dryness to give a red sticky solid, which decomposes slowly at room temperature. Yield 43 mg (44%). ^1H NMR (400 MHz, CDCl_3 , 27 °C): δ (ppm) = 6.85 (4H, s), 4.93 (2H, s).

 $((\text{PPh}_3)_2\text{Cl}_2\text{Ru}(\text{CH-}p\text{-C}_6\text{H}_4\text{C}(\text{H}))\text{RuCl}_2(\text{PPh}_3)_2$ (17)

A solution of tris(triphenylphosphine)ruthenium(II) dichloride (109 mg, 0.11 mmol) in dry dichloromethane (7 mL), cooled to -80 °C, was treated with -50 °C cold solution of **16** (9 mg, 0.057 mmol) in dry dichloromethane (1 mL). A slight color change from red brown to green brown was observed. The solution was allowed to warm up to -20 °C in 10 minutes. A green brown solid precipitated. The solvent was removed and the residue was suspended in dichloromethane (3 mL) and precipitated with dry pentane (7 mL). The overlaying solution was removed by cannula filtration. This procedure was repeated until the overlaying solution was almost colorless. The remaining solid was dried *in vacuo*. The catalyst precursor was used directly for the subsequent reaction to generate catalyst **18**.

 $((\text{PCy}_3)_2\text{Cl}_2\text{Ru}(\text{CH-}p\text{-C}_6\text{H}_4\text{C}(\text{H}))\text{RuCl}_2(\text{PCy}_3)_2$ (18) (BG1)

A solution of the catalyst precursor in dry dichloromethane (10 mL) was treated with a solution of tricyclohexylphosphine (170 mg, 0.6 mmol) in dry dichloromethane (3 mL) for 1 h. A color change from green brown to red brown was observed. The solvent was removed and the residue was washed with dry acetone and dry diethyl ether. The resulting red brown solid was dried *in vacuo*. Yield: 102 mg (38%). ^1H NMR (400 MHz, CDCl_3 , 27 °C): δ (ppm) = 20.43 (2H, s), 7.77-7.34 (4H, m), 2.36-1.04 (132H, m).

Diethyl 2-ethyl-2-(undec-10-enyl)malonate (19)

All reaction steps were performed under an atmosphere of argon. Sodium hydride (60% mineral oil dispersion, 650 mg, 16.32 mmol) was dissolved in 17 mL anhydrous tetrahydrofuran. To this solution a solution of 2-ethyl-malonic acid diethyl ester (3.23 g, 17.18 mmol) in 3 mL anhydrous THF was added drop wise at room temperature. After the evolution of hydrogen gas ceased, 11-bromoundecene (2.67 g, 11.45 mmol) were added in one shot to the reaction mixture. The mixture was refluxed and the

conversion was monitored via TLC. After complete conversion, the solvent was removed. The crude product was dissolved in chloroform. After addition of a small amount of water, the phases were allowed to separate in a separation funnel. The organic layer was dried with brine and sodium sulfate and concentrated under reduced pressure. Final purification was performed via silica gel chromatography (hexane/ethylacetate = 10:1) giving the product as a colorless oil. Yield: 3.7 g (63%). ^1H NMR (400 MHz, CDCl_3 , 27 °C): δ (ppm) = 5.80 (1H, tdd, $^3J_{\text{HH}} = 6.7$ Hz, $^3J_{\text{HH}} = 10.2$ Hz, $^3J_{\text{HH}} = 16.9$ Hz), 4.98 (1H, d, $^3J_{\text{HH}} = 17.1$ Hz), 4.92 (1H, d, $^3J_{\text{HH}} = 10.2$ Hz), 4.17 (4H, q, $^3J_{\text{HH}} = 7.1$ Hz), 2.03 (2H, q, $^3J_{\text{HH}} = 6.9$ Hz), 1.92 (2H, q, $^3J_{\text{HH}} = 7.5$ Hz), 1.85 (2H, m), 1.24 (20H, m), 0.81 (3H, t, $^3J_{\text{HH}} = 7.5$ Hz). ^{13}C NMR (100 MHz, CDCl_3 , 27 °C): δ (ppm) = 171.8, 139.1, 114.0, 60.8, 58.0, 33.8, 31.6, 29.9, 29.5, 29.4, 29.3, 29.1, 28.9, 25.2, 23.9, 14.1, 8.4.

5-ethyl-5-(undec-10-enyl)pyrimidine-2,4,6-trione (20)

Sodium hydride (60% mineral oil dispersion, 0.94 g, 23.50 mmol) was added to a solution of urea (7.2 g, 117.4 mmol) in 25 mL anhydrous DMSO. After the evolution of hydrogen gas ceased **19** (2.0 g, 5.88 mmol) was added drop wise via syringe. The reaction mixture was stirred at room temperature for 6 days. The conversion was monitored via TLC. After showing complete conversion the reaction mixture was poured onto 200 mL ice water. The solution was neutralized with KHSO_4 and extracted with chloroform (overall 1L). The combined organic layers were concentrated under reduced pressure and the remaining crude product was dissolved in ethylacetate. To this solution was added 100 mL of 10w-% aqueous NH_4Cl solution. After drying with brine and sodium sulfate, the solvent was removed under reduced pressure. Pure product **20** was obtained after silica gel chromatography (hexane/ethyl acetate = 3/1) as white solid. Yield: 1.3 g (63%). ^1H NMR (400 MHz, CDCl_3 , 27 °C): δ (ppm) = 8.89 (2H, s), 5.80 (1H, tdd, $^3J_{\text{HH}} = 6.7$ Hz, $^3J_{\text{HH}} = 10.1$ Hz, $^3J_{\text{HH}} = 16.9$ Hz), 4.98 (1H, d, $^3J_{\text{HH}} = 17.1$ Hz), 4.92 (1H, d, $^3J_{\text{HH}} = 10.2$ Hz), 2.03 (6H, m), 1.23 (14H, m), 0.89 (3H, t, $^3J_{\text{HH}} = 7.4$ Hz). ^{13}C NMR (100 MHz, CDCl_3 , 27 °C): δ (ppm) = 172.6, 148.9, 139.1, 114.1, 57.5, 38.8, 33.7, 32.5, 29.5, 29.4, 29.4, 29.2, 29.1, 28.9, 25.2, 9.5.

5,5'-(Eicos-10-ene-1,20-diyl)bis(5-ethylpyrimidine-2,4,6-trione (21)

Compound **20** (200 mg, 0.65 mmol) and Grubbs catalyst 2nd-generation (27 mg, 0.032 mmol) were weighed into a vial equipped with a magnetic stir bar. The vial was flushed with argon and sealed with a rubber septum. After dissolving the mixture with dry dichloromethane (5 mL), the vial was placed in a microwave oven (heating up with 100 W to 100 °C, 30 W, 100 °C for 15 h). Formed ethylene was removed by purging the solution every 2 h with argon. Final quenching was done with ethyl vinyl ether.

The solvent was evaporated and the crude mixture was purified via silica gel chromatography (ethyl acetate/hexane = 1/1). Yield: 140 mg (74%). ^1H NMR (400 MHz, CDCl_3 , 27 °C): δ (ppm) = 8.81 (4H, s), 5.36 (2H, m), 2.05 (12H, m), 1.23 (28H, m), 0.89 (6H, t, $^3J_{\text{HH}} = 7.4$ Hz). ^{13}C NMR (100 MHz, CDCl_3 , 27 °C): δ (ppm) = 172.8, 149.1, 130.3, 129.8, 57.5, 38.9, 32.5, 29.6, 29.5, 29.4, 29.3, 29.2, 29.1, 28.9, 28.8, 27.1, 25.3, 9.6.

5-Methyl-1-undec-10-enyl-1H-pyrimidine-2,4-dione (22)

A mixture of thymine (1.12 g, 8.9 mmol), hexamethyldisilazane (HMDS) (5.7 mL, 27 mmol) and trimethylchlorosilane (TMSCl) (1.1 mL, 8.9 mmol) was refluxed under nitrogen atmosphere until a clear solution was obtained. The excess of HMDS was evaporated. To the resulting 2,4-bis(O-trimethylsilyl)thymine were added dry DMF (7.5 mL) and 11-bromo-1-undecene (2.5 g, 10.7 mmol). The mixture was stirred for 11 days at 80 °C under an inert atmosphere. After removal of the solvent, the remaining oil was purified via column chromatography (hexane/ethyl acetate = 20/1) to obtain a pale yellow solid. Yield: 2.1 g (61%). ^1H NMR (400 MHz, CDCl_3 , 27 °C): δ (ppm) = 8.39 (1H, s), 6.96 (1H, s), 5.81 (1H, m), 4.96 (2H, dd, $^3J_{\text{HH}} = 13.6$ Hz, $^3J_{\text{HH}} = 23.0$ Hz), 3.68 (2H, t, $^3J_{\text{HH}} = 4.5$ Hz), 2.04 (2H, dd, $^3J_{\text{HH}} = 6.9$ Hz, $^3J_{\text{HH}} = 14.0$ Hz), 1.92 (3H, s), 1.67 (2H, m), 1.28 (12H, m). ^{13}C NMR (100 MHz, CDCl_3 , 27 °C): δ (ppm) = 164.0, 150.7, 140.4, 139.1, 114.1, 110.5, 48.6, 33.8, 29.4, 29.3, 29.3, 29.1, 29.1, 29.0, 28.9, 26.4, 12.3.

1,1'-(Eicos-10-ene-1,20-diyl)bis(5-methyl-1H-pyrimidine-2,4-dione) (23)

Compound **22** (200 mg, 0.72 mmol) and Grubbs catalyst 2nd-generation (30 mg, 0.036 mmol) were weighed into a vial equipped with a magnetic stir bar. After flushing with argon the vial was sealed with a rubber septum. The mixture was dissolved with dry dichloromethane (5 mL) and was then placed in a microwave oven (heating up with 100 W to 100 °C, 30 W, 100 °C for 15 h). Gaseous ethylene was removed by purging the solution every 2 h with argon. The mixture was quenched with ethyl vinyl ether and after solvent evaporation the crude mixture was purified via silica gel chromatography (ethyl acetate/hexane = 1/1). Yield: 114 mg, (60%). ^1H NMR (400 MHz, CDCl_3 , 27 °C): δ (ppm) = 8.71 (s, 2H), 6.97 (s, 2H), 5.37 (m, 2H), 3.68 (m, 4H), 1.92 (s, 6H), 1.65 (m, 4H), 1.31 (m, 28 H). ^{13}C NMR (100 MHz, CDCl_3 , 27 °C) : δ (ppm) = 163.9, 150.6, 140.2, 130.2, 110.4, 109.9, 48.6, 32.6, 29.6, 29.4, 29.3, 29.2, 29.1, 26.5, 12.4.

cis-1,4-bisacetoxo-2-butene (24) commercially available

***trans*-1,4-dibromo-2-butene (25)** commercially available

6-bromohexyl allyl ether (26)

Allyl alcohol (1.0 g, 17.24 mmol) and 1,6-dibromohexane (13.0 g, 58.28 mmol) were dissolved in 22.9 ml of hexane. To the obtained solution were added 22 g of an aqueous sodium hydroxide solution (50 w-%) and tetrabutylammonium bromide (1.5 g, 4.1 mmol). The mixture was refluxed for 17 hours. After cooling down to room temperature, the organic phase was separated, washed with water, and dried over sodium sulfate. The solution was concentrated and the crude product was purified by column chromatography (hexane/ethylacetate = 10/1) to obtain compound **26**. Yield: 3.0 g (79 %). ¹H-NMR (400 MHz, DMSO-d₆, 27 °C): δ (ppm) = 5.87 (1H, tdd, ³J_{HH} = 17.2, ³J_{HH} = 10.5 Hz, ³J_{HH} = 5.3 Hz), 5.23 (1H, d, ³J_{HH} = 17.2 Hz), 5.12 (1H, d, ³J_{HH} = 10.5 Hz), 3.90 (2H, d, ³J_{HH} = 5.3 Hz), 3.51 (2H, t, ³J_{HH} = 6.7 Hz), 3.36 (2H, t, ³J_{HH} = 6.5 Hz), 1.79 (2H, m), 1.51 (2H, m), 1.35 (4H, m).

5-methyl-1-(6-(allyloxy)hexyl)pyrimidine-2,4-(1H,3H)-dione (27)

A mixture of thymine (1.12 g, 8.9 mmol), 1,1,1,3,3,3-hexamethyldisilazane (HMDS) (5.7 ml, 13.5 mmol) and trimethylchlorosilane (TMSCl) (1.1 ml, 8.9 mmol) was refluxed under nitrogen atmosphere until a clear solution was obtained. The excess of HMDS was then evaporated with a rotary evaporator at reduced pressure. To the resulting crude bis(O-trimethylsilyl)thymine were added dry DMF (15 ml) and compound **26** (2.4 g, 10.86 mmol). The mixture was stirred for 11 days at 80 °C under a nitrogen atmosphere. The pure product was finally isolated via column chromatography (hexane/ethyl acetate, 1:4) as light yellow crystals. Yield: 0.9 g (40 %). ¹H-NMR (400 MHz, CDCl₃, 27 °C): δ (ppm) = 8.08 (1H, s), 6.96 (1H, s), 5.91 (1H, tdd, ³J_{HH} = 17.2, ³J_{HH} = 10.5 Hz, ³J_{HH} = 5.3 Hz), 5.26 (1H, d, ³J_{HH} = 17.2), 5.17 (1H, d, ³J_{HH} = 10.5), 3.96 (2H, d, ³J_{HH} = 5.6 Hz), 3.68 (2H, t, ³J_{HH} = 7.4 Hz), 3.42 (2H, t, ³J_{HH} = 6.4 Hz), 1.92 (3H, m), 1.69 (2H, m), 1.60 (2H, m), 1.38 (4H, m).

Homometathesis of 5-methyl-1-(6-(allyloxy)hexyl)pyrimidine-2,4-(1H,3H)-dione (28)

Compound **27** (450 mg, 1.76 mmol) and Grubbs catalyst 2nd generation (25 mg, 0.030 mmol) and copper(I) iodide (12 mg, 0.195 mmol) were weighed into a vial equipped with magnetic stir bar. The vial was flushed with nitrogen and sealed with a septum. Dry dichloromethane (4 ml) and dry diethyl ether (4 ml) were subsequently added into the vial to dissolve the mixture. After connecting the vial to a reflux condenser equipped with outlet tap/oil bubbler, the resulting solution was refluxed at 68 °C for 3 days.

The reaction was quenched with ethyl vinyl ether. The crude mixture was concentrated using rotary evaporator at reduced pressure and a final purification of the crude product was carried out via silica gel chromatography (ethyl acetate/methanol, 4:1), to give product **28**. Yield: 260 mg (59 %). $^1\text{H-NMR}$ (400 MHz, DMSO-d_6 , 27 °C): δ (ppm) = 11.15 (2H, s), 5.52 (2H, s), 5.69 (2H, m), 3.87 (4H, m), 3.58 (4H, t, $^3J_{\text{HH}} = 7.1$ Hz), 3.32 (4H, t, $^3J_{\text{HH}} = 6.6$ Hz), 1.74 (6H, s), 1.54 (4H, m), 1.47 (4H, m), 1.26 (8H, m).

4. References

- (1) Grubbs, R. H. *Tetrahedron* **2004**, *60*, 7117-7140.
- (2) Frenzel, U.; Müller, B. K. M.; Nuyken, O. In *Handbook of Polymer Synthesis*; 2nd ed.; CRC: 2004, p 381-427.
- (3) Schrock, R. R.; Hoveyda, A. H. *Angew. Chem. Int. Ed.* **2003**, *42*, 4592 - 4633.
- (4) Sanford, M. S.; Love, J. A. In *Handbook of Metathesis*; Grubbs, R. H., Ed.; Wiley-VCH: 2003, p 112-131.
- (5) Buchmeiser, M. R. *Chem. Rev.* **2000**, *100*, 1565-1604.
- (6) Koshravi, E. In *Handbook of Metathesis*; Grubbs, R. H., Ed.; Wiley-VCH: 2003, p 112-131.
- (7) Bielawski, C. W.; Grubbs, R. H. *Prog. Polym. Sci.* **2007**, *32*, 1-29.
- (8) Weck, M.; Schwab, P.; Grubbs, R. H. *Macromolecules* **1996**, *29*, 1789-1793.
- (9) Singh, R.; Czekelius, C.; Schrock, R. R. *Macromolecules* **2006**, *39*, 1316-1317.
- (10) Ambade, A. V.; Burd, C.; Higley, M. N.; Nair, K. P.; Weck, M. *Chem. Eur. J.* **2009**, *15*, 11904-11911.
- (11) Yang, S. K.; Ambade, A. V.; Weck, M. *J. Am. Chem. Soc.* **2010**, *132*, 1637-1645.
- (12) Matson, J. B.; Grubbs, R. H. *Macromolecules* **2010**, *43*, 213-221.
- (13) Grubbs, R. H.; *Handbook of Metathesis*; Ed.; Wiley-VCH: 2003,
- (14) Choi, T.-L.; Grubbs, R. H. *Angew. Chem. Int. Ed.* **2003**, *42*, 1743 - 1746.
- (15) Chauvin, Y.; Hérisson, P. J.-L. *Makromol. Chem.* **1971**, *141*, 161-176.
- (16) Matyjaszewski, K. *J. Polym. Sci., Part A: Polym. Chem.* **1993**, 995-999.
- (17) Buchmeiser, M. R. *Chem. Rev.* **2000**, *100*, 1565-1604.
- (18) Conrad, J. C.; Eelman, M. D.; Silva, J. A. D.; Monfette, S.; Parnas, H. H.; Snelgrove, J. L.; Fogg, D. E. *J. Am. Chem. Soc.* **2007**, *129*, 1024-1025.
- (19) Schrodi, Y.; Pederson, R. L. *Aldrichim. Acta* **2007**, *40*, 45-52.
- (20) Trnka, T. M.; Grubbs, R. H. *Acc. Chem. Res.* **2000**, *34*, 18-29.
- (21) Cazalis, C.; Héroguez, V.; Fontanille, M. *Macromol. Symp.* **2002**, *183*, 103-112.
- (22) Perrott, M. G.; Novak, B. M. *Macromolecules* **1996**, *29*, 1817-1823.
- (23) Bazan, G. C.; Khosravi, E.; Schrock, R. R.; Feast, W. J.; Gibson, V. C.; O'Regan, M. B.; Thomas, J. K.; Davis, W. M. *J. Am. Chem. Soc.* **1990**, *112*, 8378-8387.
- (24) Binder, W. H.; Kurzhals, S.; Pulamagatta, B.; Decker, U.; Manohar Pawar, G.; Wang, D.; Kühnel, C.; Buchmeiser, M. R. *Macromolecules* **2008**, *41*, 8405-8412.
- (25) Lapinte, V.; Brosse, J.-C.; Fontaine, L. *Macromol. Chem. Phys.* **2004**, *205*, 824-833.
- (26) Slugovc, C. *Macromol. Rapid Commun.* **2004**, *25*, 1283-1297.
- (27) Slugovc, C.; Demel, S.; Riegler, S.; Hobisch, J.; Stelzer, F. *Macromol. Rapid Comm.* **2004**, *25*, 475-480.
- (28) Leitgeb, A.; Wappel, J.; Slugovc, C. *Polymer* **2010**, *51*, 2927-2946.
- (29) Yoon, K.-H.; Kim, K. O.; Schaefer, M.; Yoon, D. Y. *Polymer* **2012**, *53*, 2290-2297.
- (30) Dunbar, M. A.; Balof, S. L.; LaBeaud, L. J.; Yu, B.; Lowe, A. B.; Valente, E. J.; Schanz, H. -J. *Chem. Eur. J.* **2009**, *15*, 12435-12446.
- (31) Huang, J.; Schanz, H. J.; Stevens, E. D.; Nolan, S. P. *Organometallics* **1999**, *18*, 5375-5380.
- (32) Voigtritter, K.; Ghorai, S.; Lipshutz, B. H. *J. Org. Chem.* **2011**, *76*, 4697-4702.
- (33) Sanford, M. S.; Ulman, M.; Grubbs, R. H. *J. Am. Chem. Soc.* **2001**, *123*, 749-750.
- (34) Sanford, M. S.; Love, J. A.; Grubbs, R. H. *J. Am. Chem. Soc.* **2001**, *123*, 6543-6554.
- (35) Myers, S. B.; Register, R. A. *Polymer* **2008**, *49*, 877-882.
- (36) Lee, L. B. W.; Register, R. A. *Macromolecules* **2005**, *38*, 1216-1222.

- (37) Sanford, M. S.; Love, J. A.; Grubbs, R. H. *J. Am. Chem. Soc.* **2001**, *123*, 6543-6554.
- (38) Schulz, M. D.; Wagener, K. B. *ACS Macro Letters* **2012**, *1*, 449-451.
- (39) Samojłowicz, C.; Bieniek, M.; Pazio, A.; Makal, A.; Woźniak, K.; Poater, A.; Cavallo, L.; Wójcik, J.; Zdanowski, K.; Grela, K. *Chem. Eur. J.* **2011**, *17*, 12981-12993.
- (40) Cazalis, C.; Héroguez, V.; Fontanille, M. *Macromol. Chem. Phys.* **2000**, *201*, 869-876.
- (41) Love, J. A.; Morgan, J. P.; Trnka, T. M.; Grubbs, R. H. *Angew. Chem. Int. Ed. Engl.* **2002**, *41*, 4035-4037.
- (42) The Nobel Prize in Chemistry 2002". Nobelprize.org. 4 Sep 2012 http://www.nobelprize.org/nobel_prizes/chemistry/laureates/2002/.
- (43) Schrock, R. R.; Gabert, A. J.; Singh, R.; Hock, A. S. *Organometallics* **2005**, *24*, 5058-5066.
- (44) Binder, W. H.; Pulamagatta, B.; Onur, K.; Kurzhals, S.; Barqawi, H.; Tanner, S. *Macromolecules* **2009**, *42*, 9457-9466.
- (45) Hilf, S.; Berger-Nicoletti, E.; Grubbs, R. H.; Kilbinger, A. F. M. *Angew. Chem. Int. Ed.* **2006**, *45*, 8045-8048.
- (46) Hilf, S.; Grubbs, R. H.; Kilbinger, A. F. M. *J. Am. Chem. Soc.* **2008**, *130*, 11040-11048.
- (47) Hilf, S.; Grubbs, R. H.; Kilbinger, A. F. M. *Macromolecules* **2008**, *41*, 6006-6011.
- (48) Hilf, S.; Kilbinger, A. F. M. *Macromolecules* **2009**, *42*, 1099-1106.
- (49) Hilf, S.; Kilbinger, A. F. M. *Macromolecules* **2009**, *42*, 4127-4133.
- (50) Hilf, S.; Kilbinger, A. F. M. *Nat. Chem.* **2009**, *1*, 537-546.
- (51) Hilf, S.; Kilbinger, A. F. M. *Macromolecules* **2010**, *43*, 208-212.
- (52) Nagarkar, A. A.; Crochet, A.; Fromm, K. M.; Kilbinger, A. F. M. *Macromolecules* **2012**, *45*, 4447-4453.
- (53) Scherman, O. A.; Rutenberg, I. M.; Grubbs, R. H. *J. Am. Chem. Soc.* **2003**, *125*, 8515-8522.
- (54) Biagini, S. C. G.; Gareth Davies, R.; Gibson, V. C.; Giles, M. R.; Marshall, E. L.; North, M. *Polymer* **2001**, *42*, 6669-6671.
- (55) Madkour, A. E.; Koch, A. H. R.; Lienkamp, K.; Tew, G. N. *Macromolecules* **2010**, *43*, 4557-4561.
- (56) Saetung, N.; Campistron, I.; Pascual, S.; Pilard, J.-F.; Fontaine, L. *Macromolecules* **2011**, *44*, 784-794.
- (57) Enders, C.; Tanner, S.; Binder, W. H. *Macromolecules* **2010**, *43*, 8436-8446.
- (58) Rivera-Tirado, E.; Aaserud, D. J.; Wesdemiotis, C. *J. Appl. Polym. Sci., Part A: Polym. Chem.* **2012**, *124*, 2682-2690.
- (59) Kurzhals, S.; Binder, W. H. *Macromol. Symp.* **2010**, *293*, 63-66.
- (60) Kurzhals, S.; Binder, W. H. *J. Polym. Sci., Part A: Polym. Chem.* **2010**, *48*, 5522-5532.
- (61) Yu, C.-Y.; Turner, M. L. *Angew. Chem.* **2006**, *118*, 7961-7964.
- (62) Yu, C.-Y.; Horie, M.; Spring, A. M.; Tremel, K.; Turner, M. L. *Macromolecules* **2010**, *43*, 222-232.
- (63) Gibson, V. C.; Marshall, E. L.; North, M.; Robson, D. A.; Williams, P. J. *Chem. Commun.* **1997**, 1095-1096.
- (64) Eelman, M. D.; Blacquiere, J. M.; Moriarty, M. M.; Fogg, D. E. *Angew. Chem.* **2008**, *47*, 303-306.
- (65) Zhu, W.; Wang, H.-Y.; Guo, Y.-L. *J. Mass. Spectrom.* **2012**, *47*, 352-354.
- (66) Jirásko, R.; Holčápek, M. *Mass Spectrom. Rev.* **2010**, *30*, 1013-1036.
- (67) Beierlein, C. H.; Breit, B.; Paz Schmidt, R. A.; Plattner, D. A. *Organometallics* **2010**, *29*, 2521-2532.
- (68) Aliprantis, A. O.; Canary, J. W. *J. Am. Chem. Soc.* **1994**, *116*, 6985-6986.
- (69) Fiebig, L.; Schmalz, H.-G.; Schäfer, M. *Int. J. Mass Spectrom.* **2011**, *308*, 307-310.

- (70) Santos, L. S.; Rosso, G. B.; Pilli, R. A.; Eberlin, M. N. *J. Org. Chem.* **2007**, *72*, 5809-5812.
- (71) Adlhart, C.; Peter, C. *Helv. Chim. Acta* **2000**, *83*, 2192-2196.
- (72) Adlhart, C.; Hinderling, C.; Baumann, H.; Chen, P. *J. Am. Chem. Soc.* **2000**, *122*, 8204-8214.
- (73) Volland, M. A. O.; Adlhart, C.; Kiener, C. A.; Chen, P.; Hofmann, P. *Chem. Eur. J.* **2001**, *7*, 4621-4632.
- (74) Adlhart, C.; Chen, P. *Helv. Chim. Acta* **2003**, *86*, 941-949.
- (75) Chen, P. *Angew. Chem. Int. Ed.* **2003**, *42*, 2832-2847.
- (76) Adlhart, C.; Chen, P. *J. Am. Chem. Soc.* **2004**, *126*, 3496-3510.
- (77) Torker, S.; Merki, D.; Chen, P. *J. Am. Chem. Soc.* **2008**, *130*, 4808-4814.
- (78) Wang, H.; Metzger, J. O. *Organometallics* **2008**, *27*, 2761-2766.
- (79) Hao-Yang, W.; Wai-Leung, Y.; Thorsten, K.; Jürgen, O. M. *Chem. Eur. J.* **2009**, *15*, 10948-10959.
- (80) Zhao, Z.-X.; Wang, H.-Y.; Guo, Y.-L. *Rapid Commun. Mass Spectrom.* **2011**, *25*, 3401-3410.
- (81) Wang, H.-Y.; Yim, W.-L.; Guo, Y.-L.; Metzger, J. O. *Organometallics* **2012**, *31*, 1627-1634.
- (82) Chatterjee, A. K.; Choi, T.-L.; Sanders, D. P.; Grubbs, R. H. *J. Am. Chem. Soc.* **2003**, *125*, 11360-11370.
- (83) Crowe, W. E.; Goldberg, D. R.; Zhang, Z. J. *Tetrahedron Lett.* **1996**, *37*, 2117-2120.
- (84) Wakamatsu, H.; Blechert, S. *Angew. Chem. Int. Ed.* **2002**, *41*, 2403-2405.
- (85) Harrity, J. P. A.; Visser, M. S.; Gleason, J. D.; Hoveyda, A. H. *J. Am. Chem. Soc.* **1997**, *119*, 1488-1489.
- (86) Kingsbury, J. S.; Harrity, J. P. A.; Bonitatebus, P. J.; Hoveyda, A. H. *J. Am. Chem. Soc.* **1999**, *121*, 791-799.
- (87) Garber, S. B.; Kingsbury, J. S.; Gray, B. L.; Hoveyda, A. H. *J. Am. Chem. Soc.* **2000**, *122*, 8168-8179.
- (88) Randl, S.; Gessler, S.; Wakamatsu, H.; Blechert, S. *Synlett* **2001**, *2001*, 0430-0432.
- (89) Imhof, S.; Randl, S.; Blechert, S. *Chem. Commun.* **2001**, 1692-1693.
- (90) Randl, S.; Connon, S. J.; Blechert, S. *Chem. Commun.* **2001**, 1796-1797.
- (91) Stewart, I. C.; Douglas, C. J.; Grubbs, R. H. *Org. Lett.* **2008**, *10*, 441-444.
- (92) Gessler, S.; Randl, S.; Blechert, S. *Tetrahedron Lett.* **2000**, *41*, 9973-9976.
- (93) Grela, K.; Harutyunyan, S.; Michrowska, A. *Angew. Chem.* **2002**, *114*, 4210-4212.
- (94) Love, J. A.; Morgan, J. P.; Trnka, T. M.; Grubbs, R. H. *Angew. Chem. Int. Ed.* **2002**, *41*, 4035-4037.
- (95) Gestwicki, J. E.; Cairo, C. W.; Mann, D. A.; Owen, R. M.; Kiessling, L. L. *Anal. Biochem.* **2002**, *305*, 149-155.
- (96) Gordon, E. J.; Gestwicki, J. E.; Strong, L. E.; Kiessling, L. L. *Chem. Biol.* **2000**, *7*, 9-16.
- (97) Chen, B.; Metera, K.; Sleiman, H. F. *Macromolecules* **2005**, *38*, 1084-1090.
- (98) Katayama, H.; Yonezawa, F.; Nagao, M.; Ozawa, F. *Macromolecules* **2002**, *35*, 1133-1136.
- (99) Owen, R. M.; Gestwicki, J. E.; Young, T.; Kiessling, L. L. *Org. Lett.* **2002**, *4*, 2293-2296.
- (100) Yang, S. K.; Ambade, A. V.; Weck, M. *Chem. Eur. J.* **2009**, *15*, 6605-6611.
- (101) Ambade, A. V.; Yang, S. K.; Weck, M. *Angew. Chem. Int. Ed.* **2009**, *121*, 2938-2942.
- (102) Crowe, W. E.; Mitchell, J. P.; Gibson, V. C.; Schrock, R. R. *Macromolecules* **1990**, *23*, 3534-3536.
- (103) Bielawski, C. W.; Morita, T.; Grubbs, R. H. *Macromolecules* **2000**, *33*, 678-680.
- (104) Bielawski, C. W.; Benitez, D.; Morita, T.; Grubbs, R. H. *Macromolecules* **2001**, *34*, 8610-8618.
- (105) Bielawski, C. W.; Scherman, O. A.; Grubbs, R. H. *Polymer* **2001**, *42*, 4939-4945.

- (106) Mitchell, J. P.; Gibson, V. C.; Schrock, R. R. *Macromolecules* **1991**, *24*, 1220-1221.
- (107) Mangold, S. L.; Carpenter, R. T.; Kiessling, L. L. *Org. Lett.* **2008**, *10*, 2997-3000.
- (108) Sudheendran, M.; Buchmeiser, M. R. *Macromolecules* **2010**, *43*, 9601-9607.
- (109) Hilf, S.; Hanik, N.; Kilbinger, A. F. M. *J. Polym. Sci., Part A: Polym. Chem.* **2008**, *46*, 2913-2921.
- (110) Lexer, C.; Saf, R.; Slugovc, C. *J. Polym. Sci., Part A: Polym. Chem.* **2009**, *47*, 299-305.
- (111) Matson, J. B.; Grubbs, R. H. *Macromolecules* **2008**, *41*, 5626-5631.
- (112) Higley, M. N.; Pollino, J. M.; Hollembeak, E.; Weck, M. *Chem. Eur. J.* **2005**, *11*, 2946-2953.
- (113) Maughon, B. R.; Morita, T.; Bielawski, C. W.; Grubbs, R. H. *Macromolecules* **2000**, *33*, 1929-1935.
- (114) Bai, Y.; Lu, H.; Ponnusamy, E.; Cheng, J. *Chem. Commun.* **2011**, *47*, 10830-10832.
- (115) Grudzien, K.; Malinska, M.; Barbasiewicz, M. *Organometallics* **2012**, *31*, 3636-3646.
- (116) Singh, R.; Verploegen, E.; Hammond, P. T.; Schrock, R. R. *Macromolecules* **2006**, *39*, 8241-8249.
- (117) Robson, D. A.; Gibson, V. C.; Davies, R. G.; North, M. *Macromolecules* **1999**, *32*, 6371-6373.
- (118) Burtscher, D.; Lexer, C.; Mereiter, K.; Winde, R.; Karch, R.; Slugovc, C. *J. Polym. Sci., Part A: Polym. Chem* **2008**, *46*, 4630-4635.
- (119) Haigh, D. M.; Kenwright, A. M.; Khosravi, E. *Macromolecules* **2005**, *38*, 7571-7579.
- (120) Czelusniak, I.; Heywood, J. D.; Kenwright, A. M.; Khosravi, E. *J. Mol. Catal. A: Chem.* **2008**, *280*, 29-34.
- (121) Adekunle, O.; Tanner, S.; Binder, W. H. *Beilstein J. Org. Chem.* **2010**, *6*, 59.
- (122) Keitz, B. K.; Fedorov, A.; Grubbs, R. H. *J. Am. Chem. Soc.* **2012**, *134*, 2040-2043.
- (123) Hamilton, J. G. *Polymer* **1998**, *39*, 1669-1689.
- (124) Bazan, G. C.; Renak, M. L.; Sun, B. J. *Macromolecules* **1996**, *29*, 1085-1087.
- (125) Spring, A. M.; Yu, C.-Y.; Horie, M.; Turner, M. L. *Chem. Commun.* **2009**, 2676-2678.
- (126) Yu, C. Y.; Kingsley, J. W.; Lidzey, D. G.; Turner, M. L. *Macromol. Rapid Commun.* **2009**, *30*, 1889-1892.
- (127) Yu, C.-Y.; Helliwell, M.; Raftery, J.; Turner, M. L. *Chem. Eur. J.* **2011**, *17*, 6991-6997.
- (128) Conticello, V. P.; Gin, D. L.; Grubbs, R. H. *J. Am. Chem. Soc.* **1992**, *114*, 9708-9710.
- (129) Fabris, F.; Rosso, E.; Paulon, A.; De Lucchi, O. *Tetrahedron Lett.* **2006**, *47*, 4835-4837.
- (130) Wagaman, M. W.; Bellmann, E.; Cucullu, M.; Grubbs, R. H. *J. Org. Chem.* **1997**, *62*, 9076-9082.
- (131) Yang, N. C. C.; Chen, M. J.; Chen, P. *J. Am. Chem. Soc.* **1984**, *106*, 7310-7315.
- (132) Yang, N. C. C.; Chen, M. J.; Chen, P.; Mak, K. T. *J. Am. Chem. Soc.* **1982**, *104*, 853-855.
- (133) Conticello, V. P.; Gin, D. L.; Grubbs, R. H. *J. Am. Chem. Soc.* **1992**, *114*, 9708-9710.
- (134) Evans, W. J.; Gummersheimer, T. S.; Ziller, J. W. *J. Am. Chem. Soc.* **1995**, *117*, 8999-9002.
- (135) Guthrie, J. P. *Can. J. Chem.* **1978**, *56*, 2342-2354.
- (136) Bazan, G. C.; Schrock, R. R. *Macromolecules* **1991**, *24*, 817-823.
- (137) Nomura, K.; Takahashi, S.; Imanishi, Y. *Macromolecules* **2001**, *34*, 4712-4723.
- (138) Nomura, K.; Takahashi, S.; Imanishi, Y. *Polymer* **2000**, *41*, 4345-4350.
- (139) Bishop, J. P.; Register, R. A. *Polymer* **2010**, 1-6.
- (140) Cazalis, C.; Héroguez, V.; Fontanille, M. *Macromol. Chem. Phys.* **2001**, *202*, 1513-1517.
- (141) Schrock, R. R. *Dalton Trans.* **2011**, *40*, 7484-7495.
- (142) Flook, M. M.; Ng, V. W. L.; Schrock, R. R. *J. Am. Chem. Soc.* **2011**, *133*, 1784-1786.
- (143) Stubenrauch, K.; Moitzi, C.; Fritz, G.; Glatter, O.; Trimmel, G.; Stelzer, F. *Macromolecules* **2006**, *39*, 5865-5874.

- (144) Katsumata, T.; Qu, J.; Shiotsuki, M.; Satoh, M.; Wada, J.; Igarashi, J.; Mizoguchi, K.; Masuda, T. *Macromolecules* **2008**.
- (145) Wilczek-Vera, G.; Yu, Y.; Waddell, K.; Danis, P. O.; Eisenberg, A. *Macromolecules* **1999**, *32*, 2180-2187.
- (146) Montaudo, G.; Samperi, F.; Montaudo, M. S. *Prog. Polym. Sci.* **2006**, *31*, 277-357.
- (147) Chen, H.; He, M.; Pei, J.; He, H. *Anal. Chem.* **2003**, *75*, 6531-6535.
- (148) Chen, H.; He, M. *J. Am. Soc. Mass Spectrom.* **2005**, *16*, 100-106.
- (149) Schnöll-Bitai, I.; Hrebicek, T.; Rizzi, A. *Macromol. Chem. Phys.* **2007**, *208*, 485-495.
- (150) Guttman, C. M.; Flynn, K. M.; Wallace, W. E.; Kearsley, A. J. *Macromolecules* **2009**, *42*, 1695-1702.
- (151) Walterová, Z.; Horský, J. *J. Anal. Chim. Acta* **2011**, *693*, 82-88.
- (152) Liu, X. M.; Maziarz, E. P.; Quinn, E.; Lai, Y.-C. *Int. J. Mass Spectrom.* **2004**, *238*, 227-233.
- (153) Kluger, C.; Binder, W. H. *J. Polym. Sci., Part A: Polym. Chem.* **2007**, *45*, 485-499.
- (154) Binder, W.; Zirbs, R. In *Adv. Polym. Sci.: "Hydrogen Bonded Polymers"* 2007, p 1-78.
- (155) Binder, W. H.; Kluger, C.; Josipovic, M.; Straif, C. J.; Friedbacher, G. *Macromolecules* **2006**, *39*, 8092-8101.
- (156) Zirbs, R.; Kienberger, F.; Hinterdorfer, P.; Binder, W. H. *Langmuir* **2005**, *21*, 8414-8421.
- (157) Binder, W. H.; Kluger, C.; Straif, C. J.; Friedbacher, G. *Macromolecules* **2005**, *38*, 9405-9410.
- (158) Binder, W. H.; Bernstorff, S.; Kluger, C.; Petraru, L.; Kunz, M. J. *Adv. Mater.* **2005**, *17*, 2824-2828.
- (159) Kunz, M. J.; Hayn, G.; Saf, R.; Binder, W. H. *J. Polym. Sci., Part A: Polym. Chem.* **2004**, *42*, 661-674.
- (160) Binder, W. H.; Kunz, M. J.; Kluger, C.; Hayn, G.; Saf, R. *Macromolecules* **2004**, *37*, 1749-1759.
- (161) Binder, W. H.; Kluger, C. *Macromolecules* **2004**, *37*, 9321-9330.
- (162) Ambade, A. V.; Yang, S. K.; Weck, M. *Angew. Chem. Int. Ed.* **2009**, *48*, 2894-2898.
- (163) Nair, K. P.; Breedveld, V.; Weck, M. *Macromolecules* **2008**, *41*, 3429-3438.
- (164) Weck, M. *Polym. Int.* **2007**, *56*, 453-460.
- (165) South, C. R.; Leung, K. C. F.; Lanari, D.; Stoddart, J. F.; Weck, M. *Macromolecules* **2006**, *39*, 3738-3744.
- (166) Nair, K. P.; Pollino, J. M.; Weck, M. *Macromolecules* **2006**, *39*, 931-940.
- (167) Burd, C.; Weck, M. *Macromolecules* **2005**, *38*, 7225-7230.
- (168) Binder, W. H.; Zirbs, R.; Kienberger, F.; Hinterdorfer, P. *Polym. Adv. Technol.* **2006**, *17*, 754-757.
- (169) Moreau, J. J. E.; Pichon, B. P.; Arrachart, G.; Man, M. W. C.; Bied, C. *New J. Chem.* **2005**, *29*, 653-658.
- (170) Katritzky, A. R.; El-Mowafy, A. M. *J. Org. Chem.* **1982**, *47*, 3506-3511.
- (171) Binder, W. H.; Pulamagatta, B.; Kir, O.; Kurzhals, S.; Barqawi, H.; Tanner, S. *Macromolecules* **2009**, *42*, 9457-9466.
- (172) Schulz, M.; Tanner, S.; Barqawi, H.; Binder, W. H. *J. Polym. Sci., Part A: Polym. Chem.* **2010**, *48*, 671-680.
- (173) Jamieson, A.; Venkataswamy, K. *Polymer Bull. (Berlin)* **1984**, *12*, 275-282.
- (174) Abdulahad, A. I.; Ryu, C. Y. *J. Polym. Sci. B: Polym. Phys.* **2009**, *47*, 2533-2540.
- (175) Lin, Y.-H. *Macromolecules* **1990**, *23*, 5292-5294.
- (176) Esteruelas, M. A.; González, F.; Herrero, J.; Lucio, P.; Oliván, M.; Ruiz-Labrador, B. *Polym. Bull. (Berlin)* **2007**, *58*, 923-931.
- (177) Sakurai, K.; Takahashi, T. *J. Appl. Polym. Sci.* **1989**, *38*, 1191-1194.

-
- (178) Wurm, A.; Zhuravlev, E.; Eckstein, K.; Jehnichen, D.; Pospiech, D.; Androsch, R.; Wunderlich, B.; Schick, C. *Macromolecules* **2012**, *45*, 3816-3828.
- (179) Murray, R. W.; Trozzolo, A. M. *J. Org. Chem.* **1964**, *29*, 1268-1270.
- (180) Yates, P.; Shapiro, B. L.; Yoda, N.; Fugger, J. *J. Am. Chem. Soc.* **1957**, *79*, 5756-5760.
- (181) Henderson, W. A.; Streuli, C. A. *J. Am. Chem. Soc.* **1960**, *82*, 5791-5794.
- (182) Rubin, M.; Gevorgyan, V. *Synthesis* **2004**, *5*, 796-800.
- (183) Katsumata, T.; Satoh, M.; Wada, J.; Shiotsuki, M.; Sanda, F.; Masuda, T. *Macromol. Rapid Commun.* **2006**, *27*, 1206-1211.
- (184) Plieninger, H.; Schwarz, B.; Jaggy, H.; Huber-Patz, U.; Rodewald, H.; Irngartinger, H.; Weinges, K. *Liebigs Ann. Chem.* **1986**, *1986*, 1772-1778.
- (185) Han, C.-C.; Balakumar, R. *Tetrahedron Lett.* **2006**, *47*, 8255-8258.

5. Appendix

Chapter 2.2.

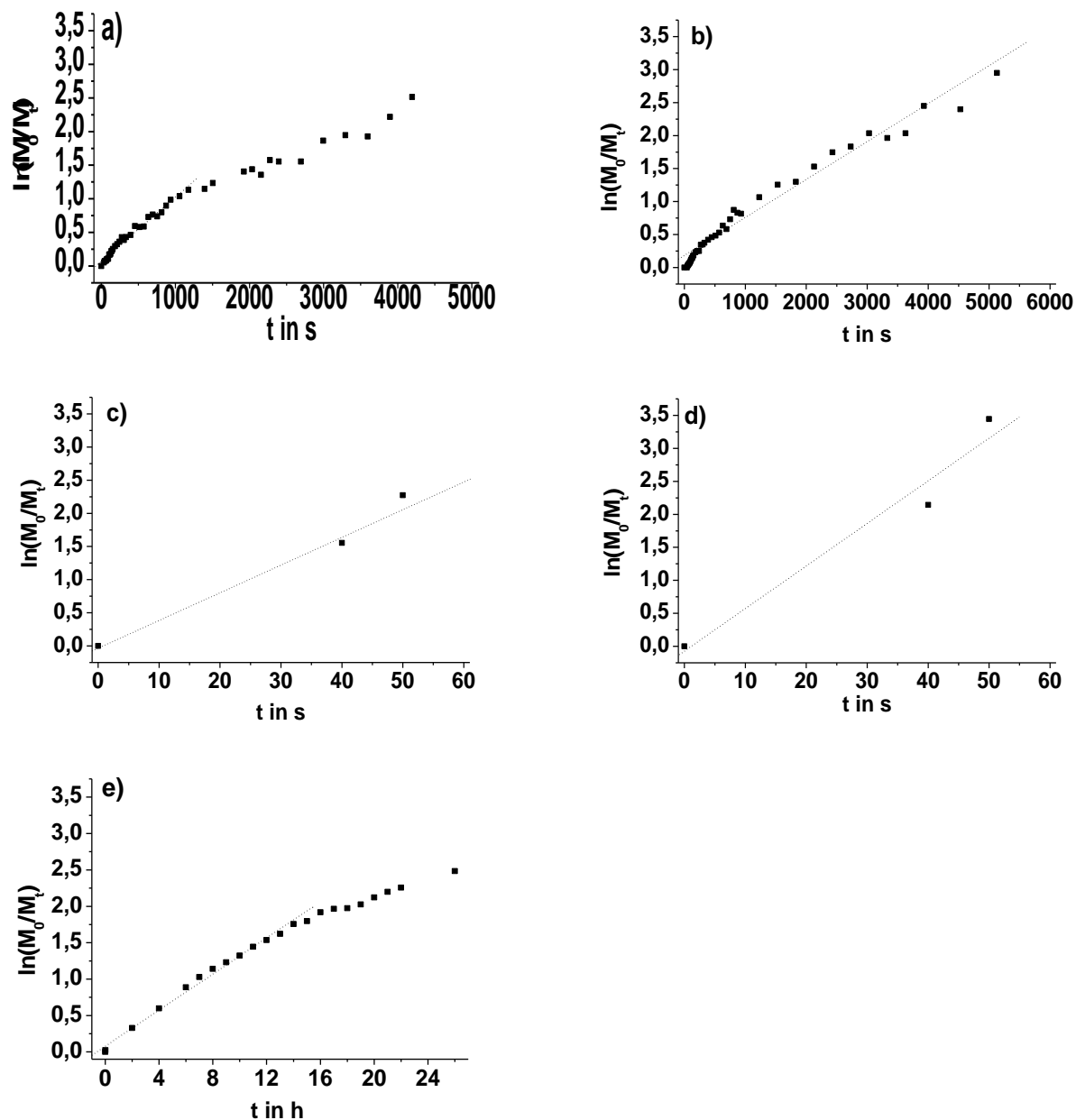


Figure 5.1. NMR kinetic plots for the polymerization of monomer **1** (5 equiv.) with a) **G1**, b) **U1**, c) **G3**, d) **U3**, e) **BG1**, polymerization of 50 equiv. of monomer **1**, the linear fit is represented by the dashed line.

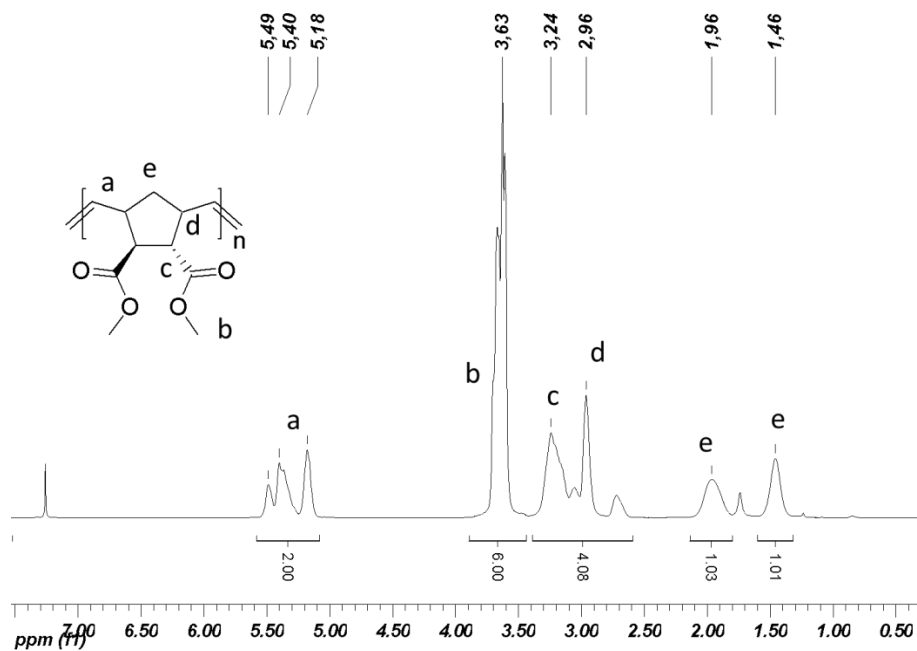


Figure 5.2. ^1H NMR of poly(1), prepared with G3, in CDCl_3 .

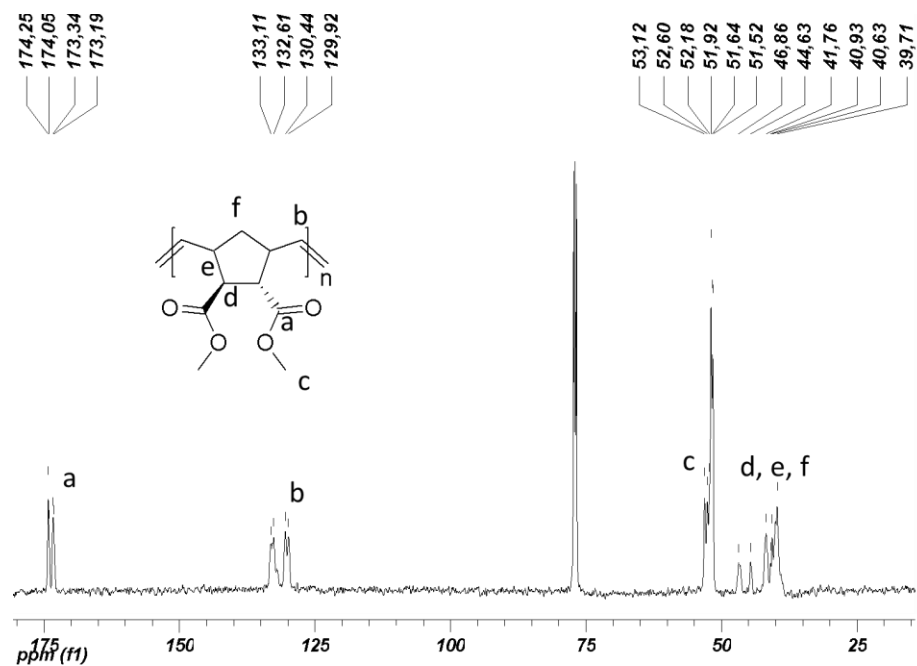
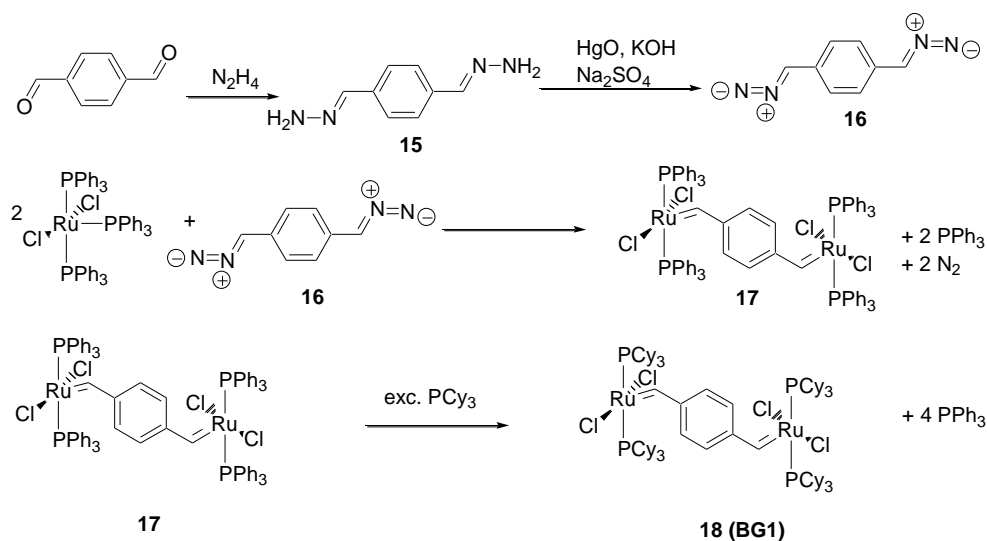


Figure 5.3. ^{13}C NMR of poly(1), prepared with G3, in CDCl_3 .

Synthesis of bimetallic catalyst BG1

Besides the monovalent catalysts (**G1-G3**, **U1-U3**) which should be used for the preparation of semi-telechelic polymers, a bimetallic catalyst should be synthesized in order to test the quenching with symmetric olefins for the preparation of telechelic polymers. As catalyst for the preparation of telechelic polymers, a bivalent Grubbs catalyst 1st-generation reported by Weck et al. was chosen.⁸ The synthetic approach^{8,179} towards this catalyst is shown in Scheme 5.1.



Scheme 5.1. Synthetic pathway towards the bimetallic Grubbs catalyst **BG1**.

In the first step, terephthalaldehyde dihydrazone (**15**) was prepared by the reaction of terephthalaldehyde with hydrazine hydrate, furnishing a yellow solid in a yield of 57%. The ^1H NMR (see Figure 5.4) shows three singlets at 7.58 ppm ($\text{CH}=\text{N}$), 7.41 ppm (CH_{ar}), and 6.15 ppm (NH_2) in an integral ratio of 2:4:4. In the second step, 1,4-bis(diazomethyl)benzene¹⁷⁹ (**16**) was prepared via oxidation of (**15**) with mercury(II) oxide in a yield of 43%. The reaction progress was monitored by IR-spectroscopy (KBr-disk), showing a strong band for the diazomethyl group (CHN_2) at 1996 cm^{-1} (literature: $2000\text{-}2100 \text{ cm}^{-1}$).¹⁸⁰ In the ^1H NMR spectrum, two singlets can be seen at 6.85 (CH_{ar}) and 4.93 ppm ($\text{CH}=\text{N}$) in an integral ratio of 4 to 2. Compound **16** decomposes at room temperature under evolution of nitrogen and therefore it has to be used quickly for the reaction with tris(triphenylphosphine)ruthenium(II) dichloride to prepare the catalyst precursor **17**. The formation of a metal alkylidene bond could be proven via ^1H NMR in deuterated dichloromethane (CD_2Cl_2) showing a singlet at 19.40 ppm ($\text{Ru}=\text{CH}$). In a subsequent reaction

the triphenylphosphine ligands were exchanged with tricyclohexylphosphine to furnish the bimetallic Grubbs catalyst 1st-generation (**BG1**) in a yield of 38% with regard to tris(triphenylphosphine)ruthenium(II) dichloride. The ligand exchange proceeds easily due to the higher basicity of tricyclohexylphosphine ($pK_a: 9.7$)¹⁸¹ compared to triphenylphosphine ($pK_a: 2.73$)¹⁸¹ binding stronger to the ruthenium complex. The ¹H NMR of the prepared bivalent catalyst is depicted in Figure 5.5, showing the alkylidene protons at 20.33 ppm (Ru=CH) and the protons of the tricyclohexylphosphine ligands in the range of 2.6-1.0 ppm (PC₁₈H₃₃).

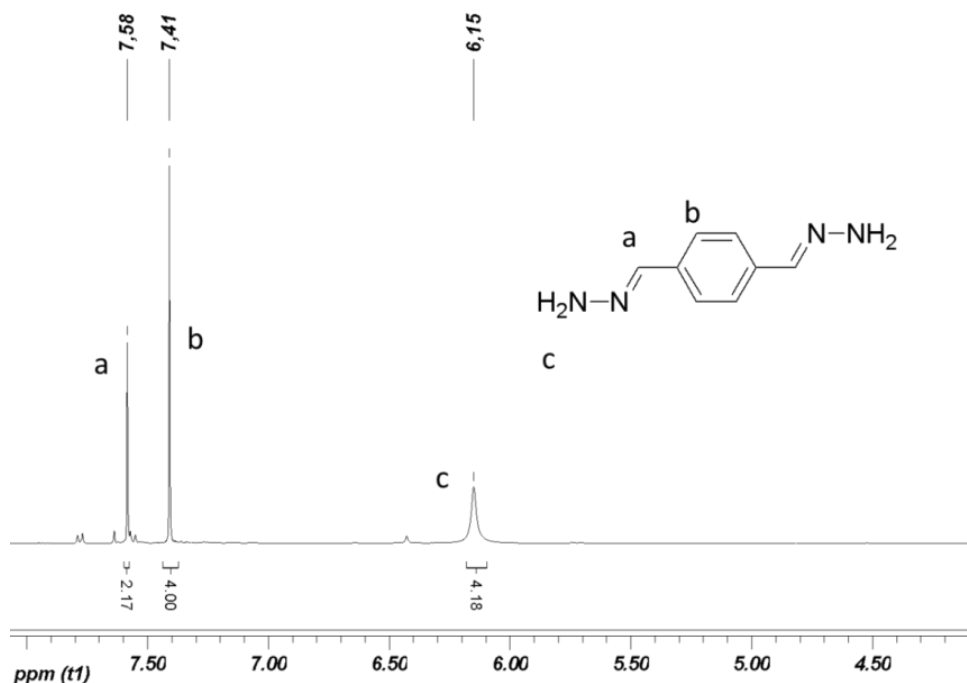


Figure 5.4. ¹H NMR of terephthalaldehyde dihydrazone (**15**) in THF-d₈.

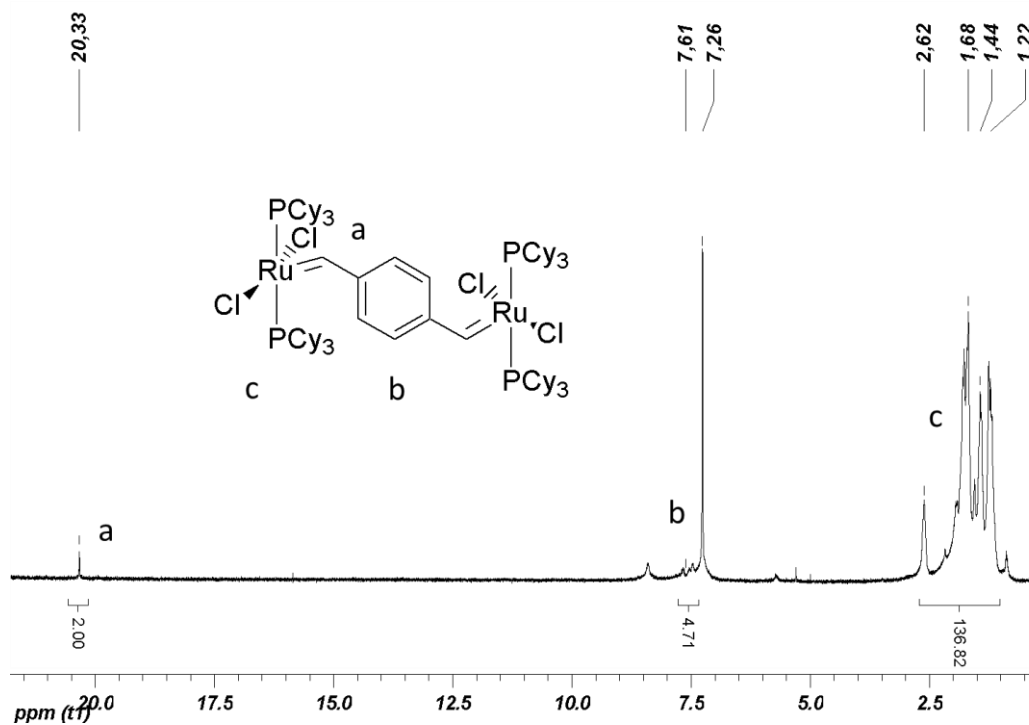


Figure 5.5. ^1H NMR of bimetallic ruthenium catalyst (BG1) in CDCl_3 .

Chapter 2.3.

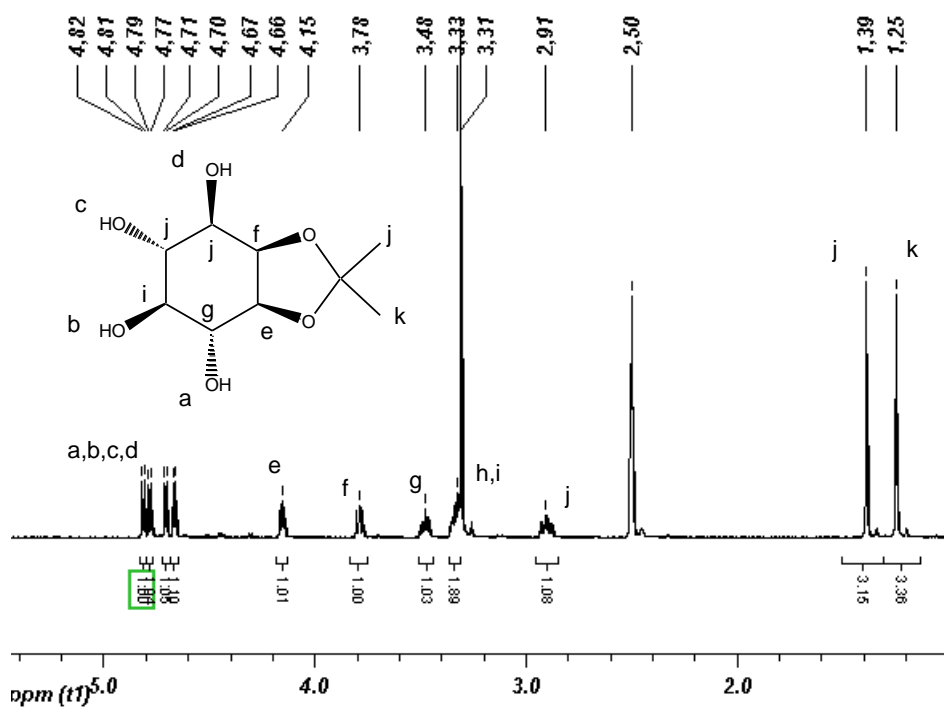


Figure 5.6. ^1H NMR of 1,2-O-isopropylidene-myoinositol (5) in DMSO-d_6 .

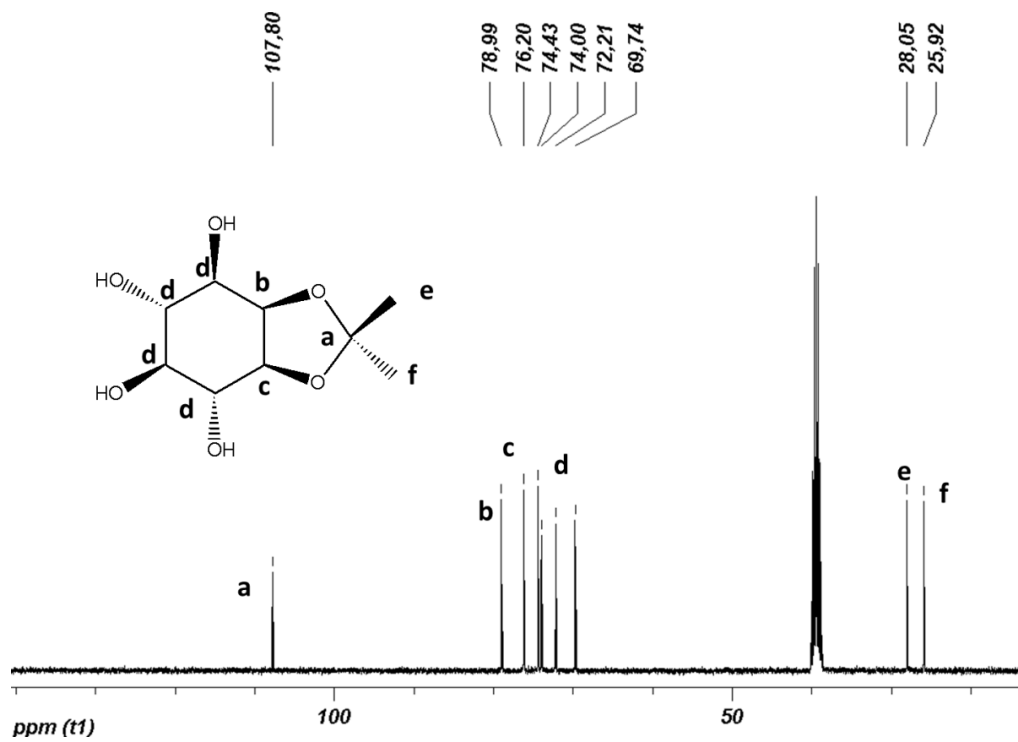
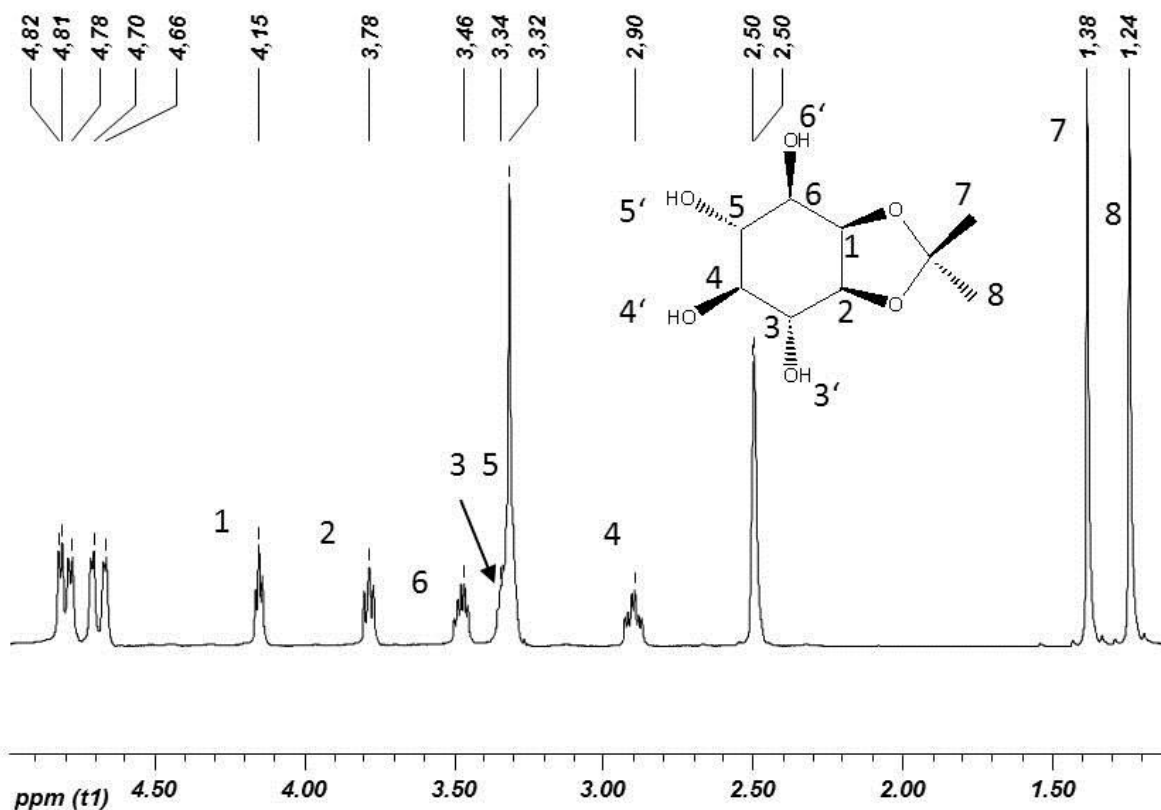


Figure 5.7. ^{13}C NMR of compound 5 in DMSO-d_6 .



Assignment to the individual protons

- 1)** 4.15 ppm (dd, 1H, $J_{1,6} = 3.9$ Hz, $J_{1,2} = 5.3$ Hz)
2) 3.78 ppm (dd, 1H, $J_{1,2} = 5.3$ Hz, $J_{2,3} = 7.4$ Hz)
3), 5) 3.33 ppm (ddd, 2H, $J = 4.8$ Hz, $J_{2,3} = 7.6$ Hz, $J_{3,4} = 9.8$ Hz)
3') 4.80 ppm (d, 1H, $J_{3,3'} = 4.8$ Hz)
4) 2.89 ppm (ddd, 1H, $J_{4,4'} = 4.4$ Hz, $J_{4,5} = 8.8$ Hz, $J_{3,4} = 9.9$ Hz)
6) 3.47 ppm (ddd, 1H, $J_{1,6} = 3.9$ Hz, $J_{6,6'} = 5.3$ Hz, $J_{5,6} = 9.2$ Hz)
6') 4.77 ppm (d, 1H, $J_{6,6'} = 5.3$ Hz)
4'), 5') 4.70 ppm (d, 1H, $J = 4.3$ Hz) 4.66 (d, 1H, $J = 4.4$ Hz)
7) 1.38 ppm (s, 3H) **8)** 1.24 ppm (s, 3H)

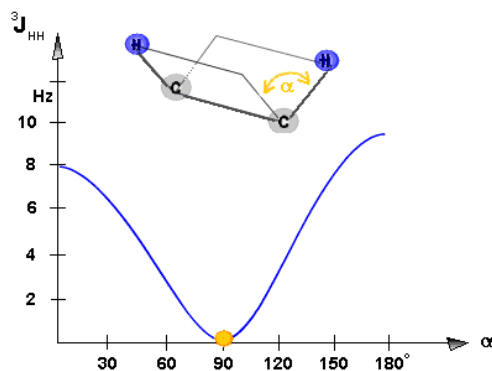


Figure 5.8. ^1H NMR spectrum of 1,2-O-isopropylidene-*myo*-inositol (**5**) in DMSO-d_6 and coupling constant analysis of compound **5**, correlation of vicinal coupling constant and dihedral angle α (Karplus curve), Figure taken from www.chemgapedia.de/vsengine/vlu/vsc/de/ch/3/anc/nmr_spek/kopplungen.vlu/Page/vsc/de/ch/3/anc/nmr_spek/m_18/nmr_4_7/kopplvicinal_m18te1100.vscml.html (11.07.2012).

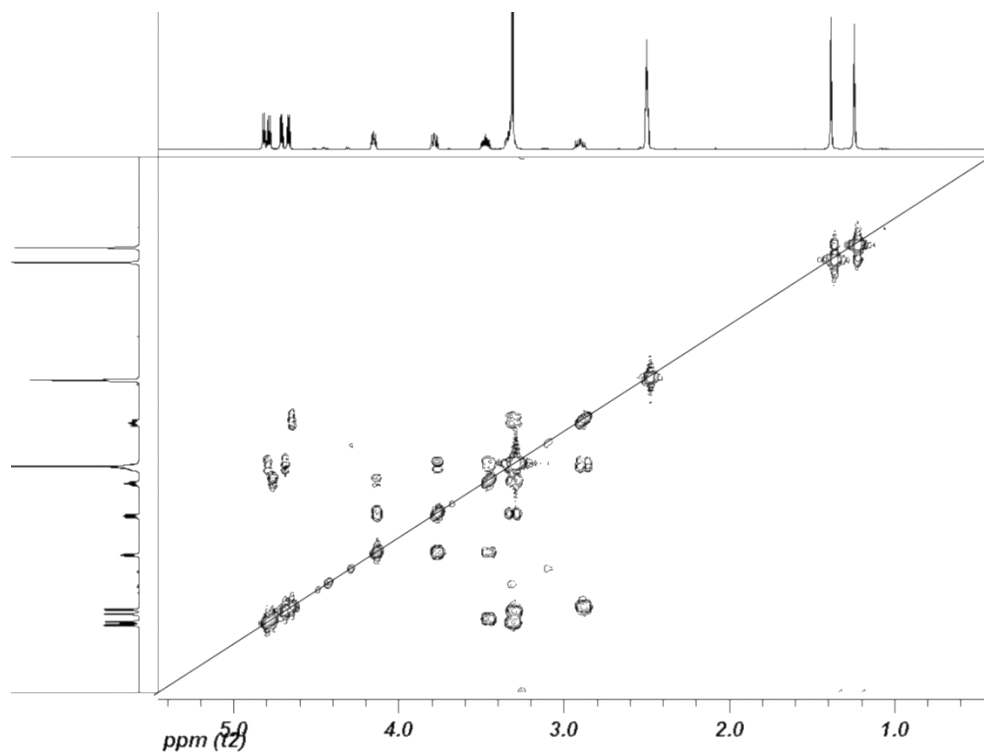


Figure 5.9. $^1\text{H}/^1\text{H}$ COSY NMR of compound 5.

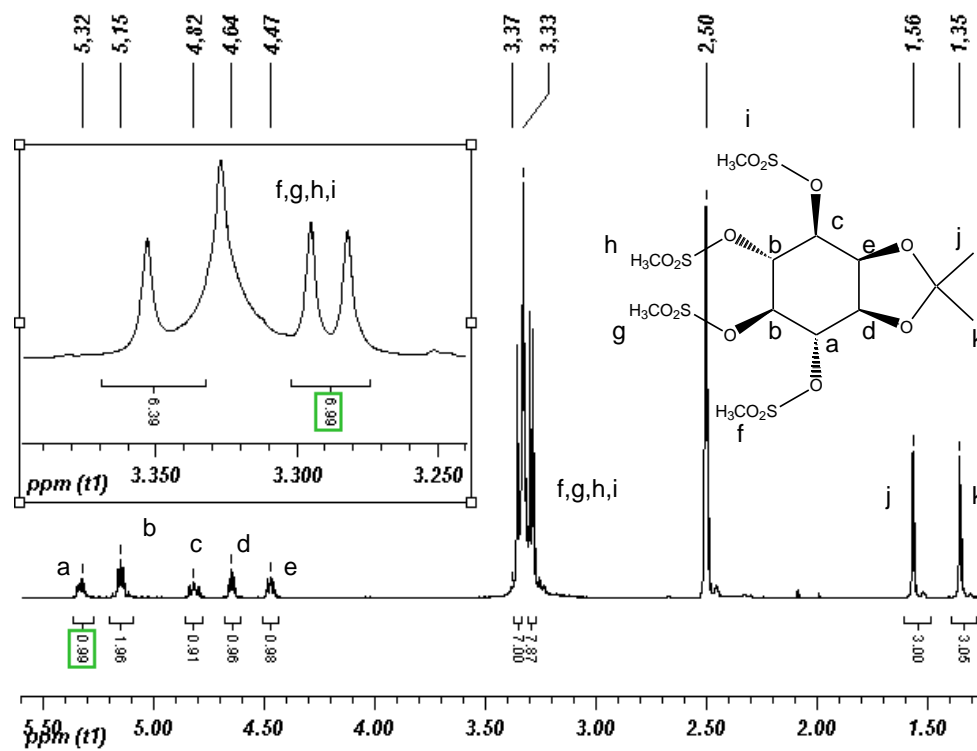


Figure 5.10. ^1H NMR of 1,2-O-isopropylidene-3,4,5,6-tetra-(methanesulfonyl)-*myo*-inositol (**6**) in DMSO-d_6 .

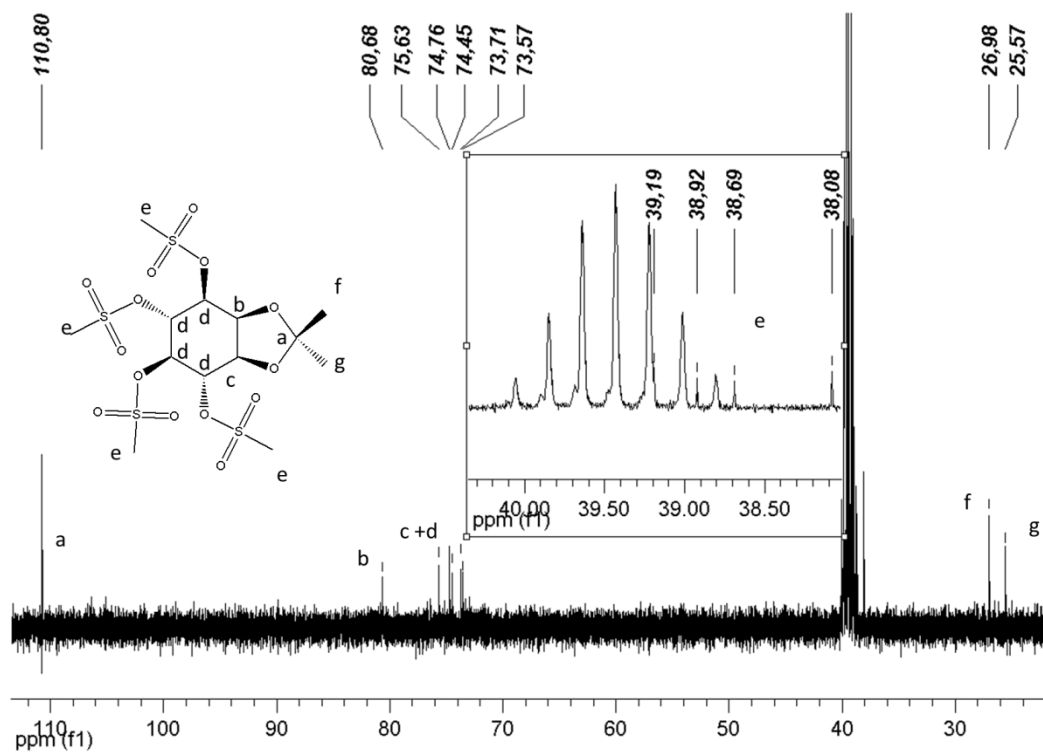


Figure 5.11. ^{13}C NMR of 1,2-O-isopropylidene-3,4,5,6-tetra-(methanesulfonyl)-*myo*-inositol (**6**) in DMSO-d_6 .

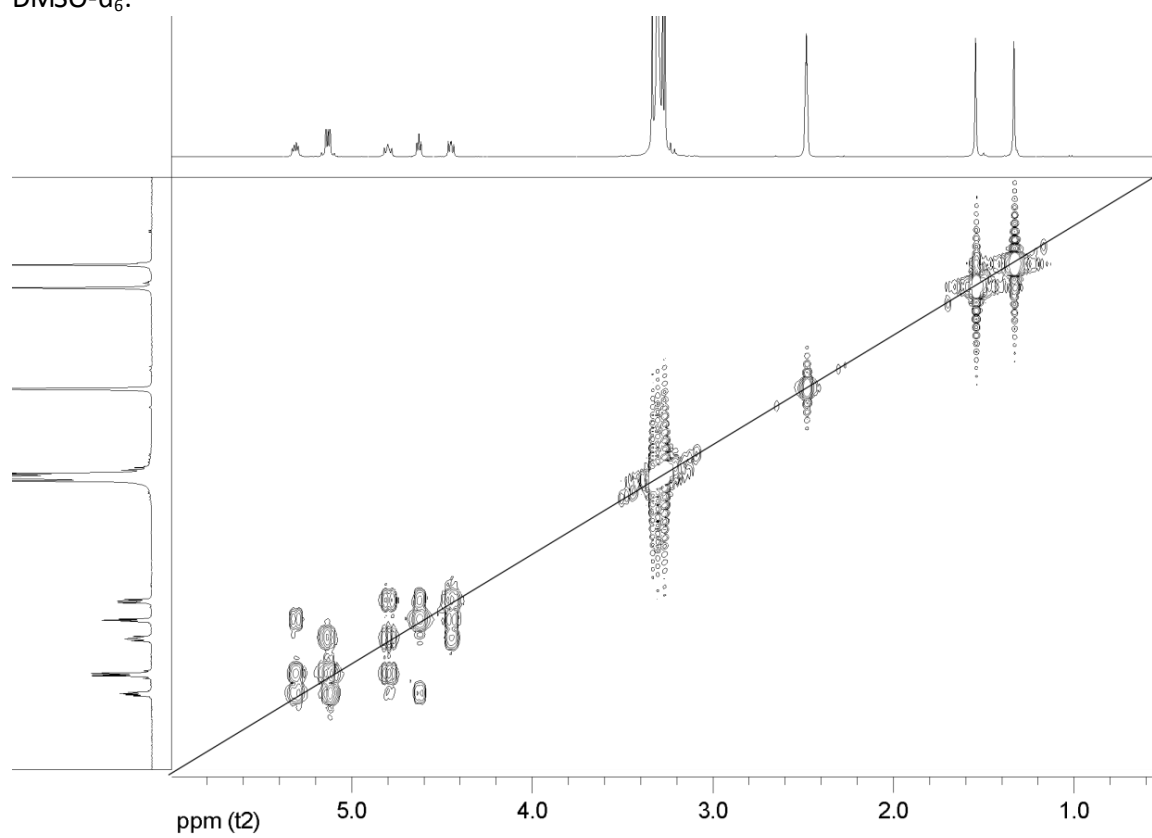


Figure 5.12. $^1\text{H}/^{13}\text{C}$ COSY of compound **6** in DMSO-d_6 .

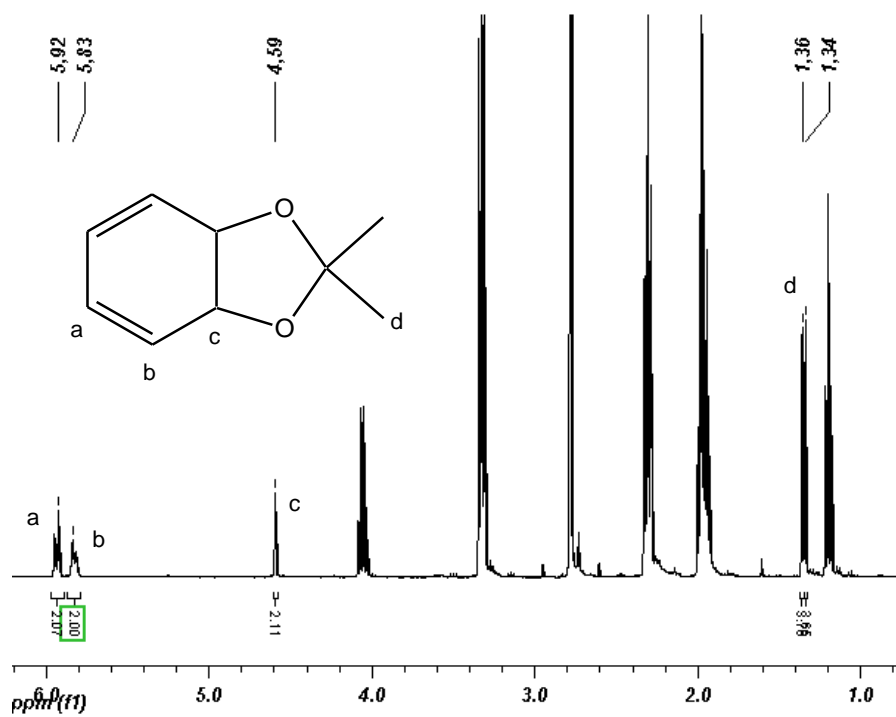


Figure 5.13. ^1H NMR of *cis*-O-isopropylidene-3,5-cyclohexadien-1,2-diol (**7**) in mixture with NMP in CDCl_3 .

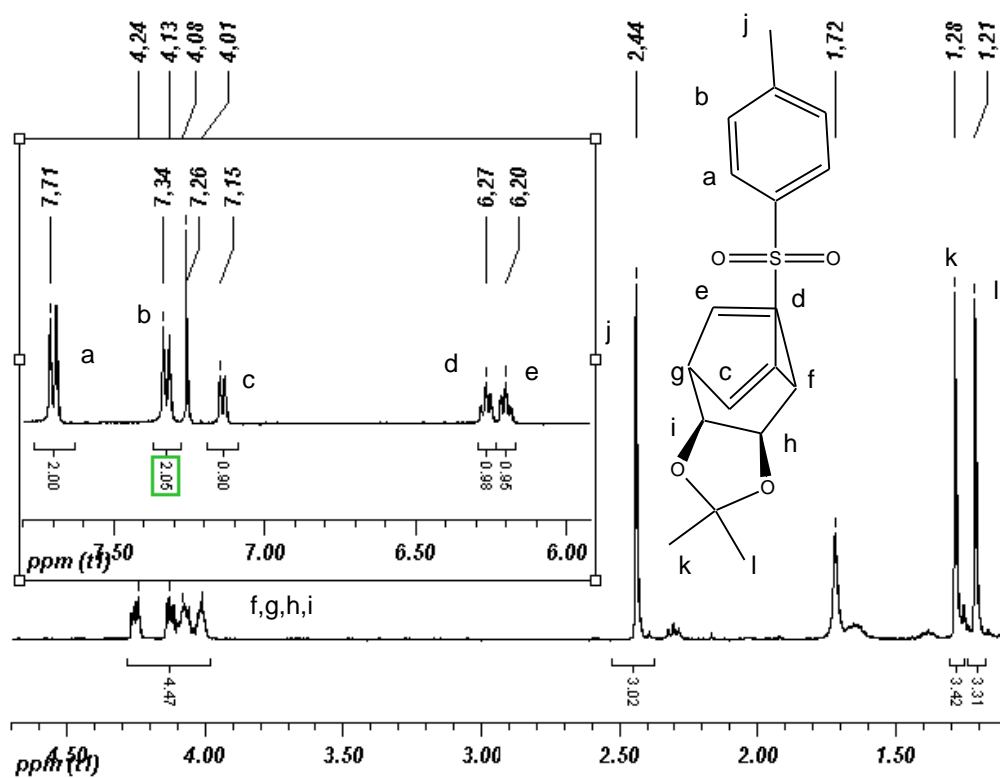


Figure 5.14. ^1H NMR of *endo*-5-(*p*-toluenesulfonyl)bicyclo[2.2.2]octa-5,7-diene 2,3-dimethyl acetal (**8**) in CDCl_3 .

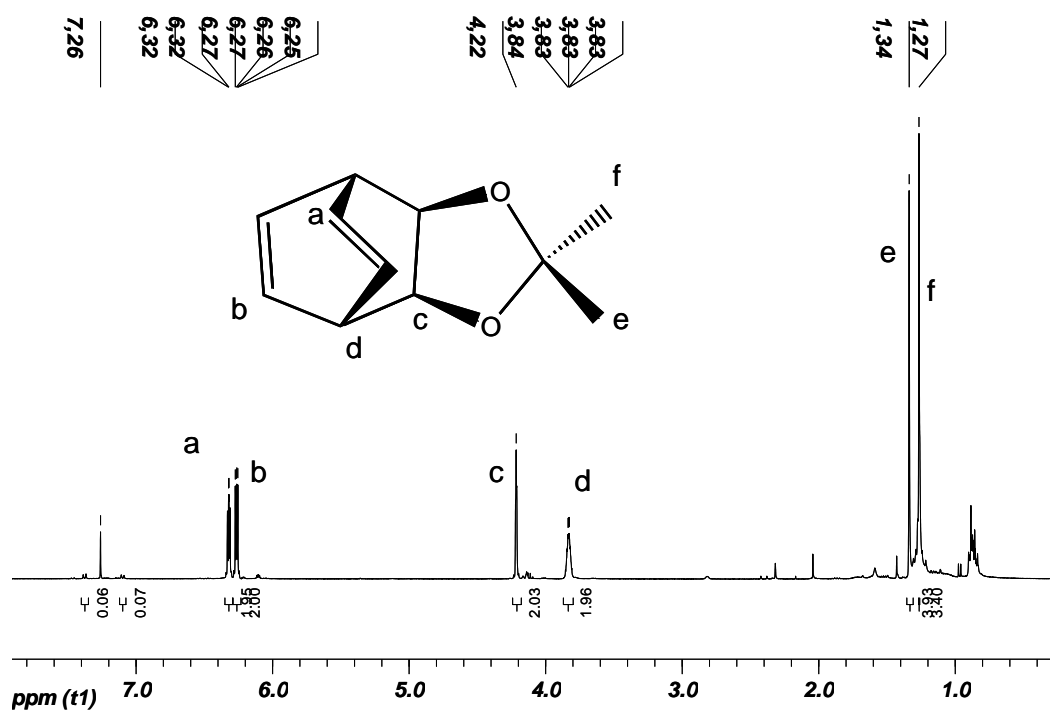


Figure 5.15. ¹H NMR 4,4-Dimethyl-3,5-dioxatricyclo[5.2.2.0(2,6)]undeca-8,10-diene (**9**) in CDCl₃.

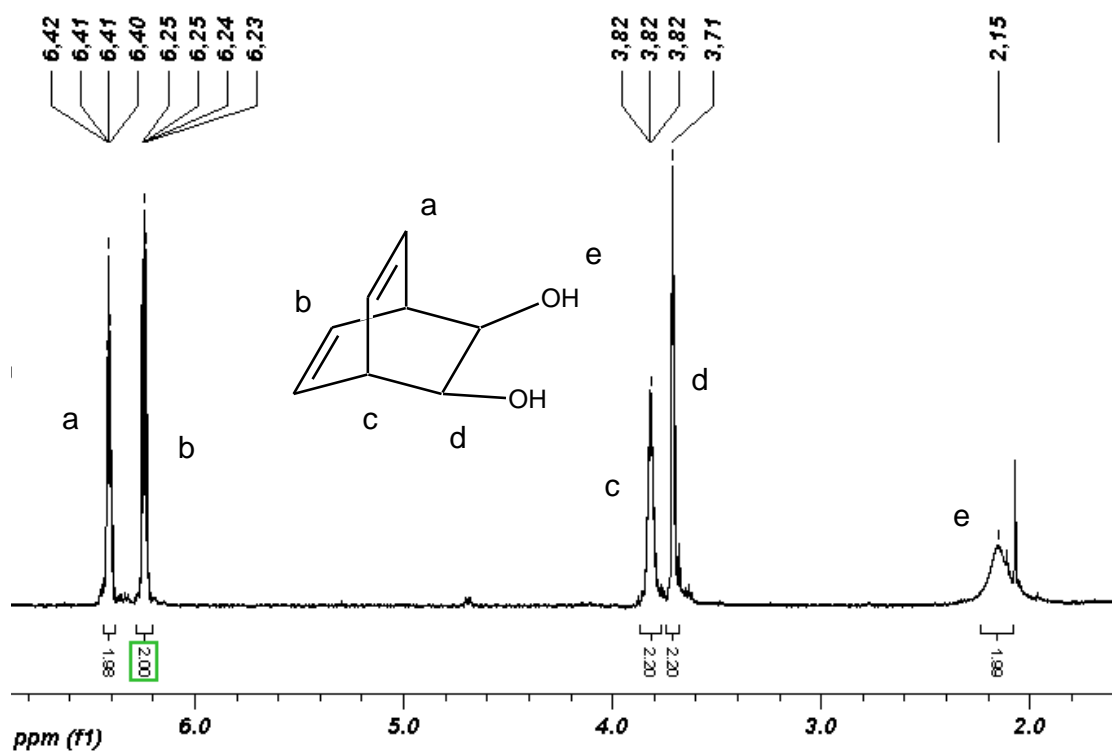
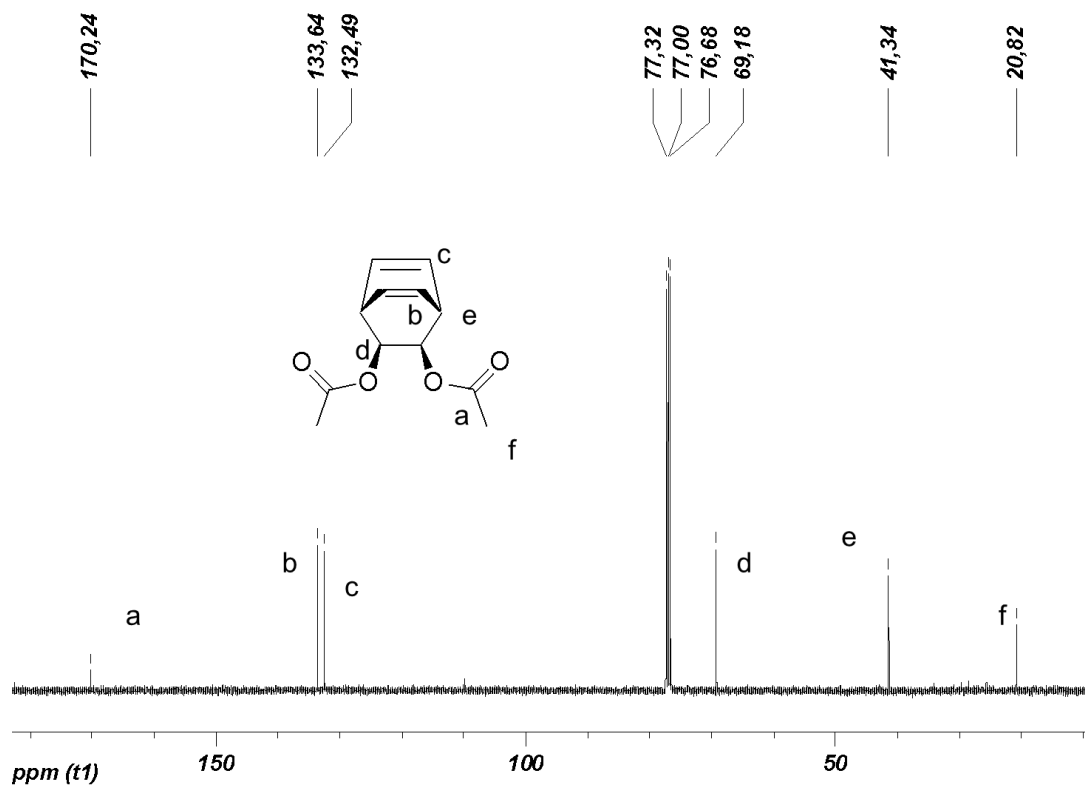
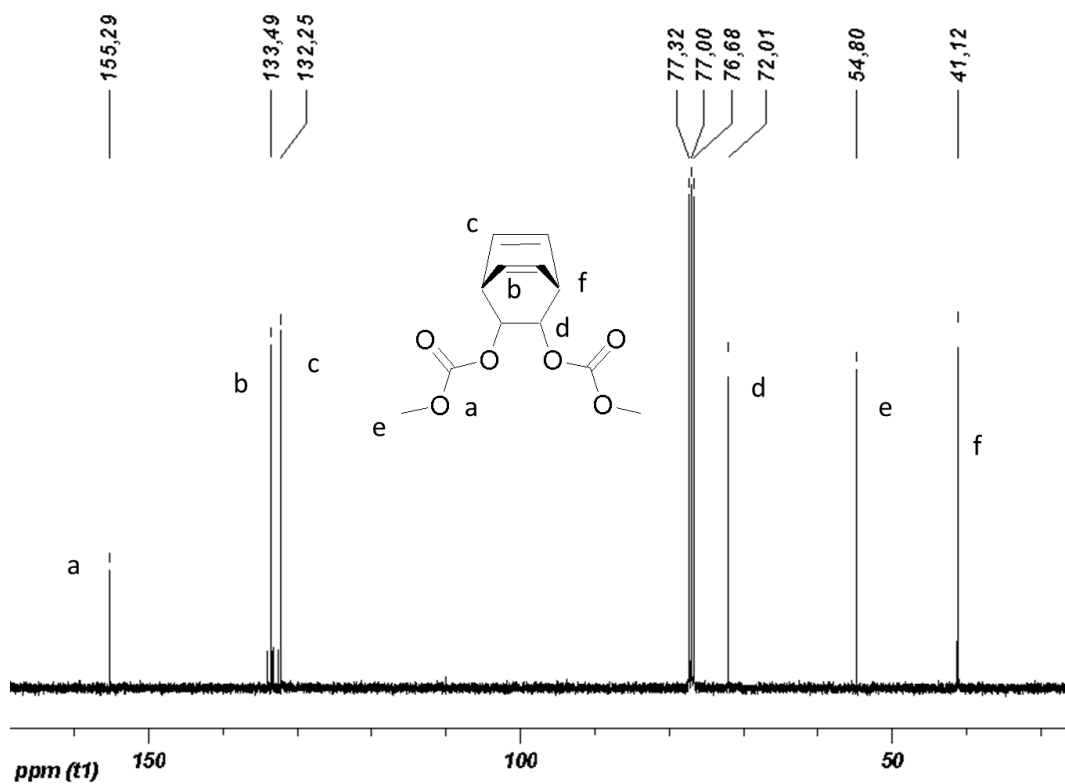


Figure 5.16. ¹H NMR of bicyclo[2.2.2]octa-5,7-diene-2,3-diol (**10**) in CDCl₃.

Figure 5.17. ¹³C NMR of **11** in CDCl₃.Figure 5.18. ¹³C NMR of **12** in CDCl₃.

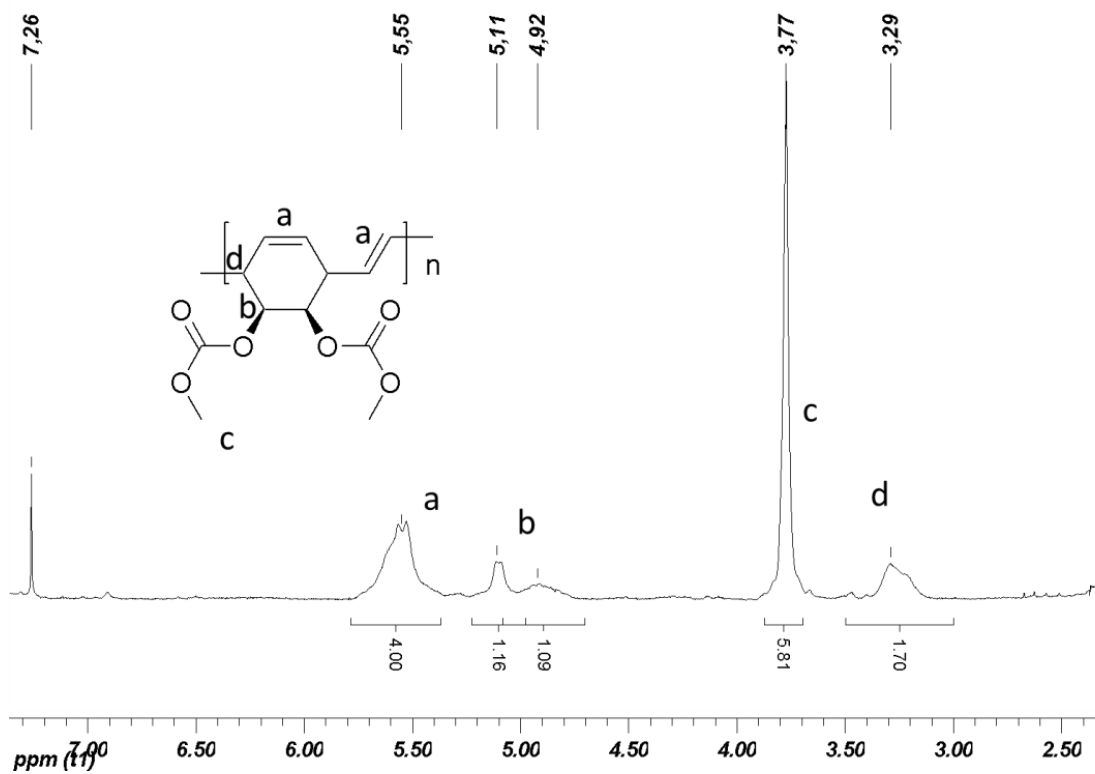


Figure 5.19. ^1H NMR of poly(**12**) prepared with Grubbs catalyst 2nd-generation (**G2**).

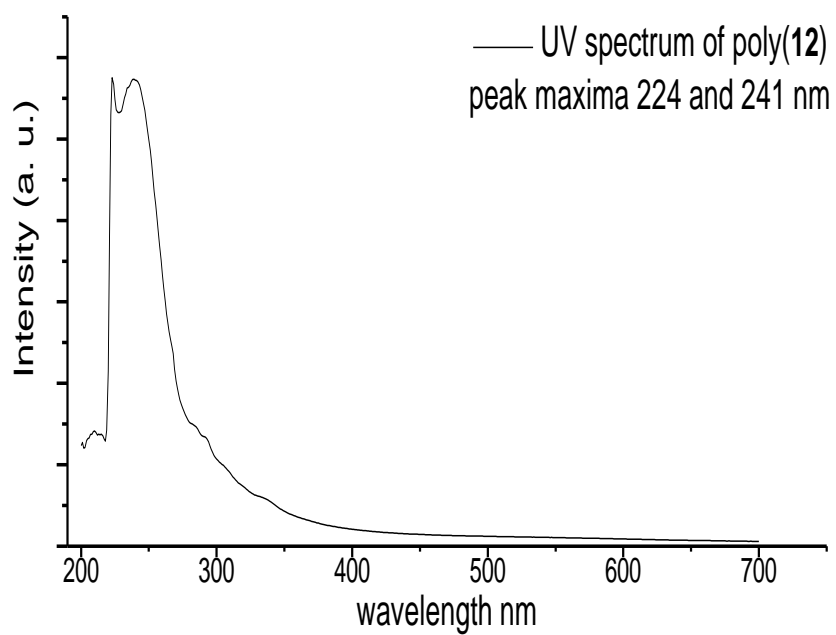


Figure 5.20. UV/VIS spectrum of poly(**12**) in dichloromethane.

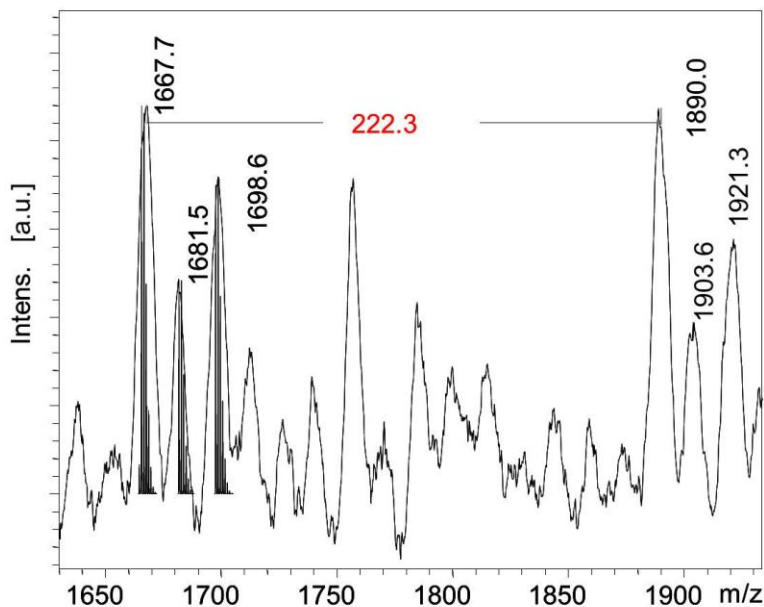


Figure 5.21. MALDI-TOF mass spectrum of poly(**11**), quenched with ethyl vinyl ether (Dithranol, sodium trifluoroacetate), expansion from 1600 to 1950 m/z, m/z (calc) = 1667.8 Da, m/z (exp) = 1667.7 Da for $(C_{12}H_{14}O_4)_7C_8H_8+Li^+$, m/z (calc) = 1682.8 Da, m/z (exp) = 1681.5 Da for $(C_{12}H_{14}O_4)_7C_8H_8+Na^+$, m/z (calc) = 1698.9 Da, m/z (exp) = 1698.6 Da for $(C_{12}H_{14}O_4)_7C_8H_8+K^+$, poly(**11**) with methylene (CH_2) and benzylidene (C_7H_6) end groups, 7 repetition units, ionized by addition of Li^+ , Na^+ and K^+ respectively.

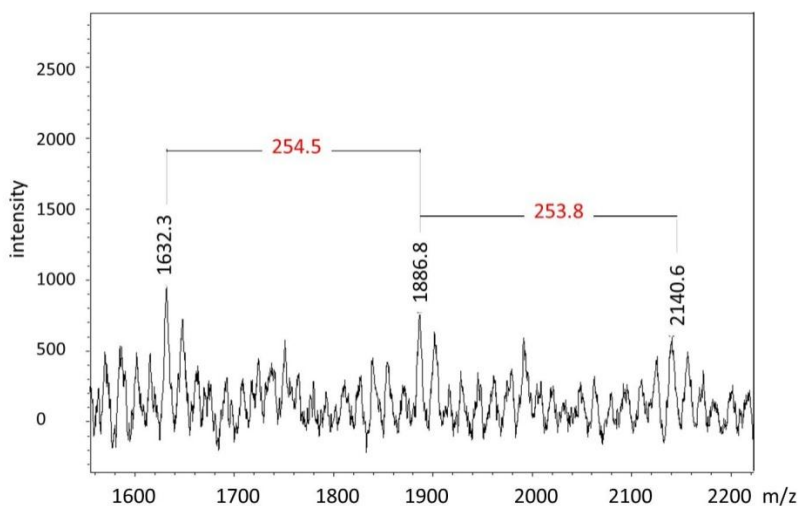
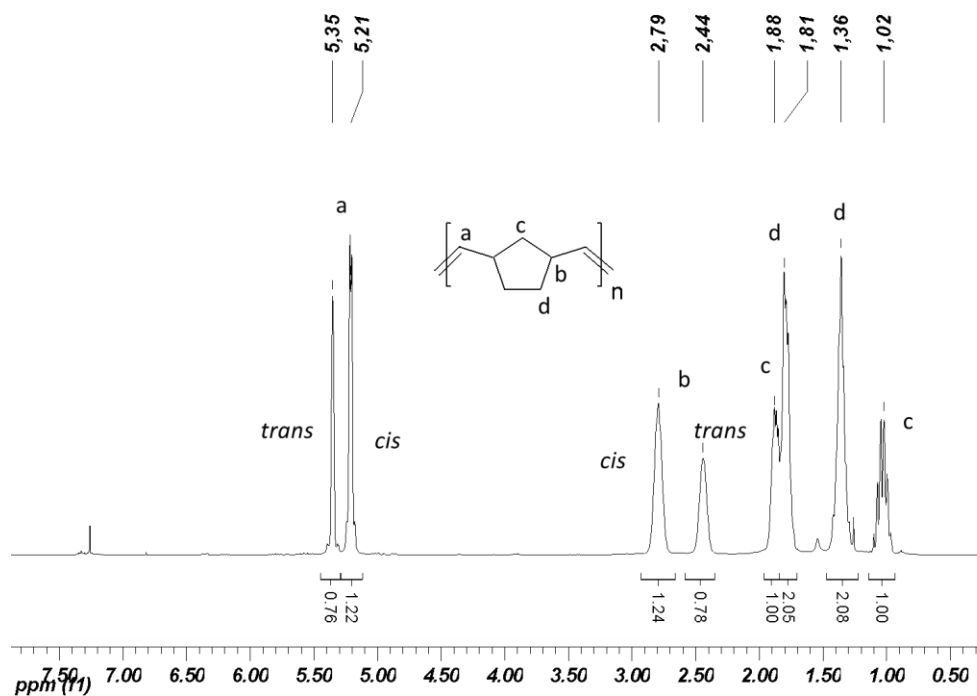
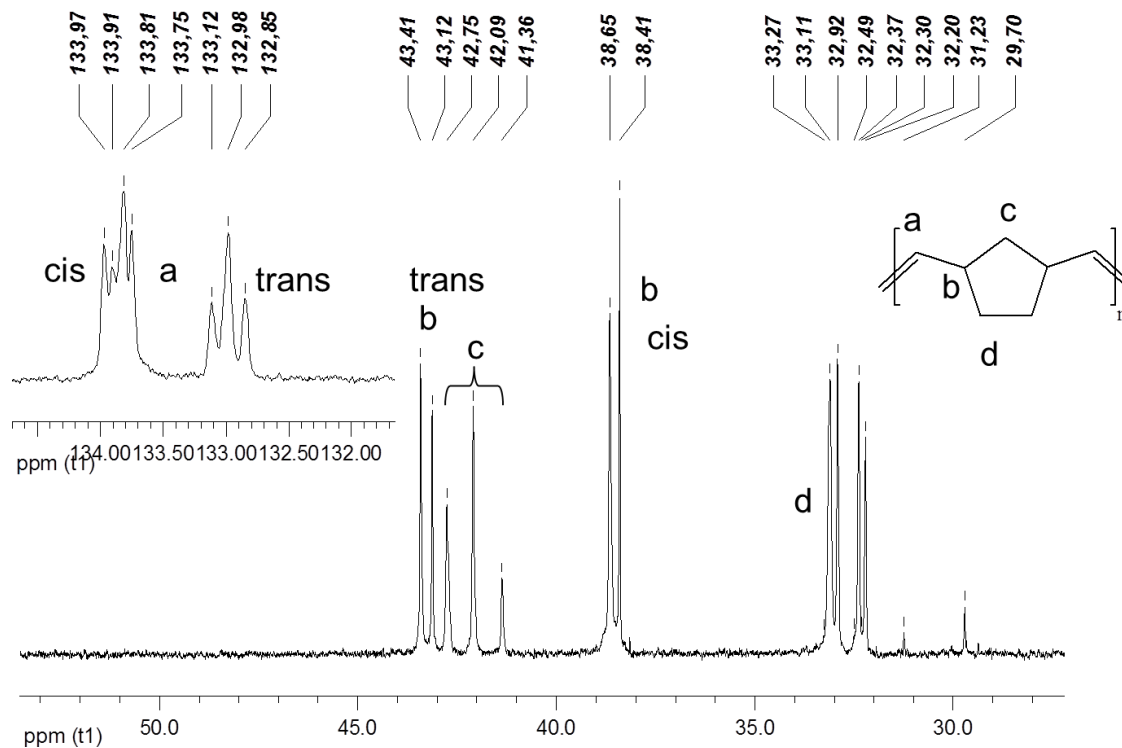


Figure 5.22. MALDI-TOF mass spectrum of poly(**12**), quenched with ethyl vinyl ether (DCTP, sodium trifluoroacetate), expansion from 1580 to 2220 m/z, m/z (calc) = 1630.6 Da, m/z (exp) = 1632.3 Da for $(C_{12}H_{14}O_6)_6C_8H_8+H^+$, poly(**12**) with methylene (CH_2) and benzylidene (C_7H_6) end groups, 6 repetition units, ionized by addition of H^+ .

Chapter 2.4.

Figure 5.23. ¹H NMR of poly(norbornene) prepared with G3.Figure 5.24. ¹³C NMR of poly(norbornene) prepared with G3.

Chapter 2.5.

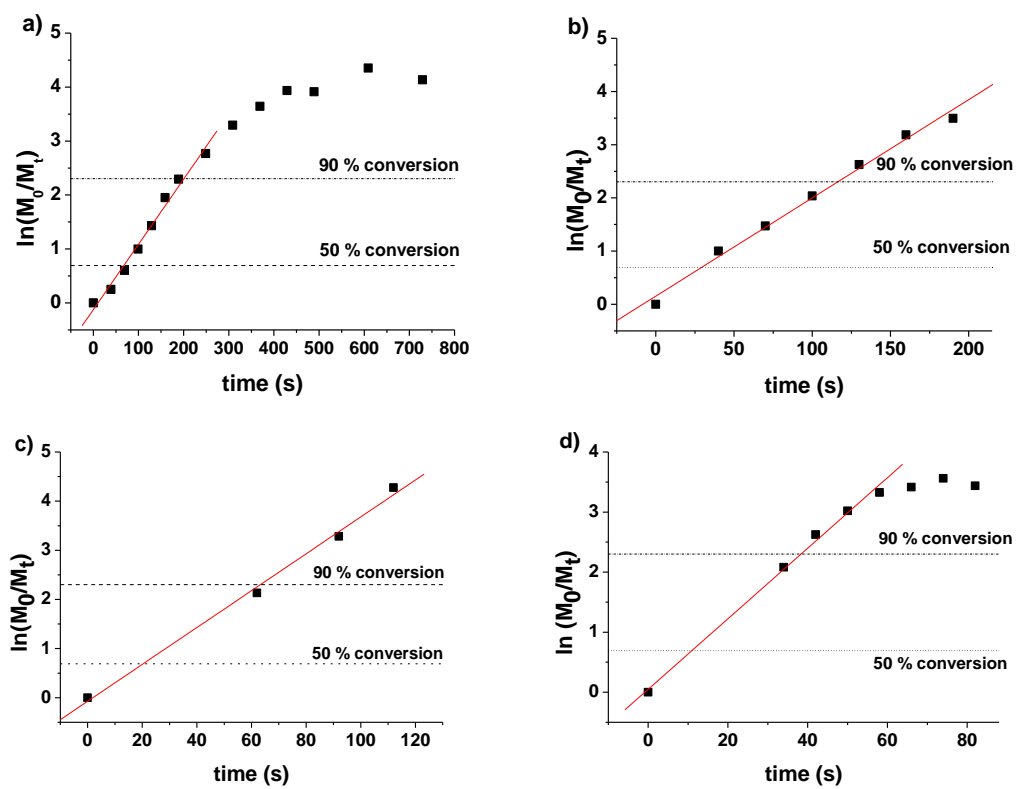


Figure 5.25. Monomer conversion v/s time (t) plots obtained from ^1H NMR a) poly(2) with catalyst G1, b) 2 in BCP (1)-b-(2) with catalyst G1, c) poly(2) with catalyst G3 and d) 2 in BCP (1)-b-(2) with catalyst G3.

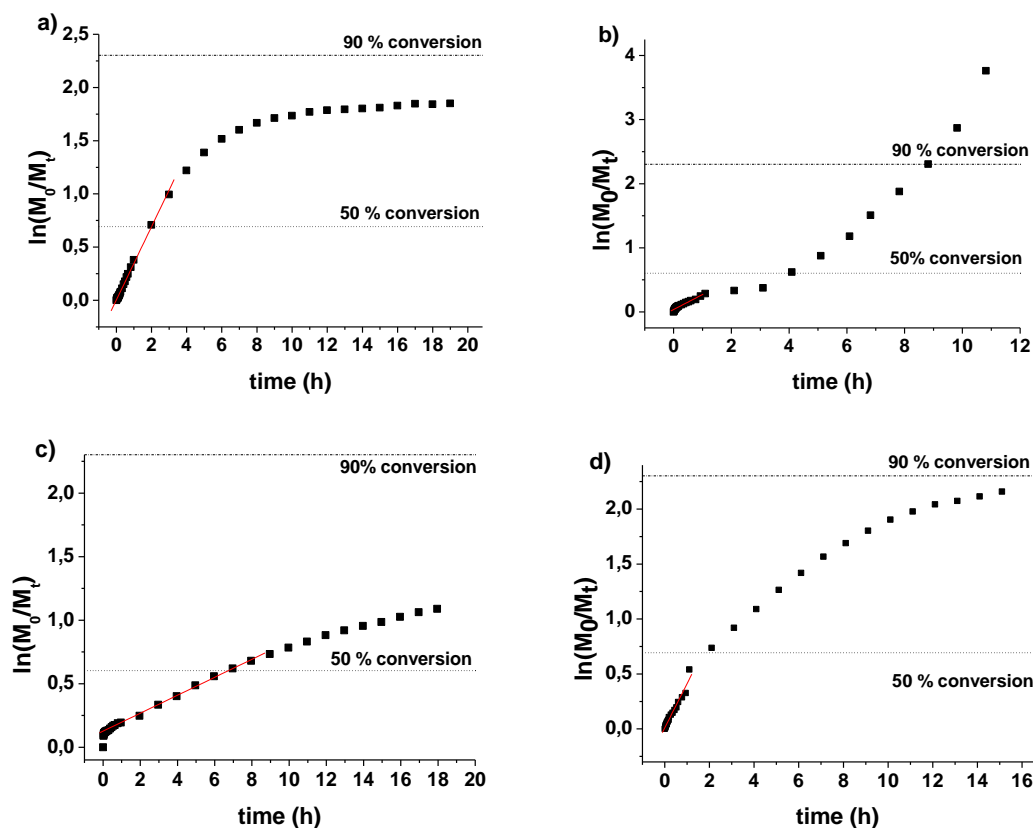


Figure 5.26. Monomer conversion v/s time (t) plots obtained from ^1H NMR a) poly(**3**) with catalyst **G1**, b) **3** in BCP (**1**)-*b*-(**3**) with catalyst **G1**, c) poly(**3**) with catalyst **G3** and d) **3** in BCP (**1**)-*b*-(**3**) with catalyst **G3**.

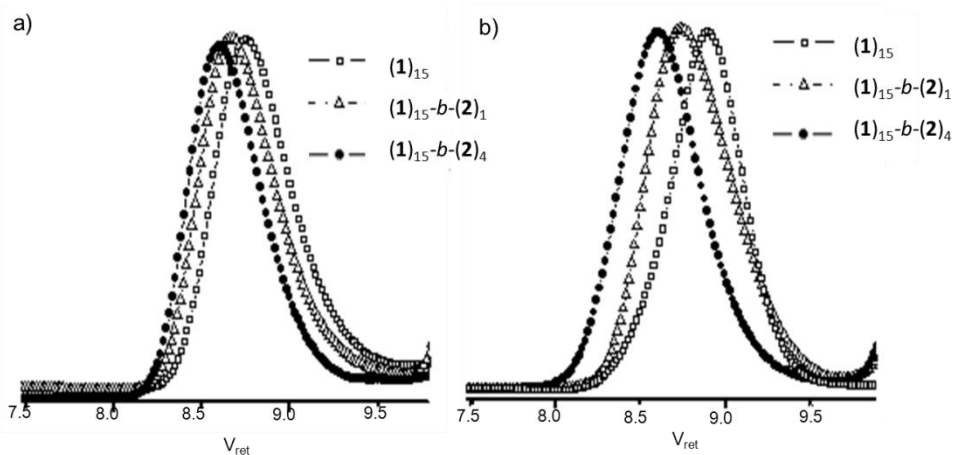


Figure 5.27. GPC curves of $(1)_{15}$ and block copolymers BCPs $(1)_{15-b-(2)_1}$ and $(1)_{15-b-(2)_4}$ prepared with a) Grubbs 1st generation catalyst (**G1**) and b) Grubbs 3rd generation catalyst (**G3**).

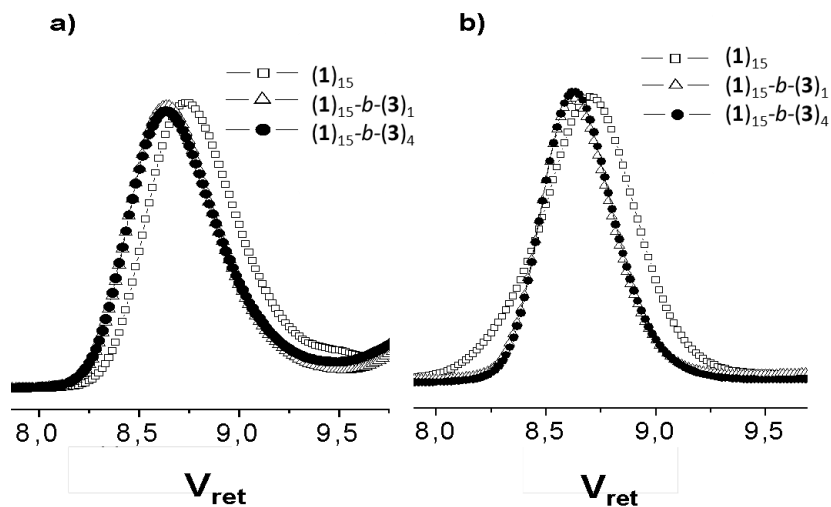


Figure 5.28. GPC curves of $(1)_{15}$ and block copolymers BCPs $(1)_{15-b-(3)_1}$ and $(1)_{15-b-(3)_4}$ prepared with a) Grubbs catalyst 1st-generation (**G1**) and b) Grubbs catalyst 3rd-generation (**G3**).

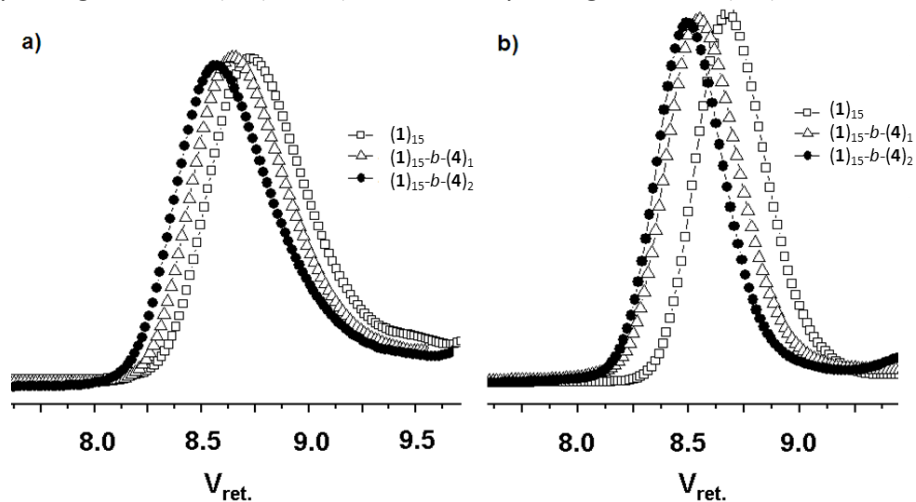


Figure 5.29. GPC curves of $(1)_{15}$ and block copolymers BCPs $(1)_{15-b-(4)_1}$ and $(1)_{15-b-(4)_2}$ prepared with a) Grubbs catalyst 1st-generation (**G1**) and b) Grubbs catalyst 3rd-generation (**G3**).

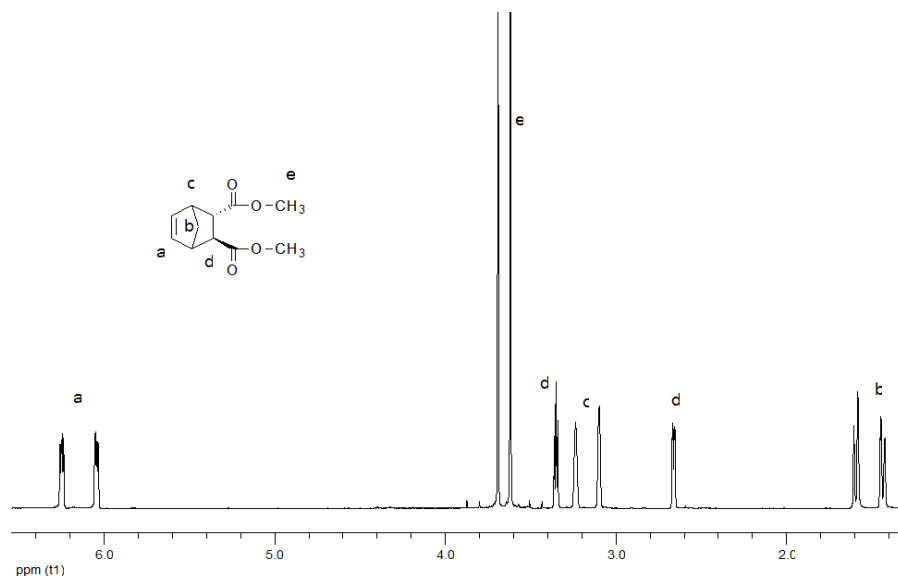


Figure 5.30. ¹H NMR Spectra of monomer **1** in CDCl₃.

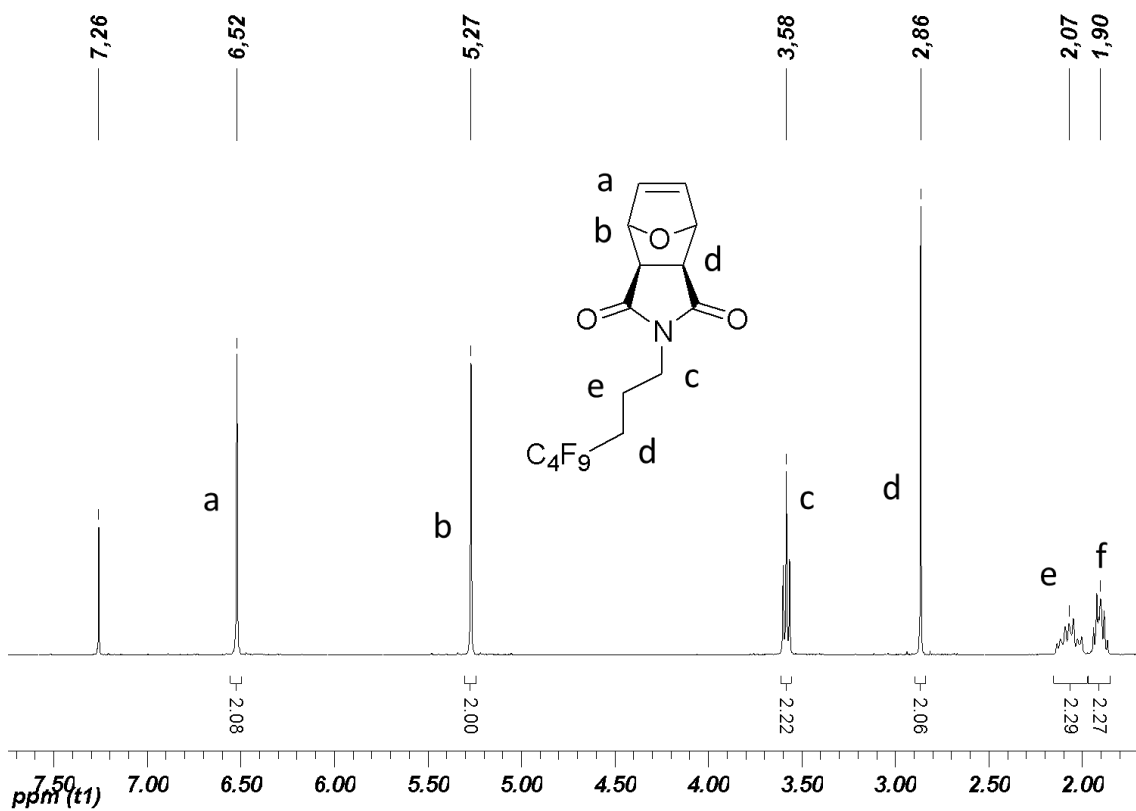


Figure 5.31. ¹H NMR Spectra of monomer **2** in CDCl₃.

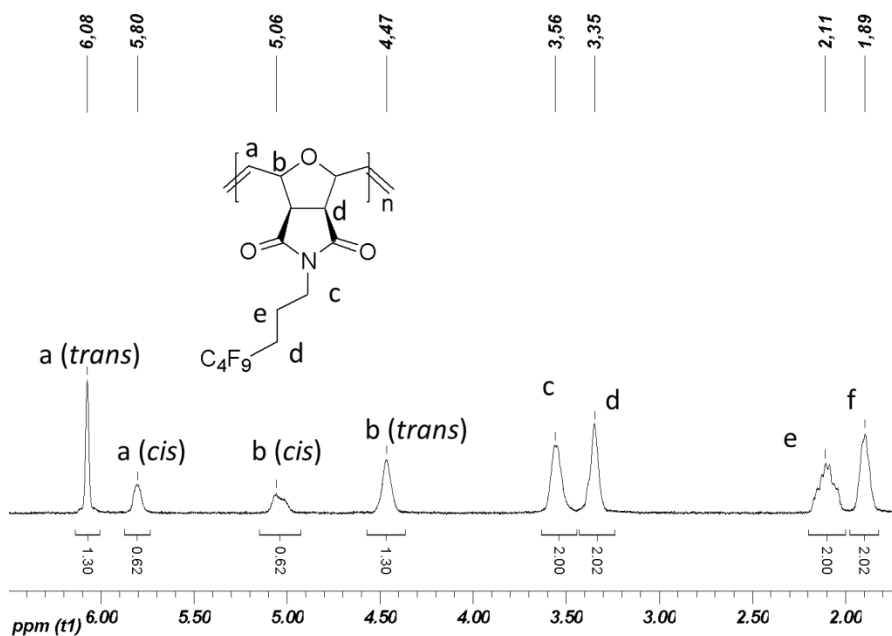


Figure 5.32. ^1H NMR Spectra of poly(2), M/C = 100, prepared with G1, cis/trans ratio = 32/68, for poly(2) prepared with G3 the cis/trans ratio changes to 51/49.

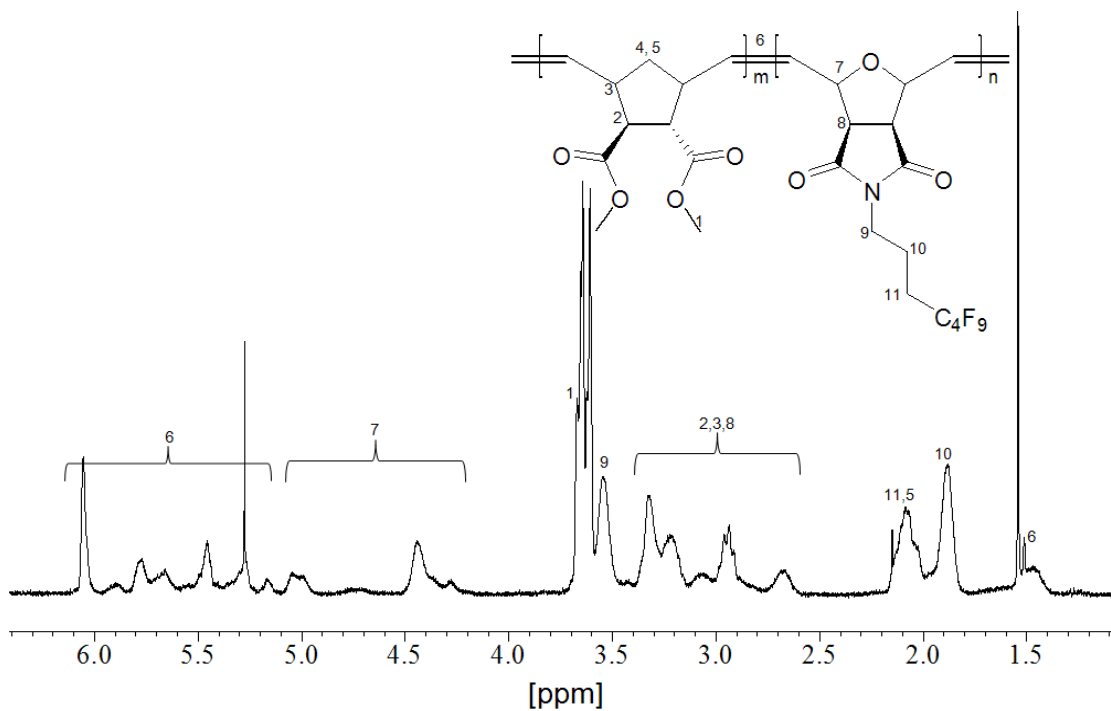


Figure 5.33. ^1H NMR Spectra of BCP (1)₁₀₀-b-(2)₁₀₀

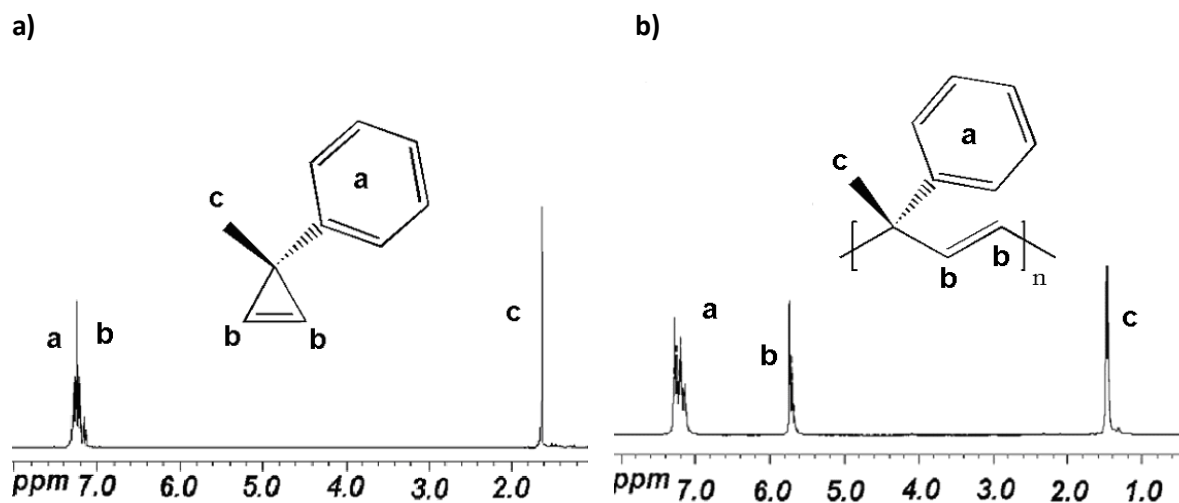


Figure 5.34. ^1H NMR (400 MHz, CDCl_3) of a) monomer **3**: 7.14-7.40 (7H, m, CH, Ph), 1.64 (3H, s, CH_3), b) poly(**3**): 7.08-7.31 (5H, m, Ph), 5.74 (2H, m, CH), 1.47 (3H, s, CH_3).

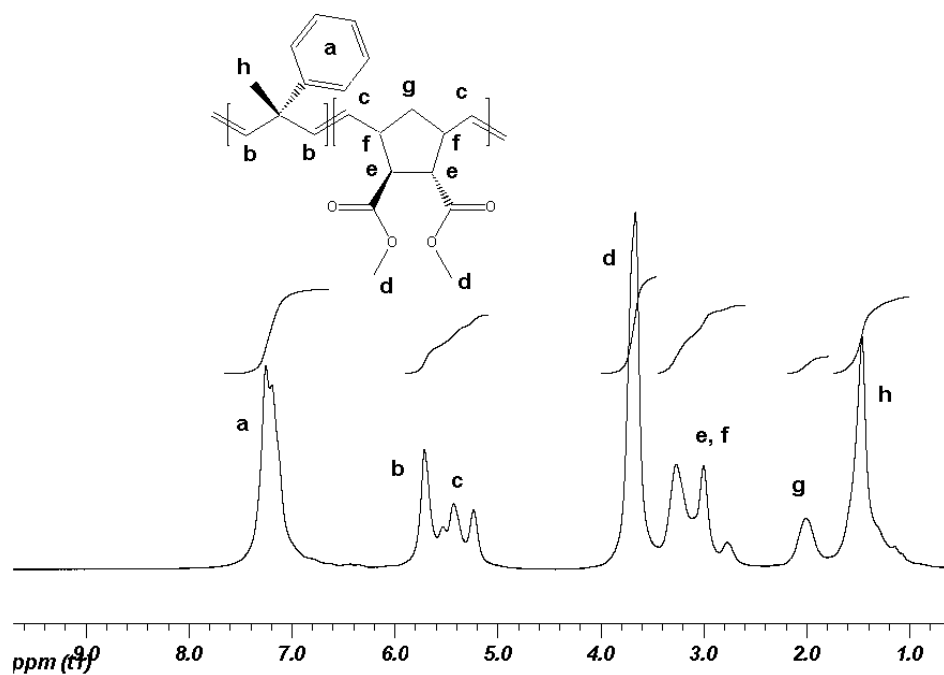


Figure 5.35. ^1H NMR of BCP (**1**)₂₅-*b*-(**3**)₂₅ in CDCl_3 .

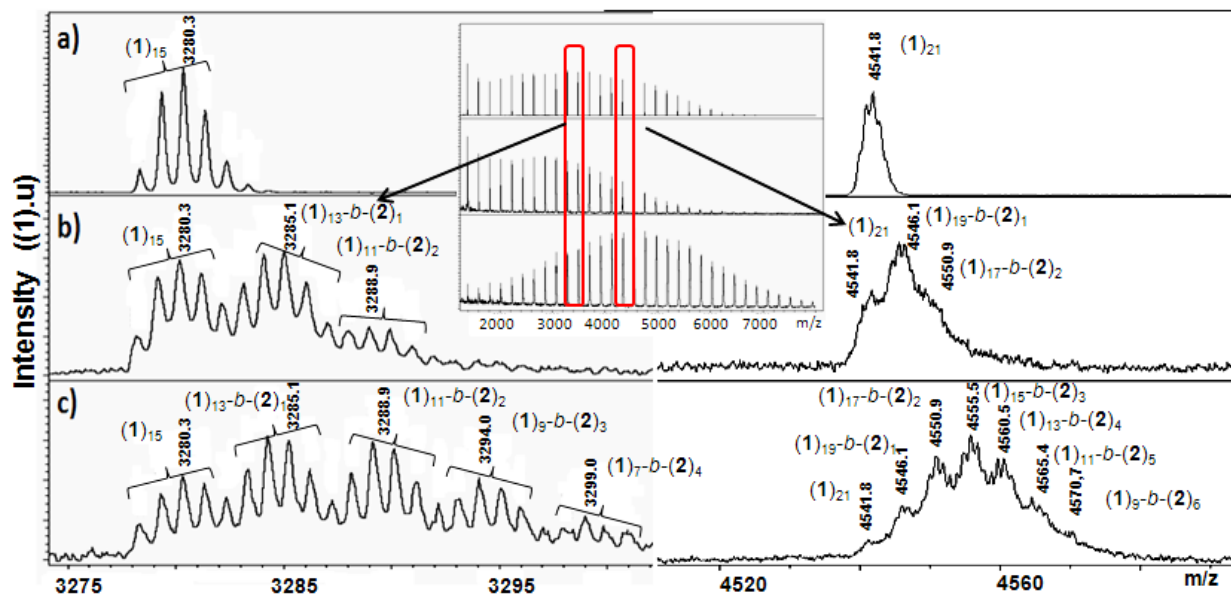


Figure 5.36. MALDI-TOF mass spectra of a) $(1)_{15}$, b) $(1)_{15-b-(2)_1}$ and c) $(1)_{15-b-(2)_4}$ prepared with catalyst **G1**. (Insert shows the complete MALDI-spectra of the sample a-c), (all chains are desorbed as $[M-Na]^+$ -ions).

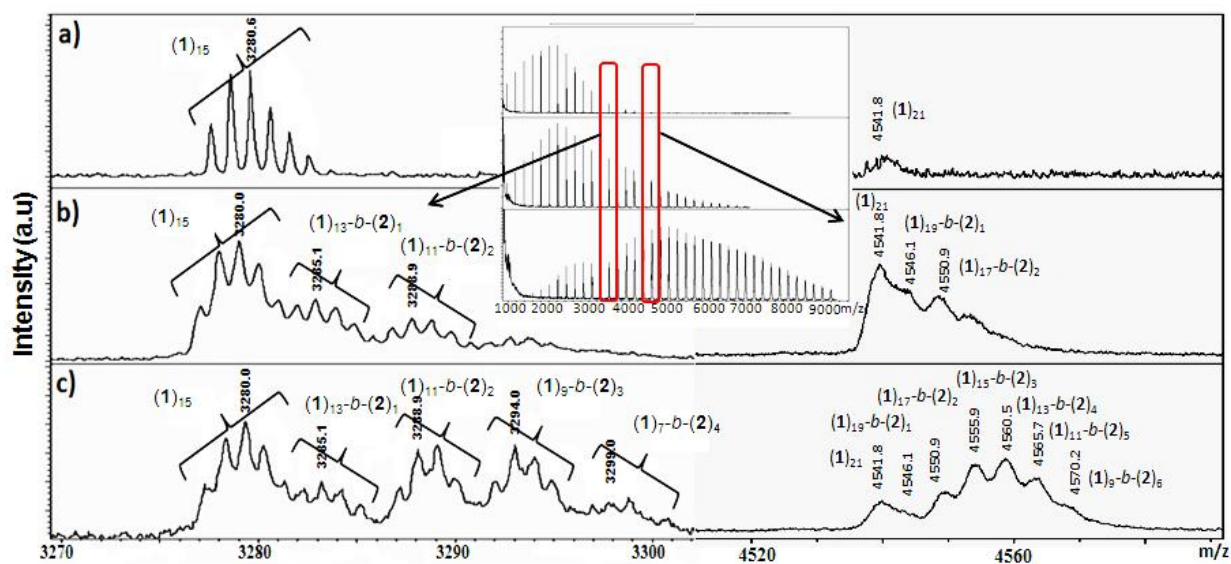


Figure 5.37. MALDI-TOF mass spectra of a) $(1)_{15}$, b) $(1)_{15-b-(2)_1}$ and c) $(1)_{15-b-(2)_4}$ prepared with catalyst **G3**. (Insert shows the complete MALDI-spectra of the sample a-c), (all chains are desorbed as $[M-Na]^+$ -ions).

Chapter 2.6.

Table 5.1. Quantification of detected ions by ESI-TOF MS for the reaction of 1 equiv. of **1** with catalyst **G1** (room temperature, 7.8 mg of catalyst **G1**, 2 mg of monomer **1** in 1 mL dichloromethane for 15 min).

species	m/z (exp)	m/z (calc)	error (ppm)	intensity	fraction (%)
G1a	787.388	787.384	5.1	2131616	60.61
G1b	507.156	507.152	7.9	135144	3.84
G1b-(1)₁	717.243	717.241	2.8	78995	2.25
G1b-(1)₂	927.330	927.331	-1.1	32129	0.91
G1b-(1)₃	1137.412	1137.421	-7.9	8825	0.25
G1b-(1)₄	1347.513	1347.510	2.2	1926	0.05
G1c	471.174	471.176	-4.2	115550	3.29
G1d	828.411	828.411	0	741945	21.09
G1d-(1)₁	1038.478	1038.501	-22.1	10993	0.31
G1d-(1)₂	1248.583	1248.590	-5.6	4496	0.13
G1d-(1)₃	1458.663	1458.680	-11.6	1548	0.04
G1e	548.182	548.179	5.5	13414	0.38
G1e-(1)₁	758.271	758.268	4.0	118655	3.37
G1e-(1)₂	968.354	968.358	4.1	65926	1.87
G1e-(1)₃	1178.444	1178.447	2.5	17688	0.50
G1e-(1)₄	1388.537	1388.537	0	3289	0.09
G1e-(1)₅	1598.635	1598.626	5.6	663	0.02
G1h	417.097	417.105	-19.2	31815	0.90
G1i	377.094	377.097	-8.0	2544	0.07

Table 5.2. Quantification of detected ions by ESI-TOF MS for the reaction of 1 equiv. of **1** with catalyst **G1** and 5 equiv. of HCl (room temperature, 7.8 mg of catalyst **G1**, 2 mg of monomer **1** in 1 mL dichloromethane, 0.03 ml (HCl in diethyl ether, (c = 1.5 M), for 15 min).

species	m/z (exp)	m/z (calc)	error (ppm)	intensity	fraction (%)
G1b	507.154	507.152	3.9	18782	5.67
G1b-(1)₁	717.241	717.241	0	107093	32.35

G1b-(1)₂	927.331	927.331	0	17150	5.18
G1b-(1)₃	1137.415	1137.421	5.2	2354	0.71
G1c	471.175	471.176	2.1	3251	0.98
G1e-(1)₁	758.269	758.268	1.3	140028	42.30
G1e-(1)₂	968.348	968.358	10.3	34738	10.49
G1e-(1)₃	1178.438	1178.447	7.6	4793	1.45
G1e-(1)₄	1388.528	1388.537	6.5	573	0.17
G1h	417.095	417.105	21.2	2262	0.68

Table 5.3. Quantification of detected ions by ESI-TOF MS for the reaction of 1 equiv. of **1** with catalyst **U1** (room temperature, 8.8 mg of catalyst **U1**, 2 mg of monomer **1** in 1 mL dichloromethane for 15 min).

species	m/z (exp)	m/z (calc)	error (ppm)	intensity	fraction (%)
U1a	887.420	887.416	4.5	2464091	38.05
U1b	607.183	607.183	0.0	72368	1.12
U1b-(1)₁	817.274	817.273	1.2	70512	1.09
U1b-(1)₂	1027.362	1027.363	-1.0	13323	0.21
U1b-(1)₃	1237.452	1237.452	0.0	3941	0.06
U1c	571.209	571.207	3.5	1704059	26.32
U1c-(1)₁	781.292	781.297	-6.4	79191	1.22
U1c-(1)₂	991.383	991.386	-3.0	25420	0.39
U1c-(1)₃	1201.471	1201.471	0.0	6196	0.10
U1d	928.444	928.443	1.1	1414867	21.85
U1e	648.210	648.210	0.0	523319	8.08
U1e-(1)₁	858.298	858.300	-2.3	61614	0.95
U1e-(1)₂	1068.384	1068.389	-4.7	26493	0.41
U1e-(1)₃	1278.482	1278.479	2.3	7931	0.12
U1e-(1)₄	1488.579	1488.568	7.4	2290	0.04

Table 5.4. Quantification of detected ions by ESI-TOF MS for the reaction of 1 equiv. of **1** with catalyst **G3** (room temperature, 8.4 mg of catalyst **G3**, 2 mg of monomer **1** in 1 mL dichloromethane for 15 min).

species	m/z (exp)	m/z (calc)	error (ppm)	intensity	fraction (%)
G3a-(1)₁	902.171	902.171	0.0	84629	1.79
G3a-(1)₂	1112.262	1112.260	1.8	57710	1.22
G3a-(1)₃	1322.351	1322.350	0.8	29823	0.63
G3a-(1)₄	1532.446	1532.440	3.9	12554	0.27
G3a-(1)₅	1742.533	1742.529	2.3	3136	0.07
G3a-(1)₆	1952.625	1952.619	3.1	924	0.02
G3b	533.131	533.130	1.9	349728	7.42
G3b-(1)₁	743.221	743.219	2.7	45296	0.96
G3b-(1)₂	953.306	953.309	-3.1	64562	1.37
G3b-(1)₃	1163.393	1163.398	-4.3	31222	0.66
G3b-(1)₄	1373.473	1373.488	-10.9	10656	0.23
G3b-(1)₅	1583.587	1583.577	6.3	3069	0.07
G3b-(1)₆	1793.641	1793.667	-14.5	871	0.02
G3c	497.147	497.153	-12.1	42727	0.91
G3c-(1)₁	707.240	707.243	-4.2	1568269	33.26
G3c-(1)₂	917.330	917.332	-2.2	676648	14.35
G3c-(1)₃	1127.420	1127.422	-1.8	272754	5.79
G3c-(1)₄	1337.509	1337.511	-1.5	62525	1.33
G3c-(1)₅	1547.597	1547.601	-2.6	12952	0.27
G3c-(1)₆	1757.669	1757.691	-12.5	2513	0.05
G3d	733.104	733.108	-5.5	10721	0.23
G3e-(1)₁	784.243	784.246	-3.8	371010	7.87
G3e-(1)₂	994.337	994.335	2.0	417671	8.86
G3e-(1)₃	1204.427	1204.425	1.7	262568	5.57
G3e-(1)₄	1414.519	1414.514	3.5	93415	1.98
G3e-(1)₅	1624.602	1624.604	-1.2	18706	0.40
G3e-(1)₆	1834.691	1834.693	-1.1	4127	0.09
G3e-(1)₇	2044.778	2044.783	-2.4	852	0.02

G3e-(1)₈	2254.901	2254.873	12.4	302	0.01
G3h	443.081	443.085	-9.0	142415	3.02
G3i	405.089	405.090	-2.5	60405	1.28

Table 5.5. Quantification of detected ions by ESI-TOF MS for the reaction of 1 equiv. of **1** with catalyst **U3** (room temperature, 7.1 mg of catalyst **U3**, 2 mg of monomer **1** in 1 mL dichloromethane for 15 min).

species	m/z (exp)	m/z (calc)	error (ppm)	intensity	fraction (%)
U3a	712.210	712.203	9.8	91657	2.58
U3a-(1)₁	922.293	922.293	0.0	81398	2.29
U3a-(1)₂	1132.385	1132.383	1.8	33935	0.95
U3a-(1)₃	1342.469	1342.472	-2.2	18655	0.52
U3a-(1)₄	1552.576	1552.562	9.0	8810	0.25
U3a-(1)₅	1762.633	1762.651	-10.2	3608	0.10
U3a-(1)₆	1972.758	1972.741	8.6	1330	0.04
U3a-(1)₇	2182.866	2182.830	16.5	493	0.01
U3b	633.163	633.161	3.2	690779	19.42
U3b-(1)₁	843.253	843.251	2.4	32648	0.92
U3b-(1)₂	1053.335	1053.340	-4.7	39066	1.10
U3b-(1)₃	1263.434	1263.430	3.2	14307	0.40
U3b-(1)₄	1473.533	1473.519	9.5	5447	0.15
U3b-(1)₅	1683.612	1683.609	1.8	2427	0.07
U3b-(1)₆	1893.697	1893.698	-0.5	945	0.03
U3b-(1)₇	2103.798	2103.788	4.8	407	0.01
U3c	597.188	597.185	5.0	223259	6.28
U3c-(1)₁	807.275	807.274	1.2	1050826	29.54
U3c-(1)₂	1017.366	1017.364	2.0	152758	4.29
U3c-(1)₃	1227.452	1227.453	-0.8	50755	1.43
U3c-(1)₄	1437.536	1437.543	-4.9	15586	0.44
U3c-(1)₅	1647.617	1647.633	-9.7	4959	0.14
U3c-(1)₆	1857.710	1857.722	-6.5	1656	0.05
U3c-(1)₇	2067.834	2067.812	10.6	568	0.02

U3e-(1)₁	884.279	884.277	2.3	333046	9.36
U3e-(1)₂	1094.369	1094.367	1.8	113311	3.19
U3e-(1)₃	1304.460	1304.456	3.1	52659	1.48
U3e-(1)₄	1515.549	1515.546	2.0	21220	0.60
U3e-(1)₅	1724.635	1724.635	0.0	7639	0.21
U3e-(1)₆	1934.734	1934.725	4.7	2650	0.07
U3e-(1)₇	2144.811	2144.814	-1.4	950	0.03
U3e-(1)₈	2356.915	2356.905	4.2	354	0.01
U3h	443.082	443.082	0.0	129477	3.64
U3h + C₅H₅N - H	521.114	521.117	-5.8	102347	2.88
U3i	405.089	405.090	-2.5	33015	0.93
U3i + 3 CH₃OH	501.168	501.169	-2.0	234507	6.59

Table 5.6. Quantification of detected ions by ESI-TOF MS for the reaction of 1 equiv. of **1** with catalyst **G1** and subsequent addition of 1 equiv. of **2** (room temperature, 7.8 mg of catalyst **G1**, 2 mg of monomer **1** in 1 mL dichloromethane for 15 min, followed by addition of 4 mg of monomer **2** in 1 mL dichloromethane and reaction for further 15 min).

species	m/z (exp)	m/z (calc)	error (ppm)	intensity	fraction (%)
G1a	787.380	787.384	-5.1	688114	73.48
G1b-(1)₂	927.327	927.331	-4.3	7619	0.81
G1c-(1)₁	681.238	681.256	23.5	2709	0.29
G1d	828.407	828.411	4.9	200414	21.40
G1e	548.169	548.179	-18.2	18908	2.02
G1e-(1)₁	758.282	758.268	18.4	2060	0.22
G1e-(1)₂	968.351	968.358	7.2	5193	0.55
G1e-(1)₃	1178.431	1178.447	13.6	2312	0.25
G1e-(1)₄	1388.531	1388.537	-4.3	1637	0.17
G1e-(1)₅	1598.580	1598.626	-28.7	876	0.09
G1e-(1)₆	1808.710	1808.716	-3.3	554	0.06
G1e-(2)₁(1)₁	1183.317	1183.336	16.1	3551	0.38
G1e-(2)₁(1)₂	1393.446	1393.425	15.1	1596	0.17
G1e-(2)₂(1)₁	1608.421	1608.404	10.6	932	0.10

Table 5.7. Quantification of detected ions by ESI-TOF MS for the reaction of 1 equiv. of **1** with catalyst **G1** and subsequent addition of 1 equiv. of **3** (room temperature, 7.8 mg of catalyst **G1**, 2 mg of monomer **1** in 1 mL dichloromethane for 15 min, followed by addition of 1.2 mg of monomer **3** in 1 mL dichloromethane and reaction for further 15 min).

species	m/z (exp)	m/z (calc)	error (ppm)	intensity	fraction (%)
G1a	787.387	787.384	3.8	1112800	63.63
G1a-(1)₁	997.461	997.474	-13.0	14408	0.82
G1a-(1)₂	1207.540	1207.564	-11.36	18020	1.03
G1a-(1)₃	1417.631	1417.653	-15.5	7118	0.41
G1a-(3)₁	917.452	917.463	-12.0	5943	0.34
G1b	507.156	507.152	7.9	44175	2.53
G1c	471.170	471.176	12.7	61262	3.50
G1c-(1)₁	681.267	681.256	16.1	9515	0.54
G1d	828.413	828.411	2.4	323435	18.49
G1d-(1)₁	1038.514	1038.501	12.5	13828	0.79
G1d-(1)₂	1248.576	1248.590	-11.2	23772	1.36
G1d-(1)₃	1458.676	1458.680	-2.7	16329	0.93
G1d-(1)₄	1668.680	1668.769	-53.3	8184	0.47
G1d-(1)₅	1878.812	1878.859	-25.0	2788	0.16
G1d-(1)₆	2088.957	2088.948	4.3	969	0.06
G1d-(3)_{1(1)₁}	1168.508	1168.579	-60.8	9918	0.57
G1d-(3)_{1(1)₂}	1378.590	1378.669	-57.3	5775	0.33
G1d-(3)_{1(1)₃}	1588.689	1588.758	-43.4	2881	0.16
G1d-(3)_{1(1)₄}	1798.768	1798.848	-44	1661	0.09
G1e-(1)₁	758.277	758.268	11.2	13786	0.79
G1e-(1)₂	968.359	968.358	1.0	23655	1.35
G1e-(1)₃	1178.458	1178.447	9.3	16215	0.93
G1e-(1)₄	1388.541	1388.537	2.9	8209	0.47
G1e-(1)₅	1598.629	1598.626	1.9	2800	0.16
G1e-(1)₆	1808.719	1808.716	1.7	975	0.06
G1e-(1)₇	2018.815	2018.805	4.9	395	0.02

Table 5.8. Quantification of detected ions by ESI-TOF MS for the reaction of 1 equiv. of **1** with catalyst **G1** + 5 equiv. of HCl and subsequent addition of 1 equiv. of **3** (room temperature, 7.8 mg of catalyst **G1**, 2 mg of monomer **1** in 1 mL dichloromethane, 0.03 ml HCl in diethyl ether ($c = 1.5$ M), for 15 min, followed by addition of 1.2 mg of monomer **3** in 1 mL dichloromethane and reaction for further 15 min).

species	m/z (exp)	m/z (calc)	error (ppm)	intensity	fraction (%)
G1b	507.158	507.152	11.8	4129	2.25
G1b-(1)₁	717.242	717.241	1.4	13981	7.61
G1b-(1)₂	927.330	927.331	-1.1	10458	5.69
G1b-(1)₃	1137.423	1137.421	1.8	4397	2.39
G1b-(3)₁(1)₁	847.320	847.320	0.0	12929	7.04
G1b-(3)₁(1)₂	1057.411	1057.410	0.9	9921	5.40
G1b-(3)₁(1)₃	1267.494	1267.499	-3.9	2846	1.55
G1b-(3)₁(1)₄	1477.594	1477.589	3.4	848	0.46
G1e-(1)₁	758.278	758.268	13.2	23055	12.55
G1e-(1)₂	968.353	968.358	-5.2	13222	7.20
G1e-(1)₃	1178.438	1178.447	-7.6	6320	3.44
G1e-(1)₄	1388.527	1388.537	-7.2	1725	0.94
G1g-(3)₁(1)₁	889.310	889.305	5.6	7784	4.24
G1g-(3)₁(1)₂	1099.398	1099.394	3.6	7334	3.99
G1g-(3)₁(1)₃	1309.482	1309.484	-1.5	2645	1.44
G1g-(3)₂(1)₁	1019.405	1019.383	21.6	2870	1.56
G1g-(3)₂(1)₂	1229.480	1229.473	5.7	1020	0.56
G1h - 3H	414.081	414.081	0.0	6247	3.40
G1h + Cl	452.072	452.074	-4.4	26794	14.59
G1h + Cl + CH₃CN	493.097	493.100	-6.1	25123	13.68

Table 5.9. Quantification of detected ions by ESI-TOF MS for the reaction of 1 equiv. of **1** with catalyst **G1** and subsequent addition of 1 equiv. of **4** (room temperature, 7.8 mg of catalyst **G1**, 2 mg of monomer **1** in 1 mL dichloromethane for 15 min, followed by addition of 4.6 mg of monomer **4** in 1 mL dichloromethane and reaction for further 15 min).

species	m/z (exp)	m/z (calc)	error (ppm)	intensity	fraction (%)
G1a	787.388	787.384	5.1	1873551	67.23
G1b	507.156	507.152	7.9	53866	1.93
G1b-(1)₁	717.243	717.241	2.8	16868	0.61

G1b-(1)₂	927.316	927.331	-16.2	18506	0.66
G1b-(1)₃	1137.417	1137.424	-3.5	3951	0.14
G1c	471.173	471.176	-6.4	106700	3.83
G1d	828.413	828.411	2.4	583452	20.94
G1d-(1)₁	1038.482	1038.501	-18.3	19693	0.71
G1d-(1)₂	1248.517	1248.590	-58.5	7278	0.26
G1d-(1)₃	1458.675	1458.680	-3.4	2656	0.10
G1d-(1)₄	1668.731	1668.769	-22.7	1138	0.04
G1d-(4)₁	1318.679	1318.716	-28.1	6030	0.22
G1d-(4)₁(1)₁	1528.750	1528.806	-36.6	1965	0.07
G1e-(1)₁	758.273	758.268	6.6	17050	0.61
G1e-(1)₂	968.346	968.358	-12.4	26965	0.97
G1e-(1)₃	1178.459	1178.447	10.2	9591	0.34
G1e-(1)₄	1388.557	1388.537	14.4	3163	0.11
G1e-(4)₁	1038.482	1038.484	-1.9	17513	0.63
G1e-(4)₂	1528.750	1528.789	-25.5	1811	0.06
G1e-(4)₁(1)₁	1248.571	1248.573	-1.6	11049	0.40
G1e-(4)₁(1)₂	1458.664	1458.663	0.7	2648	0.10
G1e-(4)₁(1)₃	1688.731	1688.752	-12.6	1140	0.04
G1e-(4)₂(1)₁	1738.843	1738.878	-20.1	661	0.02

Table 5.10. Quantification of detected ions by ESI-TOF MS for the reaction of 1 equiv. of **1** with catalyst **U1** and subsequent addition of 1 equiv. of **2** (room temperature, 8.8 mg of catalyst **U1**, 2 mg of monomer **1** in 1 mL dichloromethane for 15 min, followed by addition of 4 mg of monomer **2** in 1 mL dichloromethane and reaction for further 15 min).

species	m/z (exp)	m/z (calc)	error (ppm)	intensity	fraction (%)
U1a	887.415	887.416	-1.1	668559	33.44
U1b	607.184	607.183	1.6	22574	1.13
U1b-(1)₁	817.281	817.273	9.8	79005	3.95
U1c	571.203	571.207	-7.0	514937	25.76
U1d	928.440	928.443	-3.2	435716	21.79

U1e	648.208	648.210	-3.1	177012	8.85
U1e-(1)₁	858.295	858.300	-5.8	25740	1.29
U1e-(1)₂	1068.375	1068.389	-13.1	21440	1.07
U1e-(2)₁(1)₁	1283.353	1283.367	-10.9	30047	1.50
U1e-(2)₁(1)₂	1493.447	1493.457	-6.7	9321	0.47
U1e-(2)₂(1)₁	1708.434	1708.435	-0.6	8758	0.44
U1e-(2)₂(1)₂	1918.518	1918.525	-3.6	2205	0.11
U1e-(2)₃(1)₁	2133.499	2133.503	-1.9	2331	0.12
U1e-(2)₃(1)₂	2343.615	2343.592	9.8	864	0.04
U1e-(2)₄(1)₁	2558.603	2558.571	12.5	700	0.04

Table 5.11. Quantification of detected ions by ESI-TOF MS for the reaction of 1 equiv. of **1** with catalyst **U1** and subsequent addition of 1 equiv. of **3** (room temperature, 8.8 mg of catalyst **U1**, 2 mg of monomer **1** in 1 mL dichloromethane for 15 min, followed by addition of 1.2 mg of monomer **3** in 1 mL dichloromethane and reaction for further 15 min).

species	m/z (exp)	m/z (calc)	error (ppm)	intensity	fraction (%)
U1a	887.420	887.416	4.5	294232	31.70
U1a-(1)₁	1097.506	1097.506	0.0	1135	0.12
U1a-(1)₂	1307.582	1307.595	-9.9	785	0.08
U1a-(3)₁(1)₁	1227.625	1227.584	33.4	7488	0.81
U1b	607.182	607.183	-1.6	5684	0.61
U1b-(1)₁	817.281	817.273	9.8	13233	1.43
U1b-(1)₂	1027.366	1027.363	2.9	4943	0.53
U1b-(1)₃	1237.457	1237.452	4.0	2374	0.26
U1c	571.205	571.207	-3.5	175970	18.96
U1d	928.445	928.443	2.2	234000	25.21
U1e	648.212	648.210	3.1	143229	15.43
U1e-(1)₁	858.315	858.300	17.5	14457	1.56
U1e-(1)₂	1068.392	1068.389	2.8	10080	1.09
U1e-(1)₃	1278.482	1278.479	2.3	5227	0.56
U1e-(1)₄	1488.568	1488.568	0.0	1939	0.21

U1e-(1)₅	1698.686	1698.658	16.5	617	0.07
U1e-(3)₁(1)₁	988.379	988.378	1.0	7070	0.76
U1e-(3)₁(1)₂	1198.460	1198.468	-6.7	3822	0.41
U1e-(3)₁(1)₃	1408.549	1408.557	-5.7	1940	0.21

Table 5.12. Quantification of detected ions by ESI-TOF MS for the reaction of 1 equiv. of **1** with catalyst **U1** and subsequent addition of 1 equiv. of **4** (room temperature, 8.8 mg of catalyst **U1**, 2 mg of monomer **1** in 1 mL dichloromethane for 15 min, followed by addition of 4.6 mg of monomer **4** in 1 mL dichloromethane and reaction for further 15 min).

species	m/z (exp)	m/z (calc)	error (ppm)	intensity	fraction (%)
U1a	887.415	887.416	-1.1	869946	30.72
U1a-(1)₁	1097.492	1097.506	-12.8	5888	0.21
U1b	607.185	607.183	0.0	27366	0.97
U1b-(1)₁	817.281	817.273	9.8	53766	1.90
U1b-(1)₂	1027.349	1027.363	-13.6	7432	0.26
U1b-(1)₃	1237.454	1237.452	1.6	3881	0.14
U1b-(4)₁(1)₁	1307.568	1307.578	-7.6	4051	0.14
U1b-(4)₁(1)₂	1517.654	1517.668	-9.2	1489	0.05
U1b-(4)₁	1097.503	1097.489	12.8	5873	0.21
U1c	571.206	571.207	-1.8	841462	29.72
U1d	928.441	928.443	-2.2	589832	20.83
U1e	648.210	648.210	3.3	339877	12.00
U1e-(1)₁	858.303	858.300	3.5	21325	0.75
U1e-(1)₂	1068.387	1068.389	-1.9	18031	0.64
U1e-(1)₃	1278.475	1278.479	-3.1	7251	0.26
U1e-(1)₄	1488.552	1488.568	-10.7	2633	0.09
U1e-(4)₁	1138.503	1138.517	-12.3	16863	0.60
U1e-(4)₂	1628.828	1628.820	4.9	1345	0.05
U1e-(4)₁(1)₁	1348.597	1348.605	-5.9	6797	0.24
U1e-(4)₁(1)₂	1558.687	1558.694	-4.5	3346	0.12
U1e-(4)₁(1)₃	1768.774	1768.784	-5.7	1182	0.04

U1e-(4)₁(1)₄	1978.869	1978.873	-2.0	555	0.02
U1e-(4)₂(1)₁	1838.915	1838.910	2.7	974	0.03
U1e-(4)₂(1)₂	2048.926	2048.999	-35.6	490	0.02

Table 5.13. Quantification of detected ions by ESI-TOF MS for the reaction of 1 equiv. of **1** with catalyst **G3** and subsequent addition of 1 equiv. of **2** (room temperature, 8.4 mg of catalyst **G3**, 2 mg of monomer **1** in 1 mL dichloromethane for 15 min, followed by addition of 4 mg of monomer **2** in 1 mL dichloromethane and reaction for further 15 min).

species	m/z (exp)	m/z (calc)	error (ppm)	intensity	fraction (%)
G3a-(1)₁	902.177	902.171	6.7	19566	18.01
G3a-(1)₂	1112.260	1112.260	0.0	14185	13.06
G3a-(1)₃	1322.343	1322.350	-5.3	5948	5.47
G3b	533.131	533.130	1.9	11815	10.87
G3c-(1)₁	707.240	707.243	-4.2	10627	9.78
G3c-(1)₂	917.323	917.332	-9.8	7307	6.73
G3h	443.084	443.085	-2.3	1774	1.63
G3j-(1)₁	866.207	866.195	13.9	19860	18.28
G3j-(1)₂	1076.288	1076.284	3.7	10769	9.91
G3j-(2)₁(1)₂	1501.363	1501.352	7.3	4260	3.92
G3j-(2)₂(1)₂	1926.433	1926.420	6.7	2534	2.33

Table 5.14. Quantification of detected ions by ESI-TOF MS for the reaction of 1 equiv. of **1** with catalyst **G3** and subsequent addition of 1 equiv. of **3** (room temperature, 8.4 mg of catalyst **G3**, 2 mg of monomer **1** in 1 mL dichloromethane for 15 min, followed by addition of 1.2 mg of monomer **3** in 1 mL dichloromethane and reaction for further 15 min).

species	m/z (exp)	m/z (calc)	error (ppm)	intensity	fraction (%)
G3a-(1)₁	902.166	902.171	-5.5	7287	2.94
G3b	533.126	533.130	-7.5	8125	3.28
G3c-(1)₁	707.242	707.243	-1.4	47736	19.28
G3c-(1)₂	917.323	917.332	-9.8	30488	12.31
G3c-(1)₃	1127.415	1127.422	-6.2	15549	6.28
G3c-(1)₄	1337.508	1337.511	-2.2	5565	2.25

G3c-(3)₁	627.226	627.232	-9.6	8621	3.48
G3c-(3)₁(1)₁	837.317	837.321	-4.8	19721	7.96
G3c-(3)₁(1)₂	1047.407	1047.411	-3.8	15520	6.27
G3c-(3)₁(1)₃	1257.496	1257.500	-3.2	7492	3.03
G3e-(1)₁	784.251	784.246	6.4	15877	6.41
G3e-(1)₂	994.335	994.335	0.0	24405	9.86
G3e-(1)₃	1204.429	1204.425	3.3	15926	6.43
G3e-(1)₄	1414.514	1414.514	0.0	8614	3.48
G3e-(1)₅	1624.583	1624.604	-12.9	2389	0.96
G3e-(1)₆	1834.685	1834.693	-4.4	863	0.35
G3h	443.089	443.082	15.8	10388	4.20
G3i	405.090	405.083	17.3	3055	1.23

Table 5.15. Quantification of detected ions by ESI-TOF MS for the reaction of 1 equiv. of **1** with catalyst **G3** and subsequent addition of 1 equiv. of **4** (room temperature, 8.4 mg of catalyst **G3**, 2 mg of monomer **1** in 1 mL dichloromethane for 15 min, followed by addition of 4.6 mg of monomer **4** in 1 mL dichloromethane and reaction for further 15 min).

species	m/z (exp)	m/z (calc)	error (ppm)	intensity	fraction (%)
G3a-(1)₁	902.182	902.171	12.2	6277	2.28
G3c	533.125	533.130	-9.4	17609	6.39
G3c-(1)₁	707.240	707.243	-4.2	37903	13.75
G3c-(1)₂	917.331	917.332	-1.1	22456	8.14
G3c-(4)₁	987.453	987.458	-5.1	15056	5.46
G3c-(4)₁(1)₁	1197.544	1197.548	-3.3	8228	2.98
G3c-(4)₁(1)₂	1407.631	1407.637	-4.3	4515	1.64
G3e-(1)₁	784.252	784.246	7.7	12933	4.69
G3e-(1)₂	994.327	994.335	-8.0	20957	7.60
G3e-(1)₃	1204.425	1204.425	0.0	13409	4.86
G3e-(1)₄	1414.524	1414.514	7.1	6721	2.44
G3e-(1)₅	1624.628	1624.604	14.8	2668	0.97
G3e-(4)₁	1064.464	1064.461	2.8	15947	5.78

G3e-(4)₂	1554.747	1554.766	-12.2	6265	2.27
G3e-(4)₃	2045.035	2045.071	-17.6	1274	0.46
G3e-(4)_{1(1)₁}	1274.553	1274.551	1.6	16251	5.89
G3e-(4)_{1(1)₂}	1484.648	1484.640	5.4	10214	3.70
G3e-(4)_{1(1)₃}	1694.747	1694.730	10.0	4509	1.64
G3e-(4)_{1(1)₄}	1904.813	1904.819	-3.1	1827	0.66
G3e-(4)_{1(1)₅}	2114.981	2114.909	34.0	922	0.33
G3e-(4)_{2(1)₁}	1764.863	1764.856	4.0	4538	1.65
G3e-(4)_{2(1)₂}	1974.943	1974.945	-1.0	2025	0.73
G3e-(4)_{2(1)₃}	2185.073	2185.035	17.4	1066	0.39
G3e-(4)_{2(1)₄}	2397.137	2397.126	4.6	439	0.16
G3e-(4)_{3(1)₁}	2257.149	2257.162	-5.8	842	0.31
G3e-(4)_{3(1)₂}	2467.272	2467.252	8.1	446	0.16
G3h	443.091	443.085	13.5	31186	11.31
G3i	405.085	405.090	-12.3	9261	3.36

Table 5.16. Quantification of detected ions by ESI-TOF MS for the reaction of 1 equiv. of **1** with catalyst **U3** and subsequent addition of 1 equiv. of **2** (room temperature, 7.1 mg of catalyst **U3**, 2 mg of monomer **1** in 1 mL dichloromethane for 15 min, followed by addition of 4 mg of monomer **2** in 1 mL dichloromethane and reaction for further 15 min).

species	m/z (exp)	m/z (calc)	error (ppm)	intensity	fraction (%)
U3a	712.205	712.203	2.8	120259	3.23
U3a-(1)₁	922.286	922.293	-7.6	31008	0.83
U3a-(1)₂	1132.376	1132.383	-6.2	26589	0.71
U3a-(1)₃	1342.466	1342.472	-4.5	19243	0.52
U3a-(1)₄	1552.559	1552.562	-1.9	9633	0.26
U3a-(1)₅	1762.650	1762.651	-0.6	4334	0.12
U3a-(1)₆	1972.727	1972.741	-7.1	1915	0.05
U3a-(2)_{1(1)₁}	1347.369	1347.361	5.9	8545	0.23
U3a-(2)_{2(1)₁}	1772.447	1772.429	10.2	2342	0.06
U3a-(2)_{2(1)₂}	1982.516	1982.518	-1.0	1594	0.04
U3b	633.162	633.161	1.6	878307	23.57

U3b-(1)₁	843.247	843.251	-4.7	17004	0.46
U3b-(1)₂	1053.335	1053.340	-4.7	28527	0.77
U3b-(1)₃	1263.418	1263.430	-9.5	10074	0.27
U3b-(1)₄	1473.540	1473.519	14.3	5757	0.15
U3b-(1)₅	1683.581	1683.609	-16.6	2590	0.07
U3c	597.184	597.185	-1.7	274681	7.37
U3c-(1)₁	807.274	807.274	0.0	194813	5.23
U3c-(1)₂	1017.362	1017.364	-2.0	60642	1.63
U3c-(1)₃	1227.446	1227.453	-5.7	33477	0.90
U3c-(1)₄	1437.542	1437.543	-0.7	13348	0.36
U3c-(1)₅	1647.620	1647.633	-7.9	4302	0.12
U3c-(2)₁	1022.262	1022.253	8.8	12185	0.33
U3c-(2)₁(1)₁	1232.336	1232.342	-4.9	25462	0.68
U3c-(2)₁(1)₂	1442.448	1442.432	11.1	5425	0.15
U3c-(2)₂(1)₁	1657.403	1657.410	-4.2	6642	0.18
U3d	753.216	753.230	-18.6	12988	0.35
U3d-(2)₁	1178.306	1178.298	6.8	24575	0.66
U3d-(2)₂	1603.367	1603.366	0.6	6476	0.17
U3d-(2)₃	2028.427	2028.433	-3.0	2236	0.06
U3d-(2)₂(1)₁	1813.470	1813.455	8.3	2379	0.06
U3e-(1)₁	884.277	884.277	0.0	72110	1.94
U3e-(1)₂	1094.363	1094.367	-3.7	59086	1.59
U3e-(1)₃	1304.456	1304.456	0.0	39513	1.06
U3e-(1)₄	1515.547	1515.546	0.7	18492	0.50
U3e-(1)₅	1724.633	1724.635	-1.2	6760	0.18
U3e-(1)₆	1934.736	1934.725	2.8	2993	0.08
U3e-(2)₁	1099.264	1099.256	1.6	42818	1.15
U3e-(2)₂	1524.316	1524.324	-1.7	9094	0.24
U3e-(2)₁(1)₁	1309.337	1309.345	-7.4	17909	0.48
U3e-(2)₂(1)₁	1734.427	1734.413	-4.5	5325	0.14
U3e-(2)₂(1)₂	1944.494	1944.502	-18.6	3210	0.09

U3e-(2)₃(1)₁	2159.515	2159.481	6.8	2371	0.06
U3e-(2)₃(1)₂	2367.558	2367.570	0.6	1100	0.03
U3e-(2)₄(1)₁	2584.584	2584.548	-3.0	764	0.02
U3h	443.080	443.082	-4.5	295770	7.94
U3h + C₅H₅N - H	521.116	521.117	-1.9	549398	14.74
U3i	405.087	405.090	-7.4	91688	2.46
U3i + 3 CH₃OH	501.166	501.169	-6.0	660627	17.73

Table 5.17. Quantification of detected ions by ESI-TOF MS for the reaction of 1 equiv. of **1** with catalyst **U3** and subsequent addition of 1 equiv. of **3** (room temperature, 7.1 mg of catalyst **U3**, 2 mg of monomer **1** in 1 mL dichloromethane for 15 min, followed by addition of 1.2 mg of monomer **3** in 1 mL dichloromethane and reaction for further 15 min).

species	m/z (exp)	m/z (calc)	error (ppm)	intensity	fraction (%)
U3a	712.204	712.203	1.4	107707	3.50
U3a-(1)₁	922.278	922.293	-16.3	16328	0.53
U3a-(3)₁	842.273	842.282	-10.7	34252	1.11
U3b	633.162	633.161	1.6	521255	16.92
U3b-(1)₂	1053.333	1053.340	-6.6	20744	0.67
U3b-(3)₁	763.227	763.240	-17.0	28865	0.94
U3c	597.185	597.185	0.0	585300	19.00
U3c-(1)₁	807.273	807.274	-1.2	217210	7.05
U3c-(1)₂	1017.348	1017.364	-15.7	80819	2.62
U3c-(1)₃	1227.444	1227.453	-7.3	41937	1.36
U3c-(1)₄	1437.540	1437.543	-2.1	16931	0.55
U3c-(1)₅	1647.618	1647.633	-9.1	6171	0.20
U3c-(1)₆	1857.694	1857.722	-15.1	2274	0.07
U3c-(3)₁	727.264	727.263	1.4	55576	1.80
U3c-(3)₁(1)₁	937.343	937.353	-10.7	23574	0.77
U3c-(3)₁(1)₂	1147.443	1147.442	0.9	9449	0.31
U3c-(3)₁(1)₃	1357.514	1357.532	-13.3	5782	0.19
U3c-(3)₁ + CH₃OH	759.286	759.290	-5.3	198456	6.44
U3e-(1)₁	884.278	884.277	1.1	126473	4.11

U3e-(1)₂	1094.364	1094.367	-2.7	94134	3.06
U3e-(1)₃	1304.453	1304.456	-2.3	62313	2.02
U3e-(1)₄	1514.546	1514.546	0.0	28570	0.93
U3e-(1)₅	1724.628	1724.635	-4.1	9544	0.31
U3e-(1)₆	1934.708	1934.725	-8.8	4042	0.13
U3e-(1)₇	2144.779	2144.814	-16.3	1242	0.04
U3g-(3)₁(1)₁	1015.313	1015.314	-1.0	62780	2.04
U3h	443.084	443.082	4.5	278337	9.04
U3h + C₅H₅N – H	521.121	521.117	7.7	122990	3.99
U3i	405.090	405.090	0.0	79511	2.58
U3i + 3 CH₃OH	501.167	501.169	-4.0	237648	7.72

Table 5.18. Quantification of detected ions by ESI-TOF MS for the reaction of 1 equiv. of **1** with catalyst **U3** and subsequent addition of 1 equiv. of **4** (room temperature, 7.1 mg of catalyst **U3**, 2 mg of monomer **1** in 1 mL dichloromethane for 15 min, followed by addition of 4.6 mg of monomer **4** in 1 mL dichloromethane and reaction for further 15 min).

species	m/z (exp)	m/z (calc)	error (ppm)	intensity	fraction (%)
U3a	712.204	712.203	1.4	189137	4.30
U3a-(1)₁	922.291	922.293	-2.2	18748	0.43
U3a-(1)₂	1132.376	1132.383	-6.2	15678	0.36
U3a-(1)₃	1342.466	1342.472	-4.5	12293	0.28
U3a-(1)₄	1552.560	1552.562	-1.3	6252	0.14
U3a-(1)₅	1762.651	1762.651	0.0	3038	0.07
U3a-(1)₆	1972.729	1972.741	-6.1	1419	0.03
U3a-(4)₁	1202.509	1202.509	0.0	15530	0.35
U3a-(4)₂	1692.837	1692.814	13.6	4315	0.10
U3a-(4)₁(1)₁	1412.601	1412.598	2.1	6936	0.16
U3a-(4)₁(1)₂	1622.685	1622.688	-1.8	3807	0.09
U3a-(4)₁(1)₃	1832.780	1832.777	1.6	2063	0.05
U3a-(4)₂(1)₁	1902.890	1902.903	-6.8	2236	0.05
U3a-(4)₂(1)₂	2112.964	2112.993	-13.7	1291	0.03

U3b	633.163	633.161	3.2	1111007	25.26
U3b-(1)₁	843.244	843.251	-8.3	13214	0.30
U3b-(1)₂	1053.335	1053.340	-4.7	20545	0.47
U3c	597.185	597.185	0.0	563560	12.81
U3c-(1)₁	807.275	807.274	1.2	158797	3.61
U3c-(1)₂	1017.364	1017.364	0.0	53287	1.21
U3c-(1)₃	1227.446	1227.453	-5.7	29254	0.67
U3c-(1)₄	1437.552	1437.543	6.3	12350	0.28
U3c-(1)₅	1647.628	1647.633	-3.0	4389	0.10
U3c-(4)₁	1087.489	1087.490	-0.9	133085	3.03
U3c-(4)₂	1577.788	1577.795	-4.4	10027	0.23
U3c-(4)₁(1)₁	1297.580	1297.579	0.8	22806	0.52
U3c-(4)₁(1)₂	1507.658	1507.669	-7.3	8251	0.19
U3c-(4)₁(1)₃	1717.765	1717.759	3.5	3929	0.09
U3c-(4)₂(1)₁	1787.879	1787.885	-3.4	3590	0.08
U3c-(4)₂(1)₂	1997.976	1997.974	1.0	1771	0.04
U3d	753.234	753.230	5.3	25869	0.59
U3e-(1)₁	884.280	884.277	3.4	83226	1.89
U3e-(1)₂	1094.367	1094.367	0.0	62316	1.42
U3e-(1)₃	1304.458	1304.456	1.5	44089	1.00
U3e-(1)₄	1514.538	1514.546	-5.3	22567	0.51
U3e-(1)₅	1724.635	1724.635	0.0	11435	0.26
U3e-(4)₁	1164.495	1164.493	1.7	219075	4.98
U3e-(4)₂	1654.799	1654.798	0.6	38752	0.88
U3e-(4)₃	2145.095	2145.103	-3.7	4642	0.11
U3e-(4)₄	2637.421	2637.409	4.5	580	0.01
U3e-(4)₁(1)₁	1374.584	1374.582	1.5	48741	1.11
U3e-(4)₁(1)₂	1584.659	1584.672	-8.2	20358	0.46
U3e-(4)₁(1)₃	1794.765	1794.761	2.2	10491	0.24
U3e-(4)₁(1)₄	2004.869	2004.851	9.0	5346	0.12
U3e-(4)₁(1)₅	2205.025	2214.940	38.4	2518	0.06

U3e-(4)₁(1)₆	2427.101	2427.031	28.8	1057	0.02
U3e-(4)₂(1)₁	1864.885	1864.887	-1.1	14218	0.32
U3e-(4)₂(1)₂	2074.973	2074.977	-1.9	5727	0.13
U3e-(4)₂(1)₃	2287.061	2287.068	-3.1	2382	0.05
U3e-(4)₂(1)₄	2497.170	2497.157	5.2	1227	0.03
U3e-(4)₂(1)₅	2707.261	2707.247	5.2	623	0.01
U3e-(4)₂(1)₆	2917.301	2917.337	-12.3	421	0.01
U3e-(4)₃(1)₁	2357.155	2357.194	-16.5	1965	0.04
U3e-(4)₃(1)₂	2567.268	2567.283	-5.8	1012	0.02
U3e-(4)₃(1)₃	2777.342	2777.373	-11.2	534	0.01
U3e-(4)₃(1)₄	2987.458	2987.463	-1.7	345	0.01
U3e-(4)₄(1)₁	2847.435	2847.499	-22.5	433	0.01
U3h	443.082	443.082	0.0	250624	5.70
U3h + C₅H₅N - H	521.120	521.117	5.8	252143	5.73
U3i	405.088	405.090	-4.9	103082	2.34
U3i + 3 CH₃OH	501.168	501.169	-2.0	730675	16.61

Measured and simulated isotopic patterns

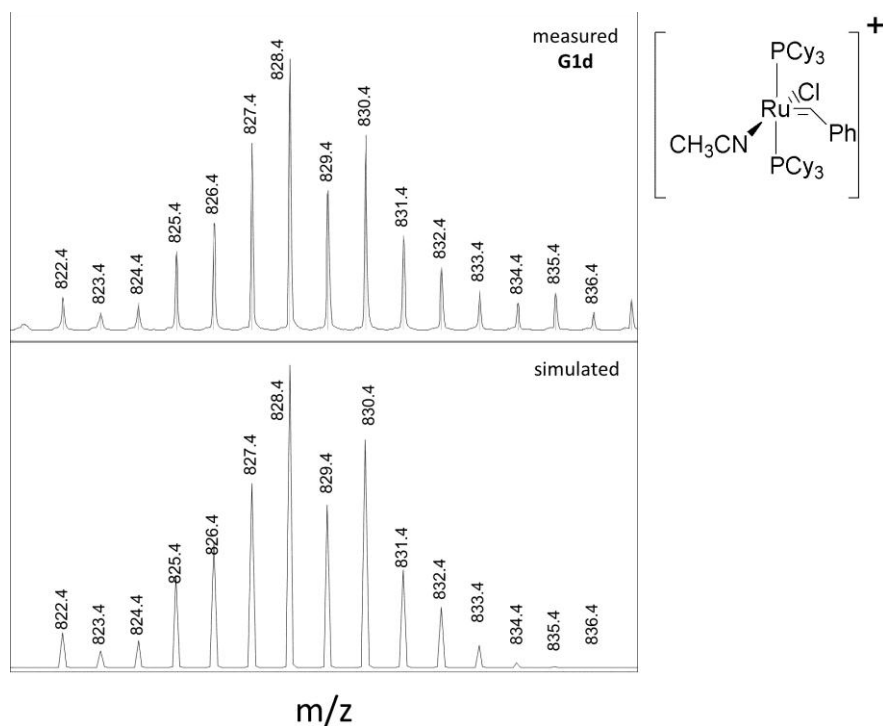


Figure 5.38. Measured and simulated isotopic pattern for **G1d**, from the reaction of catalyst **G1** with 1 equiv. **1**.

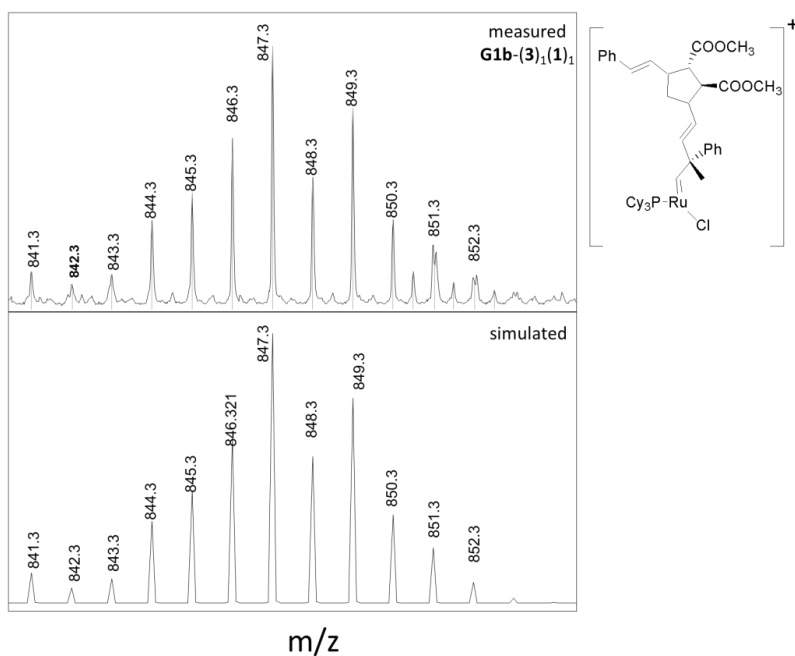


Figure 5.39. Measured and simulated isotopic pattern for **G1b-(3)₁(1)₁**, from the crossover experiment **1/3** for catalyst **G1**.

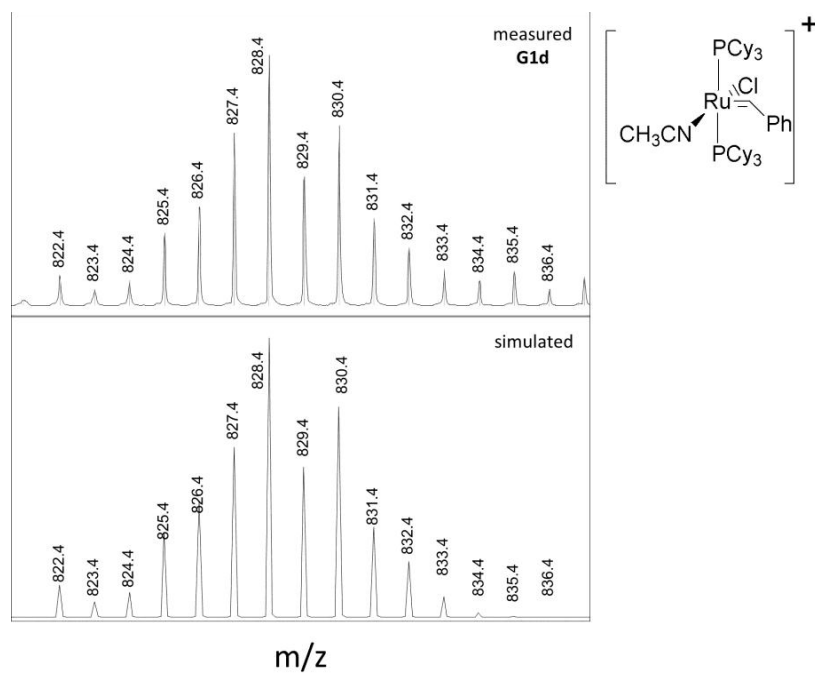


Figure 5.40. Measured and simulated isotopic pattern for **U1d**, from the reaction of catalyst **U1** with 1 equiv. of **1**.

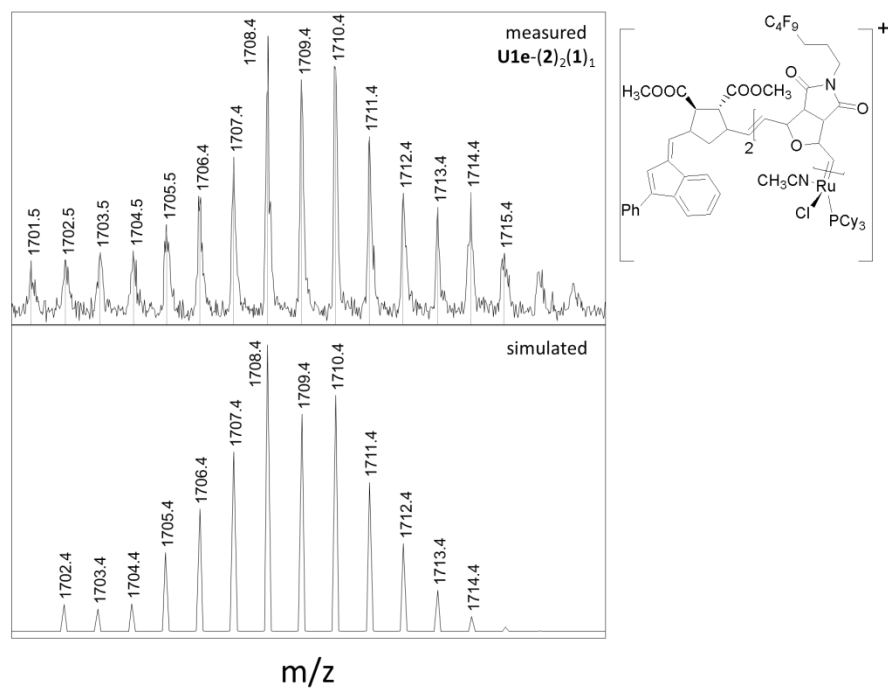


Figure 5.41. Measured and simulated isotopic pattern for **U1e-(2)₂(1)₁**, from the crossover experiment 1/2 for catalyst **U1**.

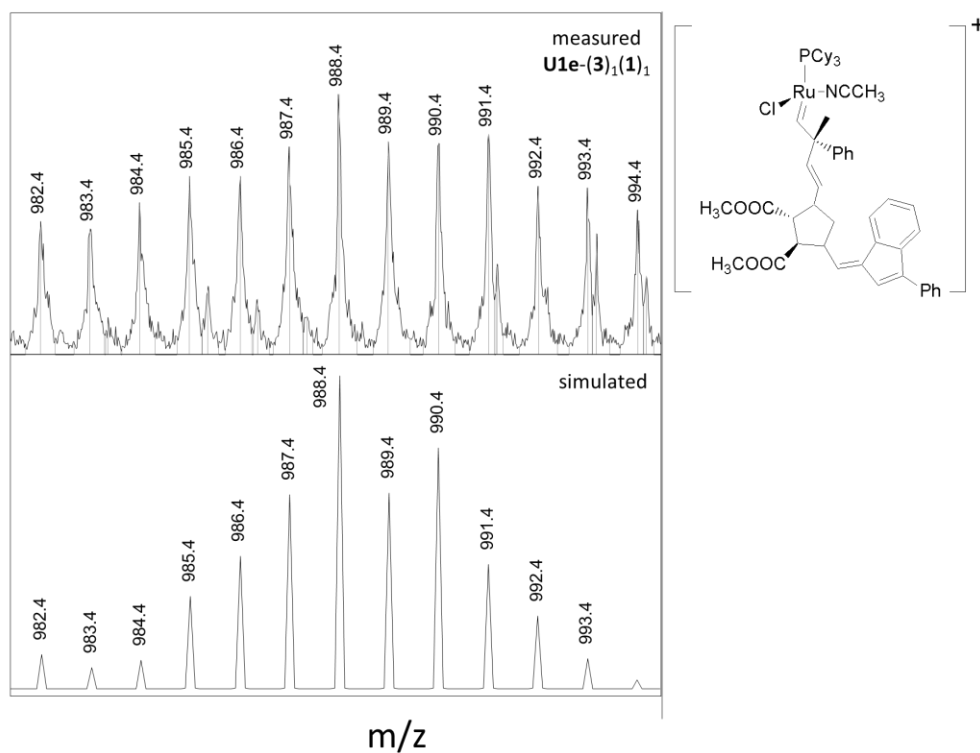


Figure 5.42. Measured and simulated isotopic pattern for $\text{U1e-(3)}_1(\mathbf{1})_1$, from the crossover experiment 1/3 for catalyst **U1**.

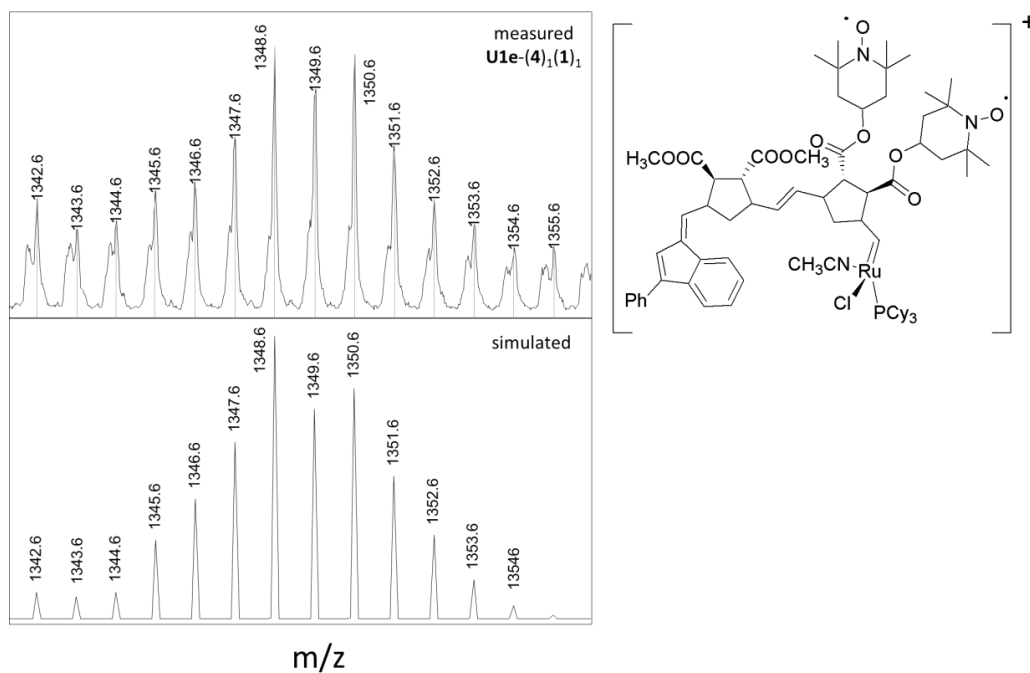


Figure 5.43. Measured and simulated isotopic pattern for $\text{U1e-(4)}_1(\mathbf{1})_1$, from the crossover experiment 1/4 for catalyst **U1**.

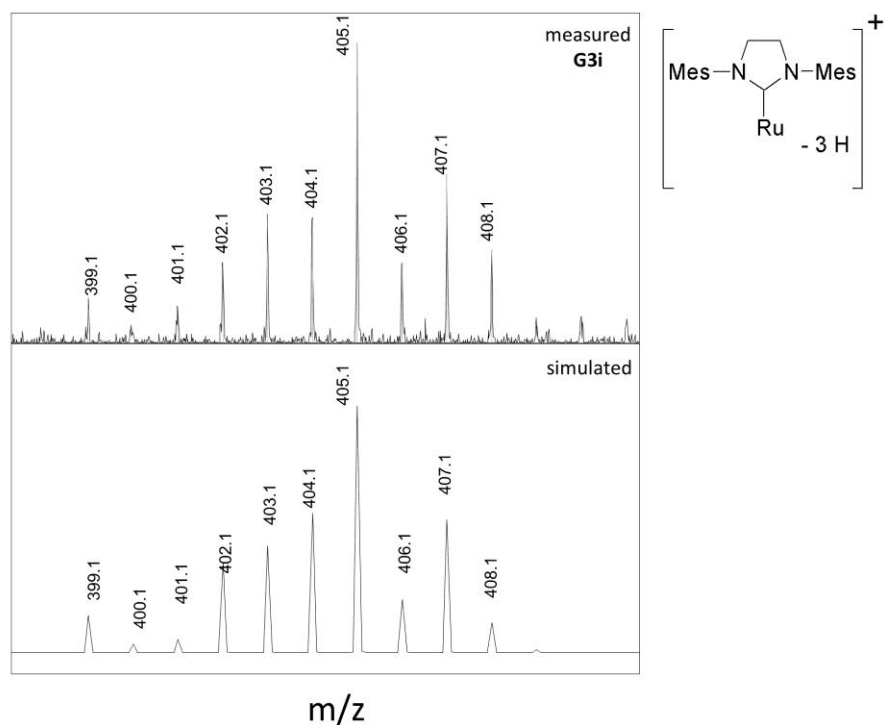


Figure 5.44. Measured and simulated isotopic pattern for **G3i**, from the crossover experiment **1/4** for catalyst **G3**.

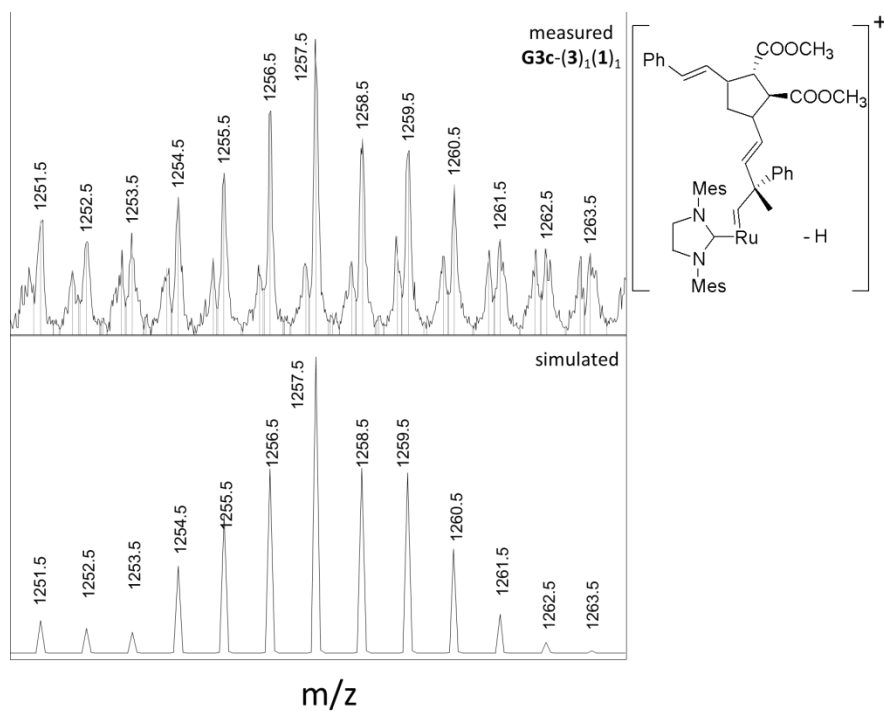


Figure 5.45. Measured and simulated isotopic pattern for **G3c-(3)₁(1)₁**, from the crossover experiment **1/3** for catalyst **G3**.

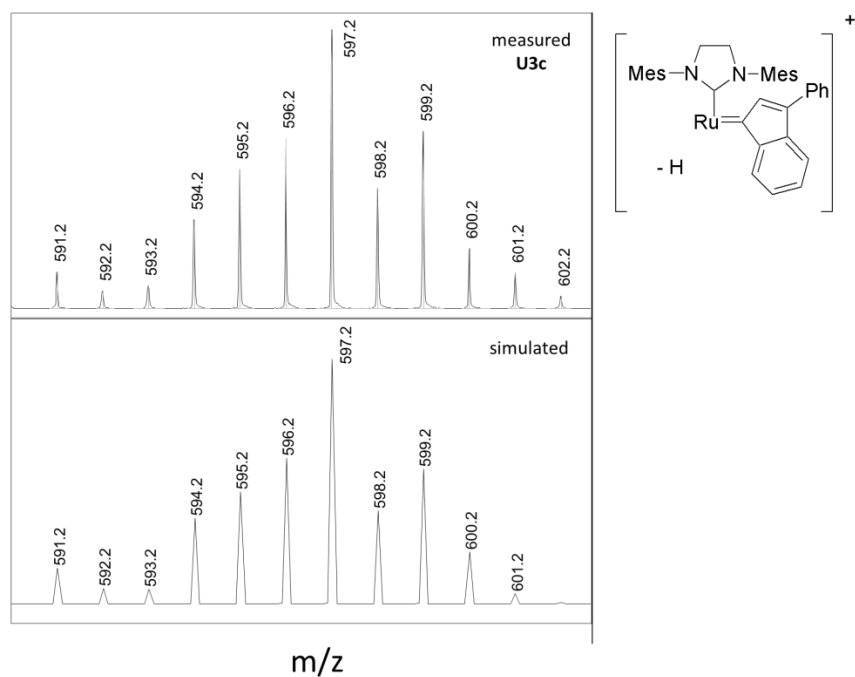


Figure 5.46. Measured and simulated isotopic pattern for **U3c**, from the reaction of catalyst **U3** with 1 equiv. of **1**.

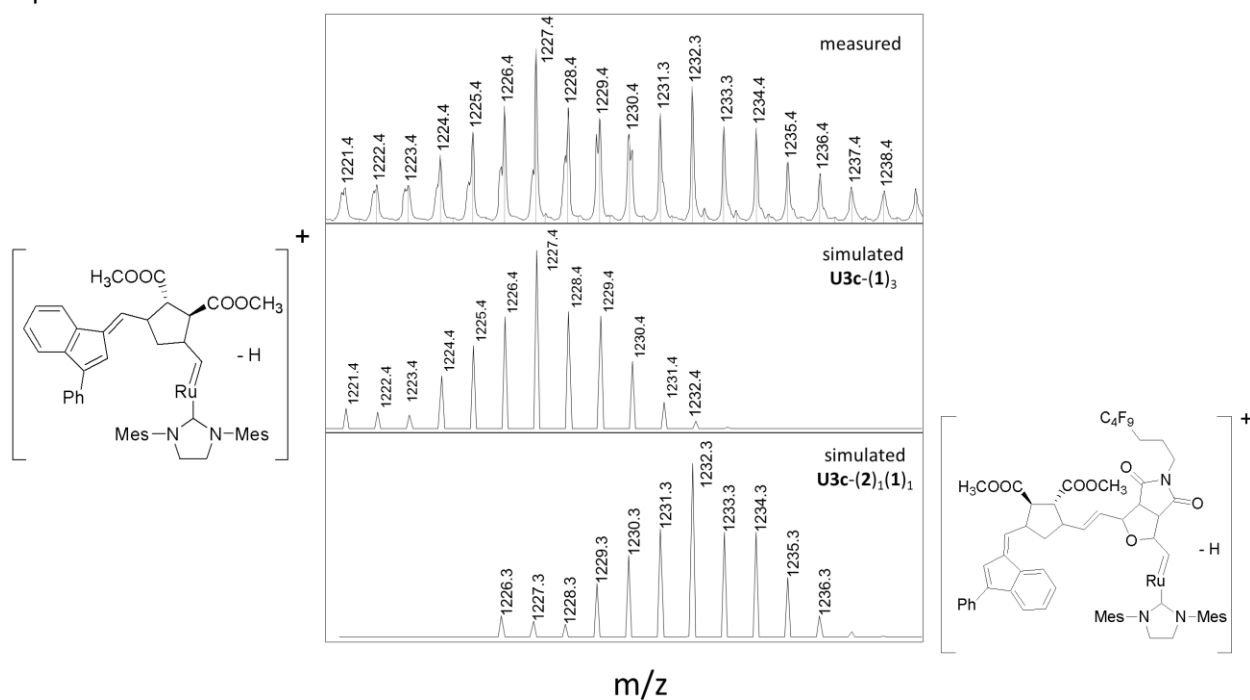


Figure 5.47. Measured and simulated isotopic pattern for **U3c-(1)₃** and **U3c-(2)₁(1)₁**, from the crossover experiment **1/2** for catalyst **U3**.

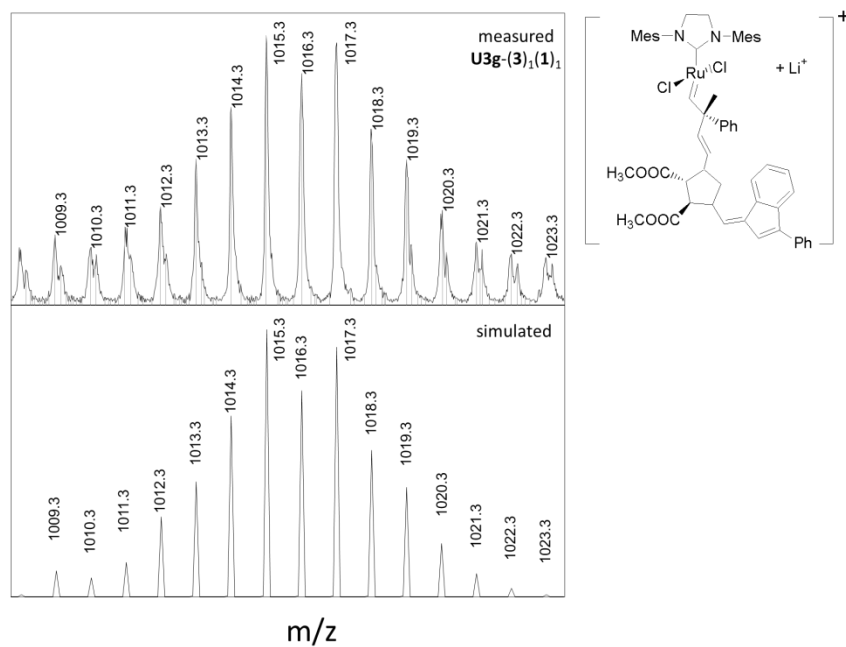


Figure 5.48. Measured and simulated isotopic pattern for **U3g-(3)₁(1)₁**, from the crossover experiment 1/3 for catalyst **U3**.

Chapter 2.7.

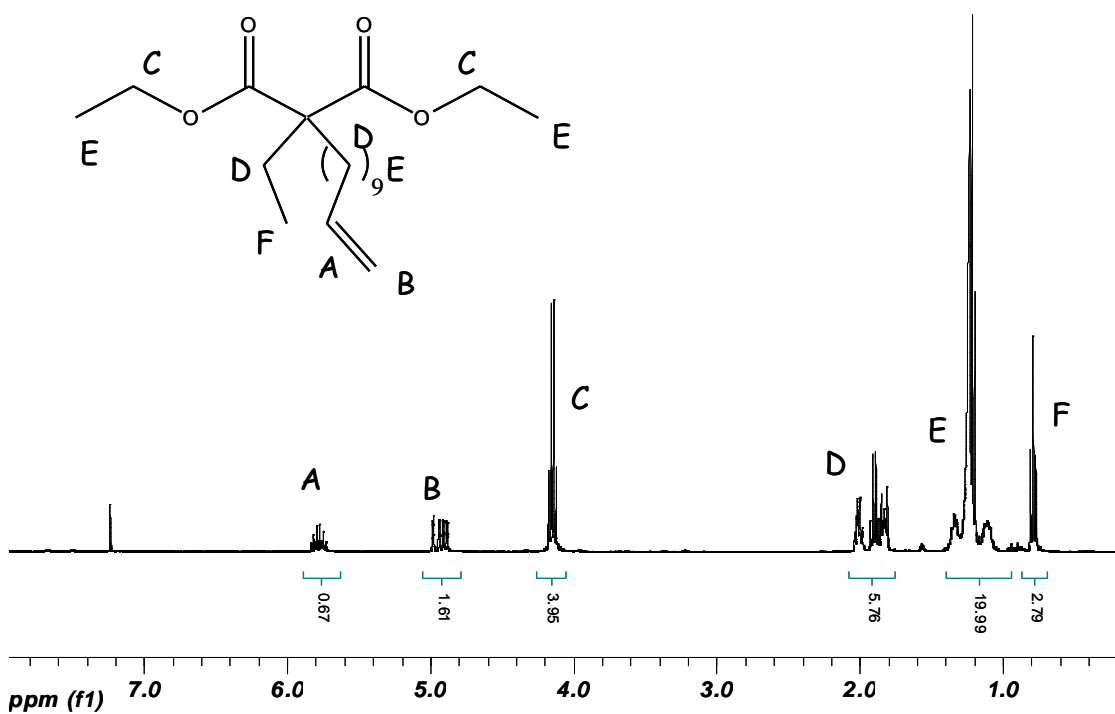
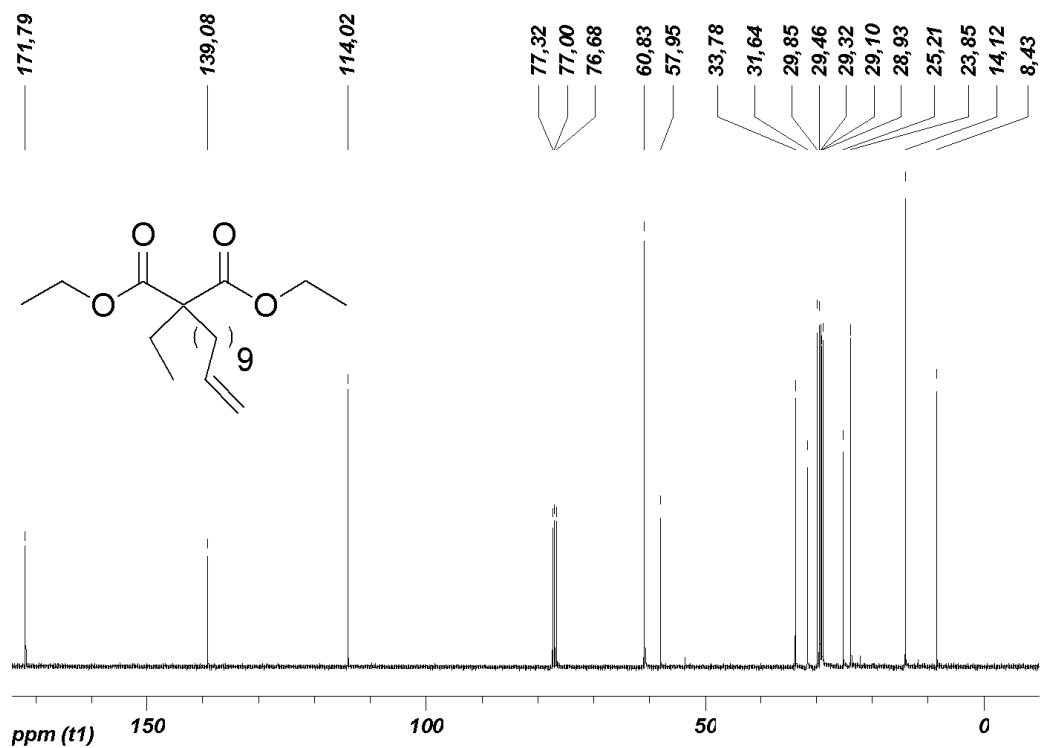
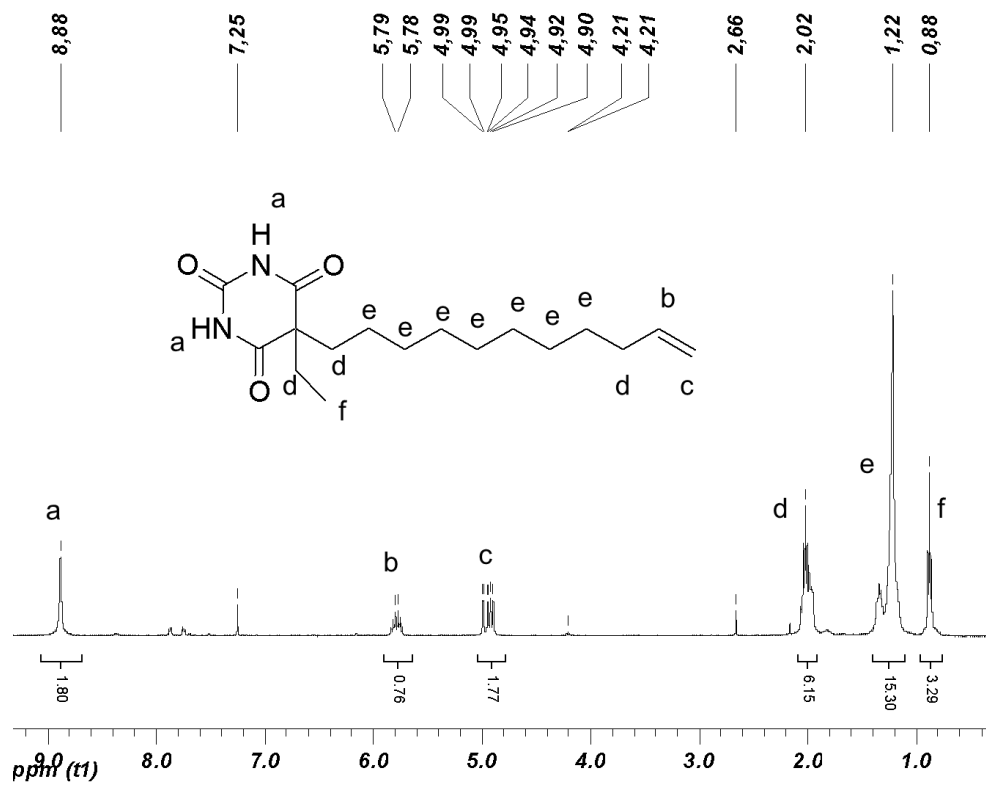


Figure 5.49. ¹H NMR of diethyl 2-ethyl-2-(undec-10-enyl)malonate (**19**).

Figure 5.50. ^{13}C NMR spectrum of compound 19.Figure 5.51. ^1H NMR of 5-ethyl-5-(undec-10-enyl)pyrimidine-2,4,6-trione (20).

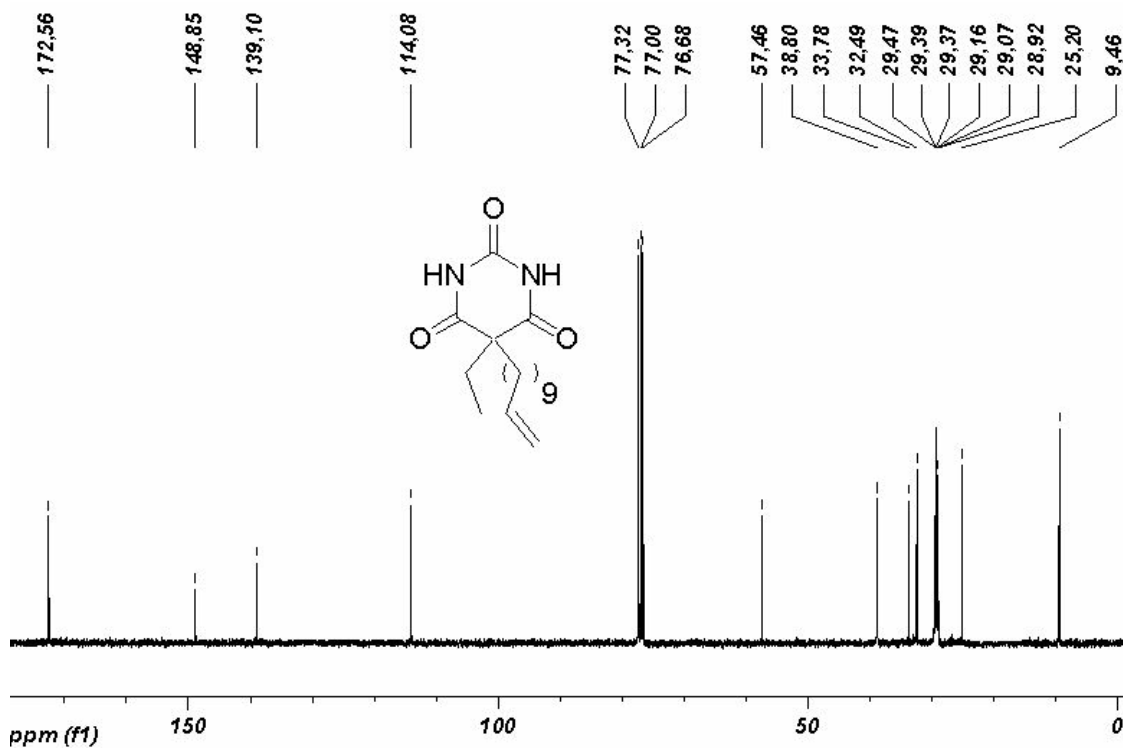


Figure 5.52. ^{13}C NMR spectrum of compound 20.

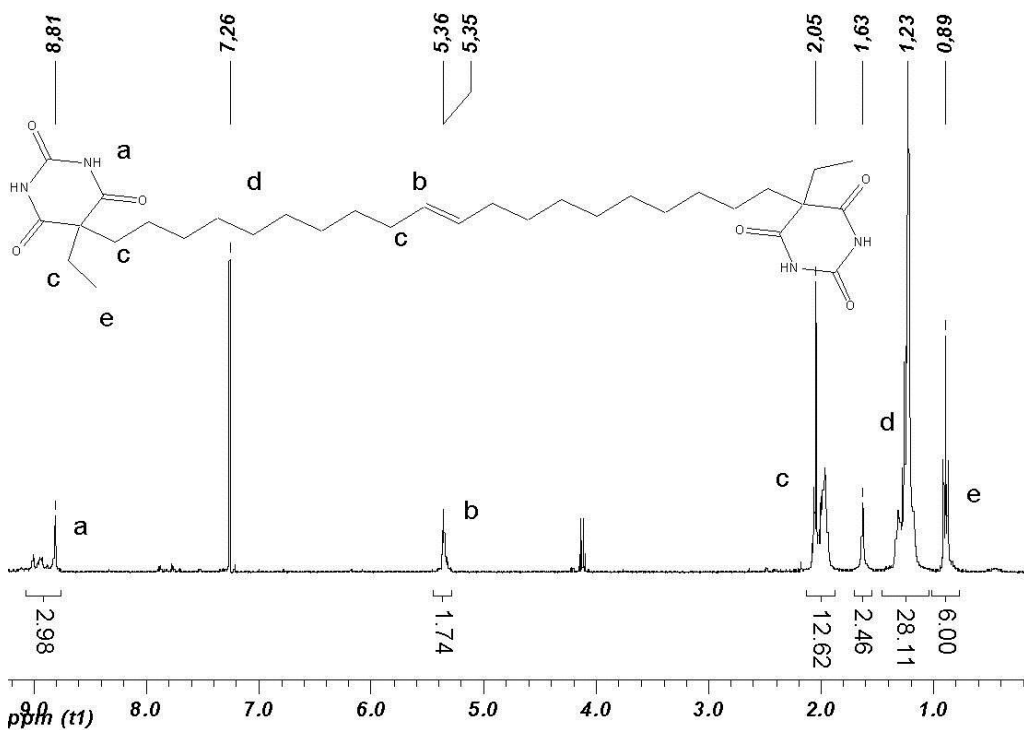
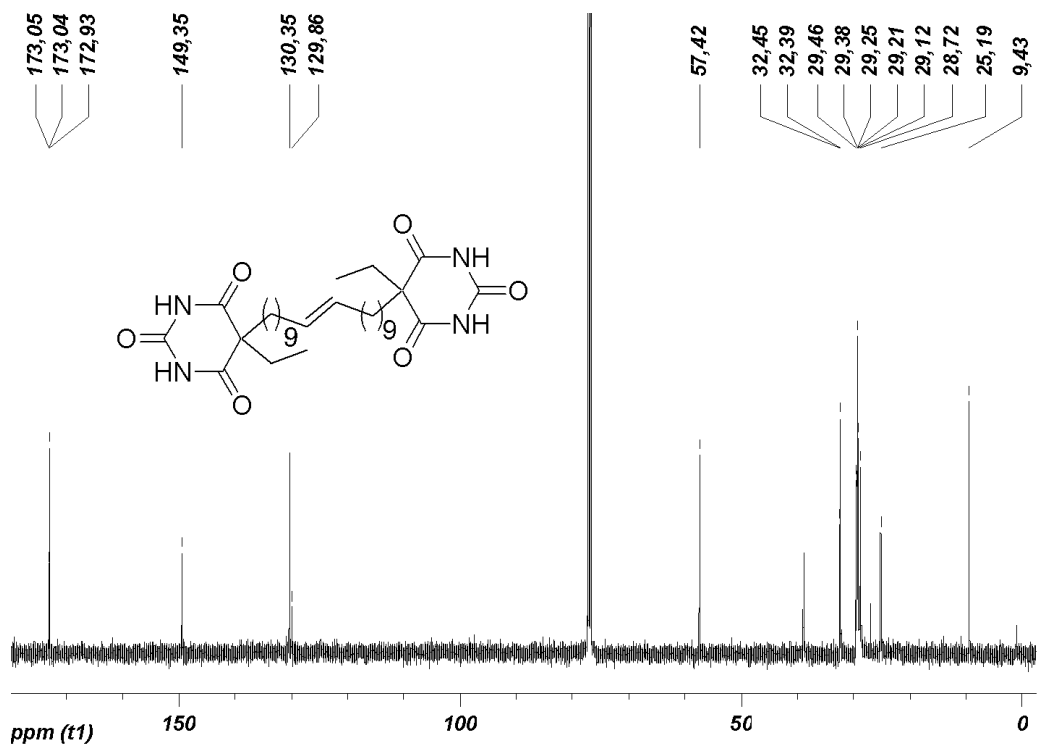
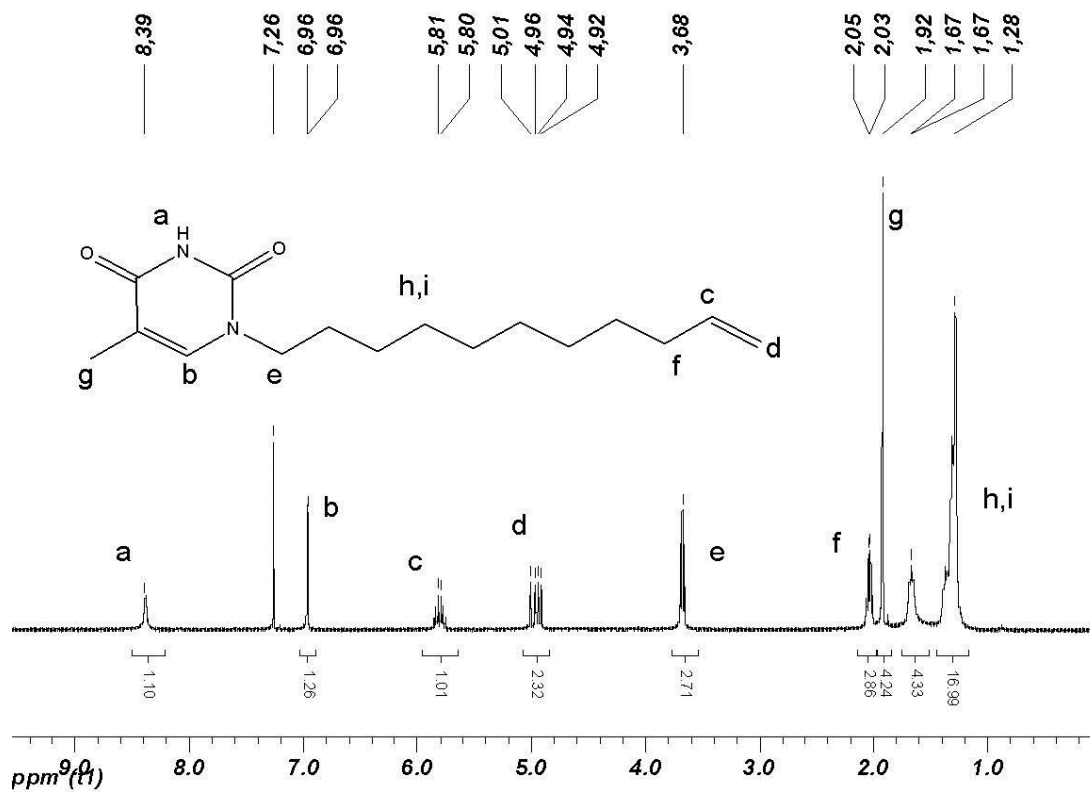
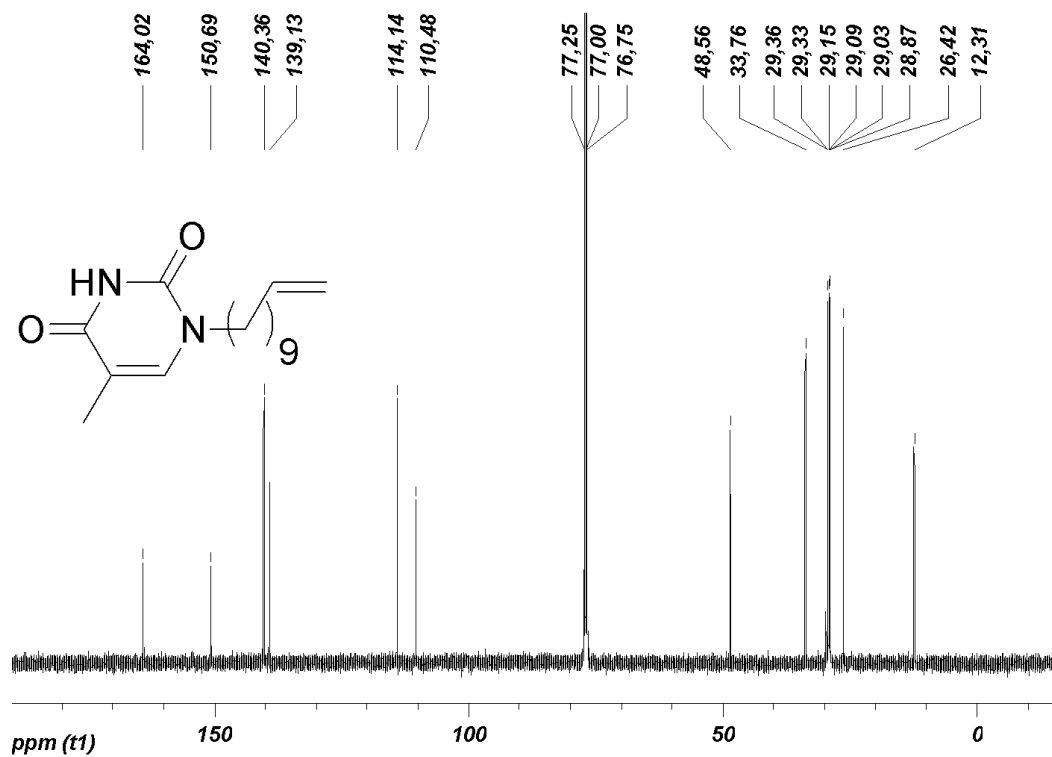
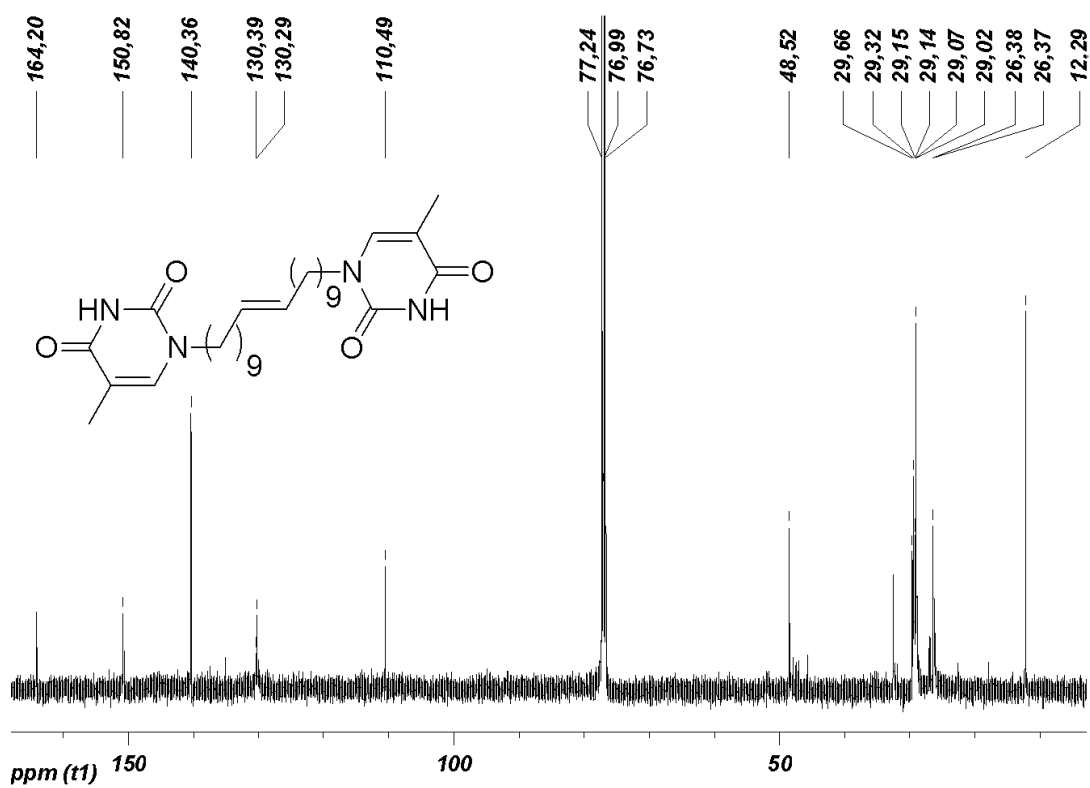


Figure 5.53. ^1H NMR of compound 21.

Figure 5.54. ^{13}C NMR spectrum of compound **21**.Figure 5.55. ^1H NMR of N-undecenylthymine (**22**)

Figure 5.56. ¹³C NMR spectrum of compound 22.Figure 5.57. ¹³C NMR spectrum of compound 23.

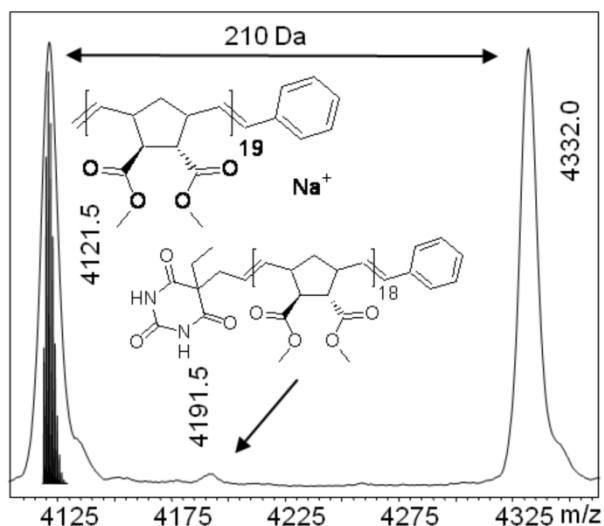


Figure 5.58. MALDI-TOF MS spectrum of poly(**1**) initiated with Grubbs catalyst 1st-generation and terminated with 10 eq. of compound **20**, reaction time 24 h, simulated isotopic pattern for methylene capped poly(**1**), n = 19, ionized with sodium.

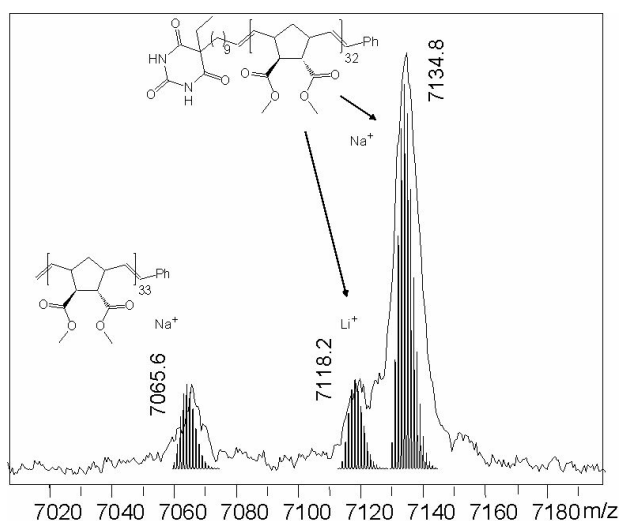
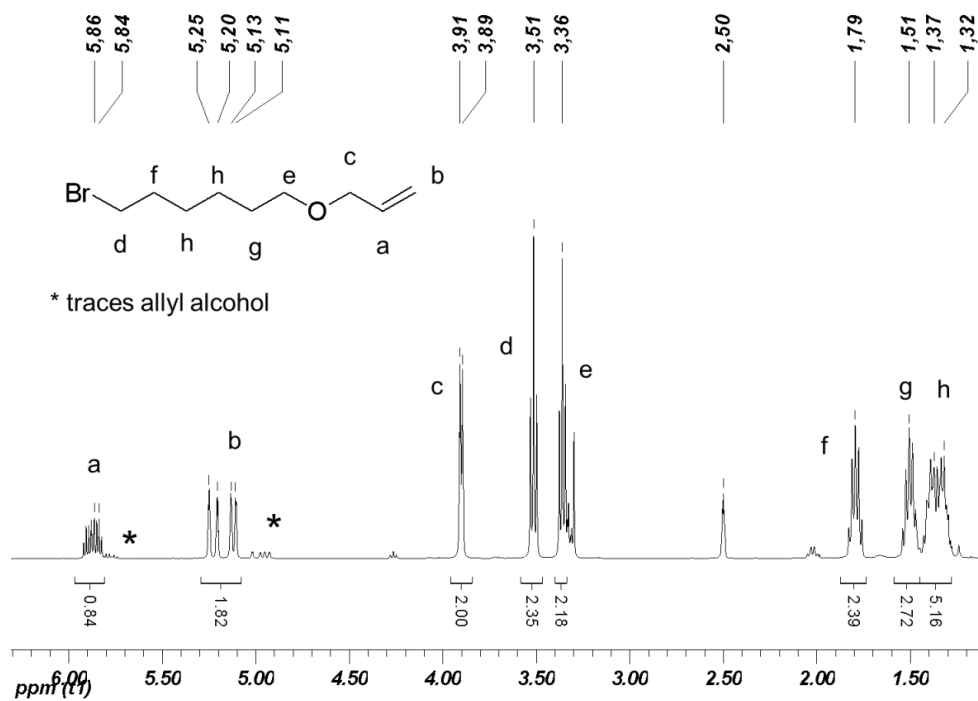
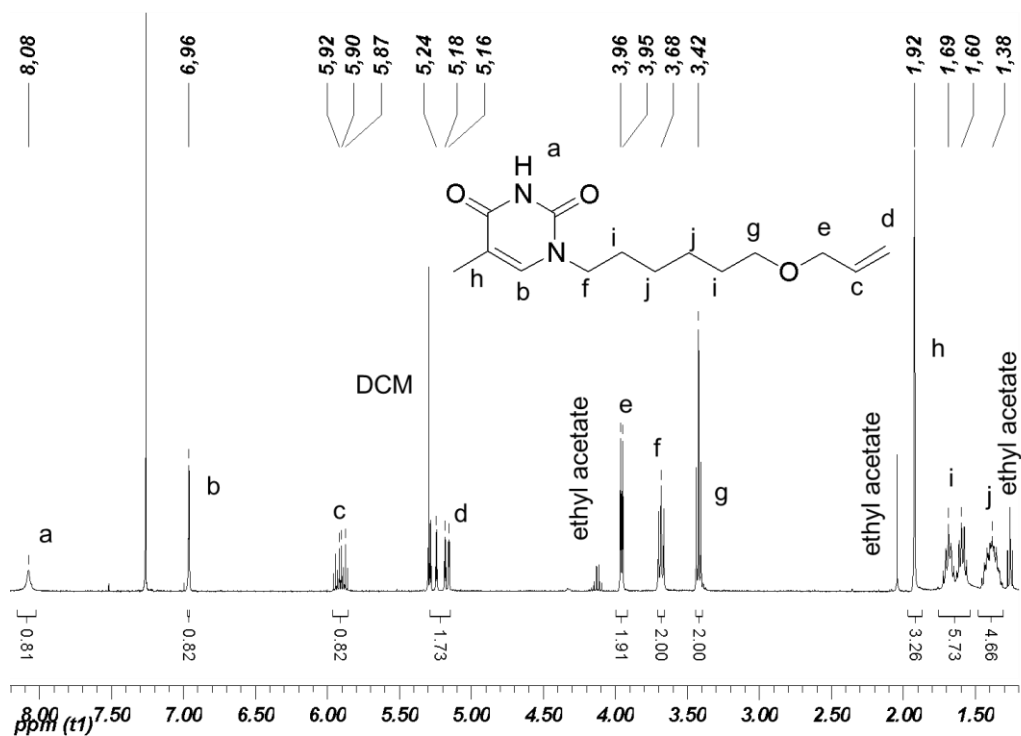


Figure 5.59. MALDI-TOF MS spectrum of poly(**1**) initiated with Grubbs catalyst 3rd-generation and terminated with 20 eq. of compound **21**, reaction time 100 h, simulated isotopic patterns for methylene capped poly(**1**), n = 33, ionized with sodium and barbiturate capped poly(**1**), n = 32, ionized with lithium and sodium.

Chapter 2.8.

Figure 5.60. ¹H NMR of compound **26** in DMSO-d₆.Figure 5.61. ¹H NMR of compound **27** in CDCl₃.

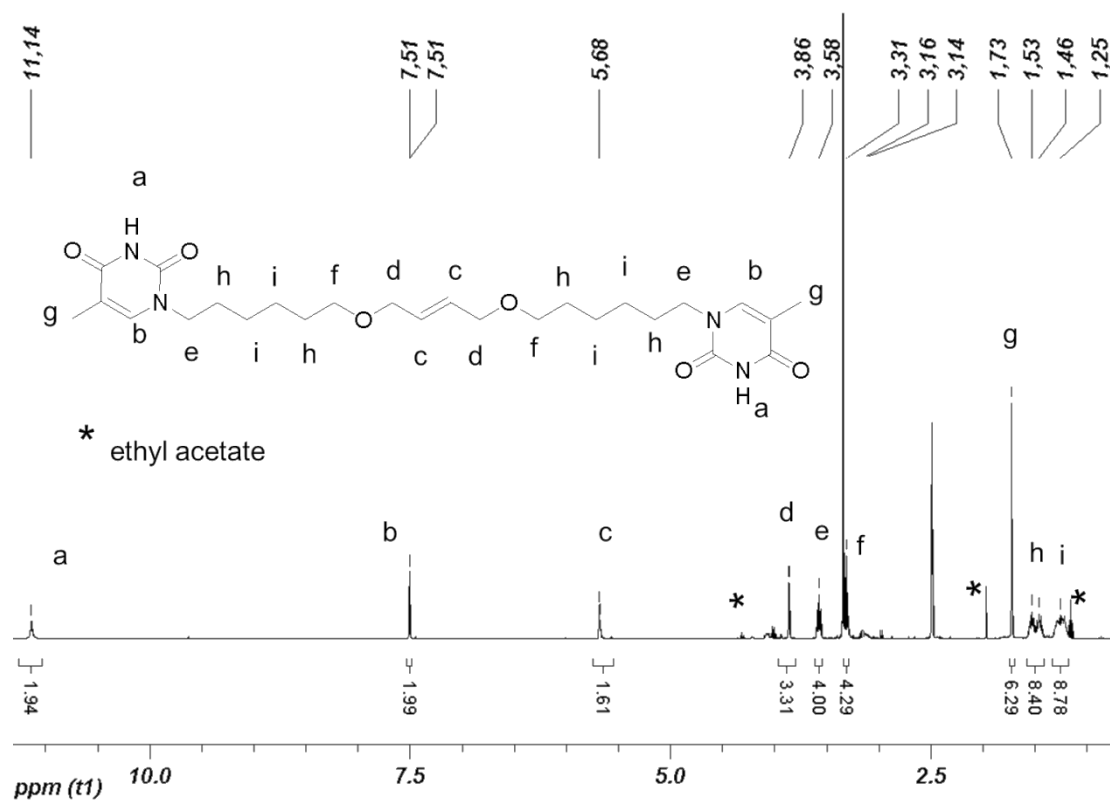


Figure 5.62. ^1H NMR of compound **28** in DMSO-d_6 .

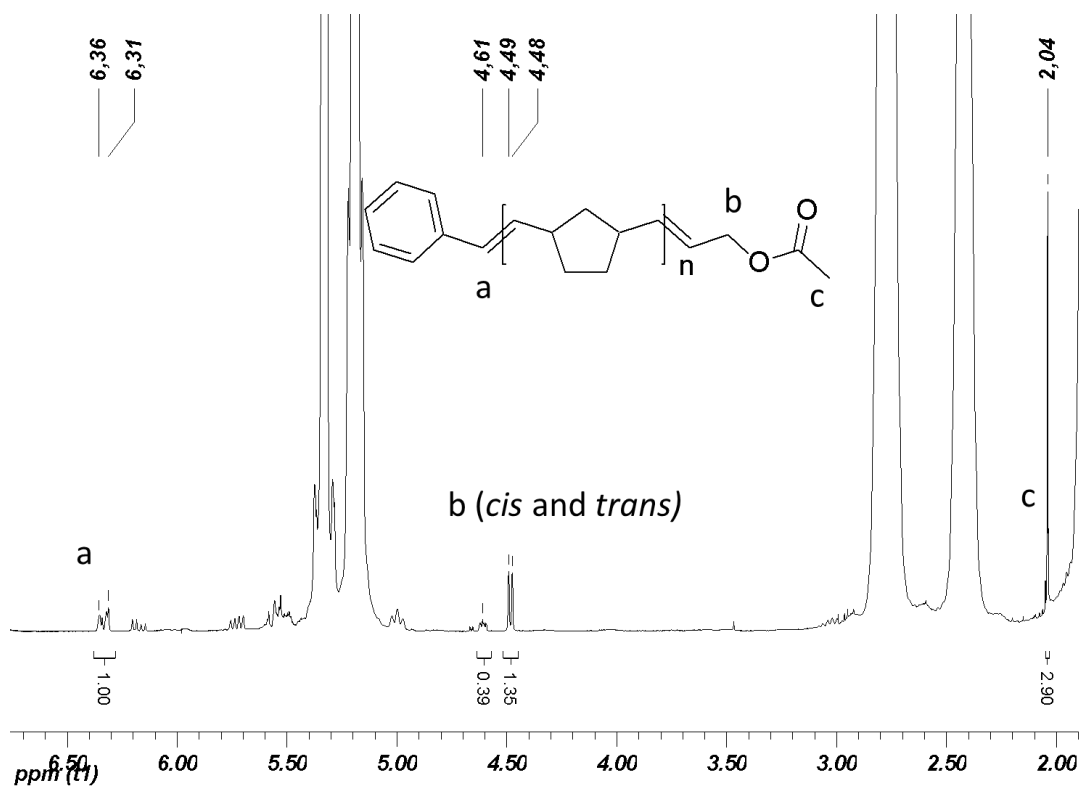


Figure 5.63. ^1H NMR (CDCl_3) of poly(**13**) quenched with compound **24** (10 equiv.), 24 h, end group fraction (89 %).

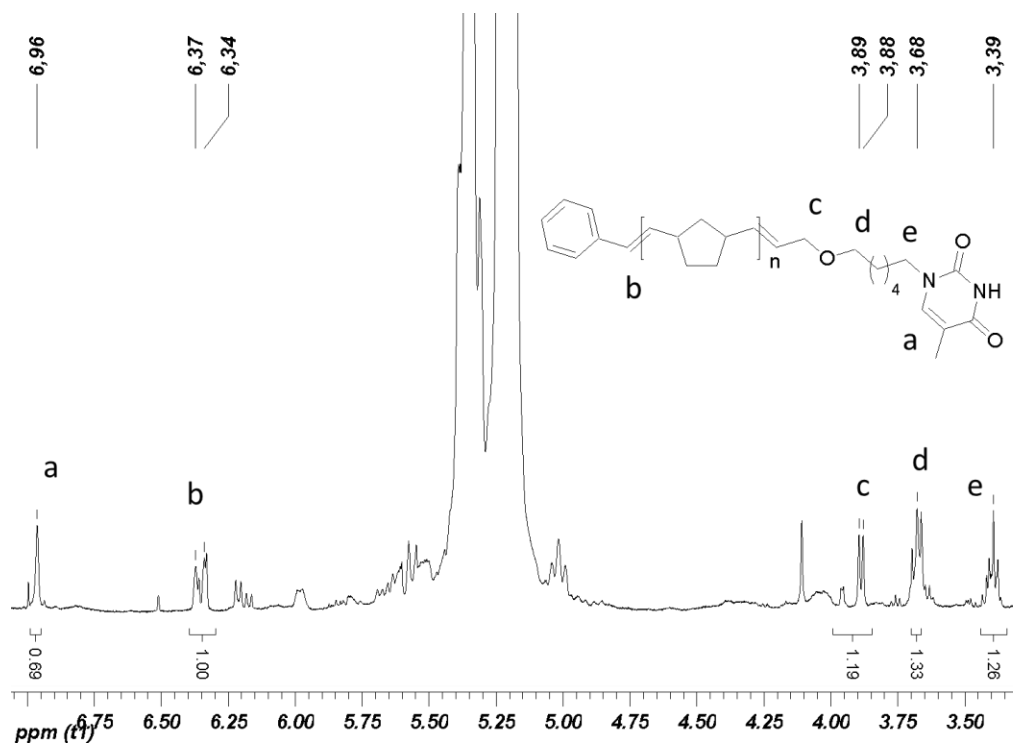


Figure 5.64. ^1H NMR (CDCl_3) of poly(**13**) quenched with compound **28** (20 equiv.), 100h, end group fraction (70 %).

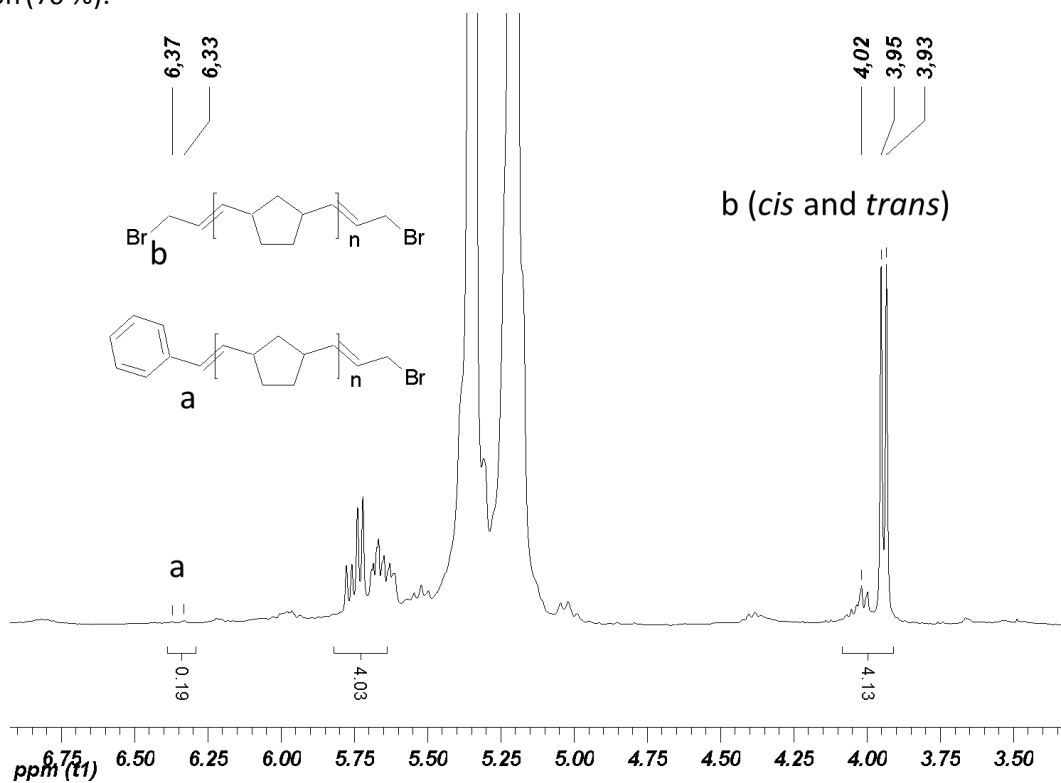


Figure 5.65. ^1H NMR (CDCl_3) of poly(**13**), using **25** as CTA and **G2** as catalyst, M/C = 2000, TA/C = 50, bromomethyl semi telechelic (20%), bromomethyl telechelic (80%).

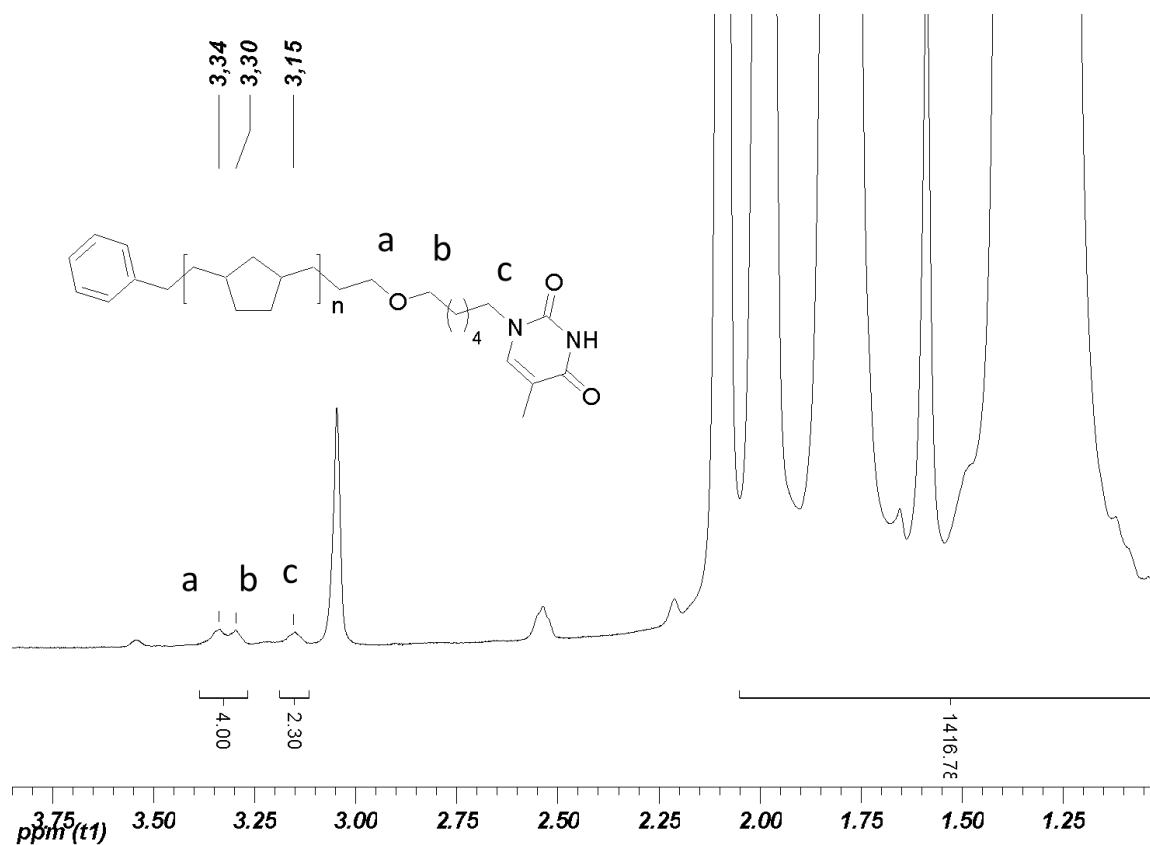


Figure 5.66. ^1H NMR (CDCl_3) of poly(**14**)-**28**, obtained by hydrogenation of poly(**13**)-**28** (thymine end group fraction for poly(**13**)-**28** = 70 %)

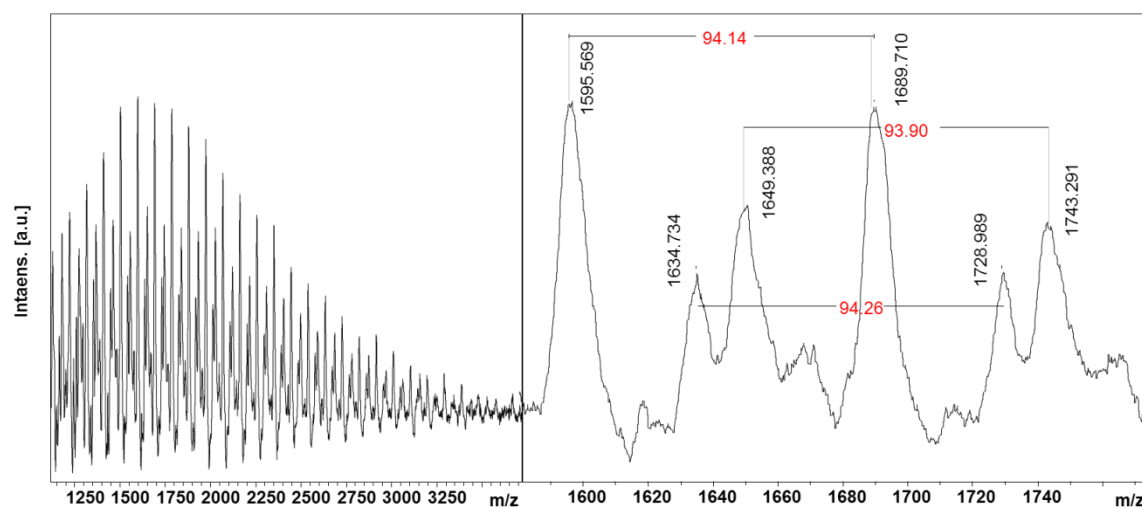


Figure 5.67. MALDI-TOF MS (DCTP, LiTFA) of poly(**13**) quenched with compound **24**. Main series assigned to semitelechelic acetoxy capped poly(**13**) ionized with lithium, e.g. m/z (exp): 1595.569 (C_7H_{10})₁₅C₇H₆C₄H₆O₂)Li⁺, simulated average mass: 1595.471 m/z .

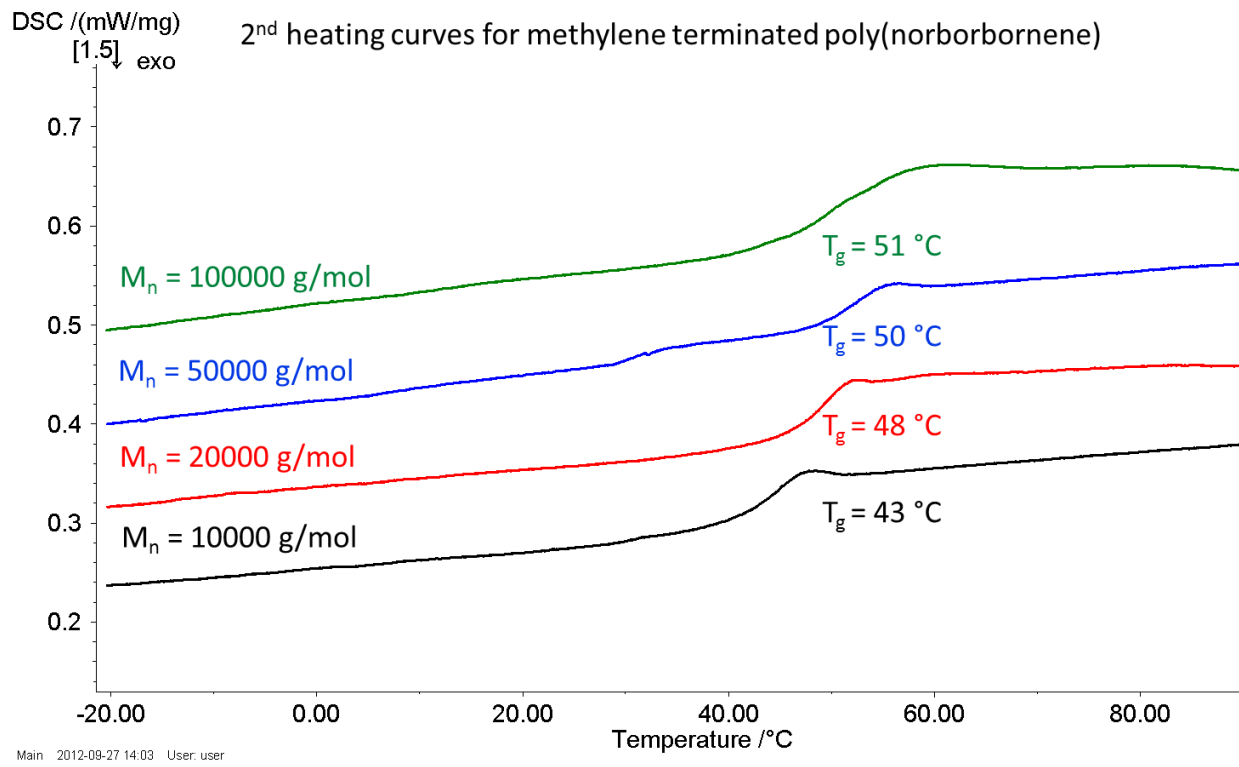


Figure 5.68. DSC, heating curves for methylene terminated poly(norbornene), 10 K/min.

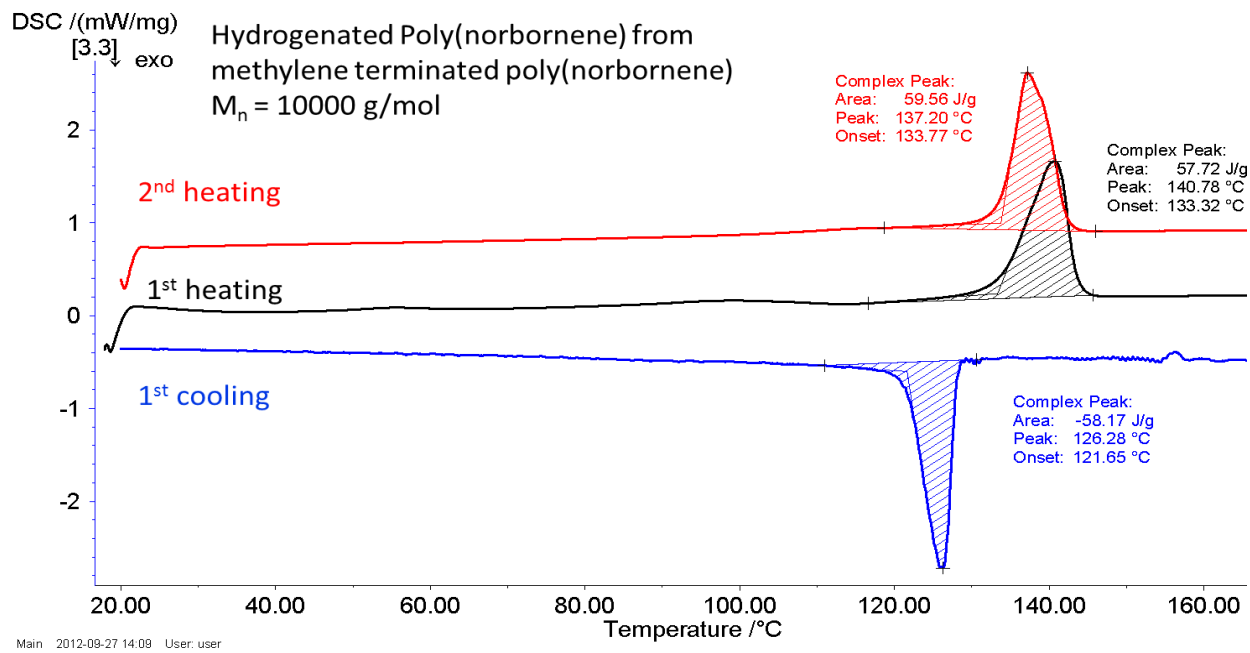


Figure 5.69. DSC, heating and cooling curves (10 K/min) for hydrogenated poly(norbornene), prepared from methylene terminated poly(norbornene), $M_n = 10000$ g/mol.

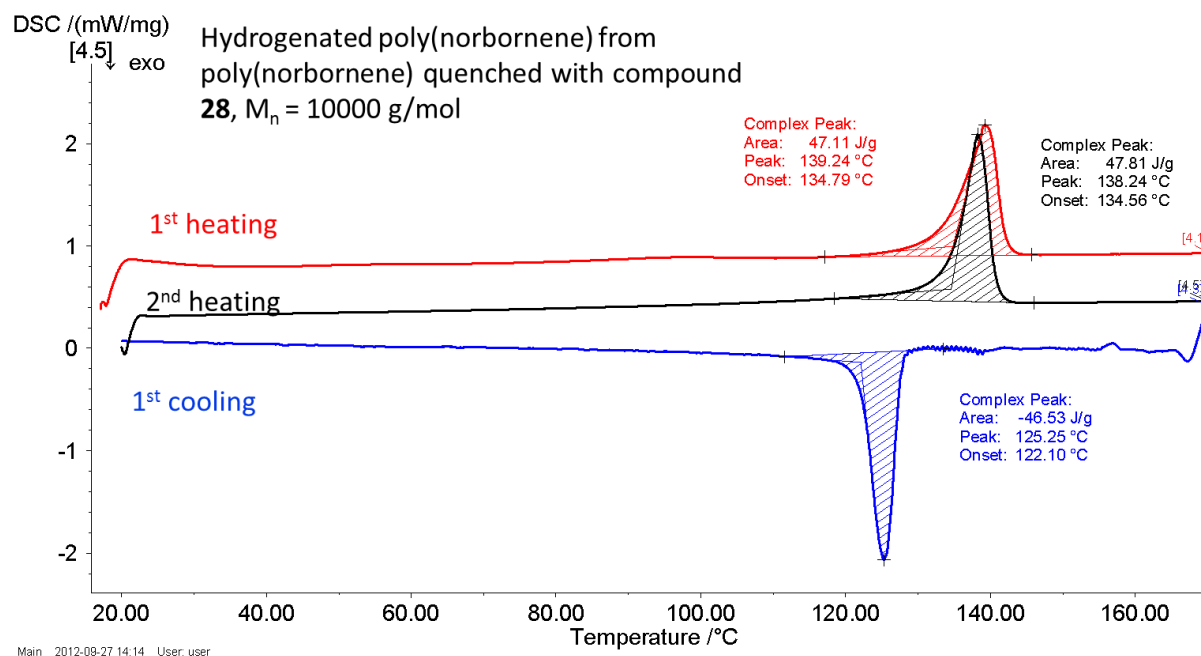


Figure 5.70. DSC, heating and cooling curves (10 K/min) for hydrogenated poly(norbornene), prepared from poly(norbornene) quenched with compound **28**, thymine end group fraction (70 %), $M_n = 10000$ g/mol.

Experimental Procedures

NMR-kinetics

A pyrene stock solution was prepared from 70 mg of pyrene dissolved in 2 mL of CDCl_3 . The NMR-tube was filled with the first monomer (i.e.: monomer **1**, 17 mg) dissolved in CDCl_3 (0.2 mL) and pyrene stock solution (0.2 mL). Before adding the catalyst solution, the ratio of the monomer to the internal standard was determined by NMR. Based on this value the monomer concentration at $t = 0$ was determined. A solution of the catalyst in CDCl_3 , ($[\text{c}] \sim 3.3$ mg in 0.2 mL of CDCl_3) was added via a syringe to yield the desired monomer to catalyst ratio. After shaking, the tube was inserted into the NMR-spectrometer and the decrease of the monomer vs. time was monitored. The second monomer (i.e.: monomer **2**, 33 mg) dissolved in CDCl_3 (0.2 mL) was added after complete conversion of the first monomer. For determination of the monomer concentration at $t = 0$ and the monomer consumption, the corresponding signals were integrated: for monomer **1** the signals at 6.27 and 6.07 ppm (2H), for monomer **2** the signal at 6.50 ppm (2H) and for monomer **3**, the signal at 1.64 ppm (3H) was compared

to the one at 8.20 ppm (4H, d, CH) from the internal standard pyrene. The time between the addition of the catalyst solution and the first measurement was added to the first measuring point.

Measurement of k_p/k_t -ratio

The NMR-tube was filled with catalyst **G1** (7.6 mg, 0.009 mmol) dissolved in CDCl_3 (0.2 mL) and pyrene stock solution (0.2 mL). Before adding the monomer solution, the ratio of the initial carbene to the internal standard was determined by NMR. A solution of monomer **1** (9.7 mg, 0.046 mmol) in CDCl_3 (0.2 mL of CDCl_3) was added via a syringe to yield the desired monomer to catalyst ratio. After shaking, the tube was inserted into the NMR-spectrometer and the decrease of the monomer and initiating carbene vs. time was monitored. The reaction was monitored until the monomer was completely converted. The time between addition of the monomer solution and the first measurement was added to the first measuring point. For monitoring the kinetics, the following signals were integrated against the resonance of the internal standard pyrene 8.20 ppm (4H, d, CH): 6.27 and 6.07 ppm (monomer **1**), 20.01 ppm (catalyst **G1**), 19.12 ppm (catalyst **G3**), 8.70 ppm (catalyst **U1**), 8.50 ppm (catalyst **U3**).

Synthesis of *endo,exo*-bicyclo[2,2,1]-hept-5-ene-2,3-dicarboxylic acid dimethylester (**1**).

A modified literature synthesis¹⁴³ was adopted. Thus methanol (3.1 g, 94.9 mmol) and pyridine (7.5 g, 95.2 mmol) were dissolved in 60 mL of dry CH_2Cl_2 . Under ice cooling *endo,exo*[2.2.1] bicyclo-2-ene-5,6-dicarboxylic acid chloride (5.2 g, 23.8 mmol) was dropped into the reaction mixture and stirred overnight at room temperature. The reaction mixture was filtered to remove the pyridinium salt and extracted with CH_2Cl_2 . The organic layer was extracted with 2N HCl solution, saturated sodium bicarbonate and dried with sodium sulfate. The solvent was removed under reduced pressure. Finally, the product was purified using column chromatography with petrol ether/ethyl acetate (10:1) as the solvent mixture to yield 3.9 g (78%) of monomer **1** as a white solid. ^1H NMR (400 MHz, CDCl_3 , 27 °C): δ (ppm) = 6.26 (1H, dd, $^3J_{\text{HH}} = 3.1$ Hz, $^3J_{\text{HH}} = 5.7$ Hz), 6.06 (1H, dd, $^3J_{\text{HH}} = 2.8$ Hz, $^3J_{\text{HH}} = 5.7$ Hz), 3.70 (3H, s), 3.63 (3H, s), 3.36 (1H, dd, $^3J_{\text{HH}} = 3.8$ Hz, $^3J_{\text{HH}} = 4.5$ Hz), 3.25 (1H, m), 3.11 (1H, m), 2.67 (1H, dd, $^3J_{\text{HH}} = 1.8$ Hz, $^3J_{\text{HH}} = 4.5$ Hz), 1.60 (1H, qd, $^2J_{\text{HH}} = 8.7$ Hz, $^3J_{\text{HH}} = 1.4$ Hz), 1.47 (1H, qd, $^2J_{\text{HH}} = 8.7$ Hz, $^3J_{\text{HH}} = 1.7$ Hz).

Exo-*N*-(4,4,5,5,6,6,7,7,7-nonafluoroheptyl)-10-oxa-4-azatricyclodec-8-ene-3,5-dione (**2**)

A two-step synthetic procedure was adopted from reference.¹⁵⁵ Freshly distilled furan (15 mL, 207.1 mmol) and maleimide (2 g, 20.6 mmol) were placed in a 100 mL large autoclave equipped with heating bath. The mixture was stirred at 90° C under argon atmosphere for 10 h. The reaction vessel was cooled

down to room temperature to regain atmospheric pressure whereupon white crystals precipitated. The white precipitate was collected by vacuum filtration, washed two times with furan and dried *in vacuo* to yield 3.3 g (96 %) of *exo*-10-oxa-4-azatricyclodec-8-ene-3,5-dione. ^1H NMR (400 MHz, DMSO- d_6 , 27 °C): δ (ppm) = 11.09 (1H, s), 6.53 (2H, m), 5.11 (2H, m), 2.85 (2H, m).

A solution of 4,4,5,5,6,6,7,7,7-nonafluoro-heptan-1-ol (1.0 g, 3.60 mmol) and tetrabromomethane (1.88 g, 5.66 mmol) in dry CH_2Cl_2 (20 mL) was cooled to 0 °C, and a solution of triphenylphosphine (1.42 g, 5.39 mmol) in dry CH_2Cl_2 (5 mL) was added slowly. The ice bath was removed, and the mixture was stirred for 12 h at ambient temperature. After complete conversion the solvent was removed under reduced pressure (care was taken not to remove the intermediate 7-bromo-1,1,1,2,2,3,3,4,4-nonafluoroheptane from the reaction mixture under reduced pressure), and the crude product was subsequently reacted without any further purification. Potassium carbonate (1.1 g, 7.91 mmol) and *exo*-10-oxa-4-azatricyclodec-8-ene-3,5-dione (0.653 g, 3.96 mmol) was added to the crude 7-bromo-1,1,1,2,2,3,3,4,4-nonafluoroheptane and resuspended in dry DMF (60 mL). The reaction mixture was stirred for 24 h at ambient temperature, and the solvent was removed subsequently under reduced pressure. The obtained crude compound was dissolved in CH_2Cl_2 and extracted with water, dried and subsequently the CH_2Cl_2 was removed under reduced pressure. Finally, the product was purified by chromatography (SiO_2 , hexane/ethyl acetate =1/1) in order to yield 1.0 g (61%) pure white crystals of monomer **2**. ^1H NMR (400 MHz, CDCl_3 , 27 °C): δ (ppm) = 6.51 (2H, m), 5.26 (2H, m), 3.57 (2H, t, $^3J_{\text{HH}} = 6.9$ Hz), 2.88-2.83 (2H, m), 2.14-1.97 (2H, m), 1.95-1.83 (2H, m).

Monomer 3 (3-methyl-3-phenylcyclopropene) was prepared according to literature procedures.^{24,182}

Monomer 4 (*endo,exo*-bicyclo[2,2,1]-hept-5-ene-2,3-dicarboxylic acid-bis-*O*-2,2,6,6-tetramethyl piperidinoxyl-ester) was prepared according to literature procedures.^{144,183}

Synthesis of poly(**1**), $M/C = 100$

A heated and argon-flushed glass tube equipped with a magnetic stirrer was charged with monomer **1** (83.0 mg, 0.39 mmol) in 1 mL of CH_2Cl_2 . To this solution was added catalyst **G1** (3.3 mg, 0.004 mmol) dissolved in 1 mL of CH_2Cl_2 . The reaction mixture was stirred for 4 hours at room temperature till all of the monomer **1** was consumed, as checked by thin layer chromatography. The reaction was then quenched with cold ethyl vinyl ether and the resulting polymer was precipitated into cold methanol (300 mL). The methanol was decanted and the product was dried under high vacuum overnight to yield 80

mg (96%) of poly(**1**). The polymerization of monomer **1** with catalyst **G3** was carried out in the same manner but with the polymerization time of 1 h due to the faster kinetics.

Block copolymer synthesis

The synthesis of block copolymers $(\mathbf{1})_x\text{-}b\text{-}(\mathbf{2})_y$, $(\mathbf{1})_x\text{-}b\text{-}(\mathbf{3})_y$ and $(\mathbf{1})_x\text{-}b\text{-}(\mathbf{4})_y$ was done analogously to methods developed in our laboratory.^{153,155,157,161} The synthesis given below is indicative of the methods used for the preparation of all block-copolymers: As example the synthesis for $(\mathbf{1})_{25}\text{-}b\text{-}(\mathbf{2})_{25}$ is given: Monomer **1** (33.1 mg, 0.16 mmol) in 0.5 mL of CH_2Cl_2 was added to the catalyst **G1** (5.18 mg, 0.006 mmol) dissolved in 1 mL of CH_2Cl_2 in a heated and argon-flushed glass vial equipped with a magnetic stir bar. The polymerization was carried out at room temperature for 1 h until all of monomer **1** was consumed, as checked by NMR and TLC. Monomer **2** (66.9 mg, 0.16 mmol) as a solution in 0.5 mL of CH_2Cl_2 was then added to the above reaction mixture and stirred for 1 h at room temperature till all of the monomer **2** was consumed, as checked by NMR and TLC. The polymerization was quenched by adding cold ethyl vinyl ether. The produced polymer was isolated by precipitating in to cold methanol or alternatively, the polymer was isolated by column chromatography (SiO_2). Finally the product was dried under high vacuum overnight to yield 97 mg (97%) of poly $(\mathbf{1})_{25}\text{-}b\text{-}(\mathbf{2})_{25}$. The other block copolymers $(\mathbf{1})_x\text{-}b\text{-}(\mathbf{3})_y$ and $(\mathbf{1})_x\text{-}b\text{-}(\mathbf{4})_y$ with catalysts **G1** and **G3** were synthesized using the above stated procedure but adopting different reaction times according to the kinetic data.

1-allylthymine (**29**)

Thymine (2 g, 16 mmol), hexamethyldisilazane (6 mL, 29 mmol) and a spatula tip of ammonium sulfate were refluxed for 24 h. The hexamethyldisilazane was coevaporated with dry toluene (2×20 mL). To the residue was added dry DMF (8 mL) and allyl bromide (8 mL, 92 mmol). The mixture was heated at 80 °C for 3 days. After evaporation of the solvent, the solid residue was recrystallized with dry toluene. Pale yellow crystals were obtained after cooling to room temperature, which were collected and dried *in vacuo*. Yield: 622 mg (24%). ^1H NMR (400 MHz, CDCl_3 , 27 °C): δ (ppm) = 8.52 (1H, s), 6.96 (1H, d, $^3J_{\text{HH}} = 1.2$ Hz), 5.87 (1H, tdd, $^3J_{\text{HH}} = 5.8$ Hz, $^3J_{\text{HH}} = 10.3$ Hz, $^3J_{\text{HH}} = 16.1$ Hz), 5.29 (2H, ddd, $^3J_{\text{HH}} = 1.0$ Hz, $^3J_{\text{HH}} = 13.7$ Hz, $^3J_{\text{HH}} = 18.0$ Hz), 4.33 (1H, td, $^3J_{\text{HH}} = 1.3$ Hz, $J = 5.8$ Hz), 1.93 (3H, d, CH_3 , $^3J_{\text{HH}} = 1.1$ Hz).

The homo metathesis of this compound failed. No product formation could be observed in the ^1H NMR. A longer spacer between terminal olefin and thymine group is necessary to avoid strong steric interactions or complexation respectively. Thus, an extension of the spacer length (from $(\text{CH}_2)_1$ to $(\text{CH}_2)_9$ → N-undecenylthymine) was performed.

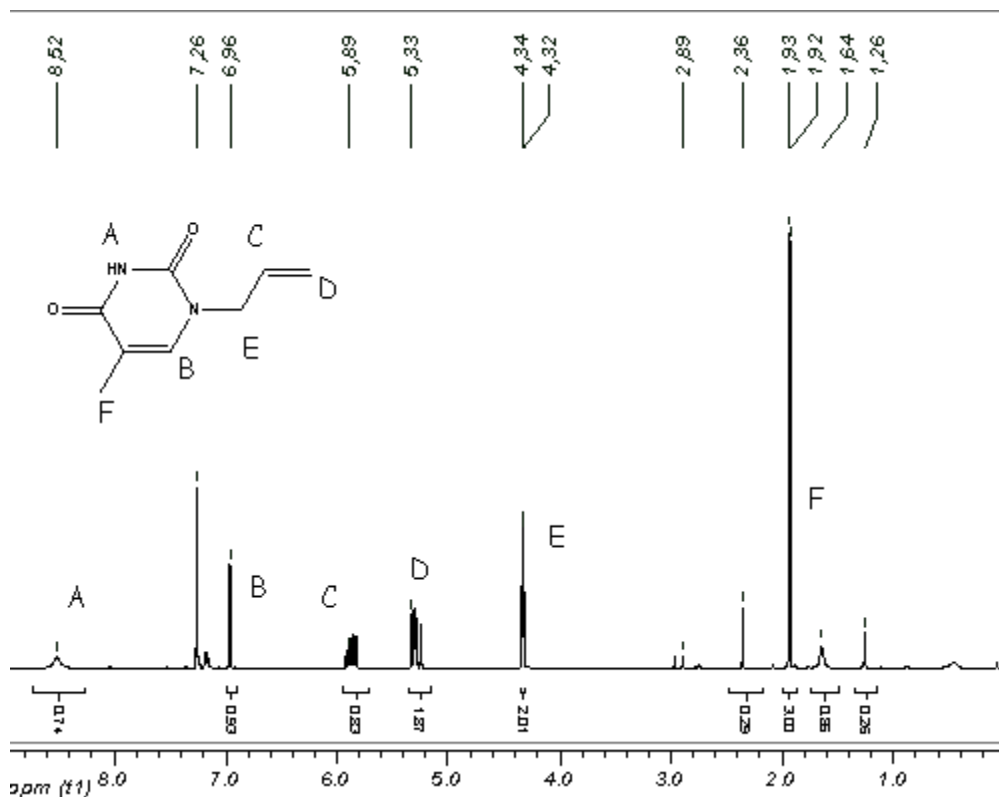


Figure 5.71. ^1H NMR of N-allylthymine (**29**)

Crotonyl chloride (**30**)

Crotonic acid (2 g, 19 mmol) and thionyl chloride (3 mL, 0.41 mmol) in dry light petroleum (6 mL) were refluxed for 4 h. Evolved HCl- and SO_2 -gas was absorbed in a washing bottle with sodium hydroxide-solution. The reaction solution was concentrated and distilled *in vacuo* (b.p. 106 °C, 600 mbar). Yield: 1.53 g (57%).

Crotonic acid diethylamide (**31**)

A solution of diethylamine (1.76 g, 28 mmol) in dry diethyl ether was cooled to 0 °C. Crotonyl chloride (1.53 g, 14 mmol) was added slowly and the solution was allowed to warm up to room temperature. The solution was filtered, concentrated and distilled *in vacuo* (B.p. 100 °C, 13 Torr). Yield: 1.1 g (53%). ^1H NMR (400 MHz, CDCl_3 , 27 °C): δ (ppm) = 6.91 (1H, qd, $^3J_{\text{HH}} = 6.8$ Hz, $^3J_{\text{HH}} = 13.7$ Hz), 6.20 (1H, d, $^3J_{\text{HH}} = 14.9$ Hz), 3.39 (4H, q, $^3J_{\text{HH}} = 6.9$ Hz), 1.87 (3H, d, $^3J_{\text{HH}} = 6.9$ Hz), 1.16 (6H, t, $^3J_{\text{HH}} = 6.7$ Hz). Application of the compound crotonic acid diethylamide as quencher has shown no selectivity. A mixture of end groups is obtained (CHCH_3 , $\text{CHC}(\text{O})\text{N}(\text{Et})_2$, CH_2 (from ethyl vinyl ether)).

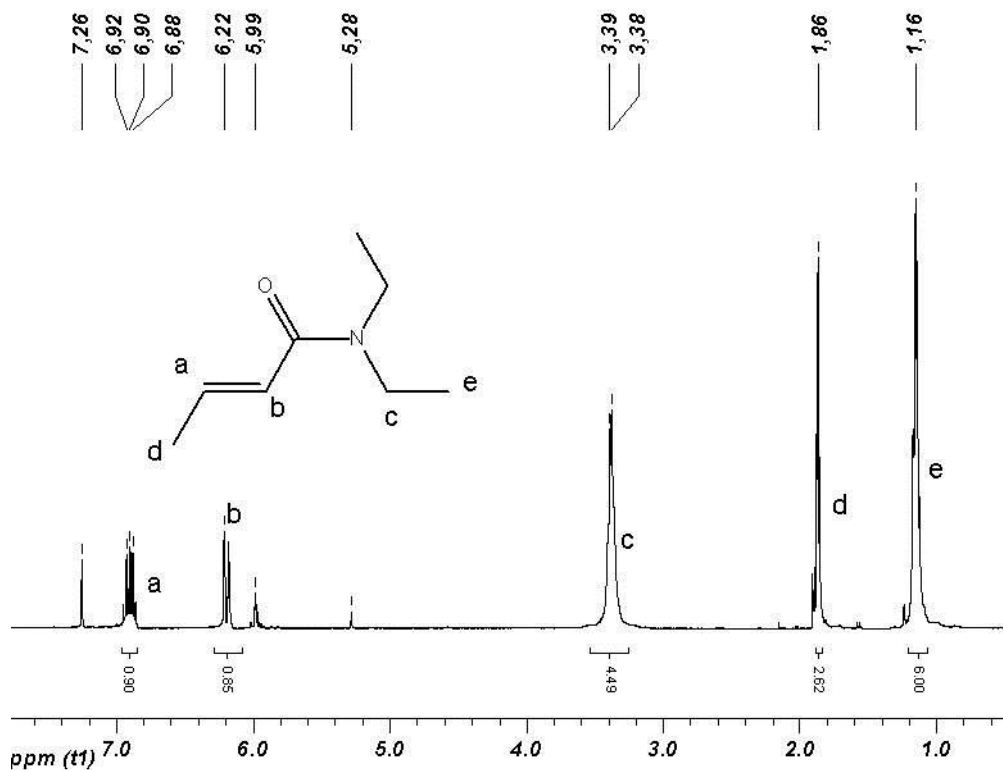


Figure 5.72. ^1H NMR of crotonic acid diethylamide (31)

4-Trimethylsiloxy benzaldehyde (32)

Synthesis was done according to Plieninger et al.¹⁸⁴ A flask, charged with 4-hydroxybenzaldehyde (6.1 g, 0.05 mol), triethylamine (5 g, 0.05 mol) and dry diethyl ether (50 mL) was cooled to 10 °C. Trimethylsilyl chloride (5.4 g, 0.05 mol) was added dropwise via syringe. After the addition, the cooling bath was removed and the stirring was continued for 1 h. The solvent was then removed and the crude product was purified by distillation with a Vigreux column, b.p. 4 mbar, 100 °C. Yield: 5.1 g (60%). ^1H NMR (400 MHz, CDCl_3 , 27 °C): δ (ppm) = 9.89 (1H, s), 7.79 (2H, d, $^3J_{\text{HH}} = 8.6$ Hz), 6.94 (2H, d, $^3J_{\text{HH}} = 8.6$ Hz), 0.31 (9H, s).

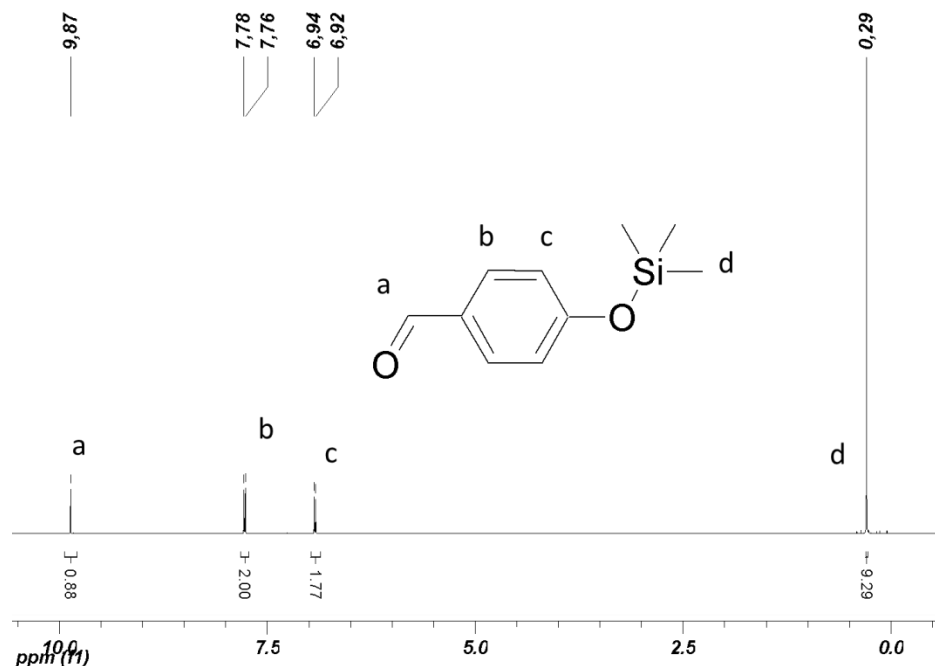


Figure 5.73. ^1H NMR of 4-trimethylsiloxybenzaldehyde in CDCl_3 .

4-bromomethyl benzaldehyde (33)

The reaction was performed under an atmosphere of nitrogen. A flask was charged with 4-bromomethylbenzonitril (6 g, mol) in anhydrous toluene (60 ml). After cooling to 0°C , a solution of diisobutylaluminium hydride in hexane (40 ml, 1 M) was added dropwise via syringe. Stirring was continued for another hour. Chloroform (80 ml) and aqueous HCl (200 ml, 10%) were added and the resulting solution was stirred for another hour. Subsequently, the organic layer was separated, washed with water and dried over sodium sulfate. The solvent was removed and the residue was filtered and washed with cold hexane to obtain 4-bromomethyl benzaldehyde. Yield: 4.2 g (70%). ^1H NMR (400 MHz, CDCl_3 , 27°C): δ (ppm) = 10.02 (1H, s), 7.87 (2H, d, $^3J_{\text{HH}} = 8.1$ Hz), 7.56 (2H, d, $^3J_{\text{HH}} = 8.1$ Hz), 4.51 (2H, s).

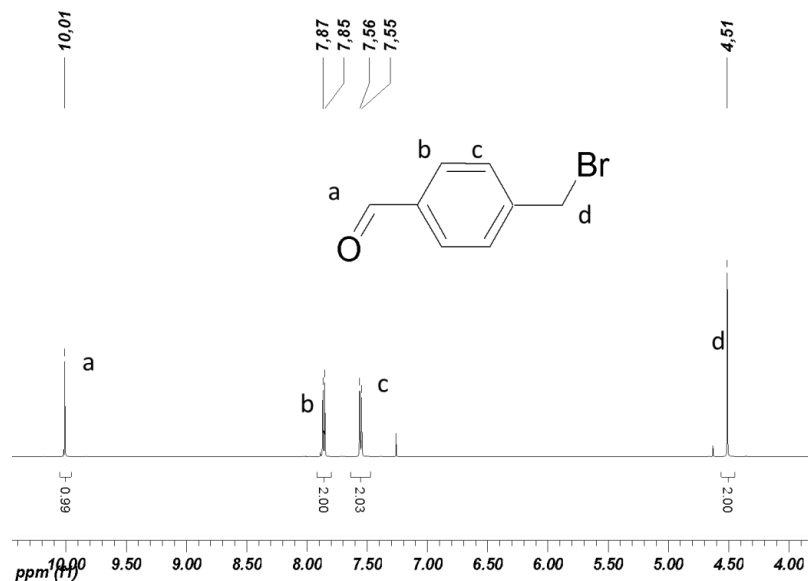
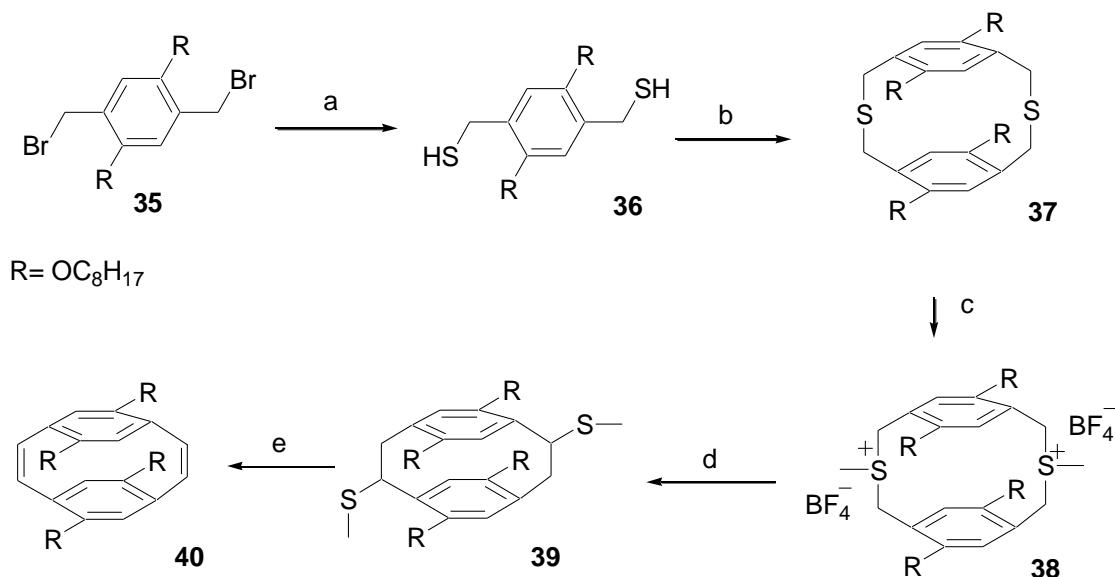


Figure 5.74. ^1H NMR of 4-bromomethylsiloxylbenzaldehyde in CDCl_3 .

Attempted synthesis of tetraoctoxycyclophanediene (**40**) according to Turner et al.¹²⁷ Procedure only pursued until compound **37**.



Scheme 5.2. Synthesis of tetraoctoxycyclophanediene (**40**), a) thiourea/ KOH_{aq} or thioacetic acid/ K_2CO_3 , b) compound **34**, K_2CO_3 , c) $(\text{CH}_3\text{O})_2\text{CH}^+\text{BF}_4^-$, d) IRA-400 OH^- , e) $(\text{CH}_3\text{O})_2\text{CH}^+\text{BF}_4^-$, NaH .

1,4-dioctoxybenzene (**34**)

Fine powdered potassium hydroxide (22.5 g, 0.4 mol) was dissolved in DMSO (50 ml). To this solution were added octyl bromide (40 g, 0.2 mol) and hydroquinone (11.1 g, 0.1 mol). Stirring was continued for

1 h after which the solution was poured in 300 mL of water. After stirring for 1 h, the brownish precipitate was filtered off, dissolved in hexane and reprecipitated in methanol (500 mL). The solid was collected on a frit and washed with methanol to obtain a white solid. Yield: 25 g (80%). ^1H NMR (400 MHz, CDCl_3 , 27 °C): δ (ppm) = 6.82 (4H, s), 3.90 (4H, t, $^3J_{\text{HH}} = 6.6$ Hz), 1.75 (4H, m), 1.45 (4H, m), 1.32 (16H, m), 0.89 (6H, t, $^3J_{\text{HH}} = 6.9$ Hz).

1,4-dioctoxy-2,5-dibromomethylbenzene (35)

The reaction was conducted with a mechanical stirrer. Paraformaldehyde (25.6 g), potassium bromide (38.4 g, 0.32 mol) and 1,4-dioctoxybenzene (20 g, 60 mmol) were dissolved in acetic acid (420 mL). A mixture of acetic acid (43 mL) and concentrated sulfuric acid (32 mL) was added to the solution during 30 minutes. After stirring the resulting solution overnight, the precipitate was filtered off and washed with water to remove acetic acid. The solid was dried and subsequently purified by Soxhlet extraction with hexane. After cooling to room temperature, the product was obtained as a pale yellow solid. Yield: 27 g (86.7%). ^1H NMR (400 MHz, CDCl_3 , 27 °C): δ (ppm) = 6.85 (2H, s), 4.53 (4H, s), 3.98 (4H, t, $^3J_{\text{HH}} = 6.4$ Hz), 1.81 (4H, m), 1.50 (4H, m), 1.33 (16H, m), 0.89 (6H, t, $^3J_{\text{HH}} = 6.8$ Hz).

1,4-dioctoxy-2,5-dimercaptomethylbenzene (36)

The reaction was conducted under an atmosphere of nitrogen according to Han et al.¹⁸⁵ A solution of 1,4-dioctoxy-2,5-dibromomethylbenzene (1 g, 1.92 mmol), potassium carbonate (1.3 g, 9.4 mmol) and thioacetic acid (0.33 mL, 4.7 mmol) in THF (6 mL) was stirred for 2 h. After adding methanol (6 mL), stirring was continued for 30 minutes, followed by acidification of the resulting solution with aqueous HCl (1 mL, 2 M). After removal of the solvent, the residue was taken up in chloroform (15 mL) and washed with water (10 mL). The organic phase was dried with sodium sulfate, filtered and concentrated to furnish the dithiol. Yield: 689 mg (83%). ^1H NMR (400 MHz, CDCl_3 , 27 °C): δ (ppm) = 6.78 (2H, s), 3.96 (4H, t, $^3J_{\text{HH}} = 6.4$ Hz), 3.69 (4H, t, $^3J_{\text{HH}} = 8.0$ Hz), 1.95 (2H, t, $^3J_{\text{HH}} = 8.0$ Hz), 1.80 (4H, m), 1.48 (4H, m), 1.32 (16H, m), 0.89 (6H, t, $^3J_{\text{HH}} = 6.7$ Hz). ^{13}C NMR (100 MHz, CDCl_3 , 27 °C): δ (ppm) = 150.1, 129.3, 113.3, 68.8, 31.8, 29.5, 29.4, 29.4, 29.3, 26.2, 24.0, 22.7, 14.7.

5,8,14,17-tetraoctyloxy-2,11-dithia-[3.3] paracyclophane (pseudo-geminal) and 6,9,14,17-tetraoctyloxy-2,11-dithia-[3.3]paracyclophane (pseudo-ortho) (37)

A solution of 1,4-dioctoxy-2,5-dibromomethylbenzene (300 mg, 0.57 mmol) in THF (23 mL) was added drop wise over a period of 6 hours to a solution of 1,4-dioctoxy-2,5-dimercaptomethylbenzene (246 mg,

0.57 mmol) and potassium carbonate (315 mg, 2.28 mmol) in a THF/DMF mixture (v/v 1:1, 23 mL). Stirring was continued after addition for another hour. After removal of the solvents, the crude mixture was purified via column chromatography (hexane/chloroform 10/1, changing then to 4/1). The compound was obtained as a mixture of two isomers. Yield: 80 mg (19%). Pseudo-geminal isomer: ^1H NMR (400 MHz, CDCl_3 , 27 °C): δ (ppm) = 6.51 (4H, s), 4.47 (4H, d, $^2J_{\text{HH}} = 15.4$ Hz), 3.94-3.47 (8H, m), 3.25 (4H, d, $^2J_{\text{HH}} = 15.4$ Hz), 1.77 (8H, m), 1.49 (8H, m), 1.31 (32H, m), 0.90 (12H, t). Pseudo-ortho isomer: ^1H NMR (400 MHz, CDCl_3 , 27 °C): δ (ppm) = 6.59 (4H, s), 4.00 (4H, d, $^2J_{\text{HH}} = 14.6$ Hz), 3.94-3.47 (8H, m), 3.44 (4H, d, $^2J_{\text{HH}} = 14.6$ Hz), 1.77 (8H, m), 1.49 (8H, m), 1.31 (32H, m), 0.90 (12H, t). Ratio: pseudo-geminal/pseudo-ortho: 40/60.

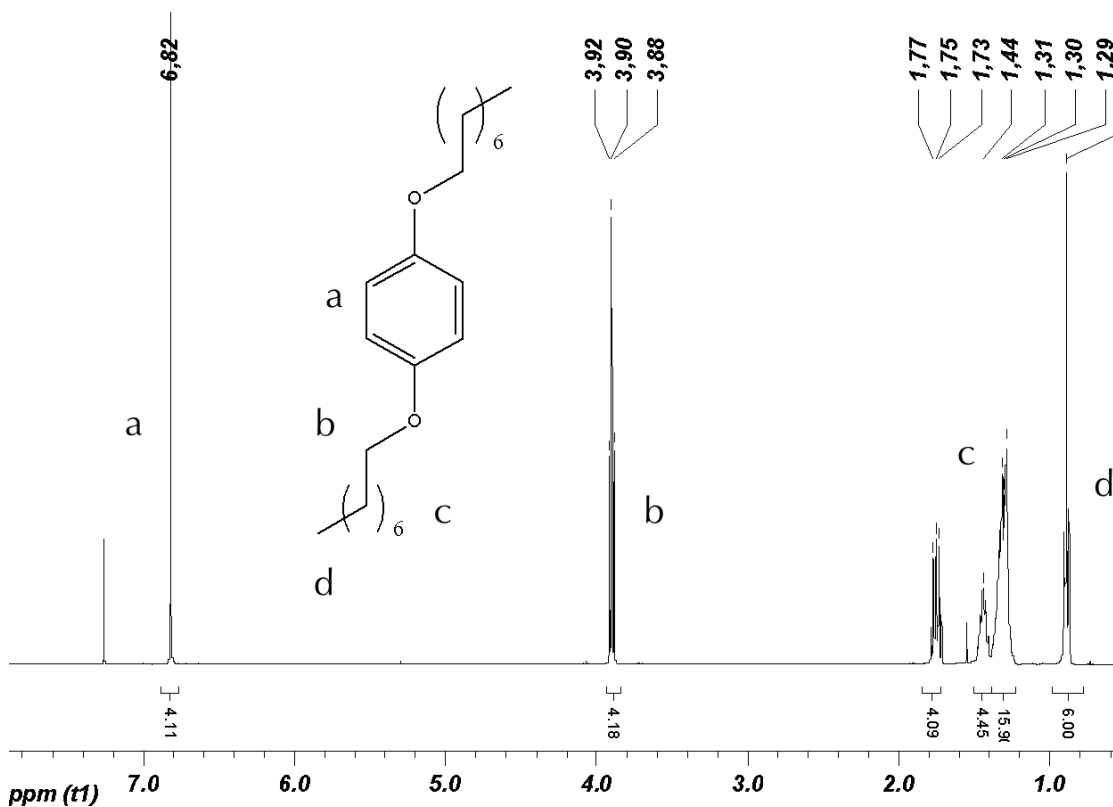


Figure 5.75. ^1H NMR of 1,4-dioctoxybenzene (**34**) in CDCl_3 .

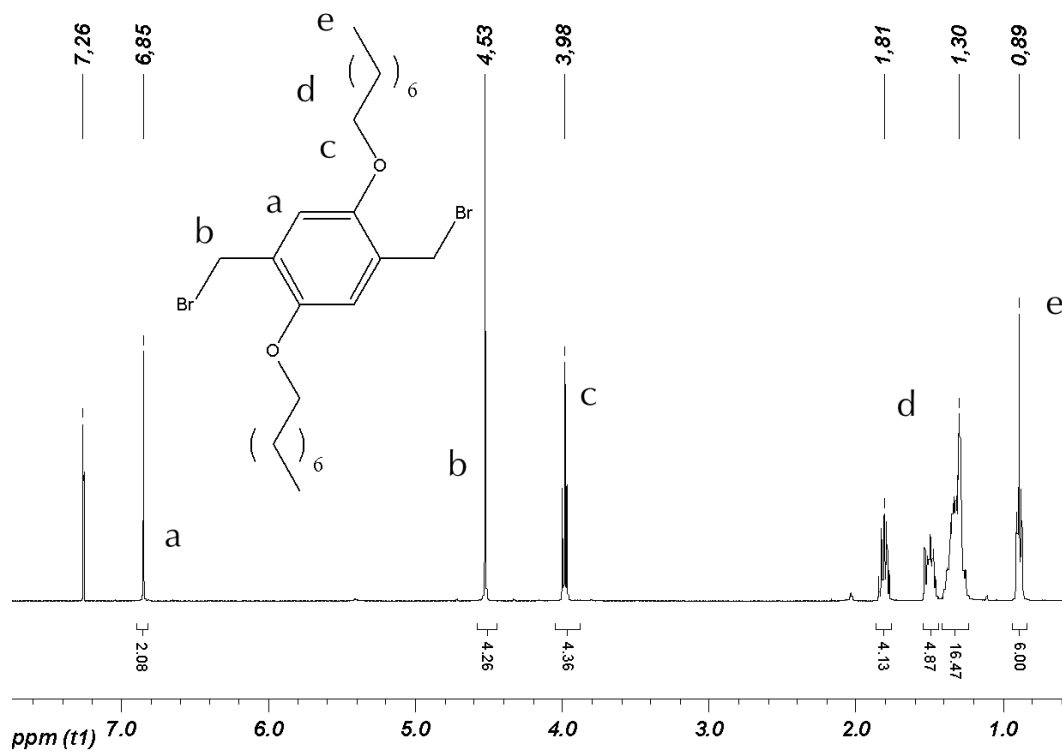


Figure 5.76. $^1\text{H-NMR}$ of 1,4-dioctoxy-2,5-dibromomethylbenzene (**35**) in CDCl_3 .

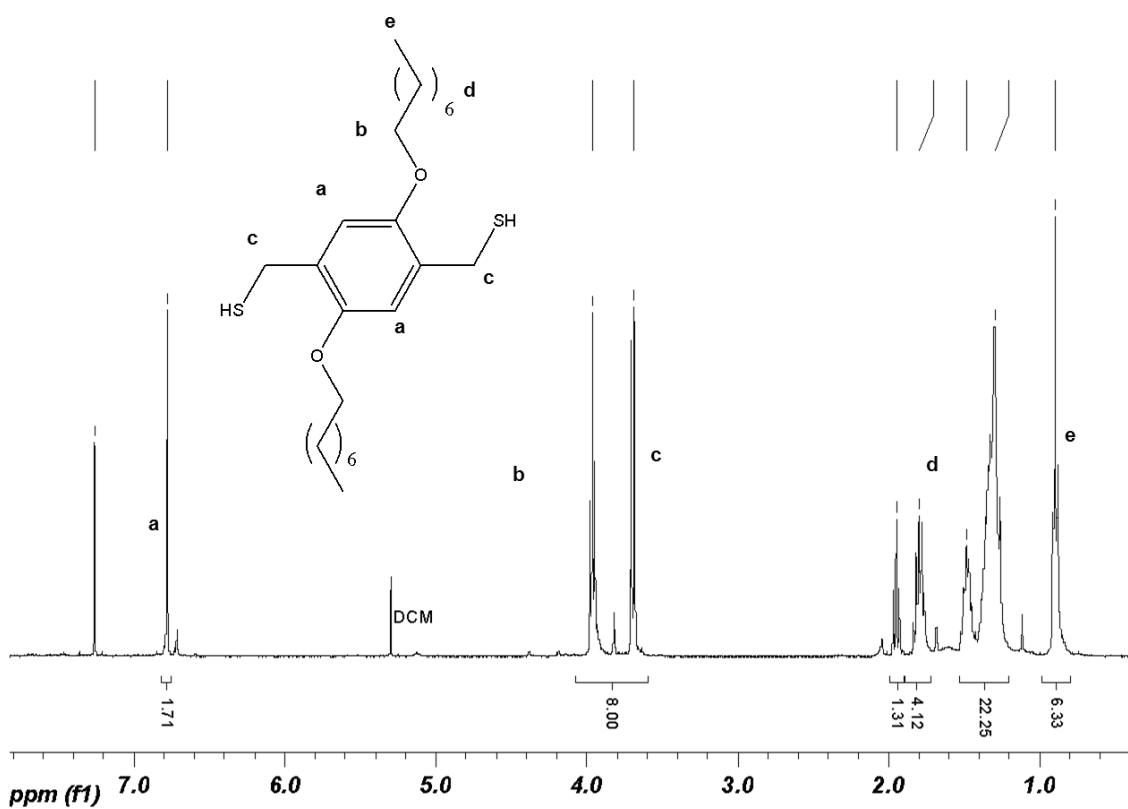
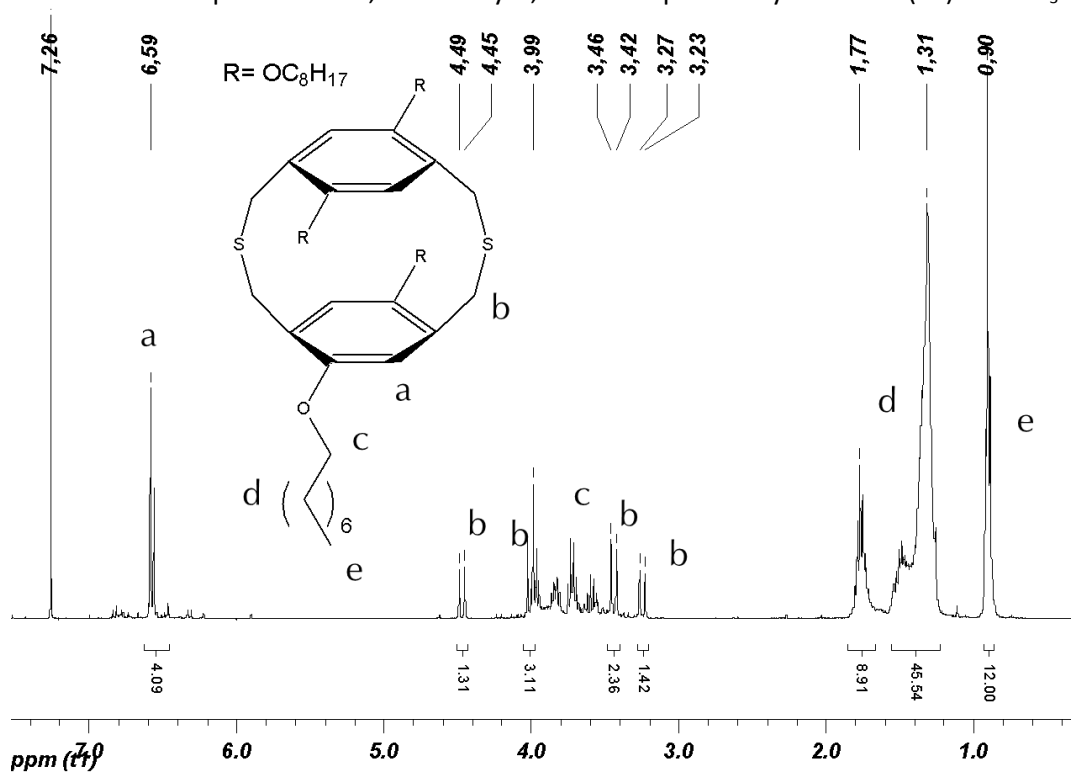
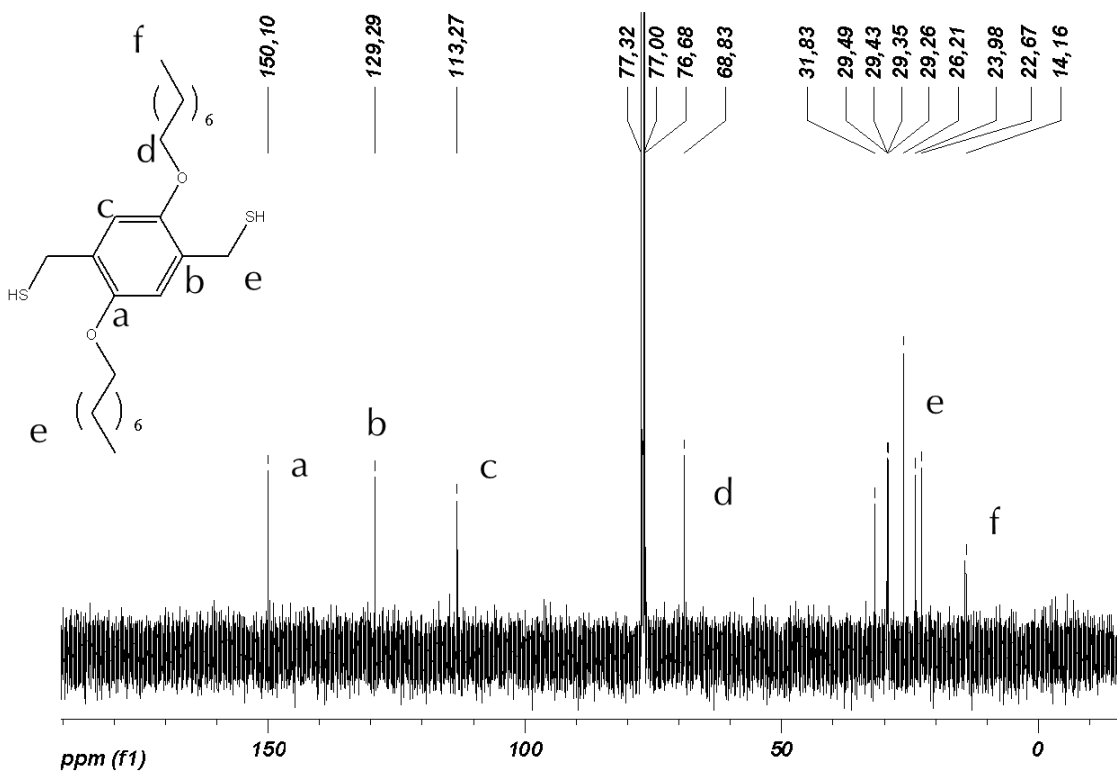


Figure 5.77. $^1\text{H NMR}$ -spectrum of 1,4-dioctoxy-2,5-dimercaptomethylbenzene (**36**) in CDCl_3 .



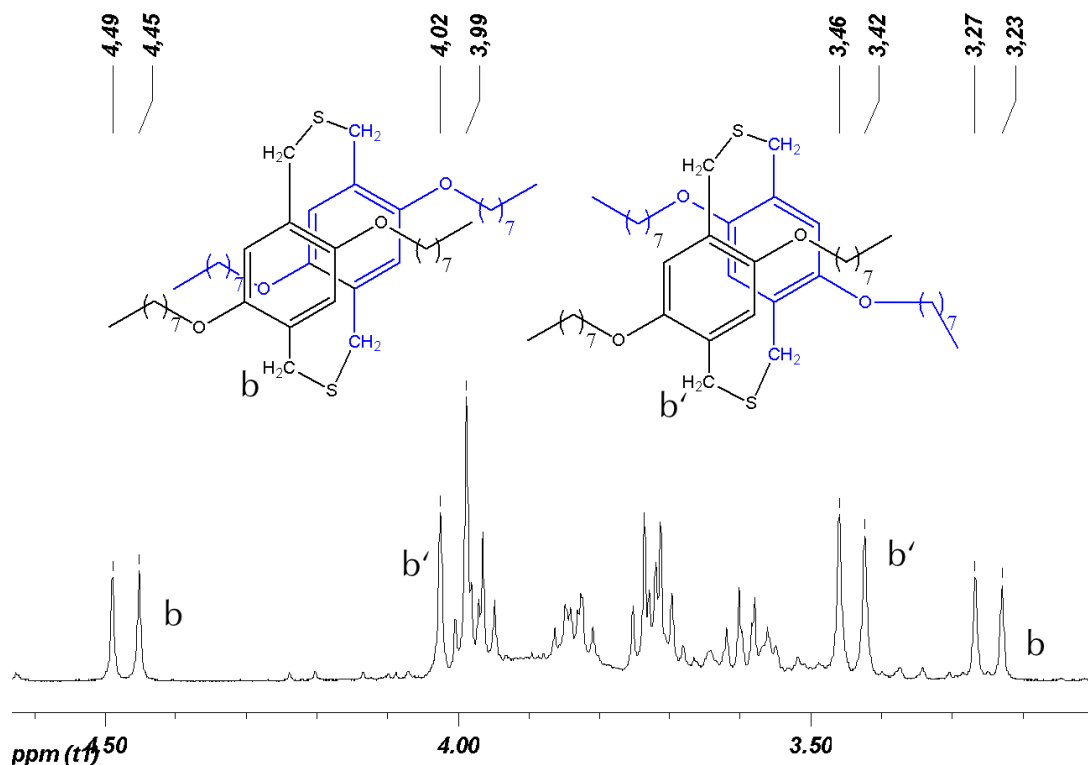


Figure 5.80. ^1H NMR of 5,8,14,17-tetraoctyloxy-2,11-dithia-[3.3] paracyclophane and 6,9,14,17-tetraoctyloxy-2,11-dithia-[3.3]paracyclophane (**37**) in CDCl_3 , magnification 3.1-4.6 ppm, ratio $b/b'=40/60$.

Attempted Synthesis of a bimetallic catalyst **46** according to Weck et al.¹⁰⁰

Ethyl-6-bromo-hexanoate (**41**)

6-Bromo-hexanoic acid (5 g, 25.6 mmol) and dry ethanol (12 mL, 0.2 mol) were refluxed for 8 h with concentrated sulfuric acid (0.2 mL). The solution was concentrated and the residue was taken up in diethyl ether and washed with water and sodium carbonate solution (5 w-%). After drying over sodium sulfate the solution was concentrated and distilled *in vacuo*, (B.p. 5 mbar, 86 °C). Yield: 4.64 g (81%).

Ethyl-6-(4-formylphenoxy)hexanoate (**42**)

4-Hydroxybenzaldehyde (517 mg, 4.2 mmol), ethyl-6-bromohexanoate (958 mg, 4.3 mmol) and dry potassium carbonate (570 mg, 4.2 mmol) in DMF (1.7 mL) were stirred at 50 °C for 3 days. The solution was filtered, concentrated and taken up in ethyl acetate. The solution was washed with brine (3 times), dried over sodium sulfate and concentrated *in vacuo*. Yield: 900 mg (80%). ^1H NMR (400 MHz, CDCl_3 , 27 °C): δ (ppm) = 9.87 (1H, s), 7.81 (2H, d, $^3J_{\text{HH}} = 8.7$ Hz), 6.97 (2H, d, $^3J_{\text{HH}} = 8.7$ Hz), 4.13 (2H, q, $^3J_{\text{HH}} = 7.1$ Hz),

4.04 (2H, t, $^3J_{\text{HH}} = 6.4$ Hz), 2.34 (2H, t, $^3J_{\text{HH}} = 7.4$ Hz), 1.84 (2H, m), 1.69 (2H, m), 1.52 (2H, m), 1.25 (3H, t, $^3J_{\text{HH}} = 7.1$ Hz)

Ethyl-6-(4-vinylphenoxy)hexanoate (43)

To a solution of methyltriphenylphosphonium bromide (1.36g, 3.8 mmol) in dry THF (32 ml) was added *n*-butyllithium (1.5 ml, 2.5 M in hexane, 1 equiv.). The yellow solution was stirred for 15 minutes before the addition of ethyl-6-(4-formylphenoxy)hexanoate (1 g, 3.8 mmol) upon which the solution turned pale yellow. The reaction was monitored via TLC. After completion of the reaction, saturated ammonium chloride solution was added and the mixture was extracted with dichloromethane and dried over sodium sulfate. The solution was concentrated and the product was purified by column chromatography. Yield: 550 mg (60%). ^1H NMR (400 MHz, CDCl_3 , 27 °C): δ (ppm) = 7.33 (2H, d, $^3J_{\text{HH}} = 8.6$ Hz), 6.84 (2H, d, $^3J_{\text{HH}} = 8.6$ Hz), 6.65 (1H, dd, $^3J_{\text{HH}} = 10.9$ Hz, $^3J_{\text{HH}} = 17.6$ Hz), 5.60 ppm (1H, d, $^3J_{\text{HH}} = 17.6$ Hz), 5.11 (1H, d, $^3J_{\text{HH}} = 10.9$ Hz), 4.13 (2H, q, $^3J_{\text{HH}} = 7.1$ Hz), 3.96 (2H, t, $^3J_{\text{HH}} = 6.4$ Hz), 2.33 (2H, t, $^3J_{\text{HH}} = 7.5$ Hz), 1.80 (2H, m), 1.71 (2H, m), 1.51 (2H, m), 1.26 (3H, t, $^3J_{\text{HH}} = 7.1$ Hz).

6-(4-vinylphenoxy)hexanoic acid (44)

Potassium hydroxide (88 mg, 1.57 mmol), ethyl-6-(4-vinylphenoxy)hexanoate (100 mg, 0.38 mmol) were dissolved in methanol (2 mL). After addition of a spatula tip of copper powder, the reaction mixture was stirred at room temperature. The reaction was monitored via TLC. After evaporation of methanol, the residue was diluted with water. The solution was acidified with cold sulfuric acid and the resulting white precipitate was filtered off. Subsequently, the white solid was dissolved in ethyl acetate and the resulting solution was dried over sodium sulfate. After filtration, the solvent was removed and 6-(4-vinylphenoxy)hexanoic acid was obtained as white solid. Yield: 62 mg (70%). ^1H NMR (400 MHz, CDCl_3 , 27 °C): δ (ppm) 7.33 (2H, d, $^3J_{\text{HH}} = 8.6$ Hz), 6.84 (2H, d, $^3J_{\text{HH}} = 8.6$ Hz), 6.66 (1H, dd, $^3J_{\text{HH}} = 10.9$ Hz, $^3J_{\text{HH}} = 17.6$ Hz), 5.60 ppm (1H, d, $^3J_{\text{HH}} = 17.6$ Hz), 5.12 (1H, d, $^3J_{\text{HH}} = 10.9$ Hz), 3.97 (2H, t, $^3J_{\text{HH}} = 6.4$ Hz), 2.40 (2H, t, $^3J_{\text{HH}} = 7.4$ Hz), 1.81 (2H, m), 1.73 (2H, m), 1.54 (2H, m). Broad resonance for carboxylic proton at 10.32 ppm.

6-(4-Vinyl-phenoxy)-hexanoic acid 4-[6-(4-vinyl-phenoxy)-hexanoyloxy]-phenyl ester (45)

Hydroquinone (14 mg, 0.12 mmol), 4-dimethylaminopyridine (4 mg, 0.03 mmol), 6-(4-vinylphenoxy)hexanoic acid (75 mg, 0.32 mmol) and EDC (60 mg, 0.41 mmol) were weighed in a heated out flask. After purging the flask with nitrogen, the mixture was dissolved in dry DMF (1 mL) and the

reaction progress was monitored via TLC. The solvent was removed and the crude product was purified via Silica gel chromatography (hexane/ethyl acetate 6/1). Yield: 112 mg (65%). $^1\text{H NMR}$ (400 MHz, CDCl_3 , 27 °C): δ (ppm) = 7.33 (2H, d, $^3J_{\text{HH}} = 8.6$ Hz), 7.08 (4H, s), 6.85 (2H, d, $^3J_{\text{HH}} = 8.7$ Hz), 6.66 (2H, d, 1H, $^3J_{\text{HH}} = 10.9$ Hz, $^3J_{\text{HH}} = 17.6$ Hz), 5.60 (2H, d, $^3J_{\text{HH}} = 17.6$ Hz), 5.12 (2H, d, $^3J_{\text{HH}} = 10.9$ Hz), 3.99 (2H, t, $^3J_{\text{HH}} = 6.3$ Hz), 2.60 (2H, t, $^3J_{\text{HH}} = 7.4$ Hz), 1.84 (8H, m), 1.60 (4H, m).

Bimetallic catalyst according to Weck et al.¹⁰⁰ (46)

A heated out and with argon flushed vial was charged with Grubbs catalyst 1st-generation (100 mg, 0.12 mmol) and 6-(4-Vinyl-phenoxy)-hexanoic acid 4-[6-(4-vinyl-phenoxy)-hexanoyloxy]-phenyl ester (15 mg, 0.027 mmol) and was then sealed with a rubber septum. The mixture was dissolved with dry degassed dichloromethane (2 mL) and was stirred for one day. The solvent was removed under *vacuo* and the bivalent initiator was isolated via column chromatography. Purification via column chromatography (hexane/chloroform 9/1, solvent predried) did not work out, decomposition of the catalyst on the column. Isolation was only possible in a mixture with Grubbs catalyst 1st-generation.

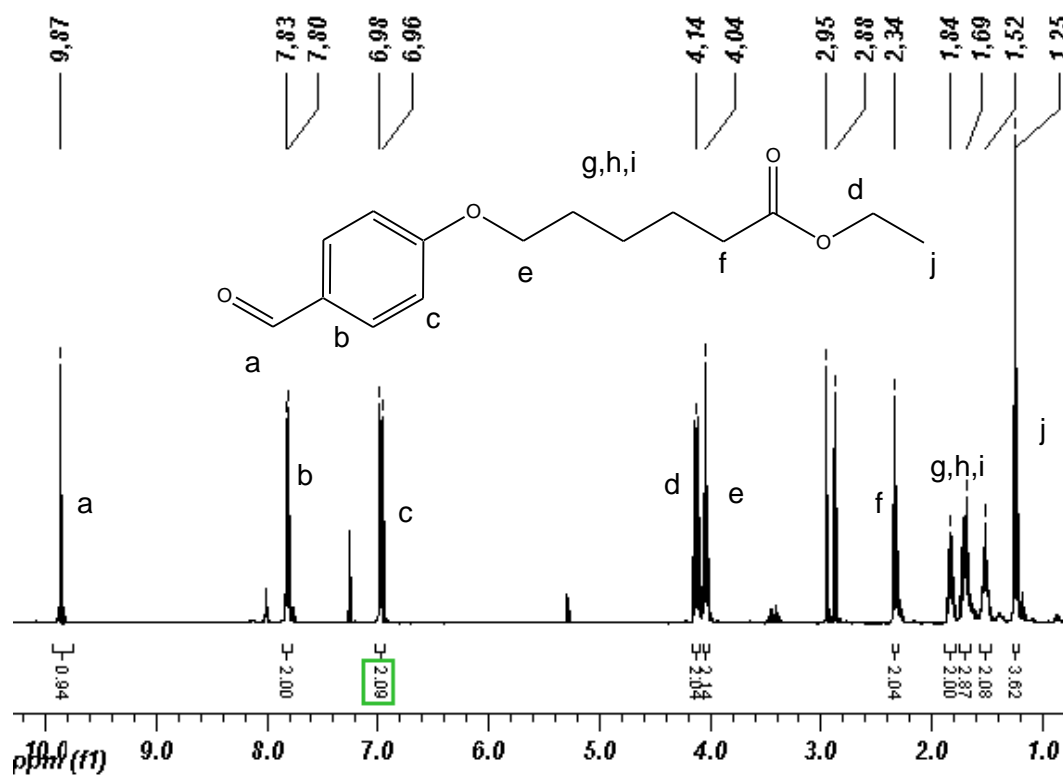


Figure 5.81. $^1\text{H NMR}$ of ethyl-6-4-formylphenoxyhexanoate (42) in CDCl_3 .

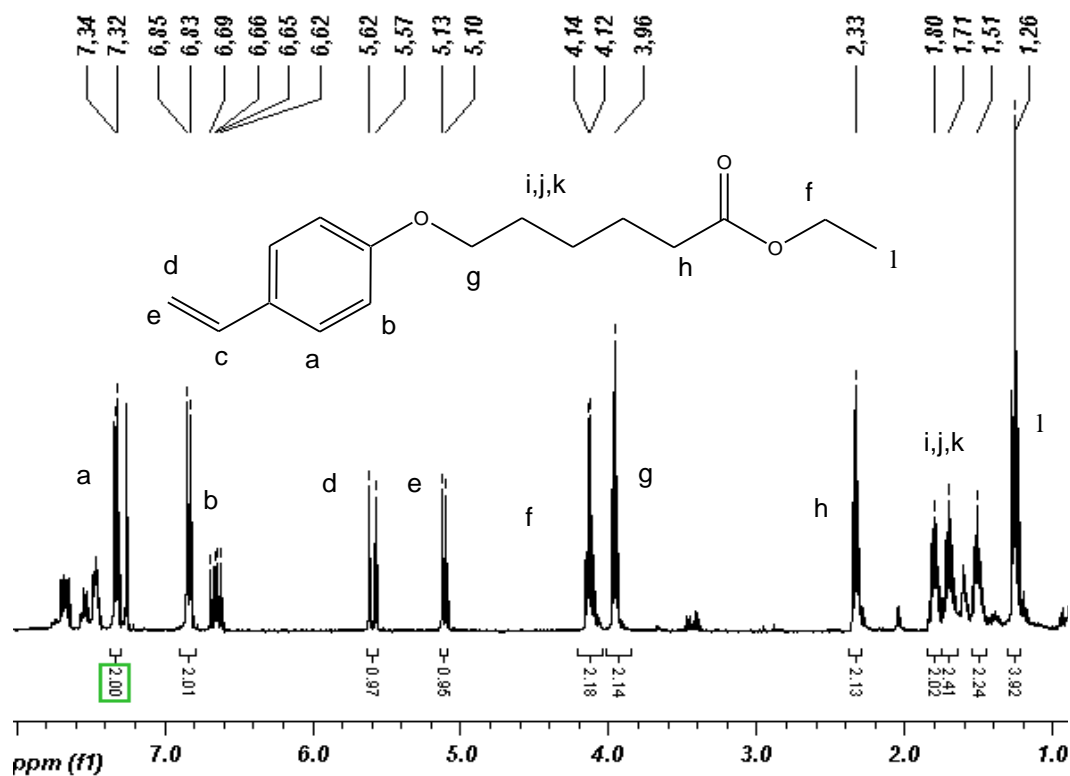


Figure 5.82. ^1H NMR of ethyl-6-(4-vinylphenoxy)hexanoate (**43**) in CDCl_3 .

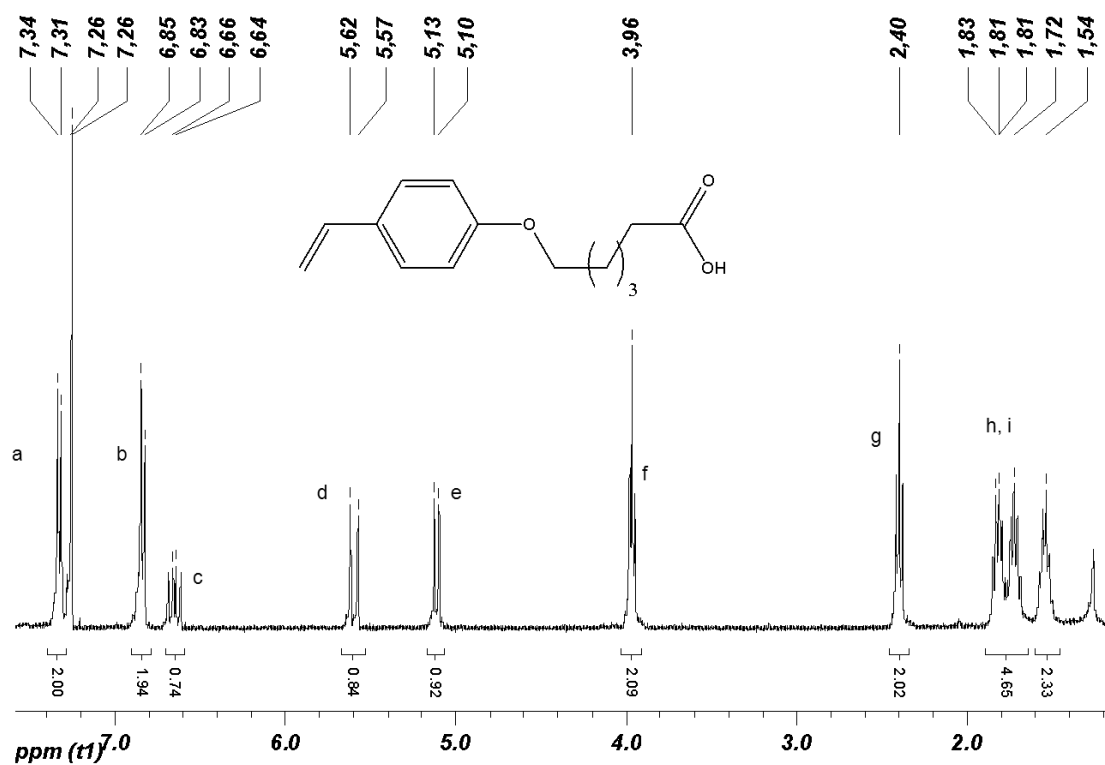


Figure 5.83. ^1H NMR of 6-(4-vinylphenoxy)hexanoic acid (**44**) in CDCl_3 .

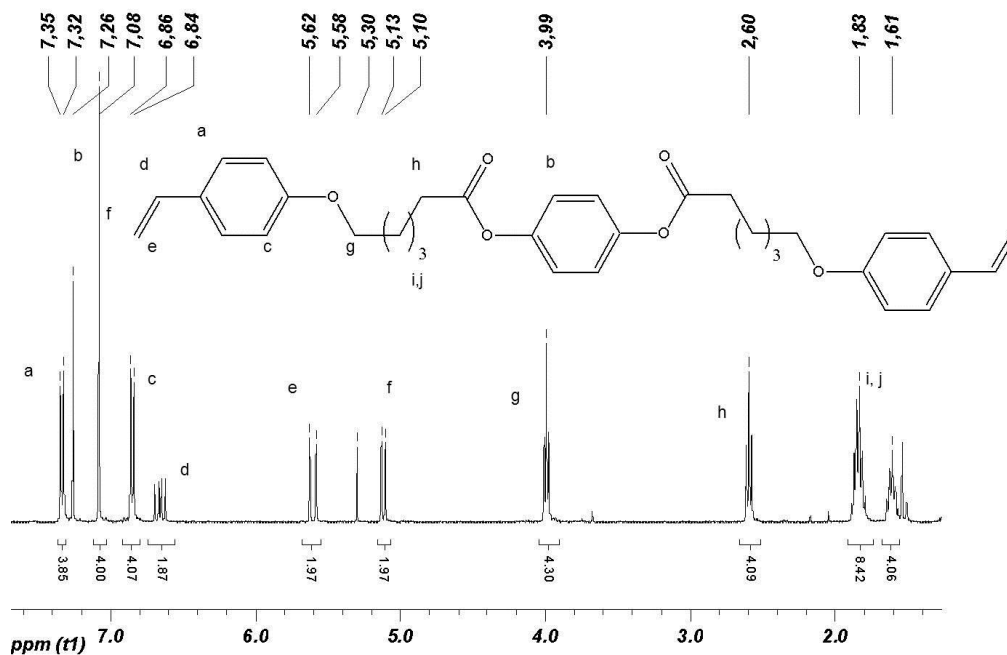


Figure 5.84. ^1H NMR of 6-(4-Vinyl-phenoxy)-hexanoic acid 4-[6-(4-vinyl-phenoxy)-hexanoyloxy]-phenyl ester (**45**) in CDCl_3 .

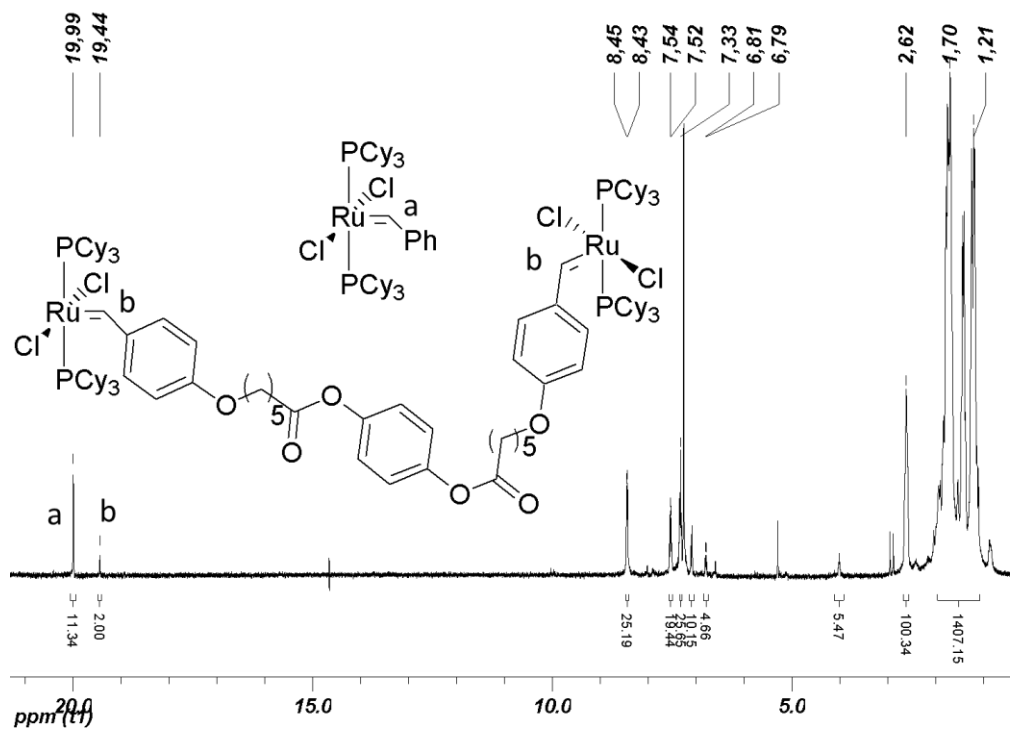


Figure 5.85. ^1H NMR of one fraction during the work up of the bimetallic catalyst (**46**) according to Weck et al.¹⁰⁰ in CDCl_3 , signals at 19.99 ppm and 19.44 ppm can be assigned to Grubbs catalyst 1st-generation and the bimetallic catalyst according to Weck et al.¹⁰⁰ in a ratio of 11.34/1.4

Halle, den 06.02.2013

Eidesstattliche Erklärung

Hiermit erkläre ich, Steffen Kurzhals, dass ich die vorliegende Arbeit selbstständig ohne fremde Hilfe angefertigt habe. Ich habe keine weiteren Quellen oder Hilfsmittel verwendet und die Werke von denen ich wörtlichen bzw. inhaltlichen Stellen entnommen habe, als solche kenntlich gemacht und angeführt.

Steffen Kurzhals

Curriculum Vitae**Persönliche Daten**

Name	Steffen Kurzhals
Geburtsdatum	06.04.1984
Geburtsort	Halle (Saale)
Adresse	Goethestr. 3 06114 Halle (Saale)
Staatsangehörigkeit	deutsch
Telefon	0176 76061872
E-Mail	steffenkurzhals@googlemail.com

Beruflicher Werdegang

11.2008-02.2013	Wissenschaftlicher Mitarbeiter an der Martin-Luther-Universität Halle-Wittenberg, Institut für Chemie, Makromolekulare Chemie, Arbeitsgruppe Prof. W. H. Binder
-----------------	---

Ausbildung

11.2008-02.2013	Promotionsarbeit in Chemie an der Martin-Luther-Universität Halle-Wittenberg, Institut für Chemie, Makromolekulare Chemie, Arbeitsgruppe Prof. W. H. Binder
09.10.2008	Abschluss als Diplomchemiker, Diplomarbeit: "Homologous Polymers via ROMP" (Note 1.0)
10.2003 - 10.2008	Studium der Chemie an der Martin-Luther-Universität Halle-Wittenberg, Vertiefungsrichtung: Makromolekulare Chemie
06.06.2003	Abschluss Abitur (Note 2.0)
08.1994-03.2003	Südstadt-Gymnasium Halle (Saale)

Auszeichnungen

Preisträger des Heinz-Bethge-Preises 2009 für die
Diplomarbeit "Approach to homologous polymers via ROMP"

Sprachkenntnisse

Deutsch: Muttersprache
Englisch: verhandlungsfähig
Französisch: Grundkenntnisse

Steffen Kurzhals

List of Publications

- (1) Kurzahls, S.; Binder, W. H. Book Chapter in “Handbook of Metathesis 2nd Edition”: Working Title “Combining Olefin Metathesis Polymerization with Click-Chemistry.” (submitted)
- (2) Kurzahls, S.; Enders, C., Binder, W. H., Monitoring ROMP Crossover Chemistry via ESI-TOF MS, *Macromolecules*, Article ASAP, DOI: 10.1021/ma302555q
- (3) Kurzahls, S.; Binder, W. H., Telechelic polynorbornenes with hydrogen bonding moieties by direct end capping of living chains. *J. Polym. Sci., Part A: Polym. Chem.* **2010**, 48, (23), 5522-5532.
- (4) Kurzahls, S.; Binder, W. H., A Synthetic Approach to Homologous Blockcopolymers. *Macromol. Symp.* **2010**, 293, (1), 63-66.
- (5) Binder, W. H.; Pulamagatta, B.; Onur, K.; Kurzahls, S.; Barqawi, H.; Tanner, S., Monitoring Block-Copolymer Crossover-Chemistry in ROMP: Catalyst Evaluation via Mass-Spectrometry (MALDI). *Macromolecules* **2009**, 42, 9457–9466.
- (6) Binder, W. H.; Kurzahls, S.; Pulamagatta, B.; Decker, U.; Manohar Pawar, G.; Wang, D.; Kühnel, C.; Buchmeiser, M. R., Homologous Poly(isobutylene): Poly(isobutylene)/High-Density Poly(ethylene) Hybrid Polymers. *Macromolecules* **2008**, 41, (22), 8405-8412.

Presentations

EPF **2011** Granada “Polymers with hydrogen bonding moieties via ROMP”

SFB-Retreat **2012** Bad Blankenburg “Crystallization in Dynamic Supramolecular Polymers”

Posters

ISOM XIII **2009** Leipzig “Approach to homologous polymers via ROMP”

ISOM XIII **2009** Leipzig “Monitoring block-copolymer crossover-chemistry in ROMP: catalyst evaluation via mass-spectrometry (MALDI)”

APME **2009** Dresden “Supramolecular Polymers via a Bimetallic Initiator”

DGMS **2010** Halle “Qualitative evaluation of the crossover reaction in ROMP with non-charged monomers via ESI-TOF MS”

12th Dresden Polymer Discussion **2010** “A general study of ROMP-crossover-reactions via MALDI methods”

P2010 **2010** Halle “Telechelic Poly-*p*-phenylenevinylenes via ROMP”

P2012 **2012** Halle "Hydrogenated poly(norbornene)s as building blocks for supramolecular block copolymers"